Xsuite
physics manual

Contents

Chapter 1

Lattice modeling and particle coordinates

The modeling of lattice and beam particles used in Xsuite is largely based on the experience of the MAD [1, 2] and Sixtrack [3] programs.

More details on the derivation of the tracking maps and the Hamiltonian formalism can be found in the references [4, 5, 6, 7, 8, 9, 10, 11].

1.1 Local reference system

This section is adapted from [1].

Figure 1.1: Local Reference System

Figure 1.1: Local Reference System

The beam line or ring to be studied is described as a sequence of beam elements placed sequentially along a reference trajectory.

The reference trajectory consists of a series of straight line segments and circular arcs. The accompanying tripod, as shown in Fig. 1.1, spans a local curvilinear right-handed coordinate system (x, y, s). The local s-axis is the tangent to the reference orbit and x and y are perpendicular to s. Typically, x is horizontal and y vertical.

We call ρ the local radius of curvature of the reference trajectory and h the local curvature defined as:

$$h = \frac{1}{\rho} \tag{1.1}$$

1.2   Global reference system

This section is adapted from [1].

The local reference system (x, y, s) may thus be referred to a global Cartesian coordinate system (X, Y, Z) as shown in Fig. 1.2.
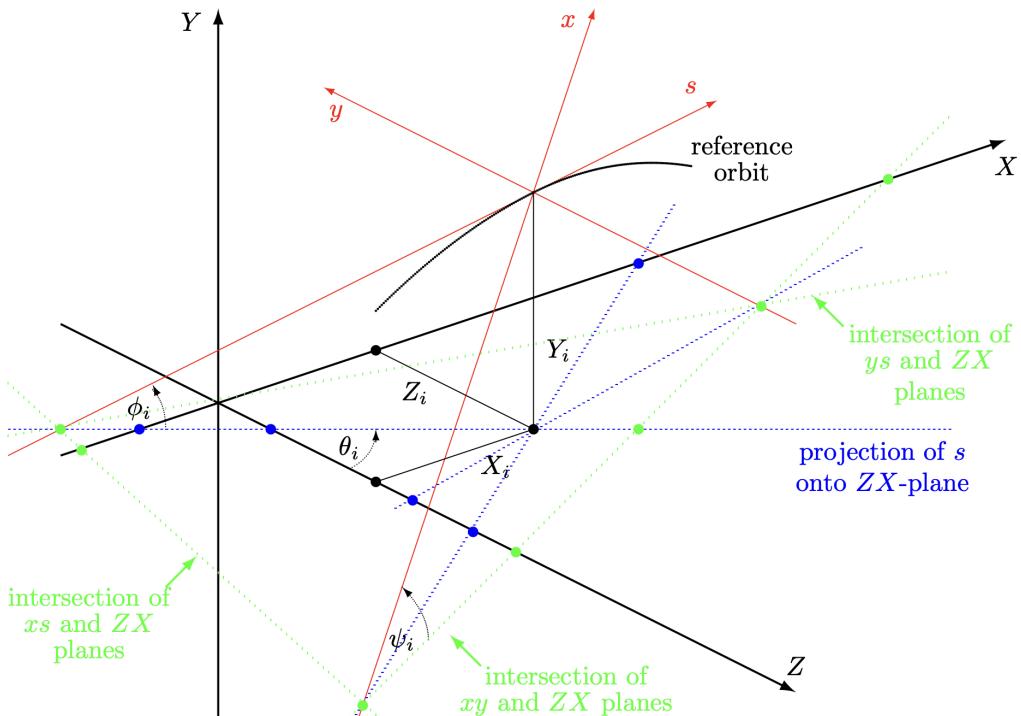
Figure 1.2: Global Reference System showing the global Cartesian system (X, Y, Z) in black and the local reference system (x, y, s) in red with the translation (X_i, Y_i, Z_i) and rotation $(\theta_i, \phi_i, \psi_i)$ relating the two.

The positions between beam elements are indexed with $i = 0, \dots, n$. The local reference system (x_i, y_i, s_i) at position i, i.e. the displacement and direction of the reference orbit with respect to the system (X, Y, Z) are defined by three displacements (X_i, Y_i, Z_i) and three angles $(\theta_i, \phi_i, \psi_i)$.

The above quantities are defined more precisely as follows:

- X Displacement of the local origin in X-direction.

- Y Displacement of the local origin in Y-direction.

- Z Displacement of the local origin in Z-direction.

- θ is the angle of rotation (azimuth) about the global Y-axis, between the global Z-axis and the projection of the reference orbit onto the (Z, X)-plane. A positive angle θ forms a right-hand screw with the Y-axis.

- ϕ is the elevation angle, i.e. the angle between the reference orbit and its projection onto the (Z, X)-plane. A positive angle ϕ corresponds to increasing Y.

  If only horizontal bends are present, the reference orbit remains in the (Z, X)-plane and ϕ is always zero.

- ψ is the roll angle about the local s-axis, i.e. the angle between the line defined by the intersection of the (x, y)-plane and (Z, X)-plane on one hand, and the local x-axis on the other hand. A positive angle ψ forms a right-hand screw with the s-axis.

Note that the angles (θ, ϕ, ψ) do not follow the usual definition of Euler angles. The reference orbit starts at the origin and points by default in the direction of the positive Z-axis.

Internally the displacement is described by a vector $\mathbf{V}$ and the orientation by a unitary matrix $\mathbf{W}$. The column vectors of $\mathbf{W}$ are the unit vectors spanning the local coordinate axes in the order (x, y, s). $\mathbf{V}$ and $\mathbf{W}$ have the values:

$$\mathbf{V} = \begin{bmatrix} X \\ Y \\ Z \end{bmatrix}, \qquad\qquad \mathbf{W} = \Theta \Phi \Psi \qquad (1.2)$$

where

$$\Theta = \begin{bmatrix} \cos\theta & 0 & \sin\theta \\ 0 & 1 & 0 \\ -\sin\theta & 0 & \cos\theta \end{bmatrix}, \quad \Phi = \begin{bmatrix} 1 & 0 & 0 \\ 0 & \cos\phi & \sin\phi \\ 0 & -\sin\phi & \cos\phi \end{bmatrix}, \quad \Psi = \begin{bmatrix} \cos\psi & \sin\psi & 0 \\ -\sin\psi & \cos\psi & 0 \\ 0 & 0 & 1 \end{bmatrix}.$$
$$(1.3)$$

When advancing through a beam element, Xsuite (like MAD) computes V_i and W_i by the recurrence relations

$$V_i = W_{i-1} R_i + V_{i-1}, \qquad\qquad W_i = W_{i-1} S_i \qquad (1.4)$$

The vector R_i is the displacement and the matrix S_i is the rotation of the local reference system introduced by the element i with respect to the entrance of the same element. The values of R_i and S_i are listed below for different physical element types.

In straight elements the local reference system is simply translated by the length of the element along the local s-axis.

The corresponding R and S are

$$R = \begin{bmatrix} 0 \\ 0 \\ L \end{bmatrix}, \qquad\qquad S = \begin{bmatrix} 1 & 0 & 0 \\ 0 & 1 & 0 \\ 0 & 0 & 1 \end{bmatrix}. \tag{1.5}$$

A rotation of the element about the s-axis has no effect on R and S, since the rotations of the reference system before and after the element cancel.

Bending magnets have a curved reference orbit. For both rectangular and sector bending magnets, the R and S are expressed as functions of the bend angle α:

$$R = \begin{bmatrix} \rho(\cos\alpha - 1) \\ 0 \\ \rho\sin\alpha \end{bmatrix}, \qquad S = \begin{bmatrix} \cos\alpha & 0 & -\sin\alpha \\ 0 & 1 & 0 \\ \sin\alpha & 0 & \cos\alpha \end{bmatrix} \tag{1.6}$$

where we have assumed that the bending occurs in the horizontal plane. A positive bend angle represents a bend to the right, i.e. towards negative x values. For sector bending magnets, the bend radius is given by ρ, and for rectangular bending magnets it has the value $\rho = L/(2\sin(\alpha/2))$. If the magnet is rotated about the s-axis by an angle ψ, R and S are transformed by

$$R = TR, \qquad\qquad S = TST^{-1} \tag{1.7}$$

where T is the orthogonal rotation matrix

$$T = \begin{bmatrix} \cos\psi & -\sin\psi & 0 \\ \sin\psi & \cos\psi & 0 \\ 0 & 0 & 1 \end{bmatrix} \tag{1.8}$$

The special value $\psi = \pi/2$ represents a bend down.

1.3   Reference particle

We introduce a reference particle with rest mass m_0, charge q_0, total energy E_0, momentum P_0, and relativistic factors β_0, γ_0. These quantities satisfy

$$E_0^2 = (P_0 c)^2 + (m_0 c^2)^2, \tag{1.9}$$

$$E_0 = m_0 \gamma_0 c^2, \tag{1.10}$$

$$P_0 = m_0 \beta_0 \gamma_0 c, \tag{1.11}$$

$$\beta_0 = \frac{P_0 c}{E_0} = \sqrt{1 - \frac{1}{\gamma_0^2}}, \tag{1.12}$$

$$\gamma_0 = \frac{1}{\sqrt{1 - \beta_0^2}}. \tag{1.13}$$

The reference particle will be used to normalize momentum and energy variables as well as electromagnetic fields and potentials. For this purpose we introduce the corresponding reference beam rigidity as

$$\text{rig}_0 = \frac{P_0}{q_0},\tag{1.14}$$

which is the momentum per unit charge used, for example, to normalize multipole strengths.

1.4 Electromagnetic potentials and fields

The electromagnetic fields $\mathbf{E}$ and $\mathbf{B}$ can be derived from the potentials $\Phi(x,y,s,t)$ and $\mathbf{A}(x,y,s,t)$, where

$$\mathbf{A}(x,y,s,t) = A_x(x,y,s,t)\hat{x}(s) + A_y(x,y,s,t)\hat{y}(s) + A_s(x,y,s,t)\hat{z}(s)\tag{1.15}$$

and for which:

$$\mathbf{E} = -\nabla\Phi - \frac{\partial\mathbf{A}}{\partial t} = -\partial_x\Phi\hat{x} - \partial_y\Phi\hat{y} - \frac{1}{1+hx}\partial_s\Phi\hat{z} - \partial_t\mathbf{A}\tag{1.16}$$

$$\mathbf{B} = \nabla\times\mathbf{A} = \left(\partial_y A_s - \frac{\partial_s A_y}{1+hx}\right)\hat{x} + \left(\frac{\partial_s A_x - \partial_x(1+hx)A_s}{1+hx}\right)\hat{y} + \left(\partial_x A_y - \partial_y A_x\right)\hat{z}.\tag{1.17}$$

We use the reference particle properties to define normalized potentials:

$$\mathbf{a}(x,y,s,t) = \frac{q_0}{P_0}\mathbf{A}(x,y,s,t)\tag{1.18}$$

$$\varphi(x,y,s,t) = \frac{q_0}{P_0 c}\Phi(x,y,s,t)\tag{1.19}$$

1.5 Convention for multipole expansion of magnetic fields

This section is adapted from [1].

1.5.1 Straight magnets ($h = 0$)

Xsuite, like MAD, uses the following Taylor expansion for the magnetic field components. Using a complex notation for the field $(B_y + iB_x)$ and the position $(x + iy)$ we write:

$$B_y + iB_x = \sum_{n=0}^{\infty} \frac{(B_n + iA_n)}{n!}(x + iy)^n\tag{1.20}$$

where, assuming that the field is piece-wise constant along s and that the local curvature h is zero, the coefficients B_n and A_n are the on-axis derivatives of the transverse field components:

$$B_n = \frac{\partial^n B_y}{\partial x^n}\bigg|_{x=0, y=0}, \qquad A_n = \frac{\partial^n B_x}{\partial x^n}\bigg|_{x=0, y=0}. \qquad (1.21)$$

The associated longitudinal vector potential for straight elements can be written as

$$A_s(x,y) = -\Re\left(\sum_{n=0}^{\infty} \frac{(B_n + iA_n)}{(n+1)!}(x+iy)^{n+1}\right), \qquad (1.22)$$

so that $B_y + iB_x = -(\partial_x - i\partial_y)A_s$ yields the field expansion above.

We define the normal multipole coefficients K_n and the skew multipole coefficients $\hat{K}_n$ using the reference beam rigidity from Eq. (1.14):

$$K_n = \frac{B_n}{\mathrm{rig}_0} \qquad (1.23)$$

and

$$\hat{K}_n = \frac{A_n}{\mathrm{rig}_0} \qquad (1.24)$$

Using these coefficients, the field expansion and the longitudinal vector potential can be written as

$$B_y + iB_x = \mathrm{rig}_0 \sum_{n=0}^{\infty} \frac{(K_n + i\hat{K}_n)}{n!}(x+iy)^n, \qquad (1.25)$$

$$A_s(x,y) = -\mathrm{rig}_0\, \Re\left(\sum_{n=0}^{\infty} \frac{(K_n + i\hat{K}_n)}{(n+1)!}(x+iy)^{n+1}\right). \qquad (1.26)$$

The normalized longitudinal potential a_s introduced in Sec. 1.4 is then

$$a_s(x,y) = \frac{q_0}{P_0} A_s(x,y) = -\Re\left(\sum_{n=0}^{\infty} \frac{(K_n + i\hat{K}_n)}{(n+1)!}(x+iy)^{n+1}\right). \qquad (1.27)$$

In the special case where only K_0, K_1, and K_2 are non-zero (all $K_{n\geq 3} = 0$ and $\hat{K}_n = 0$), the normalized longitudinal potential reduces to

$$a_s(x,y) = -\left[K_0 x + \frac{K_1}{2}\left(x^2 - y^2\right) + \frac{K_2}{6}\left(x^3 - 3xy^2\right)\right]. \qquad (1.28)$$

1.5.2   Curved magnets ($h \neq 0$)

In the case of curved magnets ($h \neq 0$), multipole components are still defined as the derivatives at the symmetry point of the magnet:

$$B_n = \frac{\partial^n B_y}{\partial x^n}\bigg|_{x=0, y=0}, \qquad (1.29)$$

$$A_n = \frac{\partial^n B_x}{\partial x^n}\bigg|_{x=0, y=0}. \qquad (1.30)$$

and the corresponding normalized multipole coefficients K_n and $\hat{K}_n$ are defined as before:

$$K_n = \frac{B_n}{\text{rig}_0}, \quad \hat{K}_n = \frac{A_n}{\text{rig}_0}. \tag{1.31}$$

The field and potential expansions are more complex than in the straight case as they must satisfy 1.17 together with the definitions (1.29) and (1.30).

For the special case where only K_0, K_1, and K_2 are non-zero, a truncated expansion for the normalized potential is:

$$a_s(x, y, s) = -K_0 \left(x - \frac{hx^2}{2(1+hx)} \right) - K_1 \left(\frac{1}{2}(x^2 - y^2) - \frac{h}{6}x^3 \right)$$
$$- K_2 \left(\frac{1}{6}(x^3 - 3xy^2) - \frac{h}{24}(x^4 - y^4) \right) \tag{1.32}$$

1.6   Particle coordinates

Xsuite uses as independent variable the position along the reference trajectory s. We call t the time coordinate, i.e. the time at which the particle passes the position s.

Xsuite can track particles of different species within the same particle ensemble. We call m and q the rest mass and charge of the individual particle and we introduce the coefficient:

$$\chi = \frac{q}{q_0} \frac{m_0}{m} \tag{1.33}$$

In the "longitudinal plane", i.e. the space spanned by time and energy coordinates, we can use any of the following pairs of conjugate variables:

$$\zeta = s\frac{\beta}{\beta_0} - \beta ct \qquad \tau = \frac{s}{\beta_0} - ct \qquad \zeta = s - \beta_0 ct \qquad \delta = \frac{P\frac{m_0}{m} - P_0}{P_0} \tag{1.34}$$

$$\delta = \frac{P\frac{m_0}{m} - P_0}{P_0} \qquad p_\tau = \frac{1}{\beta_0}\frac{E\frac{m_0}{m} - E_0}{E_0} \qquad p_\zeta = \frac{1}{\beta_0^2}\frac{E\frac{m_0}{m} - E_0}{E_0} \qquad \ell = \beta ct \tag{1.35}$$

where variables in the same column are canonically conjugate.

These variables can be easily related to each other:

$$E = m\gamma c^2 = P_0 c \left(p_\tau + \frac{1}{\beta_0} \right), \tag{1.36}$$

$$P = m\beta\gamma c = P_0(1 + \delta) \tag{1.37}$$

$$\beta = \frac{Pc}{E} = \sqrt{1 - \frac{1}{\gamma^2}} = \sqrt{1 - \frac{1 - \beta_0}{(1 + \beta_0 p_\tau)^2}}, \tag{1.38}$$

$$\gamma = \frac{1}{\sqrt{1 - \beta^2}} = \gamma_0(1 + \beta_0 p_\tau) \tag{1.39}$$

$$\zeta = s\frac{\beta}{\beta_0} - \ell = \beta\tau = \frac{\beta}{\beta_0}\zeta \tag{1.40}$$

$$\delta = \sqrt{p_\tau^2 + 2\frac{p_\tau}{\beta_0} + 1} - 1 = \beta p_\tau + \frac{\beta - \beta_0}{\beta_0} \tag{1.41}$$

$$\delta = \sqrt{\beta_0^2 p_\zeta^2 + 2p_\zeta + 1} - 1 = \beta\beta_0 p_\zeta + \frac{\beta - \beta_0}{\beta_0} \tag{1.42}$$

$$(1 + \delta)^2 = \frac{P^2}{P_0^2} = \frac{E^2 - m_0^2 c^4}{P_0^2 c^2} = \frac{E^2}{c^2 P_0^2} - \frac{1}{\beta_0^2 \gamma_0^2} = \left(p_\tau + \frac{1}{\beta_0} \right)^2 - \frac{1}{\beta_0^2 \gamma_0^2} \tag{1.43}$$

$$p_\tau = \beta_0 p_\zeta \tag{1.44}$$

$$p_\tau = \frac{\sqrt{1 + \beta_0^2 \, \delta(\delta + 2)} - 1}{\beta_0} \tag{1.45}$$

and the following derivatives:

$$\frac{\partial\delta}{\partial p_\tau} = \frac{p_\tau + 1/\beta_0}{1 + \delta} = \frac{1}{\beta} \tag{1.46}$$

$$\frac{\partial}{\partial\delta}\left(\frac{1 + \delta}{\beta\beta_0} \right) = \frac{\beta}{\beta_0} \tag{1.47}$$

For small energy deviations ($\delta \ll 1$, $p_\tau \ll 1$, $p_\zeta \ll 1$), we can neglect the terms of order δ^2, p_τ^2, p_ζ^2 and higher, hence the following approximations hold:

$$\delta \simeq \frac{p_\tau}{\beta_0} \tag{1.48}$$

$$\delta \simeq p_\zeta \tag{1.49}$$

$$\beta \simeq \beta_0 + (1 - \beta_0^2)p_\tau \tag{1.50}$$

In the transverse plane we use the coordinates x, p_x, y, p_y. The transverse canonical momenta are defined as:

$$p_x = \frac{m_0}{m}\frac{P_x}{P_0}, \qquad\qquad p_y = \frac{m_0}{m}\frac{P_y}{P_0}, \tag{1.51}$$

where:

$$P_x = m\gamma\dot{x} + qA_x, \qquad\qquad P_y = m\gamma\dot{y} + qA_y \tag{1.52}$$

in which $\dot{x}$ and $\dot{y}$ are the time derivatives of x and y.

1.7 Hamiltonian and equations of motion

The motion of a particle is described by one of the following Hamiltonian functions, depending on the choice of longitudinal coordinates:

$$
H_\delta = \frac{1+\delta}{\beta\beta_0} - (1+hx)\left(\sqrt{\left(\frac{1+\delta}{\beta} - \chi\varphi\right)^2 - \frac{1}{\beta_0^2\gamma_0^2} - (p_x - \chi a_x)^2 - (p_y - \chi a_y)^2} + \chi a_s\right)
$$

(1.53)

$$
H_\tau = \frac{p_\tau}{\beta_0} - (1+hx)\left(\sqrt{\left(p_\tau + \frac{1}{\beta_0} - \chi\varphi\right)^2 - \frac{1}{\beta_0^2\gamma_0^2} - (p_x - \chi a_x)^2 - (p_y - \chi a_y)^2} + \chi a_s\right)
$$

(1.54)

$$
H_\zeta = p_\zeta - (1+hx)\left(\sqrt{\left(\beta_0 p_\zeta + \frac{1}{\beta_0} - \chi\varphi\right)^2 - \frac{1}{\beta_0^2\gamma_0^2} - (p_x - \chi a_x)^2 - (p_y - \chi a_y)^2} + \chi a_s\right)
$$

(1.55)

Using τ and p_τ as longitudinal coordinates, the equations of motion are:

$$
\frac{\mathrm{d}p_x}{\mathrm{d}s} = -\frac{\partial H_\tau}{\partial x}
$$

(1.56)

$$
\frac{\mathrm{d}p_y}{\mathrm{d}s} = -\frac{\partial H_\tau}{\partial y}
$$

(1.57)

$$
\frac{\mathrm{d}p_\tau}{\mathrm{d}s} = -\frac{\partial H_\tau}{\partial \tau}
$$

(1.58)

$$
\frac{\mathrm{d}x}{\mathrm{d}s} = \frac{\partial H_\tau}{\partial p_x}
$$

(1.59)

$$
\frac{\mathrm{d}y}{\mathrm{d}s} = \frac{\partial H_\tau}{\partial p_y}
$$

(1.60)

$$
\frac{\mathrm{d}\tau}{\mathrm{d}s} = \frac{\partial H_\tau}{\partial p_\tau}
$$

(1.61)

The full derivation of the Hamiltonian and equations of motion can be found in Wolski [12] (note the different notation, as the symbol δ in [12] denotes the quantity that here we call p_τ).

1.8 Expanded magnet body hamiltonian

For a magnet with piece-wise constant multipole components and curvature h, we can set $a_x = 0$ and $a_y = 0$ in Eq. (1.54):

$$
H_\tau = H^{\mathrm{kin}} + H^{\mathrm{magn}}
$$

(1.62)

where

$$H^{\text{kin}} = \frac{p_\tau}{\beta_0} - (1 + hx)\sqrt{\left(p_\tau + \frac{1}{\beta_0}\right)^2 - \frac{1}{\beta_0^2 \gamma_0^2} - p_x^2 - p_y^2} \tag{1.63}$$

$$H^{\text{magn}} = -(1 + hx)\chi a_s \tag{1.64}$$

1.8.1   Approximation of the kinetic part of the hamiltonian

Using 1.43, the kinetic part can be rewritten as follows:

$$H^{\text{kin}} = \frac{p_\tau}{\beta_0} - (1 + hx)\sqrt{(1 + \delta)^2 - p_x^2 - p_y^2} \tag{1.65}$$

$$= \frac{p_\tau}{\beta_0} - \sqrt{(1 + \delta)^2 - p_x^2 - p_y^2} - hx\sqrt{(1 + \delta)^2 - p_x^2 - p_y^2} \tag{1.66}$$

Neglecting high-order terms $h^2 x^2 p_x^2$ and $h^2 x^2 p_y^2$ in the second square root, we can approximate:

$$H^{\text{kin}} = \frac{p_\tau}{\beta_0} - \sqrt{(1 + \delta)^2 - p_x^2 - p_y^2} - hx(1 + \delta) \tag{1.67}$$

$$= H_D - hx(1 + \delta) \tag{1.68}$$

where

$$H_D = \frac{p_\tau}{\beta_0} - \sqrt{(1 + \delta)^2 - p_x^2 - p_y^2} \tag{1.69}$$

is the Hamiltonian of a straight drift.
The hamiltonian for the drift can in turn be expanded as follows:

$$H_D = \frac{p_\tau}{\beta_0} - (1 + \delta)\sqrt{1 - \frac{p_x^2 + p_y^2}{(1 + \delta)^2}} \tag{1.70}$$

$$\simeq \frac{p_\tau}{\beta_0} - (1 + \delta) + \frac{1}{2}\frac{p_x^2 + p_y^2}{(1 + \delta)} \tag{1.71}$$

Replacing Eq. (1.71) in Eq. (1.68) yields the following expression for the kinetic part of the Hamiltonian:

$$H^{\text{kin}} \simeq \frac{p_\tau}{\beta_0} - \left(1 + \delta - \frac{1}{2}\frac{p_x^2 + p_y^2}{(1 + \delta)}\right) - hx(1 + \delta) \tag{1.72}$$

1.8.2   Approximation of the magnetic part of the hamiltonian

For the common case where only K_0, K_1, and K_2 are non-zero, inserting the curved-magnet potential from Eq. (1.32) in H^{magn} yields:

$$H^{\text{magn}} = (1 + hx)\chi\left[K_0\left(x - \frac{hx^2}{2(1 + hx)}\right) + K_1\left(\frac{1}{2}(x^2 - y^2) - \frac{h}{6}x^3\right)\right.$$

$$\left. + K_2\left(\frac{1}{6}(x^3 - 3xy^2) - \frac{h}{24}(x^4 - y^4)\right)\right]. \tag{1.73}$$

Discarding all terms nonlinear in h (i.e., keeping only $\mathcal{O}(h)$) yields

$$H^{\text{magn}} \simeq \chi \left[K_0 x + K_1 \frac{x^2 - y^2}{2} + K_2 \frac{x^3 - 3xy^2}{6} \right]$$
$$+ \chi h \left[\frac{K_0}{2} x^2 + K_1 \left(\frac{1}{3} x^3 - \frac{1}{2} xy^2 \right) + K_2 \left(\frac{1}{8} x^4 - \frac{1}{2} x^2 y^2 + \frac{1}{24} y^4 \right) \right]. \quad (1.74)$$

1.9 Symplectic integrators and magnet models

In Xsuite, magnets are modeled using symplectic integrators, splitting the Hamiltonian in a 'propagation' part and a 'kick' part, for which closed-form solutions of the equations of motion are available.

Hamiltonians for which closed-form solutions of the equations of motion exist and are implemented in Xsuite are reported in Table 1.1. The corresponding maps are reported in the following sections.

Different magnet models are available, which correspond to different ways of splitting the Hamiltonian. The available models are reported in Table 1.2 and the available integration schemes are reported in Table 1.3.

Map	Params.	Description	
D		Drift exact	$H_D = \frac{p_\tau}{\beta_0} - \sqrt{(1+\delta)^2 - p_x^2 - p_y^2}$
De		Drift expanded	$H_{De} = \frac{p_\tau}{\beta_0} - (1+\delta) - \frac{1}{2} \frac{p_x^2 + p_y^2}{(1+\delta)}$
R	h	Curved drift	$H_R = \frac{p_\tau}{\beta_0} - (1+hx)\sqrt{(1+\delta)^2 - p_x^2 - p_y^2}$
Br	K_0	Rectangular bend	$H_{Br} = H_D + \chi K_0 x$
B	K_0, h	Exact Bend	$H_B = H_R + \chi K_0 x + \chi h K_0 \frac{x^2}{2}$
K0	K_0	Dipole kick	$H_{K0} = \chi K_0 x$
K1	K_1	Quadrupole kick	$H_{K1} = \chi K_1 \frac{x^2 - y^2}{2}$
h	h	Curvature kick	$H_h = -hx(1+\delta)$
K0h	K_0	Weak focusing kick	$H_{K0h} = \chi h K_0 \frac{x^2}{2}$
K1h	K_1, h	Quad curv. correction	$H_{K1h} = \chi h K_1 \frac{2x^3 - 3xy^2}{6}$
Kn	$K_n, \hat{K}_n$	Multipole	$H_{Kn} = -\chi \Re \left(\sum_{n=0}^{N} (K_n + i\hat{K}_n) \frac{(x+iy)^{n+1}}{(n+1)!} \right)$
M	K_0, K_1, h	Expanded bend-quad.	$H_M = H_{De} - hx(1+\delta) + \chi K_0 x + \chi K_1 \frac{x^2 - y^2}{2} + \chi h K_0 \frac{x^2}{2}$
S	K_s	Solenoid	$H_S = \frac{p_\tau}{\beta_0} - \sqrt{(1+\delta)^2 - \left(p_x - \frac{K_s}{2} y \right)^2 - \left(p_y + \frac{K_s}{2} \right)^2}$

Table 1.1: Hamiltonians of the implemented maps.

Model	Propagation part	Kick part
rot-kick-rot	[R]	[K0 K0h K1 K1h Kn]
bend-kick-bend	[B]	[K1 K1h Kn]
matrix-kick-matrix	[M]	[K1h Kn]
drift-kick-drift-exact	[D]	[h K0 K0h K1 K1h Kn]
drift-kick-drift-expanded	[De]	[h K0 K0h K1 K1h Kn]

Table 1.2: Available magnet models.

Integrator	Description
uniform	Kicks uniformly distributed along the length of the element
teapot	TEAPOT integration scheme [13, 14]
yoshida4	Fourth order Yoshida integrator [15]

Table 1.3: Available integration schemes.

1.10   Beam element maps

1.10.1   Drift

Implemented in the Drift element.

A drift is a straight, field-free region ($h(x, y) = 0$, $V = 0$ and $\mathbf{A} = 0$). The exact and expanded Hamiltonian for a drift space are

$$H_\tau = \frac{p_\tau}{\beta_0} - \sqrt{(1+\delta)^2 - p_x^2 - p_y^2} \approx \frac{p_\tau}{\beta_0} - \delta + \frac{1}{2}\frac{p_x^2 + p_y^2}{1 + \delta}. \tag{1.75}$$

The corresponding maps can be obtained by solving the equations of motion:

$$\frac{\mathrm{d}p_i}{\mathrm{d}s} = -\frac{\partial H}{\partial q_i} \qquad\qquad \frac{\mathrm{d}q_i}{\mathrm{d}s} = \frac{\partial H}{\partial p_i} \tag{1.76}$$

As there is no explicit dependency on the position coordinates in the Hamiltonian, the momenta remain unchanged in a drift.

For the position coordinates, we get:

$$(x)' = \frac{p_x}{p_z} \approx \frac{p_x}{1+\delta} \tag{1.77}$$

$$(y)' = \frac{p_y}{p_z} \approx \frac{p_y}{1+\delta} \tag{1.78}$$

$$(\tau)' = \frac{1}{\beta_0} - \frac{1}{\beta}\frac{1+\delta}{p_z} \approx \frac{1}{\beta_0} - \frac{1}{\beta} - \frac{1}{\beta}\frac{p_x^2 + p_y^2}{2} \tag{1.79}$$

$$p_z = \sqrt{(1+\delta)^2 - p_x^2 - p_y^2} \tag{1.80}$$

Hence, the map relative to the expanded Hamiltonian for a drift of length L is:

$$x_p = \frac{p_x}{1+\delta} \tag{1.81}$$

$$y_p = \frac{p_y}{1+\delta} \tag{1.82}$$

$$x \leftarrow x + x_p L \tag{1.83}$$

$$y \leftarrow y + y_p L \tag{1.84}$$

$$\zeta \leftarrow \zeta + l\left(1 - \frac{\beta_0}{\beta}\left(1 + \frac{x_p^2 + y_p^2}{2}\right)\right) \tag{1.85}$$

and the map relative to the exact Hamiltonian for a drift of length L is:

$$x \leftarrow x + \frac{p_x}{p_z}L \tag{1.86}$$

$$y \leftarrow y + \frac{p_y}{p_z}L \tag{1.87}$$

$$\zeta \leftarrow \zeta + L\left(1 - \frac{\beta_0}{\beta}\frac{1+\delta}{p_z}\right) \tag{1.88}$$

1.10.2 Polar drift (sector curvature h)

Used in the implementation of <u>Bend</u> and <u>RBend</u> elements when model is "rot-kick-rot".
This map is ported from PTC and MAD-NG source codes.

The following map, corresponding to the motion of a particle in a field-free region in a reference frame with horizontal curvature h, is generated by the Hamiltonian:

$$H_R = \frac{p_\tau}{\beta_0} - (1+hx)\left(\sqrt{(1+\delta)^2 - p_x^2 - p_y^2}\right) \tag{1.89}$$

We call:

$$\delta_+ \equiv 1+\delta, \qquad \text{rvv} = v/c, \qquad s \equiv L.$$

Define the longitudinal momentum component

$$p_z \equiv \sqrt{\delta_+^2 - p_x^2 - p_y^2}. \tag{1.90}$$

Define the curvature radius

$$\rho \equiv \frac{1}{h},$$

(1.91)

and the trigonometric abbreviations

$$c \equiv \cos(hs), \qquad s_a \equiv \sin(hs), \qquad s_{a2} \equiv \sin\left(\frac{hs}{2}\right).$$

(1.92)

Introduce

$$\frac{1}{p_z} \equiv p_z^{-1}, \qquad p_{x,t} \equiv \frac{p_x}{p_z}, \qquad \mathcal{D} \equiv c - s_a\, p_{x,t}, \qquad \mathcal{D}^{-1} \equiv \frac{1}{\mathcal{D}}.$$

(1.93)

Define also

$$p_s \equiv (x + \rho)\, s_a\, p_z^{-1}\, \mathcal{D}^{-1}.$$

(1.94)

Transverse map

$$x_1 = \left[x + \rho \left(2s_{a2}^2 + s_a\, p_{x,t} \right) \right] \mathcal{D}^{-1},$$

(1.95)

$$p_{x1} = c\, p_x + s_a\, p_z,$$

(1.96)

$$y_1 = y + p_s\, p_y.$$

(1.97)

Path length / longitudinal map   The quantity $\Delta \ell$ computed in the code is

$$\Delta \ell = \delta_+ \frac{(x + \rho)\, s_a}{c\, p_z \left(1 - \dfrac{p_x s_a}{c\, p_z} \right)}.$$

(1.98)

The longitudinal coordinate is updated as

$$\zeta_1 = \zeta + \left(L - \frac{\Delta \ell}{\mathrm{rvv}} \right),$$

(1.99)

and the reference longitudinal position as

$$s_{\mathrm{ref},1} = s_{\mathrm{ref}} + L.$$

(1.100)

1.10.3   Curved exact bend

Implemented in the <u>Bend element</u>.

The generating Hamiltonian is:

$$H_B = \frac{p_\tau}{\beta_0} - (1 + hx) \left(\sqrt{(1 + \delta)^2 - p_x^2 - p_y^2} - K_0 \left(x - \frac{hx^2}{2(1 + hx)} \right) \right)$$

(1.101)

The corresponding map is adapted from [11]:

$$x(s) = \frac{1}{hK_0}\left(h\sqrt{(1+\delta)^2 - p_x(s)^2 - p_y^2} - \frac{dp_x(s)}{ds} - K_0\chi\right) \tag{1.102}$$

$$p_x(s) = p_x\cos(hs) + \left(\sqrt{(1+\delta)^2 - p_x^2 - p_y^2} - K_0\chi\left(\frac{1}{h} + x\right)\right)\sin(hs) \tag{1.103}$$

$$y(s) = y + \frac{p_y sh}{K_0\chi} + \frac{p_y}{K_0\chi}\left(\sin^{-1}\left(\frac{p_x}{\sqrt{(1+\delta)^2 - p_y^2}}\right) - \sin^{-1}\left(\frac{p_x(s)}{\sqrt{(1+\delta)^2 - p_y^2}}\right)\right) \tag{1.104}$$

$$p_y(s) = p_y \tag{1.105}$$

$$\delta(s) = \delta \tag{1.106}$$

$$\ell(s) = \ell + \frac{(1+\delta)sh}{K_0\chi} + \frac{(1+\delta)}{K_0\chi}\left(\sin^{-1}\left(\frac{p_x}{\sqrt{(1+\delta)^2 - p_y^2}}\right) - \sin^{-1}\left(\frac{p_x(s)}{\sqrt{(1+\delta)^2 - p_y^2}}\right)\right) \tag{1.107}$$

1.10.4 Straight exact bend

Implemented in the <u>Bend</u> and <u>RBend</u> elements for specific configurations.

The generating Hamiltonian is:

$$H_{Br} = \frac{p_\tau}{\beta_0} - \sqrt{(1+\delta)^2 - p_x^2 - p_y^2} - K_0 x \tag{1.108}$$

The corresponding map is adapted from [11]:

$$x(L) = x + \frac{1}{K_0\chi}\left(\sqrt{(1+\delta)^2 - p_x(L)^2 - p_y^2} - \sqrt{(1+\delta)^2 - p_x^2 - p_y^2}\right) \tag{1.109}$$

$$p_x(L) = p_x - K_0\chi L \tag{1.110}$$

$$y(L) = y + \frac{p_y}{K_0\chi}\left(\sin^{-1}\left(\frac{p_x}{\sqrt{(1+\delta)^2 - p_y^2}}\right) - \sin^{-1}\left(\frac{p_x(L)}{\sqrt{(1+\delta)^2 - p_y^2}}\right)\right) \tag{1.111}$$

$$p_y(L) = p_y \tag{1.112}$$

$$\delta(L) = \delta \tag{1.113}$$

$$\ell(L) = \ell + \frac{1+\delta}{K_0\chi}\left(\sin^{-1}\left(\frac{p_x}{\sqrt{(1+\delta)^2 - p_y^2}}\right) - \sin^{-1}\left(\frac{p_x(L)}{\sqrt{(1+\delta)^2 - p_y^2}}\right)\right) \tag{1.114}$$

1.10.5 Rectangular bend - straight body

Implemented in the <u>RBend</u> element.

Figure 1.3: Rectangular bend.

Xsuite supports rectangular bends with generic shifts and angles at the entrance and exit faces as shown in Fig. 1.3. In this section we report relations among the quantities defining the geometry of the magnet with respect to the reference trajectory.

The code takes as input the total bending angle α and the difference α_{diff} between the angles at entrance and exit of the reference trajectory with respect to the magnet axis:

$$\alpha = \alpha_{\text{in}} + \alpha_{\text{out}} \tag{1.115}$$

$$\alpha_{\text{diff}} = \alpha_{\text{out}} - \alpha_{\text{in}} \tag{1.116}$$

from which:

$$\alpha_{\text{in}} = \frac{\alpha - \alpha_{\text{diff}}}{2} \tag{1.117}$$

$$\alpha_{\text{out}} = \frac{\alpha + \alpha_{\text{diff}}}{2} \tag{1.118}$$

In the reference frame of the magnet body, for an on-momentum particle on the reference trajectory we can write:

$$p_{x,\text{in}} = \sin(\alpha_{\text{in}}) \tag{1.119}$$

$$p_{x,\text{out}} = -\sin(\alpha_{\text{out}}) \tag{1.120}$$

Using Eq. (1.110) we can write:

$$-\sin(\alpha_{\text{out}}) = \sin(\alpha_{\text{in}}) - hL_{\text{straight}} \tag{1.121}$$

from which we can obtain the curvature of the reference trajectory:

$$h = \frac{\sin(\alpha_{\text{in}}) + \sin(\alpha_{\text{out}})}{L_{\text{straight}}} \tag{1.122}$$

Using Eqs. (1.109) and (1.110) we can write:

$$p_{x,\text{mid}} = p_{x,\text{in}} - hL_{\text{straight}}/2 \tag{1.123}$$

$$p_{x,\text{mid}} = p_{x,\text{out}} + hL_{\text{straight}}/2 \tag{1.124}$$

$$x_{\text{in}} = x_{\text{mid}} - \frac{1}{h}\left(\sqrt{1 - p_{x,\text{mid}}^2} - \sqrt{1 - p_{x,\text{in}}^2}\right) \tag{1.125}$$

$$x_{\text{out}} = x_{\text{mid}} + \frac{1}{h}\left(\sqrt{1 - p_{x,\text{out}}^2} - \sqrt{1 - p_{x,\text{mid}}^2}\right) \tag{1.126}$$

Using Eq. (1.114) we can write:

$$L_{\text{curv}} = \frac{1}{h}\left(\sin^{-1}(p_{x,\text{out}}) - \sin^{-1}(p_{x,\text{in}})\right) = \frac{\alpha_{\text{in}} + \alpha_{\text{out}}}{h} = \frac{\alpha}{h} \tag{1.127}$$

In the special case of a sector bend ($\alpha_{\text{diff}} = 0$) we have, summing Eqs. (1.123) and (1.124):

$$\alpha_{\text{in}} = \alpha_{\text{out}} = \frac{\alpha}{2} \tag{1.128}$$

$$p_{x,\text{in}} = -p_{x,\text{out}} = \sin(\alpha/2) \tag{1.129}$$

$$p_{x,\text{mid}} = 0 \tag{1.130}$$

$$h = \frac{2\sin(\alpha/2)}{L_{\text{straight}}} \tag{1.131}$$

$$L_{\text{curv}} = \frac{\alpha}{h} = \frac{L_{\text{straight}}}{\text{sinc}(\alpha/2)} \tag{1.132}$$

$$x_{\text{in}} = x_{\text{out}} = x_{\text{mid}} - \frac{1}{h}\left(1 - \cos(\alpha/2)\right) \tag{1.133}$$

The last gives the usual equation for the sagitta of a bending magnet.

1.10.6 Expanded Bend-Quadrupole (also used for Quadrupole)

Implemented in the Bend, RBend and Quadrupole elements, for "mat-kick-mat" model.

This map is ported from MAD-X source code.

The following map is generated by the Hamiltonian:

$$H_M = \frac{p_\tau}{\beta_0} + \frac{1}{2}\frac{p_x^2 + p_y^2}{(1+\delta)} + (K_0 - h)x + \frac{K_0 h x^2}{2} + K_1\frac{x^2 - y^2}{2} \tag{1.134}$$

We consider a particle with initial canonical coordinates

$$(x, p_x, y, p_y, \zeta),$$

relative momentum deviation δ, velocity factor rvv $= v/c$, and charge/sign factor χ. The element has length L, curvature h, and (input) strengths K_0 and K_1.

Definitions

Define

$$\delta_+ \equiv 1 + \delta, \tag{1.135}$$

$$x' = \frac{p_x}{\delta_+}, \qquad y' = \frac{p_y}{\delta_+}. \tag{1.136}$$

We introduce the momentum-scaled (effective) strengths

$$\bar{K}_0 = \frac{\chi\, K_0}{\delta_+}, \qquad \bar{K}_1 = \frac{\chi\, K_1}{\delta_+}, \tag{1.137}$$

and the corresponding focusing coefficients

$$K_x = \bar{K}_0\, h + \bar{K}_1, \tag{1.138}$$

$$K_y = -\bar{K}_1. \tag{1.139}$$

Auxiliary quantities:

$$A = -K_x x - \bar{K}_0 + h, \tag{1.140}$$

$$B = x', \tag{1.141}$$

$$C = -K_y y, \tag{1.142}$$

$$D = y'. \tag{1.143}$$

Transport Functions

For an element of length L, define

$$(C_x, S_x) = \begin{cases} \left(\cos(\sqrt{K_x}L), \dfrac{\sin(\sqrt{K_x}L)}{\sqrt{K_x}} \right), & K_x > 0, \\[2ex] \left(\cosh(\sqrt{-K_x}L), \dfrac{\sinh(\sqrt{-K_x}L)}{\sqrt{-K_x}} \right), & K_x < 0, \\[2ex] (1,\, L), & K_x = 0, \end{cases}$$

$$(C_y, S_y) = \begin{cases} \left(\cos(\sqrt{K_y}L), \dfrac{\sin(\sqrt{K_y}L)}{\sqrt{K_y}} \right), & K_y > 0, \\[2ex] \left(\cosh(\sqrt{-K_y}L), \dfrac{\sinh(\sqrt{-K_y}L)}{\sqrt{-K_y}} \right), & K_y < 0, \\[2ex] (1,\, L), & K_y = 0. \end{cases}$$

Transverse Map

Positions

$$x_1 = xC_x + x'S_x + \begin{cases} \dfrac{(\bar{K}_0 - h)(C_x - 1)}{K_x}, & K_x \neq 0, \\[2ex] -\dfrac{1}{2}(\bar{K}_0 - h)L^2, & K_x = 0, \end{cases} \tag{1.144}$$

$$y_1 = yC_y + y'S_y. \tag{1.145}$$

Momenta

$$p_{x1} = \delta_+ \left(A S_x + B C_x \right),$$

(1.146)

$$p_{y1} = \delta_+ \left(C S_y + D C_y \right).$$

(1.147)

Path Length

Let L_{tot} be the total path length travelled by the particle through the element.

Horizontal contribution   For $K_x \neq 0$:

$$L_{\text{tot}} = L - \frac{h \left[(C_x - 1) x' + S_x A + L(\bar{K}_0 - h) \right]}{K_x}$$
$$+ \frac{1}{2} \left[-\frac{A^2 C_x S_x}{2 K_x} + \frac{B^2 C_x S_x}{2} + \frac{A^2 L}{2 K_x} + \frac{B^2 L}{2} \right.$$
$$\left. - \frac{A B C_x^2}{K_x} + \frac{A B}{K_x} \right].$$

(1.148)

For $K_x = 0$:

$$L_{\text{tot}} = L + \frac{hL}{6} \left(3 L x' + 6 x - (\bar{K}_0 - h) L^2 \right) + \frac{1}{2} B^2 L.$$

(1.149)

Vertical contribution   For $K_y \neq 0$:

$$L_{\text{tot}} \mathrel{+}= \frac{1}{2} \left[-\frac{C^2 C_y S_y}{2 K_y} + \frac{D^2 C_y S_y}{2} + \frac{C^2 L}{2 K_y} + \frac{D^2 L}{2} \right.$$
$$\left. - \frac{C D C_y^2}{K_y} + \frac{C D}{K_y} \right].$$

(1.150)

For $K_y = 0$:

$$L_{\text{tot}} \mathrel{+}= \frac{1}{2} D^2 L.$$

(1.151)

Longitudinal Map

The longitudinal coordinate update is

$$\Delta \zeta = L - \frac{L_{\text{tot}}}{\text{rvv}}.$$

(1.152)

Final Map

$$(x, p_x, y, p_y, \zeta) \longrightarrow (x_1, p_{x1}, y_1, p_{y1}, \zeta + \Delta \zeta), \qquad s \to s + L.$$

(1.153)

1.10.7   Thin bend

Implemented in the Multipole element.

In a curvilinear reference system with a constant curvature h in the horizontal plane a uniform magnetic field can be derived by the vector potential:

$$A_x = 0, \qquad A_y = 0, \qquad A_s = -B_y \left(x - \frac{hx^2}{2(1+hx)} \right).$$ (1.154)

With the following normalization $K_0 = \frac{q_0}{p} B_y$ is the inverse of the bending radius of the reference particle.

The exact and expanded Hamiltonian for a horizontal bending magnet is (eq. 2.12 in [5])

$$H = \frac{p_\tau}{\beta_0} - (1+hx)\sqrt{(1+\delta)^2 - p_x^2 - p_y^2} + \chi K_0 \left(x + \frac{hx^2}{2} \right)$$ (1.155)

$$\simeq \frac{p_\tau}{\beta_0} + \frac{1}{2}\frac{p_x^2 + p_y^2}{1+\delta} - (1+hx)(1+\delta) + \chi K_0 \left(x + \frac{hx^2}{2} \right)$$ (1.156)

The map for a thin dipole kick (horizontal or vertical) from the expanded Hamiltonian is (eq. 4.12 in [7]):

$$p_x \leftarrow p_x - \chi K_0 L + hL(1+\delta) - \chi K_0 hxL$$ (1.157)

$$\tau \leftarrow \tau - \frac{hx}{\beta} L.$$ (1.158)

1.10.8   Thin Multipole

Implemented in the Multipole element.

Multipolar components are defined according to the definition in Sec. 1.5.
A thin multipole models the effect of the field by taking the limit of the integration length going to zero while keeping constant the integrated strength. The Hamiltonian is:

$$H = \delta(s)\chi L \Re \left[\sum_{n=0}^{\infty} \frac{1}{(n+1)!}(K_n + i\hat{K}_n)(x + iy)^{n+1} \right].$$ (1.159)

The corresponding map is:

$$p_x \leftarrow p_x - \chi L \cdot \Re \left[\sum_{n=0}^{\infty} \frac{1}{n!}(K_n + i\hat{K}_n)(x + iy)^n \right],$$ (1.160)

$$p_y \leftarrow p_y + \chi L \cdot \Im \left[\sum_{n=0}^{\infty} \frac{1}{n!}(K_n + i\hat{K}_n)(x + iy)^n \right],$$ (1.161)

where L is the length of the modelled multipole element.
The other coordinates (x, y, δ, ζ) remain unchanged.

1.10.9 Dipole fringe field

The dipole fringe field map used in Xsuite is based on [16]. Additional information can be found in [17, 18].

The implemented map is the following:

$$p_s = \sqrt{(1+\delta)^2 - p_x^2 - p_y^2}$$

$$x_f = x + \frac{1}{2}\frac{\partial \psi}{\partial p_x} y_f^2$$

$$p_{x,f} = p_x$$

$$y_f = \frac{2y}{1 + \sqrt{1 - 2\frac{\partial \psi}{\partial p_y}y}}$$

$$p_{y,f} = p_y - \psi y_f - \frac{K_0^2}{9Fg(1+\delta)}y_f^3$$

$$\ell_f = \ell - \frac{1}{2}\frac{\partial \psi}{\partial \delta} y_f^2$$

$$\delta_f = \delta$$

with:

$$\psi = K_0 \tan\left[\arctan\left(\frac{x'}{1+y'^2}\right) - gK_0 F\left(1 + \frac{p_x^2}{p_s^2}\left(2 + \frac{p_y^2}{p_s^2}\right)\right)p_s\right] \qquad (1.162)$$

where K_0 is the normalized magnetic field, g is the magnet gap and F is the fringe field integral:

$$F = \int_{-\infty}^{+\infty} \frac{b(s)\left(K_0 - b(s)\right)}{gK_0^2}\, ds \qquad (1.163)$$

1.10.10   Dipole wedge

The following map is used to move the observation plane by an angle θ around the y axis in a uniform dipole field [11]:

$$x(\theta) = x\cos\theta + \frac{xp_x\sin(2\theta) + \sin^2\theta\left(2x\sqrt{(1+\delta)^2 - p_x^2 - p_y^2} - K_0 x^2\right)}{\sqrt{(1+\delta)^2 - p_x(\theta)^2 - p_y^2} + \sqrt{(1+\delta)^2 - p_x^2 - p_y^2}\cos\theta - p_x\sin\theta}$$

(1.164)

$$p_x(\theta) = p_x\cos\theta + \left(\sqrt{(1+\delta)^2 - p_x^2 - p_y^2} - K_0 x\right)\sin\theta \tag{1.165}$$

$$y(\theta) = y + \frac{p_y}{K_0}\theta + \frac{p_y}{K_0}\left(\sin^{-1}\left(\frac{p_x}{\sqrt{(1+\delta)^2 - p_y^2}}\right) - \sin^{-1}\left(\frac{p_x(\theta)}{\sqrt{(1+\delta)^2 - p_y^2}}\right)\right)$$

(1.166)

$$p_y(\theta) = p_y \tag{1.167}$$

$$\delta(\theta) = \delta \tag{1.168}$$

$$\ell(\theta) = \ell + \frac{(1+\delta)}{K_0}\theta + \frac{(1+\delta)}{K_0}\left(\sin^{-1}\left(\frac{p_x}{\sqrt{(1+\delta)^2 - p_y^2}}\right) - \sin^{-1}\left(\frac{p_x(\theta)}{\sqrt{(1+\delta)^2 - p_y^2}}\right)\right)$$

(1.169)

where K_0 is the normalized magnetic field.

1.10.11   Multipole fringe field

The fringe field effect for multipole magnets is implemented as described in [11]. We introduce the following auxiliary quantities:

$$f_{\pm} \approx \mp\Re\frac{c_n(x+iy)^n}{4(n+1)(1+\delta)}\left\{xp_x + yp_y + i\frac{n+2}{n}(xp_y - yp_x)\right\} \tag{1.170}$$

$$= \frac{p_x f^x + p_y f^y}{1+\delta}.$$

where $c_n = K_n + i\hat{K}_n$ is the complex multipole strength (see Sec. 1.5).
The functions f^x and f^y depend on position only. The characteristic function is chosen so as to depend on the final momenta:

$$S(\mathbf{x}, \mathbf{p}^f) = \mathbf{x}\cdot\mathbf{p}^f - \frac{p_x^f f^x + p_y^f f^y}{1+\delta}. \tag{1.171}$$

The following implicit solution is found:

$$x^f = x - \frac{f^x}{1+\delta} \tag{1.172a}$$

$$p_x = p_x^f - \frac{p_x^f(\partial_x f^x) + p_y^f(\partial_x f^y)}{1+\delta} \tag{1.172b}$$

$$y^f = y - \frac{f^y}{1+\delta} \tag{1.172c}$$

$$p_y = p_y^f - \frac{p_x^f(\partial_y f^x) + p_y^f(\partial_y f^y)}{1+\delta} \tag{1.172d}$$

$$\delta^f = \delta \tag{1.172e}$$

$$\ell = \ell^f + \frac{p_x^f f^x + p_y^f f^y}{(1+\delta)^2}. \tag{1.172f}$$

It is solved by inverting Eqs. (1.172b) and (1.172d) simultaneously to obtain the final transverse momenta.

1.10.12 Quadrupolar correction for wedge and Y rotation

If a dipole wedge or rotation around the y axis in a field-free region takes place in the presence of a quadrupole field, the following correction is applied to the transverse momenta:

$$p_x^f = p_x - K_1 x^2 \theta + K_1 \frac{y^2}{2}\theta \tag{1.173}$$

$$p_y^f = p_y + K_1 xy\theta \tag{1.174}$$

This correction is a perturbation of the wedge or Y rotation, and can in theory be applied using any integration scheme. It is currently implemented as a kick-drift approximation.

Derivation

(derived by S. Van der Schueren based on the MAD-X/PTC [1] source code)
In a curved reference frame (dropping terms of order $\mathcal{O}(y^4)$):

$$H_\tau = \frac{p_\tau}{\beta_0} - (1+hx)\left(\sqrt{(1+\delta)^2 - p_x^2 - p_y^2} - \frac{x + \frac{h}{2}x^2}{1+hx}K_0 + K_1\frac{y^2}{2} - \frac{K_1 h x^3}{3} + \frac{K_1 x^2}{2(hx+1)}\right) \tag{1.175}$$

which we can split in perturbation theory in a drift-like part H_0 and a kick-like part H_1:

$$H_0 = \frac{p_\tau}{\beta_0} - (1+hx)\sqrt{(1+\delta)^2 - p_x^2 - p_y^2} + \left(x + \frac{h}{2}x^2\right)K_0 \tag{1.176}$$

$$H_1 = -(1+hx)K_1\frac{y^2}{2} + \left(K_1 h\frac{x^3}{3} + K_1\frac{x^2}{2}\right) \tag{1.177}$$

The Hamiltonian H_0 leads to the dipole wedge 1.10.10 (or a dynamical rotation 1.10.19.2 if $b_0 = 0$) when taking the limit $1/h \to 0$, $s \to 0$, $sh \to \theta$. The Hamiltonian H_1 has equations of motion:

$$p'_x = -\frac{\partial H_1}{\partial x} = hK_1\frac{y^2}{2} - hK_1x^2 - K_1x \tag{1.178}$$

$$p'_y = -\frac{\partial H_1}{\partial y} = (1 + hx)K_1y \tag{1.179}$$

which gives integrated equations:

$$p_x(s) = p_x + hK_1\frac{y^2}{2}s - hK_1x^2s - K_1xs \tag{1.180}$$

$$p_y(s) = p_y + (1 + hx)K_1ys \tag{1.181}$$

Taking the limit to $1/h \to 0$, $s \to 0$, $sh \to \theta$ as for the dipole wedge we find the expressions for the quadrupole wedge.

1.10.13   Accelerating Cavity

Implemented in the Cavity element.

The approximated energy gain of a particle passing through an electric field of frequency $f = \frac{kc}{2\pi}$ for which:

$$V \sin(\phi - k\tau) = \int_{-l/2}^{l/2} E_s(0,0,t,s) \, \mathrm{d}s. \tag{1.182}$$

An equivalent vector potential can be derived and normalized as

$$A_s = -\frac{V}{\omega}\cos(\phi - k\tau) \qquad\qquad V_n = \frac{q_0}{P_0 c}V \tag{1.183}$$

from which one can derive the following map

$$p_\tau \leftarrow p_\tau + \chi V_n \sin(\phi - k\tau). \tag{1.184}$$

1.10.14   RF-Multipole

Implemented in the RFMultipole and Crab Cavity elements.

The RF-multipole generalizes the interaction of a particle with an electromagnetic field by assuming that

$$\Delta E(x,y,\tau) = q \int_{-L/2}^{L/2} E_z(x,y,t) \, \mathrm{d}s \tag{1.185}$$

$$\Delta P_x(x,y,\tau) = q \int_{-L/2}^{L/2} E_x(x,y,t) + \beta c B_y(x,y,t) \, \mathrm{d}s \tag{1.186}$$

$$\Delta P_y(x,y,\tau) = q \int_{-L/2}^{L/2} E_y(x,y,t) - \beta c B_x(x,y,t) \, \mathrm{d}s. \tag{1.187}$$

are harmonic in x, y and periodic in τ of frequency $f = \frac{k}{2\pi c}$ such that:

$$a_s(x, y, \tau) = \Re \left[\sum_{n=1}^{N} \left(k_n \cos(\phi_n - k\tau) + i\hat{k}_n \cos(\hat{\phi}_n - k\tau) \right) (x + iy)^n \right], \qquad (1.188)$$

The map then follows:

$$\Delta p_x = -\sum_{n=1}^{N} \frac{\chi}{n!} \Re \left[(k_n C_n + i\hat{k}_n \hat{C}_n)(x + iy)^{(n-1)} \right], \qquad (1.189)$$

$$\Delta p_y = \sum_{n=1}^{N} \frac{\chi}{n!} \Im \left[(k_n C_n + i\hat{k}_n \hat{C}_n)(x + iy)^{(n-1)} \right], \qquad (1.190)$$

$$\Delta p_\tau = -\chi k \sum_{n=1}^{N} \Re \left[(k_n S_n + i k_n \hat{S}_n)(x + iy)^n \right], \qquad (1.191)$$

where

$$C_n = \cos(\phi_n - \omega \Delta t) \qquad\qquad \hat{C}_n = \cos(\hat{\phi}_n - \omega \Delta t) \qquad (1.192)$$
$$S_n = \sin(\phi_n - \omega \Delta t) \qquad\qquad \hat{S}_n = \sin(\hat{\phi}_n - \omega \Delta t). \qquad (1.193)$$

1.10.15 Solenoid

Implemented in the UniformSolenoid and VariableSolenoid elements.

The derivation largely follows one by Forest [11], while the final map can be verified to be the same as the one by Wolski [12].
We can write the Hamiltonian for the solenoid as follows:

$$H = p_\zeta - \sqrt{(1 + \delta)^2 - \left(p_x + \frac{b_z}{2} y \right)^2 - \left(p_y - \frac{b_z}{2} x \right)^2} \qquad (1.194)$$

where we have defined the normalized quantities $b_z = B_z \frac{q_0}{P_0}$, $a_x = A_x \frac{q_0}{P_0}$, $a_y = A_y \frac{q_0}{P_0}$. This can be obtained knowing the general Hamiltonian

$$H = p_\zeta - \sqrt{(1 + \delta)^2 - (p_x - a_x)^2 - (p_y - a_y)^2} - a_z, \qquad (1.195)$$

we can extract the magnetic field potential and convince ourselves that H describes a magnetic field with only the longitudinal component equal to B_z, as expected of a solenoid:

$$\mathbf{A} = \begin{bmatrix} A_x \\ A_y \\ A_z \end{bmatrix} = \begin{bmatrix} -\frac{B_z}{2} y \\ \frac{B_z}{2} x \\ 0 \end{bmatrix} \implies \mathbf{B} = \nabla \times \mathbf{A} = \begin{bmatrix} \frac{\partial A_z}{\partial y} - \frac{\partial A_y}{\partial z} \\ \frac{\partial A_x}{\partial z} - \frac{\partial A_z}{\partial x} \\ \frac{\partial A_y}{\partial x} - \frac{\partial A_x}{\partial y} \end{bmatrix} = \begin{bmatrix} 0 \\ 0 \\ B_z \end{bmatrix}. \qquad (1.196)$$

The Hamiltonian H can be simplified, by applying the following transformation, which should be understood as the change of reference from the general coordinate system $\mathbf{X}$ to a new $\mathbf{X}_{\text{new}}$:

$$
T := \begin{bmatrix}
-\frac{1}{2} & 0 & 0 & \frac{1}{b_z} \\
0 & 1 & \frac{1}{2}b_z & 0 \\
-\frac{1}{2} & 0 & 0 & -\frac{1}{b_z} \\
0 & 1 & -\frac{1}{2}b_z & 0
\end{bmatrix}.
$$

In particular, note that if

$$
\mathbf{X} = \begin{bmatrix} x \\ p_x \\ y \\ p_y \end{bmatrix} = T^{-1}\mathbf{X}_{\text{new}} = \begin{bmatrix}
-x_{\text{new}} - y_{\text{new}} \\
\frac{1}{2}(p_{x,\text{new}} + p_{y,\text{new}}) \\
\frac{1}{b_z}(p_{x,\text{new}} - p_{y,\text{new}}) \\
\frac{b_z}{2}(x_{\text{new}} - y_{\text{new}})
\end{bmatrix},
$$

then we can rewrite H in terms of $\mathbf{X}_{\text{new}}$ (dropping the 'new' suffix, while keeping it in mind) as

$$
K := -\sqrt{(1+\delta)^2 - p_x^2 - b_z^2 x^2}.
$$

We can simplify H even further, rewriting it in terms of the following action-angle variables:

$$
x := \sqrt{\frac{2J}{|b_z|}}\cos(\phi) \quad \text{and} \quad p_x := \sqrt{2|b_z|J}\sin(\phi). \tag{1.197}
$$

The new Hamiltonian with respect to J is the following:

$$
K = -\sqrt{(1+\delta)^2 - p_x^2 - b_z^2 x^2} =
$$

$$
-\sqrt{(1+\delta)^2 - \left(\sqrt{2|b_z|J}\sin(\phi)\right)^2 - b_z^2\sqrt{\frac{2J}{|b_z|}}\cos(\phi)^2} =
$$

$$
-\sqrt{(1+\delta)^2 - \left(\sqrt{2|b_z|J}\sin(\phi)\right)^2 - \left(\sqrt{2|b_z|J}\cos(\phi)\right)^2} =
$$

$$
-\sqrt{(1+\delta)^2 - 2|b_z|J}.
$$

Then, using Hamilton's equations, we can solve for ϕ:

$$
\frac{d\phi}{dz} = \frac{\partial K}{\partial J} \implies \phi(z) = \phi(0) + z\frac{\partial K}{\partial J} = \phi(0) - z\frac{|b_z|}{K}.
$$

Let $\omega := -b_z/K$. Keeping in mind that we are still in the realm of $\mathbf{X}_{\text{new}}$, we can compute x_{new} and y_{new} substituting the above into (1.197). Note that we can drop

the modulus on b_z in both ω and the equations below, as cos is an even function, and while sin is an odd function and the signs of $\sin(\omega z)$ and b_z will cancel out anyway.

$$x = \sqrt{\frac{2J}{|b_z|}} \cos\left(\phi(0) + \left(-z\frac{|b_z|}{K}\right)\right) =$$

$$\sqrt{\frac{2J}{|b_z|}} \cos\phi(0)\cos(\omega z) - \frac{\sqrt{2J|b_z|}}{|b_z|}\sin\phi(0)\sin\left(-z\frac{|b_z|}{K}\right) =$$

$$x_0\cos(\omega z) - \frac{p_{x,0}}{b_z}\sin(\omega z)$$

$$p_x = \sqrt{2|b_z|J}\sin\left(\phi(0) + \left(-z\frac{|b_z|}{K}\right)\right) =$$

$$\sqrt{2|b_z|J}\sin\phi(0)\cos(\omega z) + |b_z|\sqrt{\frac{2J}{|b_z|}}\cos\phi(0)\sin\left(-z\frac{|b_z|}{K}\right) =$$

$$p_{x,0}\cos(\omega z) + b_z x_0 \sin(\omega z)$$

These equations give us the map for the solenoid in $\mathbf{X}_{\text{new}}$. We can write this transformation in the form of a matrix

$$R := \begin{bmatrix} \cos(\omega z) & -\frac{\sin(\omega z)}{b_z} & 0 & 0 \\ b_z\sin(\omega z) & \cos(\omega z) & 0 & 0 \\ 0 & 0 & 1 & 0 \\ 0 & 0 & 0 & 1 \end{bmatrix},$$

and therefore the whole solenoid map in $\mathbf{X}$ as follows (let $S := \sin(\omega z)$ and $C := \cos(\omega z)$):

$$M := T^{-1}RT = \begin{bmatrix} \frac{C+1}{2} & \frac{S}{b_z} & \frac{S}{2} & \frac{1-C}{b_z} \\ -\frac{b_z S}{4} & \frac{C+1}{2} & \frac{b_z(C-1)}{4} & \frac{S}{2} \\ -\frac{S}{2} & \frac{C-1}{b_z} & \frac{C+1}{2} & \frac{S}{b_z} \\ \frac{b_z(1-C)}{4} & -\frac{S}{2} & -\frac{b_z S}{4} & \frac{C+1}{2} \end{bmatrix}$$

In the tracking procedure of Xtrack (and MAD-X) the map is implemented with respect to a different quantity sk, which we will denote with k, and which represents half of magnetic field strength b_z: $k = \frac{b_z}{2}$. Let $s := \sin(\frac{zk}{H}) = \sin(\frac{\omega z}{2})$ and $c := \cos(\frac{\omega z}{2})$; then we can rewrite M using the trigonometric identities:

$$\cos(2\theta) = 2\cos^2\theta - 1 = 1 - 2\sin^2\theta \implies c^2 = \frac{C+1}{2} \text{ and } s^2 = \frac{1-C}{2},$$

$$\sin(2\theta) = 2\cos\theta\sin\theta \implies sc = \frac{S}{2},$$

as the following transfer matrix

$$M = \begin{bmatrix} c^2 & \frac{cs}{k} & cs & \frac{s^2}{k} \\ -kcs & c^2 & -ks^2 & cs \\ -cs & -\frac{s^2}{k} & c^2 & \frac{cs}{k} \\ ks^2 & -cs & -kcs & c^2 \end{bmatrix},$$

which, with relatively little effort, can be verified to correspond to the implementation of the tracking procedure. We have the following map (note the change in ζ is analogous to the drift):

$$x \leftarrow (x\cos(\theta) + y\sin(\theta))\cos(\theta) + \frac{2}{b_z}(p_x\cos(\theta) + p_y\sin(\theta))\sin(\theta)$$

$$p_x \leftarrow -\frac{1}{2}(x\cos(\theta) + y\sin(\theta))b_z\sin(\theta) + (p_x\cos(\theta) + p_y\sin(\theta))\cos(\theta)$$

$$y \leftarrow (y\cos(\theta) - x\sin(\theta))\cos(\theta) + \frac{2}{b_z}(p_y\cos(\theta) - p_x\sin(\theta))\sin(\theta)$$

$$p_y \leftarrow -\frac{1}{2}(y\cos(\theta) - x\sin(\theta))b_z\sin(\theta) + (p_y\cos(\theta) - p_x\sin(\theta))\cos(\theta)$$

$$\zeta \leftarrow \zeta + L\left(1 - \frac{\beta_0}{\beta}\frac{1+\delta}{p_z}\right),$$

where $p_z := \sqrt{(\delta+1)^2 - \left(\frac{b_z}{2}x - p_y\right)^2 - \left(\frac{b_z}{2}y + p_x\right)^2}$, $\theta := \frac{b_z L}{2p_z}$, and L is the length of the thick solenoid.

1.10.15.1   Tilted solenoid

From solenoid frame (x'-z') to beam frame (x-z) we have the following transformation:

$$x = x'\cos\theta - z'\sin\theta \tag{1.198}$$
$$z = x'\sin\theta + z'\cos\theta \tag{1.199}$$

The inverse transformation is:

$$x' = x\cos\theta + z\sin\theta \tag{1.200}$$
$$z' = -x\sin\theta + z\cos\theta \tag{1.201}$$

We write the potential for solenoid with longitudinal field dependent on z:

$$A_{x'} = -\frac{B_A(z')}{2}y' \tag{1.202}$$

$$A_{y'} = \frac{B_A(z')}{2}x' \tag{1.203}$$

$$A_{z'} = 0 \tag{1.204}$$

We compute the components in the beam frame:

$$A_x = \cos\theta \cdot A_{x'} - \sin\theta \cdot A_{z'} \tag{1.205}$$

$$A_y = A_{y'} \tag{1.206}$$

$$A_z = \sin\theta \cdot A_{x'} + \cos\theta \cdot A_{z'} \tag{1.207}$$

Replacing the coordinates x', y', z' and using the notation abuse $B_A(z) = B_A(z\,/\cos\theta)$, we obtain:

$$A_x = -\frac{B_A(z)}{2}\, y \cos\theta \tag{1.208}$$

$$A_y = \frac{B_A(z)}{2}\, x \cos\theta + \frac{B_A(z)}{2}\, z \sin\theta \tag{1.209}$$

$$A_z = -\frac{B_A(z)}{2}\, y \sin\theta \tag{1.210}$$

I do a change of gauge:

$$\mathbf{A}_{\text{new}} = \mathbf{A} + \nabla f \tag{1.211}$$

with:

$$f = -\frac{B_A(z)}{2}\, yz \sin\theta \tag{1.212}$$

obtaining:

$$A_x = -\frac{B_A(z)}{2}\, y \cos\theta \tag{1.213}$$

$$A_y = \frac{B_A(z)}{2}\, x \cos\theta \tag{1.214}$$

$$A_z = -B_A(z)\, y \sin\theta - \frac{1}{2}\frac{dB_A}{dz}\, zy \sin\theta \tag{1.215}$$

From this we compute the field $\mathbf{B} = \nabla \times \mathbf{A}$:

$$B_x(x,y,z) = -\frac{1}{2}\frac{dB_A}{dz}\, x\cos\theta - B_A(z)\sin\theta - \frac{1}{2}\frac{dB_A}{dz}\, z\sin\theta \tag{1.216}$$

$$B_y(x,y,z) = -\frac{1}{2}\frac{dB_A}{dz}\, y\cos\theta \tag{1.217}$$

$$B_z(x,y,z) = B_A(z)\cos\theta \tag{1.218}$$

We call

$$\boxed{B_{x0}(z) = B_x(0,0,z) = -B_A(z)\sin\theta - \frac{1}{2}\frac{dB_A}{dz}\, z\sin\theta} \tag{1.219}$$

$$\boxed{B_{z0}(z) = B_z(0,0,z) = B_A(z)\cos\theta} \tag{1.220}$$

We can use the above to express the field:

$$\boxed{B_x(x,y,z) = -\frac{1}{2}\frac{dB_{z0}}{dz}\, x + B_{x0}(z)} \tag{1.221}$$

$$\boxed{B_y(x,y,z) = -\frac{1}{2}\frac{dB_{z0}}{dz}\, y} \tag{1.222}$$

$$\boxed{B_z(x,y,z) = B_{z0}(z)} \tag{1.223}$$

and to express the vector potential:

$$A_x = -\frac{B_{z0}(z)}{2} y \qquad (1.224)$$

$$A_y = \frac{B_{z0}(z)}{2} x \qquad (1.225)$$

$$A_z = B_{x0}(z)y \qquad (1.226)$$

1.10.15.2   Generalization to arbitrary tilt and dipolar components

If the tilt is not in the $x - z$ plane, and if additional dipolar components are present, we can generalize the above obtaining the following vector potential:

$$A_x = -\frac{B_{z0}(z)}{2} y \qquad (1.227)$$

$$A_y = \frac{B_{z0}(z)}{2} x \qquad (1.228)$$

$$A_z = B_{x0}(z)y - B_{y0}(z)x \qquad (1.229)$$

The corresponding magnetic field is:

$$B_x(x,y,z) = -\frac{1}{2}\frac{dB_{z0}}{dz} x + B_{x0}(z) \qquad (1.230)$$

$$B_y(x,y,z) = -\frac{1}{2}\frac{dB_{z0}}{dz} y + B_{y0}(z) \qquad (1.231)$$

$$B_z(x,y,z) = B_{z0}(z) \qquad (1.232)$$

1.10.16   Wire

Implemented in the <u>Wire element</u>.

For each part we define $p_z = \sqrt{(1+\delta)^2 - x'^2 - y'^2}$, using the current values for x' and y'.

Step 1. Initial backwards drift of length $L = \frac{embl}{2}$.

$$x \to x - L \cdot \frac{x'}{p_z}$$

$$y \to y - L \cdot \frac{y'}{p_z}$$

Step 2.

$$y \to y - \frac{x \cdot \sin(t_x)}{\cos\left(\arctan\left(\frac{x'}{p_z}\right) - t_x\right)} \cdot \frac{y'}{\sqrt{(1+\delta)^2 - y'^2}}$$

$$x \to x \cdot \left[\cos(t_x) - \sin(t_x) \cdot \tan\left(\arctan\left(\frac{x'}{p_z}\right) - t_x\right)\right]$$

$$x' \to \sqrt{(1+\delta)^2 - y'^2} \cdot \sin\left(\arctan\left(\frac{x'}{p_z}\right) - t_x\right)$$

$$x \to x - \frac{y \cdot \sin(t_y)}{\cos\left(\arctan\left(\frac{y'}{p_z}\right) - t_y\right)} \cdot \frac{x'}{\sqrt{(1+\delta)^2 - x'^2}}$$

$$y \to y\left[\cos(t_y) - \sin(t_y) \cdot \tan\left(\arctan\left(\frac{y'}{p_z}\right) - t_y\right)\right]$$

$$y' \to \sqrt{(1+\delta)^2 - x'^2}\sin\left(\arctan\left(\frac{y'}{p_z}\right) - t_y\right)$$

Step 3. Drift part of length $L = lin$.

$$x \to x + L \cdot \frac{x'}{p_z}$$

$$y \to y + L \cdot \frac{y'}{p_z}$$

Step 4. Here $x_i = x - r_x$ and $y = y - r_y$.

$$x' \to x' - \frac{\frac{cur \cdot 10^{-7}}{chi} \cdot x_i}{x_i^2 + y_i^2}\left[\sqrt{(lin+l)^2 + x_i^2 + y_i^2} - \sqrt{(lin-l)^2 + x_i^2 + y_i^2}\right]$$

$$y' \to y' - \frac{\frac{cur \cdot 10^{-7}}{chi} \cdot y_i}{x_i^2 + y_i^2}\left[\sqrt{(lin+l)^2 + x_i^2 + y_i^2} - \sqrt{(lin-l)^2 + x_i^2 + y_i^2}\right]$$

Step 5. Drift of length $L = leff - lin$.

$$x \to x + L\frac{x'}{p_z}$$

$$y \to y + L\frac{y'}{p_z}$$

Step 6.

$$x \to x - \frac{y \cdot \sin(-t_y)}{\cos\left(\arctan\left(\frac{y'}{p_z}\right) + t_y\right)} \cdot \frac{x'}{\sqrt{(1+\delta)^2 - x'^2}}$$

$$y \to y \cdot \left[\cos(-t_y) - \sin(-t_y) \cdot \tan\left(\arctan\left(\frac{y'}{p_z}\right) + t_y\right)\right]$$

$$y' \to \sqrt{(1+\delta)^2 - x'^2} \cdot \sin\left(\arctan\left(\frac{y'}{p_z}\right) + t_y\right)$$

$$y \to y - \frac{x \cdot \sin(-t_x)}{\cos\left(\arctan\left(\frac{x'}{p_z}\right) + t_x\right)} \cdot \frac{y'}{\sqrt{(1+\delta)^2 - y'^2}}$$

$$x \to x \left[\cos(-t_x) - \sin(-t_x) \cdot \tan\left(\arctan\left(\frac{x'}{p_z}\right) + t_x\right)\right]$$

$$x' \to \sqrt{(1+\delta)^2 - y'^2} \cdot \sin\left(\arctan\left(\frac{x'}{p_z}\right) + t_x\right)$$

Step 7. Shift.

$$x \to x + embl \cdot \tan(t_x)$$

$$y \to y + embl \cdot \frac{\tan(t_y)}{\cos(t_x)}$$

Step 8. Negative drift of length $L = \frac{embl}{2}$.

$$x \to x - L \cdot \frac{x'}{p_z}$$

$$y \to y - L \cdot \frac{y'}{p_z}$$

1.10.17   Electron Lens

Implemented in the Elens element.

1.10.17.1   Hollow electron lens - uniform annular profile

For a uniform distribution of the electron beam between R_1 and R_2, the radial kick can be described by a shape function $f(r)$ and a maximum kick strength θ_{max}:

$$\theta(r) = \frac{f(r)}{(r/R_2)} \cdot \theta_{max} \tag{1.233}$$

with $r = \sqrt{x^2 + y^2}$ and θ_{max} independent of r. The shape function $f(r)$ is defined as

$$f(r) = \frac{I(r)}{I_T} = \frac{2\pi}{I_T} \int_0^r r\rho(r)dr \tag{1.234}$$

where I_T is the total electron beam current, $I(r)$ is the current enclosed in a radius r and $\rho(r)$ is the electron beam density distribution.

For a uniform profile one then obtains:

$$
\begin{cases}
0 & , \quad r < R_1 \\
\frac{r^2 - R_1^2}{R_2^2 - R_1^2} & , \quad R_1 \leq r < R_2 \\
1 & , \quad R_2 \leq r
\end{cases}
\tag{1.235}
$$

and

$$
\theta_{\max} = \theta(R_2) = \frac{2LI_T(1 \pm \beta_e \beta_p)}{4\pi\epsilon_0 \, (B\rho)_p \, \beta_e \beta_p c^2} \cdot \frac{1}{R_2}
\tag{1.236}
$$

where L is the length of the e-lens, I_T the total electron beam current, $\beta_{e/p}$ the relativistic β of electron/proton beam, $B\rho$ the magnetic rigidity, c the speed of light and ϵ_0 the vacuum permittivity. The $\pm$-sign represents the two cases of the electron beam traveling in the direction of the proton beam $(+)$ or in the opposite direction $(-)$. For hollow electron beam collimation, electron and proton beam travel in the same direction.

The kick in (x', y') can then be expressed as (note $\frac{x}{r} = \cos(\phi)$, $\frac{y}{r} = \sin(\phi)$):

$$
x' = x' - \theta_{\max} \cdot \frac{r_2}{r^2} \cdot f(r) \cdot x
\tag{1.237}
$$

$$
y' = y' - \theta_{\max} \cdot \frac{r_2}{r^2} \cdot f(r) \cdot y
\tag{1.238}
$$

If the electron lens is offset by $(x_{\text{offset}}, y_{\text{offset}})$, the coordinates (x, y) are simply transferred to:

$$
\tilde{x} = x + x_{\text{offset}}
\tag{1.239}
$$

$$
\tilde{y} = y + y_{\text{offset}}
\tag{1.240}
$$

$$
\tilde{r} = \sqrt{\tilde{x}^2 + \tilde{y}^2}
\tag{1.241}
$$

and the kick is then given by:

$$
x' = x' - \theta_{\max} \cdot \frac{r_2}{\tilde{r}^2} \cdot f(\tilde{r}) \cdot \tilde{x}
\tag{1.242}
$$

$$
y' = y' - \theta_{\max} \cdot \frac{r_2}{\tilde{r}^2} \cdot f(\tilde{r}) \cdot \tilde{y}
\tag{1.243}
$$

1.10.18   Electron Cooler

Implemented in the ElectronCooler element.

The Parkhomchuk electron cooler in Xsuite applies a kick to the circulating ion based on the following equation:

$$
\mathbf{F} = -\frac{n_e q^2 e^4}{4\pi^2 \epsilon_0^2 m_e} \cdot \frac{d\mathbf{V}}{V_{\text{tot}}^3} \ln\left(\frac{\rho_{\max} + \rho_{\min} + \rho_L}{\rho_{\min} + \rho_L}\right),
\tag{1.244}
$$

Where **F** is the friction force acting on the circulating particle, n_e is the electron density (per unit volume), q is the charge of the circulating particle, e is the elementary charge, m_e is the electron mass, $d\mathbf{V}$ is the velocity difference between the circulating particle and the local electron velocity. $\rho_{\max}$ and $\rho_{\min}$ are the maximum and minimum impact parameters, respectively, and ρ_{L} is Larmor radius of the electrons (also known as the radius of gyration). V_{tot} represents the total velocity difference between the electrons and ion, which is given by:

$$V_{\mathrm{tot}} = \sqrt{dV^2 + \Delta_{\parallel}^2 + \Delta_{\mathrm{magnet}}^2}, \tag{1.245}$$

Where $dV^2 = dV_x^2 + dV_y^2 + dV_z^2$ is the squared norm of the relative velocity difference between the ion and electron. To prevent the cooling force from diverging as $dV \to 0$, regularization terms are added. The most logical approach is to add the temperatures as regularization terms because they provide the RMS velocity difference when $dV = 0$. This is why $\Delta_{\parallel}$ the longitudinal electron velocity spread associated with their temperature is added to Equation (1.245). Lastly, Δ_{magnet} is the additional velocity spread induced by imperfections in the magnetic field of the electron cooler solenoid, which is given by:

$$\Delta_{\mathrm{magnet}} = c\gamma \frac{B_{\perp}}{B_{\parallel}} \tag{1.246}$$

Where $\frac{B_{\perp}}{B_{\parallel}}$ is the ratio of the transverse component of the magnetic field with respect to the longitudinal component. The transverse temperature is not included in Equation (1.245) because it is suppressed due to the gyration motion of the electrons in the magnetic field. The transverse temperature indirectly plays a role in the Parkhomchuk model via the Larmor radius ρ_{L}, which is given by:

$$\rho_{\mathrm{L}} = \frac{m_e \Delta_{\perp}}{eB} \tag{1.247}$$

Where $\Delta_{\perp}$ is the transverse velocity due to the transverse electron temperature and B is the magnetic field. The minimum impact parameter $\rho_{\min}$ is given by:

$$\rho_{\min} = \frac{Ze^2}{4\pi\varepsilon_0 m_e \mathbf{V}^2} \tag{1.248}$$

The maximum impact parameter determines the maximum length scale at which a Coulomb interaction takes place, which can be limited by various physical effects, such as the Debye length and it is given by:

$$\rho_d = \frac{\Delta_{\parallel}}{\omega_p}, \tag{1.249}$$

Where the longitudinal velocity spread of the electrons $\Delta_{\parallel}$ is given by:

$$\Delta_{\parallel} = \sqrt{\frac{k_B T}{m_e}} \tag{1.250}$$

The plasma frequency ω_{p} represents the natural oscillation frequency of the electron due to a perturbation in its charge distribution, which is given by:

$$\omega_{\mathrm{p}} = \sqrt{\frac{n_e e^2}{m_e \epsilon_0}}. \tag{1.251}$$

The Debye radius is not the only limitation for the maximum interaction length. In the case where the velocity difference between the ion and electron $d\mathbf{V}$ is sufficiently larger than the velocity spread of the electron $\Delta_{\parallel}$, then the maximum shielding radius ρ_{s} is given by:

$$\rho_{\mathrm{s}} = \frac{d\mathbf{V}}{\omega_p}. \tag{1.252}$$

In principle, it is necessary to compute both ρ_{d} and ρ_{s} and compare them to see which one is the bottleneck and use that as the maximum impact parameter, which is given by:

$$\rho_{\max} = \min(\rho_{\mathrm{d}}, \rho_{\mathrm{s}})$$

However, in the code, the two shielding impact parameters are merged into a single effective impact parameter, given by:

$$\rho_{\mathrm{shield}} = \frac{V_{\mathrm{tot}}}{\omega_p}. \tag{1.253}$$

Here, V_{tot} is the total velocity difference between the electron and ion from Equation 1.245. Combining these effects in one term ensures that the shielding parameter reflects the combined influence of the ion's motion and the internal velocity distribution of the electron beam, which is affected by the temperature of the electrons as well as the imperfections in the magnetic field. An advantage of this formulation is that it ensures that the impact parameter varies smoothly as a function of the relative ion velocity $d\mathbf{V}$, which changes continuously throughout the cooling process. By using the combined expression for ρ_{shield} from Equation (1.253), the code avoids any abrupt changes in the friction force that could arise from sharp transitions in the shielding distance.

In addition to ρ_{shield}, the maximum impact parameter can also be limited by the distance an ion travels inside the electron cooler. This distance-based limit is expressed as:

$$\rho_{\mathrm{interaction}} = V_{\mathrm{tot}}\tau \tag{1.254}$$

Where τ is $\frac{L}{\beta_0 c \gamma_0}$, which is the time it takes for the ion to pass through the electron cooler. Finally, the maximum impact parameter in the Xsuite implementation is the minimum of $\rho_{\mathrm{interaction}}$ and ρ_{shield}, which is given by:

$$\rho_{\max} = \min(\rho_{\mathrm{shield}}, \rho_{\mathrm{interaction}}) \tag{1.255}$$

1.10.18.1 Electron beam space charge

An additional effect of electron cooling that needs to be taken into consideration is the space charge of the electron beam. Moreover, the electron beam will assume a

parabolic profile with respect to the radius, which is given by [19]:

$$\frac{\Delta E(r)}{E_0} = \frac{Ir_e}{ec}\frac{\gamma+1}{\beta_0^3\gamma^2}\left(\frac{r}{r_0}\right)^2 \approx 1.2 \times 10^{-4}\frac{I}{\beta_0^3}\left(\frac{r}{r_{e-beam}}\right)^2 \qquad (1.256)$$

Equation 1.256 says that the electrons at the edge electron beam have a larger momentum than the electrons at the center. This means that the ions at the edge of the beam pipe will reach a larger equilibrium momentum than the ions at the core because the ions will assume the momentum of the electrons.

The Xsuite electron cooler allows for the inclusion of an optional effect called "space charge neutralization," which is determined by the parameter "space charge factor." A value of 0 for this parameter indicates that there is no space charge in the electron beam, while a value of 1 indicates that the electron beam will follow a parabolic profile as described in Equation 1.256.

An additional effect due to space charge is the rotation of the electron beam around the beam axis due to the magnetic field of the electron cooler. The angular velocity of the rotation is given by [19]:

$$\omega = \frac{\mathbf{F}\times\mathbf{B}}{er|B|^2} = \frac{I}{2\pi\epsilon_0 cr_{e-\ beam}^2}\frac{1}{\beta\gamma^2 B_{\parallel}} \approx 60\frac{I}{r_{e\text{-beam}}^2}\frac{1}{\beta\gamma^2 B_{\parallel}} \qquad (1.257)$$

This effect can also be disabled by setting "space charge factor" to zero. A value of 0 indicates that there is no rotation of the electron beam, while a value of 1 indicates that the electron beam will rotate with the angular frequency described in Equation 1.257.

1.10.19   Rotations

We assume the conventions for the directions of rotation for compatibility with MAD-X, as visualised in Fig. 1.4, and give the maps to convert the particle coordinates to the reference frames rotated by ϕ, θ, and ψ, respectively.

Figure 1.4: Rotation directions in the beam coordinate system (right-handed system).

The longitudinal momentum is

$$p_z = \sqrt{(1+\delta)^2 - p_x^2 - p_y^2}.$$

1.10.19.1 X Rotation

We define a scaling factor κ arising from the coordinate system being tilted by ϕ about the x-axis:

$$\kappa := 1 - \frac{\tan \phi \; p_y}{p_z}.$$

The coordinate updates can be described as follows:

$$y \leftarrow \frac{y}{\kappa \cos \phi}, \quad p_y \leftarrow p_y \cos \phi + p_z \sin \phi,$$

$$x \leftarrow x + \frac{y p_x \tan \phi}{\kappa p_z}, \quad \zeta \leftarrow \zeta - \frac{y \tan \phi \, (1 + \beta_0 p_\tau)}{\kappa p_z}.$$

1.10.19.2 Y Rotation

We define a scaling factor κ arising from the coordinate system being tilted by θ about the y-axis:

$$\kappa := 1 + \frac{\tan \theta \; p_x}{p_z}.$$

The coordinate updates can be described as follows (which can be verified with [11], noting the opposite convention of the angle θ):

$$x \leftarrow \frac{x}{\kappa \cos \theta}, \quad p_x \leftarrow p_x \cos \theta - p_z \sin \theta,$$

$$y \leftarrow y - \frac{x \, p_y \, \tan \theta}{\kappa \, p_z}, \quad \zeta \leftarrow \zeta + \frac{x \tan \theta \, (1 + \beta_0 p_\tau)}{\kappa \, p_z}.$$

1.10.19.3 S Rotation

We perform a rotation in the x-y plane by an angle ψ:

$$x \leftarrow x \cos \psi + y \sin \psi, \quad y \leftarrow -x \sin \psi + y \cos \psi,$$

$$p_x \leftarrow p_x \cos \psi + p_y \sin \psi, \quad p_y \leftarrow -p_x \sin \psi + p_y \cos \psi.$$

1.11 Cavity time, energy errors and acceleration

A cavity kick depends on:

$$\sin(2\pi f T + \phi) \tag{1.258}$$

where T is laboratory time.
For the most general case:

$$\sin(2\pi f T + \phi) = \sin\left(2\pi f \frac{s-\zeta}{\beta_0 c} + \phi\right) \tag{1.259}$$

Most codes drop the term $2\pi f s/(\beta_0 c)$ that is

$$\sin(2\pi f T + \phi) \rightarrow \sin\left(-2\pi f \frac{\zeta}{\beta_0 c} + \phi\right) \tag{1.260}$$

to make sure that a particle that is synchronous to the reference trajectory is in phase with the cavity.

1.11.1   Implementing energy errors

One can define

$$
\begin{aligned}
s &= s_0 + n(L_0 - L) + nL \\
f_{\mathrm{rev}} &= \beta_0 c / L \\
f &= h f_{\mathrm{rev}}
\end{aligned}
\tag{1.261}
$$

where s_0 is the path length at the cavity turn at 0, L_0 is the design circumference, n is the turn number, h is the harmonic number, L is the new path length with an energy error. Indeed one could write $L = L_0(1 + \eta \delta_s)$ where η is a constant property of the lattice.
Multiple cavities can have their own defined L.
Using these definitions, then

$$\sin(2\pi f T + \phi) = \sin\left(2\pi h f_{\mathrm{rev}} \frac{s_0 + n(L_0 - L) - \zeta}{\beta_0 c} + \phi\right) \tag{1.262}$$

$$= \sin\left(2\pi h f_{\mathrm{rev}} \frac{n(L_0 - L) - \zeta}{\beta_0 c} + \phi'\right) \tag{1.263}$$

where $\phi' = \frac{2\pi h s_0}{L} + \phi$.
In MAD-X Twiss and MAD8, the longitudinal coordinate is directly $\zeta' = n(L_0 - L) - \zeta$ and the term $n(L_0 - L)$ is added smoothly in each thick element. This forces all the cavities to share the same L or f_{rev}.
In SixTrack or MAD-X track, one could simply define a turn-dependent phase

$$\phi = \phi_0 + 2\pi h f_{\mathrm{rev}} n(L_0 - L) \tag{1.264}$$

which is very general, or alternatively add a special element that performs at each turn the following transformation:

$$\zeta_{\mathrm{new}} = (L_0 - L) - \zeta_{\mathrm{old}} \tag{1.265}$$

1.11.2 Acceleration

Acceleration can be achieved by renormalizing the relative variables using a new momentum reference. This has the side effect that the fields of the magnets (expressed in normalized strength) follow the energy ramp and that the cavity frequency (if expressed in terms of the harmonic number; NB we should perhaps change this in the Xtrack interface) is updated.

The re-normalization if done once at each turn is:

$$p_{x,\text{new}} = p_{x,\text{old}} \frac{P_{0,\text{old}}}{P_{0,\text{new}}} \qquad\qquad p_{y,\text{new}} = p_{y,\text{old}} \frac{P_{0,\text{old}}}{P_{0,\text{new}}} \tag{1.266}$$

$$\delta_{\text{new}} = (\delta_{\text{old}} + 1) \frac{P_{0,\text{old}}}{P_{0,\text{new}}} - 1 \qquad p_{\tau,\text{new}} = \frac{p_{\tau,\text{old}} P_{0,\text{old}} c + E_{0,\text{old}} - E_{0,\text{new}}}{P_{0,\text{new}} c} \tag{1.267}$$

$$\zeta_{\text{new}} = s\beta_0 \left(\frac{1}{\beta_{0,\text{new}}} - \frac{1}{\beta_{0,\text{old}}} \right) - \zeta_{\text{old}} \qquad \tau_{\text{new}} = s \left(\frac{1}{\beta_{0,\text{new}}} - \frac{1}{\beta_{0,\text{old}}} \right) - \tau_{\text{old}} \tag{1.268}$$

$$\tag{1.269}$$

Chapter 2

Misalignments

2.1 Definitions

For defining the misalignments, we use the MAD-like coordinate system, where s is the axis tangent to the reference trajectory at the entrance to the element, and x and y are the transverse beam coordinates.

A misalignment of an element is characterized by seven quantities, as illustrated in Figs. 2.1, 2.2, and 2.3:

- A reference point (anchor) along the reference trajectory through the unperturbed element;

- 6 parameters specifying the shifts and rotations of the element with respect to the reference frame defined at the anchor point.

In the derivation we omit Δ in the naming of shifts and drifts and we call
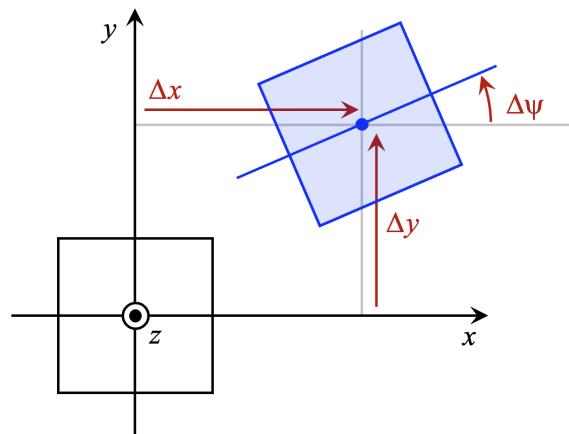
$$f = \frac{\Delta s_{\text{anchor}}}{L} \tag{2.1}$$

the relative position of the anchor along the element of length L.

Note that the rotation about the y axis does not follow the classical right-handed approach: a positive ϕ rotation is clockwise when viewed from positive x side, i.e., it goes from the s to the y axis, as opposed to from y to s.

For our calculations, we will represent the reference frame transformations using 4×4 augmented matrices. We shall assume the following notation convention: each matrix M consists of entries from M_{00} (top left corner), through M_{03} (top right corner), to M_{33} (bottom right corner). In particular, we distinguish 4 basic transformations:

$$\mathrm{T}(x,y,s) := \begin{bmatrix} 1 & 0 & 0 & x \\ 0 & 1 & 0 & y \\ 0 & 0 & 1 & s \\ 0 & 0 & 0 & 1 \end{bmatrix} \quad \text{(translation)}$$

Figure 2.1: Misalignment in the s-x plane.

Figure 2.2: Misalignment in the s-y plane.

Figure 2.3: Misalignment in the x-y plane.

$$R_x(\phi) := \begin{bmatrix} 1 & 0 & 0 & 0 \\ 0 & \cos(\phi) & \sin(\phi) & 0 \\ 0 & -\sin(\phi) & \cos(\phi) & 0 \\ 0 & 0 & 0 & 1 \end{bmatrix} \quad \text{(rotation around the } x \text{ axis)}$$

$$R_y(\theta) := \begin{bmatrix} \cos(\theta) & 0 & \sin(\theta) & 0 \\ 0 & 1 & 0 & 0 \\ -\sin(\theta) & 0 & \cos(\theta) & 0 \\ 0 & 0 & 0 & 1 \end{bmatrix} \quad \text{(rotation around the } y \text{ axis)}$$

$$R_s(\psi) := \begin{bmatrix} \cos(\psi) & -\sin(\psi) & 0 & 0 \\ \sin(\psi) & \cos(\psi) & 0 & 0 \\ 0 & 0 & 1 & 0 \\ 0 & 0 & 0 & 1 \end{bmatrix} \quad \text{(rotation around the } s \text{ axis)}$$

We allow the notation $T_x(\Delta x)$ to mean $T(\Delta x, 0, 0)$, and so on, for $T_y(\Delta y)$ and $T_s(\Delta s)$.

Figure 2.4: MAD-like coordinate system

2.2 Misalignment at arbitrary s without a tilt

We consider a potentially curved element misaligned with respect to an arbitrary position along its length.
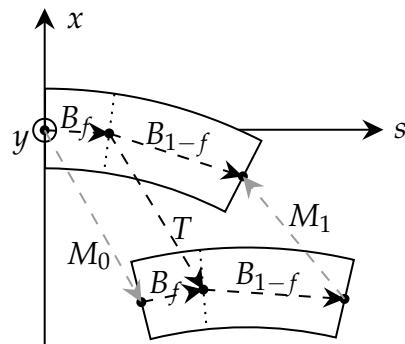
Figure 2.5: Transformations for a curved element misaligned at an arbitrary s.

Assuming a curved element of length L that bends the reference frame by α (and therefore a radius of curvature $\rho = L/\alpha$), we can represent B as a combination of a translation and a rotation, $B := T(\Delta x, 0, \Delta s) R_y(-\alpha)$, where

$$\Delta x = \rho(\cos(\alpha) - 1) = -L\operatorname{sinc}(\alpha/2)\sin(\alpha/2),$$
$$\Delta s = \rho\sin(\alpha) = L\operatorname{sinc}(\alpha).$$

$$(2.2)$$

Note, that the second formulations of Δx and Δs let us avoid division by zero if $\alpha = 0$, catering also to the case of a straight element for a truly general case.

Let us say that our element is misaligned at position ΔL along its length L. Then we can decompose our reference-frame-bending transformation B into parts B_f and B_{1-f} so that $B = B_f B_{1-f}$. The respective bending angles of the two parts are simply $f\alpha$ and $(1-f)\alpha$, where $f := \Delta L/L = \Delta L/(\rho\alpha)$ and ρ is the curvature. Knowing these parameters, it is trivial to construct B_f and B_{1-f} analogously to B, as shown in eq. 2.2. Then, we compute the following transformation, which will take us from the normal to the misaligned element entry frame:

$$M_0 = B_f T B_f^{-1},$$

whereas for returning to the normal frame from the exit

$$B_f T B_{1-f} M_1 = B = B_f B_{1-f},$$
$$M_1 = (T B_{1-f})^{-1} B_{1-f} = B_{1-f}^{-1} T^{-1} B_{1-f}.$$

When evaluated, the matrix for the curved element in the general case is

$$B_f := \begin{bmatrix} \cos(\alpha f) & 0 & -\sin(\alpha f) & \rho(\cos(\alpha f) - 1) \\ 0 & 1 & 0 & 0 \\ \sin(\alpha f) & 0 & \cos(\alpha f) & \rho\sin(\alpha f) \\ 0 & 0 & 0 & 1 \end{bmatrix},$$

and so

$$B_f^{-1} := \begin{bmatrix} \cos(\alpha f) & 0 & \sin(\alpha f) & \rho(\cos(\alpha f) - 1) \\ 0 & 1 & 0 & 0 \\ -\sin(\alpha f) & 0 & \cos(\alpha f) & -\rho\sin(\alpha f) \\ 0 & 0 & 0 & 1 \end{bmatrix}.$$

Note that $B_{f,03} = (B_f^{-1})_{03} = -Lf\operatorname{sinc}(\alpha f/2)\sin(\alpha f/2)$ and $B_{f,23} = -(B_f^{-1})_{23} = Lf\operatorname{sinc}(\alpha f)$.

Meanwhile, the misalignment matrix is (let $s_\phi := \sin(\phi)$, $c_\psi := \cos(\psi)$, etc., for space-saving reasons)

$$T = \begin{bmatrix} -s_\phi s_\psi s_\theta + c_\psi c_\theta & -c_\psi s_\phi s_\theta - c_\theta s_\psi & c_\phi s_\theta & x \\ c_\phi s_\psi & c_\phi c_\psi & s_\phi & y \\ -c_\theta s_\phi s_\psi - c_\psi s_\theta & -c_\psi c_\theta s_\phi + s_\psi s_\theta & c_\phi c_\theta & s \\ 0 & 0 & 0 & 1 \end{bmatrix}$$

and its inverse, since T is a rigid affine transformation, can be computed with

$$T^{-1} = \begin{bmatrix} R^T & -R^T t \\ 0 & 1 \end{bmatrix}, \text{ given } \begin{bmatrix} R & t \\ 0 & 1 \end{bmatrix} := T.$$

For the conversion from M_0 and M_1 to the basic tracking transformations, we can use the decomposition, $M_0 = T(x_0, y_0, s_0) R_y(\theta_0) R_x(\phi_0) R_s(\psi_0)$, for which the parameters are as follows

$$\theta_0 = \arctan_2(M_{0,02}, M_{0,22}),$$
$$\phi_0 = \arctan_2(M_{0,12}, \sqrt{M_{0,10}^2 + M_{0,11}^2}),$$
$$\psi_0 = \arctan_2(M_{0,10}, M_{0,11}),$$
$$x_0 = M_{0,03},$$
$$y_0 = M_{0,13},$$
$$s_0 = M_{0,23},$$

and for the exit, $M_1 = T(x_1, y_1, s_1) R_y(\theta_1) R_x(\phi_1) R_s(\psi_1)$,

$$\theta_1 = \arctan_2(M_{1,02}, M_{1,22}),$$
$$\phi_1 = \arctan_2(M_{1,12}, \sqrt{M_{1,10}^2 + M_{1,11}^2}),$$
$$\psi_1 = \arctan_2(M_{1,10}, M_{1,11}),$$
$$x_1 = M_{1,03},$$
$$y_1 = M_{1,13},$$
$$s_1 = M_{1,23}.$$

Note that many decompositions are possible, and their order can lead to more or less clean closed formulae for the parameters; in this case, however, we do not expect any 'nice' closed-form solutions (as opposed to the case of the subsequent section!) The above decomposition corresponds to the following tracking sequence:

- (M_0:) XYShift(x_0, y_0), SShift(s_0), YRot(θ_0), XRot(ϕ_0), SRot(ψ_0),

- (B:) Element(L, α),

- (M_1:) XYShift(x_1, y_1), SShift(s_1), YRot(θ_1), XRot(ϕ_1), SRot(ψ_1).

2.3 Misalignment at arbitrary s (the straight case)

Analogously to the previous section, we split D into $D_f D_{1-f}$:

Figure 2.6: A straight element misaligned at an arbitrary location.

We simply have that $D_f := T(0,0,fL)$ and $D_{1-f} := T(0,0,(1-f)L)$. To get to the misaligned entry frame we have

$$M_0 := D_f T D_f^{-1} = T_s(fL)\ T\ T_s(-fL),$$

whereas for returning to the normal frame from the exit

$$M_1 := D_{1-f}^{-1} T^{-1} D_{1-f} = T_s((f-1)L)\ T^{-1}\ T_s((1-f)L).$$

It is intuitively obvious, that due to lack of curvature, the entry and exit transformations should be possible to simplify. Specifically, we would want M_0 to involve some translation followed by rotations $R_y(\theta)R_x(\phi)R_s(\psi)$, and M_1, since it 'undoes' the effect of M_0, into rotations $R_s(-\psi)R_x(-\phi)R_y(-\theta)$ followed by some other translation. First we decompose the entry matrix $M_0 = T(x_0, y_0, s_0)R_y(\theta_0)R_x(\phi_0)R_s(\psi_0)$, i.e. with the same method as in the previous section. After some algebra we observe that the angles and shifts indeed simplify:

$$\begin{aligned}
\theta_0 &= \arctan_2(M_{0,02}, M_{0,22}) = \theta, \\
\phi_0 &= \arctan_2(M_{0,12}, \sqrt{M_{0,10}^2 + M_{0,11}^2}) = \phi, \\
\psi_0 &= \arctan_2(M_{0,10}, M_{0,11}) = \psi, \\
x_0 &= T_{0,03} = x - Lf\cos(\phi)\sin(\theta), \\
y_0 &= T_{0,13} = y - Lf\sin(\phi), \\
s_0 &= T_{0,23} = s - Lf(\cos(\phi)\cos(\theta) - 1).
\end{aligned}$$

Let us now decompose the matrix M_1 into $R_s(\psi_1)R_x(\phi_1)R_y(\theta_1)T(x_1, y_1, s_1)$. To this end, let us write separately as M_{rot} and M_{tr} the rotation and translation part of the above decomposition, i.e. let $M_{rot} = R_s(\psi_1)R_x(\phi_1)R_y(\theta_1)$ and let $M_{tr} := T(x_1, y_1, s_1)$. In such a decomposition, the rotation part of M_{rot} is the same as that of M_1, and so we can simply extract it from there. Afterwards, knowing M_{rot} we can compute

$M_{tr} = M_{rot}^{-1} M_1$ to get the shifts. We indeed observe the angles and shifts simplifying:

$$\theta_1 = -\arctan_2(M_{1,20}, M_{1,22}) = -\theta,$$

$$\phi_1 = -\arctan_2(M_{1,21}, \sqrt{M_{1,01}^2 + M_{1,11}^2}) = -\phi,$$

$$\psi_1 = \arctan_2(M_{1,01}, M_{1,11}) = -\psi,$$

$$x_1 = M_{tr,03} = (f-1)L\cos(\phi)\sin(\theta) - x,$$

$$y_1 = M_{tr,13} = (f-1)L\sin(\phi) - y,$$

$$s_1 = M_{tr,23} = (f-1)L(\cos(\phi)\cos(\theta) - 1) - s.$$

This way, our tracking procedure can be significantly less computationally expensive, compare to that of the preceding section, as no matrix operations are required:

- XYShift$(x - Lf\cos(\phi)\sin(\theta), y - Lf\sin(\phi))$

- SShift$(s - Lf(1 - \cos(\phi)\cos(\theta)))$

- YRot(θ), XRot(ϕ), SRot(ψ),

- Element(L),

- SRot$(-\psi)$, XRot$(-\phi)$, YRot$(-\theta)$,

- SShift$((f-1)L(\cos(\phi)\cos(\theta) - 1) - s)$,

- XYShift$((f-1)L\cos(\phi)\sin(\theta) - x, (f-1)L\sin(\phi) - y)$.

2.4 Misalignment at arbitrary s with a tilt

We consider a tilted curved element misaligned with respect to an arbitrary position along its length.

Figure 2.7: A tilted curved element misaligned at an arbitrary location.

Compared with the earlier discussion of misaligned curved elements (see Section 2.2), when considering a tilted element, we need to include the tilting in our transformation B (which, as before, is decomposed as $B_f B_{1-f}$ in Figure 2.7).

In order to include this effect we need to realise that in the previous case the curvature of the reference frame was only applied in the $s-x$ plane, whereas in the case of Figure 2.7, it will be applied in the plane obtained by tilting $s-x$ by some angle κ. Therefore, taking B_{sx} as the earlier transformation, i.e.,

$$
B_{sx} := \begin{bmatrix} \cos(\alpha) & 0 & -\sin(\alpha) & \rho(\cos(\alpha)-1) \\ 0 & 1 & 0 & 0 \\ \sin(\alpha) & 0 & \cos(\alpha) & \rho\sin(\alpha) \\ 0 & 0 & 0 & 1 \end{bmatrix},
$$

and taking $s_\alpha = \sin(\alpha)$, $c_\alpha = \cos(\alpha)$, etc. for space-saving reasons, we can express B as $R_s(\kappa)\, B_{sx}\, R_s(-\kappa)$, which evaluates to

$$
B := \begin{bmatrix} (c_\alpha-1)c_\kappa^2+1 & (c_\alpha-1)c_\kappa s_\kappa & -c_\kappa s_\alpha & \rho(c_\alpha-1)c_\kappa \\ (c_\alpha-1)c_\kappa s_\kappa & (c_\alpha-1)s_\kappa^2+1 & -s_\alpha s_\kappa & \rho(c_\alpha-1)s_\kappa \\ c_\kappa s_\alpha & s_\alpha s_\kappa & c_\alpha & \rho s_\alpha \\ 0 & 0 & 0 & 1 \end{bmatrix}.
$$

We can obtain the matrices B_f and B_{1-f} by substituting $f\alpha$ and $(1-f)\alpha$ for α in the above. To obtain the tracking procedure in this case it suffices to follow the steps of Section 2.2, substituting the new matrices.

2.5   Misalignment at arbitrary s with a tilt (straight case)

We can generalise the matrix of the above section to a straight case by recalling that $\rho(\cos(\alpha)-1) = -L\mathrm{sinc}(\alpha/2)\sin(\alpha/2)$ and $\rho\sin(\alpha) = L\mathrm{sinc}(\alpha)$. Then, we can see that when $\alpha = 0$, the matrix B of the preceding section simplifies to

$$
B|_{\alpha=0} = \begin{bmatrix} 1 & 0 & 0 & 0 \\ 0 & 1 & 0 & 0 \\ 0 & 0 & 1 & L \\ 0 & 0 & 0 & 1 \end{bmatrix} = T_s(L) = D.
$$

This means that the effect of the roll is disregarded in the calculation of the reference frame change for the purposes of a misalignment, and, therefore, that we can apply the exact procedure outlined in Section 2.3 also for tilted elements. This makes intuitive sense, as, in our setup, the tilt indeed only affects the direction of curvature of the element: if the element is straight, there is no work to be done for the misalignment, and the element map alone fully describes the effect of the tilt on the particles.

2.6   S Shift – ζ correction

In the tracking procedures shown in the preceding sections, we use the tracking map we refer to as an SShift, which we use to transport the particles in a straight line by a

displacement in s. We can presume the SShift to be a variant of DriftExact, however there are special considerations that we need to take here, with respect to the path length s and the delay ζ of our particles.
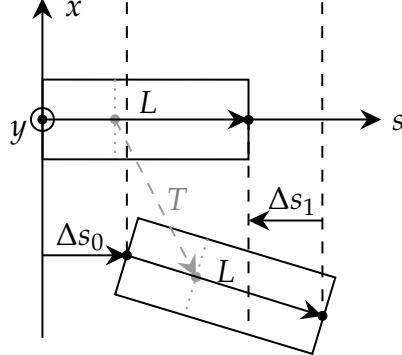
Figure 2.8: Visualisation of the s-coordinate transformations without correction.

In the visualization in Fig. 2.8 we can see the different s-coordinate updates taking place when we track through a misalignment: in particular, we can see that the total path of the particle travelled, should SShift be simply a drift, is $\Delta s = \Delta s_0 + L + \Delta s_1$. Clearly, $\Delta s_0 \neq -\Delta s_1$, and so the path length changes between the aligned and misaligned element. However, what we desire is the opposite, i.e. that the path length does not change: it is inconvenient to have the length of our accelerator change due to a misalignment. Therefore, the simplest correction we can make in this instance is to disregard the update of the s coordinate in our drift/s-shift.

A further correction needs to be made with respect to the ζ coordinate. Since ζ is related to the path length by $\zeta = s - \beta_0 ct$, and since, in our setup, the synchronous particle arrival time is not expected to change between the normal and misaligned entry to the element we expect that $\Delta\zeta = \Delta s$ between those two points. However, as we have already established for our correction of s, we expect the s coordinate to be unchanged, so we can adjust ζ in exactly the same fashion as we do s:

$$\text{SShift}(\Delta s) := (\text{DriftExact}(\Delta s), \ s \leftarrow s - \Delta s, \ \zeta \leftarrow \zeta - \Delta s).$$

Chapter 3

Linear optics

We define z as the vector of $2k$ coordinates,

$$z = (z_1, \ldots, z_{2k})^T = (x - x_0, p_x - p_{x0}, y - y_0, p_y - p_{y0}, \zeta - \zeta_0, p_\zeta - p_{\zeta 0})^T \qquad (3.1)$$

one can define linear transfer maps (e.g. $M_{1\to 2}$ that propagates coordinates between two points s_1, s_2) and the one-turn map (e.g. M_1 that combines the effects for one turn starting from s_1):

$$z(s_2) = M_{1\to 2}z(s_1) \qquad\qquad z(C + s_1) = M_1 z(s_1). \qquad (3.2)$$

In the following we will describe the optics calculation based on the Ripken formalism described in [20]. A good summary is also given in the MAD8 physics manual [2].

3.1   Linear normal form

Since the matrices derive from symplectic maps, the eigenvalue spectrum of the one-turn map M consists of $2k$ distinct eigenvalues and linearly independent eigenvectors. In addition, for the motion to be stable the eigenvalues $\lambda_k^\pm$ with eigenvectors $v_k^\pm$ have to be complex [20]:

$$Mv_k^\pm = \lambda_k^\pm v_k^\pm, \ k = 1, \ldots, 3 \qquad (3.3)$$

$$v_k^+ = (v_k^-)^*, \quad \lambda_k^+ = (\lambda_k^-)^*, \quad |\lambda_k^\pm| = 1 \qquad (3.4)$$

As the eigenvectors are linearly independent M can be diagonalized with

$$M = V\Lambda V^{-1}, \qquad (3.5)$$

where V consists of the eigenvectors and Λ of the eigenvalues:

$$V = \begin{pmatrix} v_{1,1}^+ & v_{1,1}^- & \cdots & v_{3,1}^- \\ v_{1,2}^+ & v_{1,2}^- & \cdots & v_{3,2}^- \\ \vdots & \vdots & \vdots & \vdots \end{pmatrix} \qquad \Lambda = \begin{pmatrix} \lambda_1^+ & & & \\ & \lambda_1^- & & \\ & & \ddots & \\ & & & \lambda_3^- \end{pmatrix} \qquad (3.6)$$

for which $v_{i,j}^{\pm}$ is the component j of eigenvector $v_i^{\pm}$.

The same calculation can be carried out with real numbers by the following defini-
tions:

$$v_k^{\pm} = a_k \pm i b_k, \qquad \lambda_k^{\pm} = \cos \mu_k \pm i \sin \mu_k, \qquad \mu_k, a_k, b_k \in \mathbb{R} \qquad (3.7)$$

such that:

$$M = WRW^{-1} \qquad (3.8)$$

with

$$R = R(\mu_k) = \begin{pmatrix} \cos \mu_1 & \sin \mu_1 & & & & \\ -\sin \mu_1 & \cos \mu_1 & & & & \\ & & \ddots & & & \\ & & & \cos \mu_3 & \sin \mu_3 \\ & & & -\sin \mu_3 & \cos \mu_3 \end{pmatrix}, \qquad (3.9)$$

$$W = \begin{pmatrix} a_{1,1} & b_{1,1} & \cdots & a_{3,1} & b_{3,1} \\ a_{1,2} & b_{1,2} & \cdots & a_{3,2} & b_{3,2} \\ \vdots & \vdots & \vdots & \vdots \\ a_{1,6} & b_{1,6} & \cdots & a_{3,6} & b_{3,6} \end{pmatrix} \qquad (3.10)$$

Equation 3.8 is called the linear normal form of the one-turn map M. The matrix R
describes a rotation in the 3 planes by angles μ_k.

Usually μ_k is written as $\mu_k = 2\pi Q_k$, where Q_k is then the tune of the mode k. By
convention, the eigenvectors and values are normalized, sorted and rotated so that
the following three conditions are fulfilled:

1. Plane 1 is associated with the horizontal, plane 2 with the vertical and plane 3
   with the longitudinal plane. This is achieved by first normalizing the eigenvec-
   tors $v_k^{\pm}$ and then sorting them so that:

$$|v_{j,2j-1}^+| = |v_{j,2j-1}^-| = \max_{k=1,2,3} v_{k,j}, \quad j = 1,\ldots,3 \qquad (3.11)$$

2. The eigenvectors are then rotated with a phase term ψ_k

$$v_k \rightarrow v_k \exp(i\psi_k) \qquad (3.12)$$

   such that

$$\text{angle}(v_{k,2k-1}^+) = 0 \leftrightarrow \psi_k = -\text{angle}(v_{k,2k-1}^+) \qquad (3.13)$$

   In real space, Eqn. 3.11 and 3.13 then become equivalent to:

$$|a_{j,2j-1}| = \max_{k=1,2,3} |a_{k,j}|, \qquad b_{j,2j-1} = 0, \qquad j = 1,\ldots,3 \qquad (3.14)$$

   This has the effect that a particle with $x = 0$ is transformed to $\tilde{x}$ in the normal-
   ized phase space.

3. The sign of $b_{k,j}$ is fixed by the symplectic condition on W

$$W^T S W = S \tag{3.15}$$

with S defined as

$$S = \begin{pmatrix} 0 & 1 & \\ -1 & 0 & \\ & & \ddots \end{pmatrix} \tag{3.16}$$

which is equivalent to:

$$
\begin{aligned}
a_k^T \cdot S \cdot b_k &= 1, \quad b_k^T \cdot S \cdot a_k = -1, & \text{for } k = l \\
a_k^T \cdot S \cdot b_l &= 0, & \text{for } k \neq l \\
a_k^T \cdot S \cdot a_l &= 0, \quad b_k^T \cdot S \cdot b_l = 0, & k, l = 1, \ldots, 3
\end{aligned} \tag{3.17}
$$

Eqn. 3.17 yields that in phase space a_k is thus obtained by an anticlockwise rotation of b_k by $\pi/2$ and a scaling of its length with $|a_k| = \frac{1}{|b_k|}$.

We will show in the following that in the normalized phase space the propagation of particle coordinates $z(s)$ from s_1 to s_2 is just a rotation by an angle ϕ_k in the $k = 1, \ldots, 3$ planes, while the amplitude I_k and initial phase $\phi_{k,0}$ stay constant, explicitly $z(s)$ is then given by:

$$z(s) = \sum_{k=1}^{3} \sqrt{2I_k} \left(a_k(s) \cos\left(\phi_{k,0} + \phi_k(s) \right) - b_k(s) \sin\left(\phi_{k,0} + \phi_k(s) \right) \right) \tag{3.18}$$

and

$$
\begin{aligned}
z(s_2) &= W(s_2) R(\phi_k) W(s_1)^{-1} z(s_1), \\
&\text{with } \phi_k = \phi_k(s_2) - \phi_k(s_1)
\end{aligned} \tag{3.19}
$$

This implies that one turn is simply a rotation by $\phi_k = 2\pi Q_k$ where Q_k is the tune of the mode k. In the transverse plane the tune $(Q_{I,II})$ is usually positive and the particles rotate clockwise, while in the longitudinal plane the tune (Q_{III}) is negative above γ_T leading to an anticlockwise rotation.

For the derivation the following steps are needed:

1. The effect of one turn on the normalized variable $\tilde{z}(s) = W^{-1}(s)z(s)$ is a rotation:

$$\tilde{z}(C + s) = W^{-1} z(s + C) \stackrel{\text{(Eqn.3.8)}}{=} W^{-1} W R W^{-1} z(s) = R\tilde{z}(s), \tag{3.20}$$

As M and R are symplectic also W is symplectic, and its inverse is thus given by $S^{-1}W^T S$, explicitly:

$$
W^{-1} =
\begin{pmatrix}
b_{12} & -b_{11} & b_{14} & -b_{13} & b_{16} & -b_{15} \\
-a_{12} & a_{11} & -a_{14} & a_{13} & -a_{16} & a_{15} \\
b_{22} & -b_{21} & b_{24} & -b_{23} & b_{26} & -b_{25} \\
-a_{22} & a_{21} & -a_{24} & a_{23} & -a_{26} & a_{25} \\
b_{32} & -b_{31} & b_{34} & -b_{33} & b_{36} & -b_{35} \\
-a_{32} & a_{31} & -a_{34} & a_{33} & -a_{36} & a_{35}
\end{pmatrix}
\tag{3.21}
$$

2. The one-turn map and W-matrix can be propagated from s_1 to s_2 by

$$
M_2 = M_{1\to2} M_1 M_{1\to2}^{-1} \qquad\qquad W_2 = M_{1\to2} W_1 \tag{3.22}
$$

As Eqn. 3.20 represents a similarity transformation, the eigenvalues are thus independent of the position s and as the rotation matrix R consists of the eigenvalues of M, the angle of the rotation $\mu_k = 2\pi Q_k$ is thus also independent of s.

3. As Eqn. 3.8 represents a basis transformation from the standard $\mathbb{R}^2$ basis to the eigenvector basis, the vectors a_k and b_k are projected onto (Eqn. 3.17):

$$
\begin{aligned}
\tilde{a}_1 = W^{-1}a_1 &= -SW^T S a_1 \\
&= -S(a_1 S a_1, b_1 S a_1, \ldots, b_3 S a_1)^T = (1, 0, \ldots, 0) \\
\tilde{b}_1 = W^{-1}b_1 &= -SW^T S b_1 \\
&= -S(a_1 S b_1, b_1 S b_1, \ldots, b_3 S b_1)^T = (0, 1, \ldots, 0) \\
&\quad\cdots \\
\tilde{b}_3 = W^{-1}b_3 &= -SW^T S b_3 \\
&= -S(a_1 S b_3, b_1 S b_3, \ldots, b_3 S b_3)^T = (0, 0, \ldots, 1)
\end{aligned}
\tag{3.23}
$$

in the normalized phase space.

4. From Eqn. 3.20 it follows that the amplitude I_k and initial phase ϕ_{k0} of $\tilde{z} = W^{-1}z = (\tilde{z}_{a_1}, \tilde{z}_{b_1}, \ldots, \tilde{z}_{b_3})$

$$
I_k = \frac{(\tilde{z}_{a_k})^2 + (\tilde{z}_{b_k})^2}{2}, \quad k = 1, \ldots, 3 \tag{3.24}
$$

$$
\tan \phi_{k0} = -\frac{\tilde{z}_{b_k}}{\tilde{z}_{a_k}} \tag{3.25}
$$

are constants of the motion. The initial phase is defined with a minus sign in view of the definition of the Twiss parameters, where the initial phase is then

added (and not subtracted) to the phase advance. The components of $\tilde{z}$ are then explicitly given by:

$$\tilde{z}_{a_k} = \sum_{j=1}^{3} b_{k,2j} z_{2j-1} - b_{k,2j-1} z_{2j}, \quad k = 1, \ldots, 3 \tag{3.26}$$

$$\tilde{z}_{b_k} = \sum_{j=1}^{3} a_{k,2j-1} z_{2j} - a_{k,2j} z_{2j-1}, \quad k = 1, \ldots, 3. \tag{3.27}$$

An arbitrary vector $z(s)$ can thus be written in the following form:

$$
\begin{aligned}
z(s) &= W(s)\tilde{z}(s) \\
&= W(s) \left(\sum_{k=1}^{3} \tilde{z}_{a_k} \tilde{a}_k + \tilde{z}_{b_k} \tilde{b}_k \right) \\
&= \sum_{k=1}^{3} \tilde{z}_{a_k} W(s) \tilde{a}_k + \tilde{z}_{b_k} W(s) \tilde{b}_k \overset{\text{Eqn. 3.23}}{=} \sum_{k=1}^{3} \tilde{z}_{a_k} a_k + \tilde{z}_{b_k} b_k \\
&\overset{\text{Eqns. 3.24,3.25}}{=} \sum_{k=1}^{3} \sqrt{2I_k} \left(a_k \cos \phi_{k0} - b_k \sin \phi_{k0} \right)
\end{aligned}
\tag{3.28}
$$

3.2 Twiss parameters

In the following the parameter k will always be used for the mode k and the parameter $j = 1, 2, 3$ for the horizontal (x, p_x), vertical (y, p_y) and longitudinal plane (ζ, p_ζ) in the phase space. z_{2j-1} then stands for the coordinates (x, y, ζ) and z_{2j} for $(p_{x,y}, p_\zeta)$.
The Twiss parameters can be introduced by writing the components of the eigenvector basis $(a_k(s), b_k(s))$ as the product of two envelope functions $\sqrt{\beta_{k,j}(s)}$, $\sqrt{\gamma_{k,j}(s)}$ and phase functions $\phi_{k,j}(s)$, $\bar{\phi}_{k,j}(s) = \phi_{k,j}(s) - \arctan(1/\alpha_{k,j})$, also called Twiss parameters or lattice functions, with

$$a_{k,2j-1}(s) = \sqrt{\beta_{k,j}(s)} \cos \phi_{k,j}(s),$$

$$b_{k,2j-1}(s) = \sqrt{\beta_{k,j}(s)} \sin \phi_{k,j}(s), \; k, j = 1, \ldots, 3, \tag{3.29}$$

$$a_{k,2j}(s) = \sqrt{\gamma_{k,j}(s)} \cos \bar{\phi}_{k,j}(s),$$

$$b_{k,2j}(s) = \sqrt{\gamma_{k,j}(s)} \sin \bar{\phi}_{k,j}(s), \; k, j = 1, \ldots, 3 \tag{3.30}$$

where $\beta_{k,j}(s), \alpha_{k,j}(s), \gamma_{k,j}(s)$ represent the projection of the ellipse of mode k on the plane of coordinates $z_{2k-1} - z_{2k}$.
Using Eqns. 3.18, 3.29, 3.30 and $\cos(x + y) = \cos x \cos y - \sin x \sin y$, the coordinates $z(s)$ can be expressed by:

$$z_{2j-1}(s) = \sum_{k=1}^{3} \sqrt{2I_k \beta_{k,j}(s)} \cos \left(\phi_{k,j}(s) + \phi_{k,0} \right) \tag{3.31}$$

$$z_{2j}(s) = \sum_{k=1}^{3} \sqrt{2I_k \gamma_{k,j}(s)} \cos \left(\bar{\phi}_{k,j}(s) + \phi_{k,0} \right), \; j = 1, \ldots, 3 \tag{3.32}$$

Conversely the lattice functions can also be expressed by a_k and b_k with

$$\beta_{k,j}(s) = a_{k,2j-1}(s)^2 + b_{k,2j-1}(s)^2 \tag{3.33}$$

$$\alpha_{k,j}(s) = -a_{k,2j-1}(s)a_{k,2j}(s) - b_{k,2j-1}(s)b_{k,2j}(s) \tag{3.34}$$

$$\gamma_{k,j}(s) = a_{k,2j}(s)^2 + b_{k,2j}(s)^2, \tag{3.35}$$

The well known relations between the lattice functions

$$\sum_{j=1}^{3} \beta_{k,j}\phi'_{k,j} = 1 \tag{3.36}$$

$$\gamma_{k,j} = \frac{\beta_{k,j}^2 \phi'^2_{k,j} + \alpha_{k,j}^2}{\beta_{k,j}}, \text{ with} \tag{3.37}$$

$$\alpha_{k,j} := -\frac{1}{2}\beta'_{k,j} \tag{3.38}$$

can then be derived with the help of the normalization condition (Eqn. 3.17)

$$a_k^T S b_k = 1 \tag{3.39}$$

by the following steps:

1. As $x' = \frac{dx}{ds}$, $y' = \frac{dy}{ds}$ the following relations hold also for a_k and b_k:

$$a_{k,2j} = a'_{k,2j-1} = \frac{d}{ds}(a_{k,2j-1}), \tag{3.40}$$

$$b_{k,2j} = b'_{k,2j-1} = \frac{d}{ds}(b_{k,2j-1}), \ k,j = 1,\ldots,3 \tag{3.41}$$

2. The normalization condition Eqn. 3.17 can then be written as

$$a_k^T S b_k = \sum_{j=1}^{3} \sqrt{\beta_{k,j}} \cos \phi_{k,j} \left(\sqrt{\beta_{k,j}} \sin \phi_{k,j} \right)'$$

$$- \left(\sqrt{\beta_{k,j}} \cos \phi_{k,j} \right)' \sqrt{\beta_{k,j}} \sin \phi_{k,j}$$

$$= \sum_{j=1}^{3} \beta_{k,j} \phi'_{k,j}$$

$$= 1 \tag{3.42}$$

Note that Eqn. 3.42 yields the following relation between the phase advance ϕ and β in 2D:

$$\phi(s) = \phi(0) + \int_{s_0}^{s} \frac{1}{\beta(\bar{s})} d\bar{s} \tag{3.43}$$

3. Using the abbreviation $\alpha_{k,j} := -\frac{1}{2}\beta_{k,j}'$, one finds for each mode k and plane j

$$\sqrt{\gamma_{k,j}}\cos\phi_{k,j} = a_{k,2j} = a'_{k,2j-1} = (\sqrt{\beta_{k,j}}\cos\phi_{k,j})' \tag{1}$$

$$\sqrt{\gamma_{k,j}}\sin\phi_{k,j} = b_{k,2j} = b'_{k,2j-1} = (\sqrt{\beta_{k,j}}\sin\phi_{k,j})' \tag{2}$$

$$\overset{(1)^2+(2)^2}{\Longrightarrow} \gamma_{k,j} = \frac{\beta_{k,j}^2\phi_{k,j}'^2 + \alpha_{k,j}^2}{\beta_{k,j}}, \quad k,j = 1,\dots,3 \tag{3.44}$$

which simplifies in the 2D case to:

$$\gamma \overset{\text{Eqn. 3.42}}{=} \frac{1+\alpha^2}{\beta} \tag{3.45}$$

3.3 Transformation to normalized coordinates

The W matrix can be used to transform normalized coordinates into physical coordinates and vice versa:

$$\begin{pmatrix} x \\ p_x \\ y \\ p_y \\ \zeta \\ p_\zeta \end{pmatrix} = W \begin{pmatrix} \hat{x} \\ \hat{p}_x \\ \hat{y} \\ \hat{p}_y \\ \hat{\zeta} \\ \hat{p}_\zeta \end{pmatrix} = W \begin{pmatrix} \sqrt{\varepsilon_x}\tilde{x} \\ \sqrt{\varepsilon_x}\tilde{p}_x \\ \sqrt{\varepsilon_y}\tilde{y} \\ \sqrt{\varepsilon_y}\tilde{p}_y \\ \sqrt{\varepsilon_\zeta}\tilde{\zeta} \\ \sqrt{\varepsilon_\zeta}\tilde{p}_\zeta \end{pmatrix} \tag{3.46}$$

where

$$\begin{pmatrix} \tilde{x} & \tilde{p}_x & \tilde{y} & \tilde{p}_y & \tilde{\zeta} & \tilde{p}_\zeta \end{pmatrix} \tag{3.47}$$

are normalized coordinates in sigmas and ε_x, ε_y and ε_ζ are the geometric emittances.

3.4 Action, amplitude and emittance

We define the action associated to the three modes:

$$J_x = \frac{\hat{x}^2 + \hat{p}_x^2}{2}, \quad J_y = \frac{\hat{y}^2 + \hat{p}_y^2}{2}, \quad J_\zeta = \frac{\hat{\zeta}^2 + \hat{p}_\zeta^2}{2} \tag{3.48}$$

The corresponding amplitudes are defined such that:

$$A_x = \sqrt{\hat{x}^2 + \hat{p}_x^2} = \sqrt{2J_x}, \tag{3.49}$$

$$A_y = \sqrt{\hat{y}^2 + \hat{p}_y^2} = \sqrt{2J_y} \tag{3.50}$$

$$A_\zeta = \sqrt{\hat{\zeta}^2 + \hat{p}_\zeta^2} = \sqrt{2J_\zeta} \tag{3.51}$$

A Gaussian distribution is defined such that the density with respect to each action can be written as:

$$f(J_x) = Ke^{-J_x/\varepsilon_x} \tag{3.52}$$

where the emittance ε_x is

$$\varepsilon_x = <J_x> = \int J_x f(J_x)\, dJ_x \tag{3.53}$$

3.5   Dispersion and crab dispersion

For a particle having no betatron amplitude ($\hat{x} = \hat{p}_x = \hat{y} = \hat{p}_y = 0$) we can write:

$$x = W_{15}\hat{\zeta} + W_{16}\hat{p}_\zeta \tag{3.54}$$
$$\zeta = W_{55}\hat{\zeta} + W_{56}\hat{p}_\zeta \tag{3.55}$$
$$p_\zeta = W_{65}\hat{\zeta} + W_{66}\hat{p}_\zeta \tag{3.56}$$

3.5.1   Dispersion

The dispersion is:

$$D_x^{p_\zeta} = \frac{dx}{dp_\zeta} \quad \text{for } \zeta = 0 \tag{3.57}$$

By imposing $\zeta = 0$ in Eq. 3.55 we obtain:

$$\hat{\zeta} = -\frac{W_{56}}{W_{55}}\hat{p}_\zeta \tag{3.58}$$

We replace in Eq. 3.56:

$$\hat{p}_\zeta = \left(W_{66} - \frac{W_{65}W_{56}}{W_{55}}\right)^{-1} p_\zeta \tag{3.59}$$

From Eq. 3.58 we obtain:

$$\hat{\zeta} = -\frac{W_{56}}{W_{55}}\left(W_{66} - \frac{W_{65}W_{56}}{W_{55}}\right)^{-1} p_\zeta \tag{3.60}$$

Replacing the last two into Eq. 3.54 we obtain:

$$x = \left(W_{16} - \frac{W_{15}W_{56}}{W_{55}}\right)\left(W_{66} - \frac{W_{65}W_{56}}{W_{55}}\right)^{-1} p_\zeta \tag{3.61}$$

which gives the dispersion:

$$D_x^{p_\zeta} = \left(W_{16} - \frac{W_{15}W_{56}}{W_{55}}\right)\left(W_{66} - \frac{W_{65}W_{56}}{W_{55}}\right)^{-1} \tag{3.62}$$

A similar type of calculation can be done for the other planes, and for the transverse momentum dispersion, obtaining $D_{px}^{p\zeta}$: which gives the dispersion:

$$D_{px}^{p\zeta} = \left(W_{26} - \frac{W_{25}W_{56}}{W_{55}} \right) \left(W_{66} - \frac{W_{65}W_{56}}{W_{55}} \right)^{-1} \tag{3.63}$$

$$D_{y}^{p\zeta} = \left(W_{36} - \frac{W_{35}W_{56}}{W_{55}} \right) \left(W_{66} - \frac{W_{65}W_{56}}{W_{55}} \right)^{-1} \tag{3.64}$$

$$D_{py}^{p\zeta} = \left(W_{46} - \frac{W_{45}W_{56}}{W_{55}} \right) \left(W_{66} - \frac{W_{65}W_{56}}{W_{55}} \right)^{-1} \tag{3.65}$$

3.5.2 Crab dispersion

The crab dispersion is:

$$D_{x}^{\zeta} = \frac{dx}{dz} \quad \text{for } p_{\zeta} = 0 \tag{3.66}$$

By imposing $p_{\zeta} = 0$ in Eq. 3.56 we obtain:

$$\hat{p}_{\zeta} = -\frac{W_{65}}{W_{66}}\hat{\zeta} \tag{3.67}$$

We replace in Eq. 3.55:

$$\hat{\zeta} = \left(W_{55} - \frac{W_{56}W_{65}}{W_{66}} \right)^{-1} \zeta \tag{3.68}$$

From Eq. 3.67 we obtain:

$$\hat{p}_{\zeta} = -\frac{W_{65}}{W_{66}} \left(W_{55} - \frac{W_{56}W_{65}}{W_{66}} \right)^{-1} \zeta \tag{3.69}$$

Replacing the last two into Eq. 3.54 we obtain:

$$x = \left(W_{15} - \frac{W_{16}W_{65}}{W_{66}} \right) \left(W_{55} - \frac{W_{56}W_{65}}{W_{66}} \right)^{-1} \zeta \tag{3.70}$$

which gives the crab dispersion:

$$D_{x}^{\zeta} = \left(W_{15} - \frac{W_{16}W_{65}}{W_{66}} \right) \left(W_{55} - \frac{W_{56}W_{65}}{W_{66}} \right)^{-1} \tag{3.71}$$

A similar type of calculation can be done for the other planes, and for transverse momentum crab dispersion obtaining:

$$D_{px}^{\zeta} = \left(W_{25} - \frac{W_{26}W_{65}}{W_{66}} \right) \left(W_{55} - \frac{W_{56}W_{65}}{W_{66}} \right)^{-1} \tag{3.72}$$

$$D_{y}^{\zeta} = \left(W_{35} - \frac{W_{36}W_{65}}{W_{66}} \right) \left(W_{55} - \frac{W_{56}W_{65}}{W_{66}} \right)^{-1} \tag{3.73}$$

$$D_{py}^{\zeta} = \left(W_{45} - \frac{W_{46}W_{65}}{W_{66}} \right) \left(W_{55} - \frac{W_{56}W_{65}}{W_{66}} \right)^{-1} \tag{3.74}$$

3.6   Linear coupling indicators

The following is based on [21] and [22].

In the presence of betatron coupling the transverse on-momentum motion can be written as:

$$
\begin{cases}
x_n = A_{1,x} \cos\left[2\pi Q_1(n-1) + \phi_{1,x}\right] + A_{2,x} \cos\left[2\pi Q_2(n-1) + \phi_{2,x}\right] \\
y_n = A_{1,y} \cos\left[2\pi Q_1(n-1) + \phi_{1,y}\right] + A_{2,y} \cos\left[2\pi Q_2(n-1) + \phi_{2,y}\right]
\end{cases}
\tag{3.75}
$$

We can define:

$$
\begin{cases}
r_1 = \left|A_{1,y}\right| / \left|A_{1,x}\right| = \beta_{1y}/\beta_{1x} \\
r_2 = \left|A_{2,x}\right| / \left|A_{2,y}\right| = \beta_{2x}/\beta_{2y}
\end{cases}
\tag{3.76}
$$

$$
\begin{cases}
\Delta\phi_1 = \phi_{1,y} - \phi_{1,x} \\
\Delta\phi_2 = \phi_{2,x} - \phi_{2,y}
\end{cases}
\tag{3.77}
$$

These quantities can be obtained from the normalized W matrix as:

$$
\begin{cases}
r_1 = \sqrt{W_{31}^2 + W_{32}^2}/W_{11} \\
r_2 = \sqrt{W_{13}^2 + W_{14}^2}/W_{33}
\end{cases}
\tag{3.78}
$$

$$
\begin{cases}
\Delta\phi_{1,0} = \arctan\left(W_{32}/W_{31}\right) \\
\Delta\phi_{2,0} = \arctan\left(W_{14}/W_{13}\right)
\end{cases}
\tag{3.79}
$$

From these we can compute the following quantities as [22]:

$$
\left|C^-\right| = \frac{2\sqrt{r_1 r_2}\left|Q_1 - Q_2\right|}{(1 + r_1 r_2)}
\tag{3.80}
$$

$$
\chi(s) = \Delta\phi_{1,0}(s)
\tag{3.81}
$$

$$
C^-(s) = \left|C^-\right| e^{i\chi(s)}
\tag{3.82}
$$

where Q_1 and Q_2 are the tunes of the betatron eigenmodes. Note that only the phase of $C^-(s)$ is s dependent.
It is possible to prove that C^- is related to the skew quadrupole strengths along the ring by the following relation:

$$
C^- = \left|C^-\right| e^{i\chi} = \frac{1}{2\pi} \int_0^L \sqrt{\beta_x \beta_y} k_s e^{i\left[\Phi_x - \Phi_y - 2\pi\Delta \cdot s/L\right]} dl.
\tag{3.83}
$$

where Δ is the difference of the unperturbed fractional tunes.
To have a more robust estimate, Eq. 3.80 is evaluated at all s positions and averaged over the ring, as suggested in [23].

3.6.1 Edwards-Teng formalism

This section is based on [24] and [25].
Consider the linear one-turn matrix R in two degrees of freedom, partitioned into four 2×2 blocks:

$$R = \begin{pmatrix} A & B \\ C & D \end{pmatrix}. \tag{3.84}$$

We can block-diagonalize R as follows:

$$g^2 \begin{pmatrix} I & -\bar{R}_{\text{ET}} \\ R_{\text{ET}} & I \end{pmatrix} \begin{pmatrix} A & B \\ C & D \end{pmatrix} \begin{pmatrix} I & \bar{R}_{\text{ET}} \\ -R_{\text{ET}} & I \end{pmatrix} = \begin{pmatrix} E & 0 \\ 0 & F \end{pmatrix} \tag{3.85}$$

Here R_{ET} is a 2×2 matrix with unit determinant.
The notation $\bar{Z}$ denotes the symplectic conjugate of matrix Z:

$$\bar{Z} = -S Z^T S \tag{3.86}$$

The matrix R_{ET} is given by:

$$R_{\text{ET}} = - \left(\frac{1}{2}(\operatorname{tr} A - \operatorname{tr} D) + \operatorname{sign}(\operatorname{tr} A - \operatorname{tr} D) \sqrt{\Delta} \right)^{-1} (C + \bar{B}) \tag{3.87}$$

where:

$$\Delta = \frac{1}{4}(\operatorname{tr} A - \operatorname{tr} D)^2 + |C + \bar{B}| \tag{3.88}$$

The matrices E and F are given by:

$$E = A - B R_{\text{ET}} \tag{3.89}$$
$$F = D + R_{\text{ET}} B \tag{3.90}$$

Twiss parameters can be found from E (and F):

$$E = \begin{pmatrix} E_{1,1} & E_{1,2} \\ E_{2,1} & E_{2,2} \end{pmatrix} = \begin{pmatrix} \cos \mu_A + \alpha_A \sin \mu_A & \beta_A \sin \mu_A \\ -\gamma_A \sin \mu_A & \cos \mu_A - \alpha_A \sin \mu_A \end{pmatrix} \tag{3.91}$$

from which:

$$\cos \mu_A = \tfrac{1}{2} \operatorname{tr} E, \tag{3.92}$$

$$\sin \mu_A = \operatorname{sign}(E_{1,2}) \sqrt{-E_{1,2} E_{2,1} - \left(\frac{E_{1,1} - E_{2,2}}{2} \right)^2} \tag{3.93}$$

$$\beta_A = \frac{E_{1,2}}{\sin \mu_A} \tag{3.94}$$

$$\gamma_A = -\frac{E_{2,1}}{\sin \mu_A} \tag{3.95}$$

$$\alpha_A = \frac{E_{1,1} - E_{2,2}}{2 \sin \mu_A}. \tag{3.96}$$

3.6.1.1   Propagation of Edwards-Teng parameters

Consider two positions a and b along the lattice, with the linear transfer map

$$R^{ab} = \begin{pmatrix} A^{ab} & B^{ab} \\ C^{ab} & D^{ab} \end{pmatrix}. \tag{3.97}$$

Using the Edwards-Teng parametrization $\{E^a, F^a, R^a_{\text{ET}}\}$ at a, the parameters at b are obtained from

$$E^b = E^{ab} E^a \overline{E}^{ab} / |E^{ab}|, \tag{3.98}$$

$$F^b = F^{ab} F^a \overline{F}^{ab} / |F^{ab}|, \tag{3.99}$$

$$R^b_{\text{ET}} = -\left(C^{ab} - D^{ab} R^a_{\text{ET}} \right) \overline{E}^{ab} / |E^{ab}|. \tag{3.100}$$

where:

$$E^{ab} = A^{ab} - B^{ab} R^a_{\text{ET}}, \tag{3.101}$$

$$F^{ab} = D^{ab} + C^{ab} \overline{R}^a_{\text{ET}}. \tag{3.102}$$

Here $\overline{(\cdot)}$ denotes the symplectic conjugate, and $|X|$ the determinant of matrix X. Let $E^{ab}_{i,j}$ denote the elements of E^{ab}. The Edwards-Teng Twiss parameters propagate as

$$\beta^b_x = \frac{\left(E^{ab}_{1,1} \beta^a_x - E^{ab}_{1,2} \alpha^a_x \right)^2 + \left(E^{ab}_{1,2} \right)^2}{|E^{ab}| \, \beta^a_x}, \tag{3.103}$$

$$\alpha^b_x = -\frac{\left(E^{ab}_{2,1} \beta^a_x - E^{ab}_{2,2} \alpha^a_x \right)\left(E^{ab}_{1,1} \beta^a_x - E^{ab}_{1,2} \alpha^a_x \right) + E^{ab}_{1,2} E^{ab}_{2,2}}{|E^{ab}| \, \beta^a_x}, \tag{3.104}$$

$$\mu^b_x = \mu^a_x + \text{atan2}\left(E^{ab}_{1,2}, \; E^{ab}_{1,1} \beta^a_x - E^{ab}_{1,2} \alpha^a_x \right), \tag{3.105}$$

$$\gamma^b_x = \frac{1 + \left(\alpha^b_x \right)^2}{\beta^b_x}. \tag{3.106}$$

The same relations apply to the vertical plane, replacing E^{ab} by F^{ab} and the subscript x by y.

Chapter 4

Resonant Driving Terms

This chapter follows the formulation in [26, 27].

4.1 Courant–Snyder normalized coordinates

We work in Courant–Snyder normalized transverse coordinates $(\tilde{u}, \tilde{p}_u)$ with $u \in \{x, y\}$, obtained from (u, p_u) via

$$
\begin{pmatrix} \tilde{u} \\ \tilde{p}_u \end{pmatrix} = \begin{pmatrix} \beta_u^{-1/2} & 0 \\ \alpha_u \beta_u^{-1/2} & \beta_u^{1/2} \end{pmatrix} \begin{pmatrix} u \\ p_u \end{pmatrix},
\tag{4.1}
$$

where the Twiss parameters (α_u, β_u) are evaluated at the observation point s.

4.2 Complex Courant–Snyder coordinates

For $q \in \{x, y\}$ we introduce the complex Courant–Snyder coordinates

$$
h_{q,\pm} = \tilde{q} \pm i \tilde{p}_q = \sqrt{2 I_q} \, e^{\mp i (\psi_q + \psi_{q,0})},
\tag{4.2}
$$

where I_q is the action and ψ_q the betatron phase advance (with initial phase $\psi_{q,0}$). From $\tilde{q}$ and $\tilde{p}_q$ we recover

$$
I_q = \frac{\tilde{q}^2 + \tilde{p}_q^2}{2},
\tag{4.3}
$$

$$
\psi_q = -\psi_{q,0} - \operatorname{atan2}\left(\tilde{p}_q, \tilde{q}\right).
\tag{4.4}
$$

4.3   Motion expressed through resonant driving terms

The transverse motion written in terms of resonant driving terms (RDTs) reads

$$
h_{x,-}(s,N) = \sqrt{2I_x}\, e^{i(2\pi Q_x N + \psi_{s,x,0})} - 2i \sum_{pqrt} p\, f_{pqrt}^{(s)} \left(2I_x\right)^{\frac{p+q-1}{2}} \left(2I_y\right)^{\frac{r+t}{2}}
$$

$$
\times\, e^{i\left[(1-p+q)(2\pi Q_x N + \psi_{s,x,0}) + (t-r)\left(2\pi Q_y N + \psi_{s,y,0}\right)\right]}, \tag{4.5}
$$

$$
h_{y,-}(s,N) = \sqrt{2I_y}\, e^{i\left(2\pi Q_y N + \psi_{s,y,0}\right)} - 2i \sum_{pqrt} r\, f_{pqrt}^{(s)} \left(2I_x\right)^{\frac{p+q}{2}} \left(2I_y\right)^{\frac{r+t-1}{2}}
$$

$$
\times\, e^{i\left[(q-p)(2\pi Q_x N + \psi_{s,x,0}) + (1-r+t)\left(2\pi Q_y N + \psi_{s,y,0}\right)\right]}, \tag{4.6}
$$

where N is the turn number, $Q_{x,y}$ the tunes, $I_{x,y}$ the invariants and $\psi_{s,x,0}$, $\psi_{s,y,0}$ the initial phases at the observation point s.

4.4   Expression of RDTs from first-order perturbation theory

The coefficients f_{pqrt} at the element j are computed from first-order perturbation theory obtaining:

$$
f_{pqrt}(j) = \frac{\displaystyle\sum_{m=1}^{M} h_{m,pqrt}\, e^{i\left[(p-q)\Delta\phi_{x,mj} + (r-t)\Delta\phi_{y,mj}\right]}}{1 - e^{2\pi i\left[(p-q)Q_x + (r-t)Q_y\right]}}, \tag{4.7}
$$

where the numerator runs over the M elements of the ring and where

$$
h_{m,pqrt} = -\frac{K_{m,n-1}\,\Omega(r+t) + i\,\hat{K}_{m,n-1}\,\Omega(r+t+1)}{p!\, q!\, r!\, t!\, 2^{p+q+r+t}}\, i^{r+t} \left(\beta_{m,x}\right)^{\frac{p+q}{2}} \left(\beta_{m,y}\right)^{\frac{r+t}{2}}, \tag{4.8}
$$

with $n = p + q + r + t$ and where $K_{m,n-1}$ and $\hat{K}_{m,n-1}$ are the normal and skew multipole strengths of order $n-1$ in element m. The parity selector is

$$
\Omega(i) = \begin{cases} 1, & \text{if } i \text{ is even,} \\ 0, & \text{if } i \text{ is odd.} \end{cases} \tag{4.9}
$$

The phase advances between element m and observation point j follow

$$
\Delta\phi_{x,mj} = \begin{cases} \phi_{x,j} - \phi_{x,m}, & \phi_{x,j} > \phi_{x,m}, \\ \phi_{x,j} - \phi_{x,m} + 2\pi Q_x, & \phi_{x,j} < \phi_{x,m}, \end{cases} \tag{4.10}
$$

$$
\Delta\phi_{y,mj} = \begin{cases} \phi_{y,j} - \phi_{y,m}, & \phi_{y,j} > \phi_{y,m}, \\ \phi_{y,j} - \phi_{y,m} + 2\pi Q_y, & \phi_{y,j} < \phi_{y,m}. \end{cases} \tag{4.11}
$$

Note that $h_{m,pqrt}$ in Eq. (4.8) is a Hamiltonian coefficient and shall not be confused with the complex Courant–Snyder coordinates $h_{x,y}$ appearing in Eqs. (4.5)–(4.6).

4.5 Feed-down and misalignments

When evaluating RDTs, the multipole strengths must be taken on the closed orbit and corrected for magnet tilts and transverse shifts. Using the complex transverse coordinate $z = x + iy$ (lab frame), the normalized longitudinal potential is

$$a_s(z) = -\Re \left[\sum_{n=0}^{\infty} \frac{K_n + i\hat{K}_n}{(n+1)!} z^{n+1} \right], \tag{4.12}$$

where K_n and $\hat{K}_n$ are the normal and skew multipole coefficients of order n (dipole $n = 0$, quadrupole $n = 1$, etc.) in the magnet reference frame. We consider a magnet whose center is transversely shifted by $\Delta = \Delta x + i\Delta y$ and tilted by an angle ψ around the longitudinal axis (positive ψ rotates the magnet frame counter-clockwise relative to the lab frame).

4.5.1 Coordinate transformation

From the lab coordinate z, the coordinate in the magnet frame is obtained by first translating by $-\Delta$ and then rotating by $-\psi$:

$$z_{\text{mag}} = e^{-i\psi} (z - \Delta). \tag{4.13}$$

Substituting (4.13) into (4.12) gives

$$a_s(z) = -\Re \left[\sum_{n=0}^{\infty} \frac{K_n + i\hat{K}_n}{(n+1)!} e^{-i(n+1)\psi} (z - \Delta)^{n+1} \right]. \tag{4.14}$$

4.5.2 Feed-down expansion

Expanding the shifted power with the binomial theorem,

$$(z - \Delta)^{n+1} = \sum_{m=0}^{n+1} \binom{n+1}{m+1} z^{m+1} (-\Delta)^{n-m}, \tag{4.15}$$

and re-collecting terms proportional to z^{m+1}, we write

$$a_s(z) = -\Re \left[\sum_{m=0}^{\infty} \frac{K'_m + i\hat{K}'_m}{(m+1)!} z^{m+1} \right], \tag{4.16}$$

with effective (feed-down) multipole coefficients

$$K'_m + i\hat{K}'_m = \sum_{n=m}^{\infty} \frac{K_n + i\hat{K}_n}{(n-m)!} (-\Delta)^{n-m} e^{-i(n+1)\psi}. \tag{4.17}$$

Expressing the transverse shift in the magnet frame, $\tilde{\Delta} = e^{-i\psi}\Delta$, and using $n = m + p$ gives

$$K'_m + i\hat{K}'_m = e^{-i(m+1)\psi} \sum_{p=0}^{\infty} \frac{K_{m+p} + i\hat{K}_{m+p}}{p!} (-\tilde{\Delta})^p. \tag{4.18}$$

4.5.3   Expansion around a closed orbit x_0, y_0

Let $z_0 = x_0 + iy_0$ denote the closed orbit in the lab frame and write $z = z_0 + u$, where u is the small transverse excursion. The magnet-frame coordinate becomes

$$z_{\text{mag}} = e^{-i\psi}\,(z_0 - \Delta + u) = \tilde{b} + e^{-i\psi}u, \quad \text{with} \quad \tilde{b} \equiv e^{-i\psi}(z_0 - \Delta). \tag{4.19}$$

Expanding the potential in powers of u as in (4.16) yields effective multipoles around the closed orbit:

$$K_m^{(\text{orb})} + i\hat{K}_m^{(\text{orb})} = e^{-i(m+1)\psi} \sum_{p=0}^{\infty} \frac{K_{m+p} + i\hat{K}_{m+p}}{p!}\, (\tilde{b})^{\,p}. \tag{4.20}$$

This is the same feed-down structure as (4.18), with $\tilde{\Delta}$ replaced by the orbit-corrected offset $\tilde{b} = e^{-i\psi}(z_0 - \Delta)$. For $z_0 = 0$ the result reduces to (4.18); for a centered magnet ($\Delta = 0$), $\tilde{b}$ captures the intrinsic feed-down from the closed-orbit displacement.

Chapter 5

Synchrotron motion

We collect here some relevant properties and quantities of the longitudinal particle motion.

The momentum compaction factor is defined as:

$$\alpha_c = \frac{\Delta C/C}{\delta} \tag{5.1}$$

where C is the closed orbit path length. The slip factor is defined as (positive above transition):

$$\eta = -\frac{\Delta f/f_0}{\delta} = \alpha_c - \frac{1}{\gamma_0^2} = \frac{1}{\gamma_t^2} - \frac{1}{\gamma_0^2} \tag{5.2}$$

The slippage over a single turn is given by:

$$\Delta\zeta = -\beta_0 c \Delta T = -\beta_0 c (T - T_0) = -\beta_0 c \left(\frac{1}{f} - \frac{1}{f_0} \right) \tag{5.3}$$

$$= -\frac{\beta_0 c}{f_0} \left(\frac{1}{1 + \Delta f/f_0} - 1 \right) \simeq \frac{\beta_0 c}{f_0} \frac{\Delta f}{f_0} = -\eta \frac{\beta_0 c}{f_0} \delta = -\eta C \delta \tag{5.4}$$

The kick in energy from an RF cavity is given by:

$$\Delta E = q V_{RF} \sin\left(2\pi h_{RF} f_0 t + \phi_{RF}\right) \tag{5.5}$$

$$= q V_{RF} \sin\left(-2\pi h_{RF} \frac{\zeta}{C} + \phi_{RF}\right) \tag{5.6}$$

$$= q V_{RF} \sin\left(-2\pi f_{RF} \frac{\zeta}{\beta_0 c} + \phi_{RF}\right) \tag{5.7}$$

from which:

$$\Delta p_\zeta = \frac{\Delta E}{\beta_0^2 E_0} = \frac{q V_{RF}}{\beta_0^2 E_0} \sin\left(-2\pi f_{RF} \frac{\zeta}{\beta_0 c} + \phi_{RF}\right) \tag{5.8}$$

5.1   Linearized motion

We expand around the synchronous fixed point at longitudinal position ζ_0, where the RF frequency is $f_{RF} = h_{RF} f_0 = h_{RF} \beta_0 c / C$:

$$\Delta p_\zeta \approx \frac{q V_{RF}}{\beta_0^2 E_0} \sin \left(-2\pi f_{RF} \frac{\zeta_0}{\beta_0 c} + \phi_{RF} \right) - \frac{2\pi q f_{RF} V_{RF}}{\beta_0^3 E_0 c} (\zeta - \zeta_0) \cos \left(-2\pi f_{RF} \frac{\zeta_0}{\beta_0 c} + \phi_{RF} \right)$$
$$(5.9)$$

We define the synchronous phase as

$$\phi_s = -2\pi f_{RF} \frac{\zeta_0}{\beta_0 c} + \phi_{RF} \tag{5.10}$$

and the longitudinal displacement as

$$\bar{\zeta} = \zeta - \zeta_0 \tag{5.11}$$

obtaining:

$$\Delta p_\zeta \approx \frac{q V_{RF}}{\beta_0^2 E_0} \sin \phi_s - \frac{2\pi q f_{RF} V_{RF}}{\beta_0^3 E_0 c} \bar{\zeta} \cos \phi_s \tag{5.12}$$

We assume that the energy deviation of the stable fixed point is zero, giving

$$\Delta p_\zeta \approx -\frac{2\pi q f_{RF} V_{RF}}{\beta_0^3 E_0 c} \cos \phi_s \bar{\zeta} \tag{5.13}$$

5.2   Smooth approximation

In the smooth approximation we smear the RF kicks and the slippage uniformly along the ring. The equations of motion become:

$$\frac{dp_\zeta}{ds} = \frac{\Delta p_\zeta}{C} = K_s \bar{\zeta} \tag{5.14}$$

$$\frac{d\bar{\zeta}}{ds} = \frac{\Delta \zeta}{C} = -\eta p_\zeta \tag{5.15}$$

where we have used the approximation from Eq. 1.49:

$$\delta \ll 1 \Rightarrow \delta \simeq p_\zeta \tag{5.16}$$

and we have defined the smooth-approximation longitudinal focusing factor:

$$K_s = -\frac{2\pi q V_{RF} f_{RF}}{\beta_0^3 C E_0 c} \cos \phi_s \tag{5.17}$$

We derive the second equation and replace the first:

$$\frac{d^2 \bar{\zeta}}{ds^2} + \eta K_s \bar{\zeta} = 0 \tag{5.18}$$

The motion is stable if

$$\eta K_s > 0 \quad \Leftrightarrow \quad \eta \cos \phi_s < 0 \tag{5.19}$$

In that case the solution is harmonic:

$$\begin{aligned}
\bar{\zeta}(s) &= \bar{\zeta}_A \cos\left(\sqrt{\eta K_s}\, s\right) + B \sin\left(\sqrt{\eta K_s}\, s\right) \\
&= \bar{\zeta}_A \cos\left(2\pi Q_s s / C\right) + B \sin\left(2\pi Q_s s / C\right)
\end{aligned} \tag{5.20}$$

where $\bar{\zeta}_A = \bar{\zeta}(0)$ and $p_{\zeta_A} = p_\zeta(0)$ denote the initial conditions. The synchrotron tune is

$$Q_s = \sqrt{\eta K_s} \frac{C}{2\pi} = \sqrt{-\frac{q\eta f_{RF} C V_{RF}}{2\pi \beta_0^3 E_0 c} \cos \phi_s} \tag{5.21}$$

We replace

$$f_{RF} = \frac{h_{RF} \beta_0 c}{C} \tag{5.22}$$

obtaining:

$$Q_s = \sqrt{-\frac{q\eta h_{RF} V_{RF}}{2\pi \beta_0^2 E_0} \cos \phi_s} \tag{5.23}$$

Replacing Eq. 5.20 in Eq. 5.15:

$$p_\zeta = -\frac{2\pi Q_s}{\eta C}\left(-\bar{\zeta}_A \sin\left(2\pi Q_s s / C\right) + B \cos\left(2\pi Q_s s / C\right)\right) \tag{5.24}$$

Replacing $s = 0$:

$$p_{\zeta_A} = -\frac{2\pi Q_s}{\eta C} B \tag{5.25}$$

from which:

$$B = -\frac{\eta C}{2\pi Q_s} p_{\zeta_A} = -\beta_\zeta p_{\zeta_A}, \tag{5.26}$$

where we have defined:

$$\beta_\zeta = \frac{\eta C}{2\pi Q_s} \tag{5.27}$$

Replacing

$$\bar{\zeta}(s) = \bar{\zeta}_A \cos\left(2\pi Q_s \frac{s}{C}\right) - p_{\zeta_A} \beta_\zeta \sin\left(2\pi Q_s \frac{s}{C}\right) \tag{5.28}$$

$$p_\zeta(s) = \frac{\bar{\zeta}_A}{\beta_\zeta} \sin\left(2\pi Q_s \frac{s}{C}\right) + p_{\zeta_A} \cos\left(2\pi Q_s \frac{s}{C}\right) \tag{5.29}$$

These expressions can be recast in Courant–Snyder form:

$$\bar{\zeta}(s) = \sqrt{\beta_\zeta \, \varepsilon_s} \, \cos\left(2\pi Q_s \frac{s}{C} + \Phi_{s,\bar{\zeta}}\right) \tag{5.30}$$

$$p_\zeta(s) = \sqrt{\frac{\varepsilon_s}{\beta_\zeta}} \, \cos\left(2\pi Q_s \frac{s}{C} + \Phi_{s,p_\zeta}\right) \tag{5.31}$$

with the longitudinal emittance and phases determined by the initial conditions $\bar{\zeta}_A = \bar{\zeta}(0)$ and $p_{\zeta_A} = p_\zeta(0)$:

$$\varepsilon_s = \frac{\bar{\zeta}_A^2}{\beta_\zeta} + \beta_\zeta p_{\zeta_A}^2 \tag{5.32}$$

$$\Phi_{s,\bar{\zeta}} = \mathrm{atan2}\left(\beta_\zeta p_{\zeta_A}, \, \bar{\zeta}_A\right) \tag{5.33}$$

$$\Phi_{s,p_\zeta} = \mathrm{atan2}\left(-\bar{\zeta}_A/\beta_\zeta, \, p_{\zeta_A}\right) \tag{5.34}$$

The two phase offsets differ by $\pi/2$ (modulo 2π), consistently with the sine/cosine quadrature between coordinate and momentum in a simple harmonic oscillator.
In the longitudinal plane we can take the Twiss parameter $\alpha_\zeta = 0$, since the longitudinal focusing is weak compared to the revolution scale and can be treated as constant around the ring.
For a matched bunch with longitudinal emittance ε_s, the rms beam sizes read

$$\sigma_{\bar{\zeta}} = \sqrt{\beta_\zeta \, \varepsilon_s} \tag{5.35}$$

$$\sigma_{p_\zeta} = \sqrt{\frac{\varepsilon_s}{\beta_\zeta}} \tag{5.36}$$

so that

$$\sigma_{\bar{\zeta}} \sigma_{p_\zeta} = \varepsilon_s \tag{5.37}$$

and equivalently

$$\beta_\zeta = \frac{\sigma_{\bar{\zeta}}}{\sigma_{p_\zeta}} \tag{5.38}$$

and the longitudinal envelope rotates in phase space with tune Q_s.

5.3   Kick-drift model

For the kick-drift mode we want to rewrite the Eq. 5.13:

$$\Delta p_\zeta = C K_s \bar{\zeta} \tag{5.39}$$

5.4 Hamiltonian of the synchrotron motion

In this section we use the time in the laboratory frame as independent variable as done in the PyHEADTAIL longitudinal treatment. In this section we also include the effect of a reference momentum change of ΔP_0 per turn.

We assume small energy deviations, hence we can consider the coordinates (ζ, δ) to be canonically conjugate ($\delta \ll 1 \Rightarrow \delta \simeq p_\zeta$ – see Eq. 1.49).

The longitudinal motion can be described by the following Hamiltonian:

$$H(\zeta, \delta) = -\frac{1}{2}\eta\beta_0 c\delta^2 + \frac{\beta_0 c}{C}\frac{\Delta P_0}{P_0}\zeta - \frac{q_0}{P_0}\sum_i \frac{1}{2\pi h_i}V_i\cos\left(-2\pi h_i\frac{\zeta}{C} + \phi_i\right) \tag{5.40}$$

This can be proven using Hamilton's equations:

$$\frac{d\zeta}{dt} = \frac{\partial H}{\partial \delta} = -\eta\beta_0 c\delta \tag{5.41}$$

$$\frac{d\delta}{dt} = -\frac{\partial H}{\partial \zeta} = -\frac{\beta_0 c}{C}\frac{\Delta P_0}{P_0} + \frac{q_0}{P_0 C}\sum_i V_i\sin\left(-2\pi h_i\frac{\zeta}{C} + \phi_i\right) \tag{5.42}$$

The coordinate change over one revolution is:

$$\Delta\zeta = \frac{d\zeta}{dt}\frac{C}{\beta_0 c} = -\eta C\delta \tag{5.43}$$

$$\Delta\delta = \frac{d\delta}{dt}\frac{C}{\beta_0 c} = -\frac{\Delta P_0}{P_0} + \frac{q_0}{\beta_0 c P_0}\sum_i V_i\sin\left(-2\pi h_i\frac{\zeta}{C} + \phi_i\right) \tag{5.44}$$

which are consistent with those found in Sec. 5.

5.4.1 Fixed points

The fixed points can be found by imposing $\Delta\zeta = 0$ and $\Delta\delta = 0$. If only a single harmonic is present a closed solution can be found:

$$-\frac{\Delta P_0}{P_0} + \frac{q_0}{\beta_0 c P_0}V_{\text{RF}}\sin\left(-2\pi h_{\text{RF}}\frac{\zeta}{C} + \phi_i\right) = 0 \tag{5.45}$$

We want to get an explicit expression for ζ:

$$\frac{\Delta P_0 \beta_0 c}{q_0 V_{\text{RF}}} = \sin\left(-2\pi h_{\text{RF}}\frac{\zeta}{C} + \phi_i\right) \tag{5.46}$$

There are two families of solutions:

$$\arcsin\left(\frac{\Delta P_0 \beta_0 c}{q_0 V_{\text{RF}}}\right) + 2n\pi = -2\pi h_{\text{RF}}\frac{\zeta}{C} + \phi_{\text{RF}} \tag{5.47}$$

$$\pi - \arcsin\left(\frac{\Delta P_0 \beta_0 c}{q_0 V_{\text{RF}}}\right) + 2n\pi = -2\pi h_{\text{RF}}\frac{\zeta}{C} + \phi_{\text{RF}} \tag{5.48}$$

where n is an integer number. Depending on the sign of η only one family of fixed points is stable.

We solve for ζ:

$$\zeta = \frac{C}{2\pi h_{\mathrm{RF}}} \left(\phi_{\mathrm{RF}} - \arcsin\left(\frac{\Delta P_0 \beta_0 c}{q_0 V_{\mathrm{RF}}} \right) + 2n\pi \right) \tag{5.49}$$

$$\zeta = \frac{C}{2\pi h_{\mathrm{RF}}} \left(\phi_{\mathrm{RF}} + \pi + \arcsin\left(\frac{\Delta P_0 \beta_0 c}{q_0 V_{\mathrm{RF}}} \right) + 2n\pi \right) \tag{5.50}$$

It is possible to set ϕ_{RF} to place a fixed point of either family in $\zeta = 0$:

$$\phi_{\mathrm{RF}} = \arcsin\left(\frac{\Delta P_0 \beta_0 c}{q_0 V_{\mathrm{RF}}} \right) \tag{5.51}$$

$$\phi_{\mathrm{RF}} = \pi - \arcsin\left(\frac{\Delta P_0 \beta_0 c}{q_0 V_{\mathrm{RF}}} \right) \tag{5.52}$$

It can be shown that, to have a stable fixed point in $\zeta = 0$, one needs to use Eq. 5.51 when $\eta < 0$ (below transition) and Eq. 5.52 when $\eta > 0$ (above transition).

Chapter 6

Counter-rotating beams

In machines having counter-rotating beams, such as the LHC, it is useful to be able to express beam coordinates for one of the beams in the reference frame of the other. Furthermore it is also useful to be able to define the two sequences using the same orientation. For the LHC, for example, the sequence of the LHC beam 2 is defined following the orientation of the LHC beam 1. In this case the properties of the elements are specified in such a way that the built sequence is able to backtrack the physical beam and the sequence required to track the physical beam (usually called Beam 4 sequence) can be obtained with suitable transformations.

6.1 Reversed reference frame

The reference frames for beam 4 and beam 2 are related by the following transformations:

$$\tilde{x} = -x \tag{6.1}$$
$$\tilde{y} = y \tag{6.2}$$
$$\tilde{s} = -s \tag{6.3}$$
$$\tilde{t} = -t \tag{6.4}$$
$$\tilde{\zeta} = -\zeta \tag{6.5}$$
$$\tilde{p_x} = p_x \tag{6.6}$$
$$\tilde{p_y} = -p_y \tag{6.7}$$
$$\tilde{p_\zeta} = p_\zeta \tag{6.8}$$
$$\tilde{\delta} = \delta \tag{6.9}$$

where the tilde indicates the coordinates in the reversed reference frame.

6.2 Transformation of beam elements

The elements are transformed in such a way that the map implements the backtrack of the physical beam as seen in the reversed reference frame.

6.2.1   Horizontal deflecting cavity

In the case of a horizontal deflecting cavity we can proceed as follows.
For Beam 4 we can write:

$$\Delta p_x = V_x \sin(\phi - \omega t) \tag{6.10}$$

and for Beam 2 we can write:

$$\Delta \tilde{p}_x = \tilde{V}_x \sin(\tilde{\phi} - \omega \tilde{t}), \tag{6.11}$$

Since we define the element as backtracking we can write:

$$\Delta \tilde{p}_x = - \Delta p_x \tag{6.12}$$

where the minus sign comes from the backtracking and no additional sign change
comes from the reference frame transformation (see Eq. 6.6).
Combining the equations above we obtain:

$$\tilde{V}_x \sin(\tilde{\phi} - \omega \tilde{t}) = - V_x \sin(\phi - \omega t) \tag{6.13}$$

Using Eq. 6.4 we can write:

$$\tilde{V}_x \sin(\tilde{\phi} + \omega t) = - V_x \sin(\phi - \omega t) \tag{6.14}$$

We choose to reverse the voltage definition since also the electric field is expressed in
the reversed reference frame:

$$\boxed{\tilde{V}_x = - V_x} \tag{6.15}$$

obtaining:

$$\sin(\tilde{\phi} + \omega t) = \sin(\phi - \omega t) \tag{6.16}$$

Using trigonometric properties we can write:

$$- \sin(-\tilde{\phi} - \omega t) = \sin(\phi - \omega t) \tag{6.17}$$

and then:

$$\sin(\pi - \tilde{\phi} - \omega t) = \sin(\phi - \omega t) \tag{6.18}$$

From this we obtain:

$$\boxed{\tilde{\phi} = \pi - \phi} \tag{6.19}$$

6.2.2   Vertical deflecting cavity

The case of a vertical deflecting cavity is similar but not identical.
For Beam 4 we can write:

$$\Delta p_y = V_y \sin(\phi - \omega t) \tag{6.20}$$

and for Beam 2 we can write:

$$\Delta \tilde{p}_y = \tilde{V}_y \sin(\tilde{\phi} - \omega \tilde{t}), \tag{6.21}$$

Since we define the element as backtracking we can write:

$$\Delta \tilde{p}_y = -(-\Delta p_y) \tag{6.22}$$

where one minus sign comes from the backtracking and an additional sign change comes from the reference frame transformation (see Eq. 6.7).
Combining the equations above we obtain:

$$\tilde{V}_y \sin(\tilde{\phi} - \omega \tilde{t}) = V_y \sin(\phi - \omega t) \tag{6.23}$$

Using Eq. 6.4 we can write:

$$\tilde{V}_y \sin(\tilde{\phi} + \omega t) = -V_y \sin(\phi - \omega t) \tag{6.24}$$

We do not reverse the voltage definition as the vertical component of the electric field does not change sign due to the reference frame transformation:

$$\boxed{\tilde{V}_y = V_y} \tag{6.25}$$

Hence we obtain:

$$\sin(\tilde{\phi} + \omega t) = \sin(\phi - \omega t) \tag{6.26}$$

Using trigonometric properties we can write:

$$-\sin(-\tilde{\phi} - \omega t) = \sin(\phi - \omega t) \tag{6.27}$$

and then:

$$\sin(\pi - \tilde{\phi} - \omega t) = \sin(\phi - \omega t) \tag{6.28}$$

From this we obtain:

$$\boxed{\tilde{\phi} = \pi - \phi} \tag{6.29}$$

Chapter 7

Synchrotron radiation

We collect here some relevant properties of synchrotron radiation [28]:
We assume $B = |B_\perp|$.
Classical particle radius:

$$r_0 = Q^2 / \left(4\pi\epsilon_0 m_0 c^2\right) \tag{7.1}$$

Curvature, rigidity, field:

$$\frac{1}{\rho} = \frac{QB}{p} = \frac{QB}{m_0 c \beta \gamma} \tag{7.2}$$

Emitted power:

$$P_s = \frac{2r_0 c^3 Q^2 \beta^2 \gamma^2 B^2}{3m_0 c^2} \tag{7.3}$$

Critical frequency:

$$\omega_c = \frac{3Q\beta^2\gamma^2 B}{2m_0} \tag{7.4}$$

Critical energy:

$$E_{\gamma c} = \hbar\omega_c = \frac{3Q\hbar\beta^2\gamma^2 B}{2m_0} \tag{7.5}$$

Number of photons per unit time:

$$\dot{n}_s = \frac{15\sqrt{3}}{8} \frac{P_s}{E_{\gamma c}} = \frac{60\sqrt{3}}{72} \frac{r_0 c Q B}{\hbar} \tag{7.6}$$

Average photon energy:

$$\langle E_\gamma \rangle = \frac{8\sqrt{3}}{45} E_{\gamma c} = \frac{8\sqrt{3}}{15} \frac{Q\hbar\beta^2\gamma^2 B}{2m_0} \tag{7.7}$$

Photon energy variance:

$$\left\langle E_\gamma^2 \right\rangle = \frac{11}{27} E_{\gamma c}^2 = \frac{11}{12} \frac{Q^2\hbar^2\beta^4\gamma^4 B^2}{m_0^2} \tag{7.8}$$

$$\left\langle \dot{n}_s \Delta \delta^2 \right\rangle = \frac{\left\langle \dot{n}_s E_\gamma^2 \right\rangle}{E_0^2} = \frac{11}{12} \frac{1}{m_0^2 c^4 \gamma_0^2} \frac{Q^2 \hbar^2 \beta^4 \gamma^4 B^2}{m_0^2} \frac{60\sqrt{3}}{72} \frac{cQB}{\hbar} \frac{Q^2}{4\pi\epsilon_0 m_0 c^2} \tag{7.9}$$

The algorithm to generate photon energies with the appropriate distribution is described in [29].

7.1 Damping from synchrotron radiation

The damping constants from synchrotron radiation can be easily obtained from magnitude of the eigenvalues of the one-turn matrix:

$$\alpha_x = -\log(|\lambda_x|) \tag{7.10}$$
$$\alpha_y = -\log(|\lambda_y|) \tag{7.11}$$
$$\alpha_\zeta = -\log(|\lambda_\zeta|) \tag{7.12}$$

The damping acts such that:

$$\frac{1}{A_x} \frac{dA_x}{dt} = -\frac{\alpha_x}{T_0} \tag{7.13}$$

where T_0 is the revolution period. From Eq. 3.49 we obtain:

$$\frac{dJ_x}{dt} = -\frac{2\alpha_x}{T_0} J_x \tag{7.14}$$

By averaging over the beam distribution we obtain:

$$\frac{d\varepsilon_x}{dt} = -\frac{2\alpha_x}{T_0} \varepsilon_x \tag{7.15}$$

7.2 Equilibrium emittance

This section is based on the approach described in [30].
To account for the kicks experienced by the particles due to quantum excitation we note that the transverse momentum change due to an energy kick in the direction of the particle motion can be written as:

$$P_{x,y}^{\text{new}} = P_{x,y}^{\text{old}} \frac{P^{\text{new}}}{P^{\text{old}}} \tag{7.16}$$

From this:

$$P_{x,y}^{\text{new}} - P_{x,y}^{\text{old}} = P_{x,y}^{\text{old}} \left(\frac{P^{\text{new}} - P^{\text{old}}}{P^{\text{old}}} \right) \tag{7.17}$$

Dividing by P_0:

$$\frac{P_{x,y}^{\text{new}} - P_{x,y}^{\text{old}}}{P_0} = \frac{P_{x,y}^{\text{old}}}{P_0} \left(\frac{P^{\text{new}} - P^{\text{old}}}{P_0} \right) \frac{P_0}{P^{\text{old}}} \tag{7.18}$$

Using the accelerator coordinates definitions (Eqs. 1.34 and 1.35), we obtain:

$$\Delta p_{x,y} = \frac{p_{x,y}}{1+\delta}\Delta\delta \tag{7.19}$$

The corresponding change in normalized coordinates can be computed from Eq. 3.46:

$$
\begin{pmatrix}
\Delta\tilde{x} \\
\Delta\tilde{p}_x \\
\Delta\tilde{y} \\
\Delta\tilde{p}_y \\
\Delta\tilde{\zeta} \\
\Delta\tilde{p}_\zeta
\end{pmatrix}
= W^{-1}
\begin{pmatrix}
0 \\
\dfrac{p_x}{1+\delta}\Delta\delta \\
0 \\
\dfrac{p_y}{1+\delta}\Delta\delta \\
0 \\
\Delta\delta
\end{pmatrix}
\tag{7.20}
$$

Using the Eq. 3.21 we obtain:

$$\Delta\hat{x} = \mathcal{K}_x\Delta\delta \tag{7.21}$$
$$\Delta\hat{p}_x = \mathcal{K}_{p_x}\Delta\delta \tag{7.22}$$
$$\Delta\hat{y} = \mathcal{K}_y\Delta\delta \tag{7.23}$$
$$\Delta\hat{p}_y = \mathcal{K}_{p_y}\Delta\delta \tag{7.24}$$
$$\Delta\hat{\zeta} = \mathcal{K}_\zeta\Delta\delta \tag{7.25}$$
$$\Delta\hat{p}_\zeta = \mathcal{K}_{p_\zeta}\Delta\delta \tag{7.26}$$

where:

$$\mathcal{K}_x = \left(\frac{a_{11}p_x + a_{13}p_y}{1+\delta} + a_{15}\right) \tag{7.27}$$

$$\mathcal{K}_{p_x} = \left(\frac{b_{11}p_x + b_{13}p_y}{1+\delta} + b_{15}\right) \tag{7.28}$$

$$\mathcal{K}_y = \left(\frac{a_{21}p_x + a_{23}p_y}{1+\delta} + a_{25}\right) \tag{7.29}$$

$$\mathcal{K}_{p_y} = \left(\frac{b_{21}p_x + b_{23}p_y}{1+\delta} + b_{25}\right) \tag{7.30}$$

$$\mathcal{K}_\zeta = \left(\frac{a_{31}p_x + a_{33}p_y}{1+\delta} + a_{35}\right) \tag{7.31}$$

$$\mathcal{K}_{p_\zeta} = \left(\frac{b_{31}p_x + b_{33}p_y}{1+\delta} + b_{35}\right) \tag{7.32}$$

The change in action (see Eq. 3.48) associated to the first mode, due to the emission of

a photon can be written as:

$$\Delta J_x = \frac{1}{2}\left[(\hat{x} + \Delta\hat{x})^2 + (\hat{p}_x + \Delta\hat{p}_x)^2 - \hat{x}^2 - \hat{p}_x^2\right] \tag{7.33}$$

$$= \frac{1}{2}\left[\Delta\hat{x}^2 + \Delta\hat{p}_x^2 + 2\hat{x}\Delta\hat{x} + 2\hat{p}_x\Delta\hat{p}_x\right] \tag{7.34}$$

Averaging over all particles in the beam we obtain:

$$\Delta\varepsilon_x = <\Delta J_x> = \frac{1}{2}\left(<\Delta\hat{x}^2> + <\Delta\hat{p}_x^2>\right) \tag{7.35}$$

Using Eqs. 7.21 and 7.22 we obtain:

$$\Delta\varepsilon_x = <\Delta J_x> = \frac{1}{2}\left(\mathcal{K}_x^2 + \mathcal{K}_{p_x}^2\right)<\Delta\delta^2> \tag{7.36}$$

Assuming that the kicks are uncorrelated we can obtain the emittance growth rate from quantum excitation integrating over a full turn:

$$\left(\frac{d\varepsilon_x}{dt}\right)_{\text{quant}} = \frac{1}{2T_0 c}\int_0^C \left(\mathcal{K}_x^2 + \mathcal{K}_{p_x}^2\right)<\dot{N}\Delta\delta^2> ds \tag{7.37}$$

where $\dot{N}$ is the photon emission rate (number of photons per unit time), T_0 is the revolution period, C is the circumference.

By summing Eqs. 7.15 and 7.37 we obtain the total instantaneous growth rate:

$$\frac{d\varepsilon_x}{dt} = \left(\frac{d\varepsilon_x}{dt}\right)_{\text{damp}} + \left(\frac{d\varepsilon_x}{dt}\right)_{\text{quant}} = -\frac{2\alpha_x}{T_0}\varepsilon_x + \frac{1}{2T_0 c}\int_0^C \left(\mathcal{K}_x^2 + \mathcal{K}_{p_x}^2\right)<\dot{N}\Delta\delta^2> ds$$

$$\tag{7.38}$$

By imposing the derivative to be zero we obtain the value of the equilibrium emittance:

$$\varepsilon_x = \frac{1}{4\alpha_x c}\int_0^C \left(\mathcal{K}_x^2 + \mathcal{K}_{p_x}^2\right)<\dot{N}\Delta\delta^2> ds \tag{7.39}$$

In the ultra-relativistic approximation:

$$<\dot{N}\Delta\delta^2> = \frac{<\dot{N}(\Delta E)^2>}{E_0^2} \tag{7.40}$$

7.3 Radiation integrals

Xsuite can compute the following radiation integrals:

$$I_1 = \oint \left(h_{0x} D_x + h_{0y} D_y \right) \, \mathrm{d}s \tag{7.41}$$

$$I_2 = \oint |h|^2 \, \mathrm{d}s \tag{7.42}$$

$$I_3 = \oint |h|^3 \, \mathrm{d}s \tag{7.43}$$

$$I_{4x} = \oint \left(|h|^2 h_{0x} + 2 h_x k_1 \right) D_x \, \mathrm{d}s \tag{7.44}$$

$$I_{4y} = \oint \left(|h|^2 h_{0y} - 2 h_y k_1 \right) D_y \, \mathrm{d}s \tag{7.45}$$

$$I_4 = I_{4x} + I_{4y} = \oint \left[2 k_1 \left(h_x D_x - h_y D_y \right) + |h|^2 (h_{0x} D_x + h_{0y} D_y) \right] \, \mathrm{d}s \tag{7.46}$$

$$I_{5x} = \oint h^3 \mathcal{H}_x \, \mathrm{d}s \tag{7.47}$$

$$I_{5y} = \oint h^3 \mathcal{H}_y \, \mathrm{d}s \tag{7.48}$$

The following quantities are used in the calculation.

- Horizontal and curvature of the particle trajectory:

$$h_x = \frac{B_y Q}{m_0 c \gamma} \tag{7.49}$$

$$h_y = -\frac{B_x Q}{m_0 c \gamma} \tag{7.50}$$

- Total transverse curvature and relation to the transverse magnetic field:

$$h = \sqrt{h_x^2 + h_y^2} \tag{7.51}$$

which is related to the transverse magnetic field by:

$$B = \sqrt{B_x^2 + B_y^2} = h \frac{m_0 \beta c \gamma}{Q} \tag{7.52}$$

- "Curly H" functions:

$$\mathcal{H}_x = \gamma_x D_x^2 + 2 \alpha_x D_x D_x' + \beta_x D_x'^2 \tag{7.53}$$
$$\mathcal{H}_y = \gamma_y D_y^2 + 2 \alpha_y D_y D_y' + \beta_y D_y'^2 \tag{7.54}$$

- The derivative of the dispersion $D_{x,y}'$ can be obtained from the transverse momentum dispersion $D_{p_{x,y}}$ using the relation:

$$D_{x,y}' = \frac{\mathrm{d} D_{x,y}}{\mathrm{d}s} = \frac{\mathrm{d}x'}{\mathrm{d}\delta} = \frac{\mathrm{d}}{\mathrm{d}\delta} \frac{p_{x,y}}{1 + \delta} = (1 - \delta) D_{p_{x,y}} - p_{x,y} \tag{7.55}$$

- h_{0x} and h_{0y} are the curvatures of the reference trajectory. The path length on the particle trajectory is related to the path length on the reference trajectory by:

$$\mathrm{d}s' = (1 + h_{0x}x + h_{0y}y)\,\mathrm{d}s \tag{7.56}$$

The radiation integrals can be used to compute the following quantities (where C_0 is the ring circumference, r_0 is the classical particle radius, $\hbar$ is the reduced Planck's constant) :

- Momentum compaction factor (unitless):

$$\alpha_c = \frac{I_1}{C_0} \tag{7.57}$$

- Energy loss per turn:

$$U_s = \frac{2}{3}r_0 E_0 \gamma^3 I_2 \tag{7.58}$$

- Damping partition numbers:

$$J_x = 1 - \frac{I_{4x}}{I_2} \tag{7.59}$$

$$J_y = 1 - \frac{I_{4y}}{I_2} \tag{7.60}$$

$$J_z = 2 + \frac{I_4}{I_2} \tag{7.61}$$

  which satisfy Robinson's theorem:

$$J_x + J_y + J_z = 4 \tag{7.62}$$

- Longitudinal damping rate in $[\mathrm{s}^{-1}]$:

$$\alpha_\epsilon = \frac{cr_0\gamma^3}{3C_0}(2I_2 + I_4) \tag{7.63}$$

- Transverse damping rates in $[\mathrm{s}^{-1}]$:

$$\alpha_x = \frac{cr_0\gamma^3}{3C_0}(I_2 - I_{4x}) \tag{7.64}$$

$$\alpha_y = \frac{cr_0\gamma^3}{3C_0}(I_2 - I_{4y}) \tag{7.65}$$

- Energy spread (unitless):

$$\sigma_\delta^2 = \frac{55\sqrt{3}}{96}\frac{\hbar\gamma^2}{m_0 c}\frac{I_3}{2I_2 + I_4} \tag{7.66}$$

- Transverse equilibrium emittances in $[\mathrm{m\ rad}]$:

$$\epsilon_x = \frac{55\sqrt{3}}{96}\frac{\hbar\gamma^2}{m_0 c}\frac{I_{5x}}{I_2 - I_{4x}} \tag{7.67}$$

$$\epsilon_y = \frac{55\sqrt{3}}{96}\frac{\hbar\gamma^2}{m_0 c}\frac{I_{5y}}{I_2 - I_{4y}} \tag{7.68}$$

7.3.1 Derivations

7.3.1.1 Energy Loss and Second Radiation Integral

From the instantaneous radiated power,

$$P_s = \frac{2}{3} \frac{c^3 r_0 Q^2 E^2 B^2}{(m_0 c^2)^3} = \frac{2}{3} c r_0 E \gamma^3 |h|^2 \tag{7.69}$$

The energy loss per turn is obtained by integration around one turn.

$$U_s = \int P_s(t) \, \mathrm{d}t \approx \frac{1}{c} \oint P_s(s') \, \mathrm{d}s' = \frac{2}{3} r_0 E \gamma^3 \oint |h|^2 \, \mathrm{d}s' \tag{7.70}$$

We can assume $(h_{0x} x + h_{0y} y) \ll 1$, obtaining:

$$U_s = \frac{2}{3} r_0 E \gamma^3 I_2 \tag{7.71}$$

where we have defined the second radiation integral:

$$I_2 = \oint |h|^2 \, \mathrm{d}s \tag{7.72}$$

7.3.1.2 Longitudinal Damping Rate and Fourth Radiation Integral

Following Hofmann's analysis, the longitudinal damping rate can be written as [28]:

$$\alpha_\epsilon = \frac{1}{2} \frac{1}{T_{\mathrm{rev}}} \frac{\mathrm{d}U_s}{\mathrm{d}E} \tag{7.73}$$

We calculate:

$$\frac{\mathrm{d}U_s}{\mathrm{d}E} = \frac{1}{c} \frac{\mathrm{d}}{\mathrm{d}E} \oint P_s(s') \, \mathrm{d}s' = \frac{1}{c} \frac{\mathrm{d}}{\mathrm{d}E} \oint P_s \left(1 + h_{0x} x(E) + h_{0y} y(E)\right) \mathrm{d}s \tag{7.74}$$

Using the dispersion to express $x(E)$ and $y(E)$:

$$\frac{\mathrm{d}U_s}{\mathrm{d}E} = \frac{\mathrm{d}}{\mathrm{d}E} \frac{1}{c} \oint P_s \left(1 + h_{0x} D_x \delta + h_{0y} D_y \delta\right) \mathrm{d}s \tag{7.75}$$

The derivative w.r.t. E is related to the derivative w.r.t. δ by:

$$\frac{\mathrm{d}}{\mathrm{d}E} = \frac{\mathrm{d}\delta}{\mathrm{d}E} \frac{\mathrm{d}}{\mathrm{d}\delta} = \frac{\mathrm{d}}{\mathrm{d}E} \left(\frac{E - E_0}{E_0}\right) \frac{\mathrm{d}}{\mathrm{d}\delta} = \frac{1}{E_0} \frac{\mathrm{d}}{\mathrm{d}\delta} \tag{7.76}$$

Writing out the derivative then gives:

$$\begin{aligned}
\frac{\mathrm{d}U_s}{\mathrm{d}E} &= \frac{1}{c} \oint \frac{\mathrm{d}P_s}{\mathrm{d}E} \left(1 + h_{0x} D_x \delta + h_{0y} D_y \delta\right) + \frac{P_s}{E_0} \frac{\mathrm{d}}{\mathrm{d}\delta} \left(1 + h_{0x} D_x \delta + h_{0y} D_y \delta\right) \mathrm{d}s \\
&= \frac{1}{c} \oint \frac{\mathrm{d}P_s}{\mathrm{d}E} \left(1 + h_{0x} D_x \delta + h_{0y} D_y \delta\right) + \frac{P_s}{E_0} \left(h_{0x} D_x + h_{0y} D_y\right) \mathrm{d}s
\end{aligned} \tag{7.77}$$

The derivative of P_s w.r.t. E can be rewritten as:

$$\frac{dP_s}{dE} = 2P_s \left[\frac{1}{E} + \frac{1}{B} \left(\frac{\partial B}{\partial x} \frac{dx}{dE} + \frac{\partial B}{\partial y} \frac{dy}{dE} \right) \right] \tag{7.78}$$

The derivatives of the positions w.r.t. E are related to the dispersions through Eq. 7.76

$$\frac{dx}{dE} = \frac{1}{E_0} \frac{dx}{d\delta} = \frac{1}{E_0} D_x \tag{7.79}$$

$$\frac{dy}{dE} = \frac{1}{E_0} \frac{dy}{d\delta} = \frac{1}{E_0} D_y \tag{7.80}$$

Using the fact that $B = \sqrt{B_x^2 + B_y^2}$, the derivatives of B w.r.t. x and y are:

$$\frac{\partial B}{\partial x} = \frac{B_x}{B} \frac{\partial B_x}{\partial x} + \frac{B_y}{B} \frac{\partial B_y}{\partial x} \tag{7.81}$$

$$\frac{\partial B}{\partial y} = \frac{B_x}{B} \frac{\partial B_x}{\partial y} + \frac{B_y}{B} \frac{\partial B_y}{\partial y} \tag{7.82}$$

The magnetic field gradients are defined as:

$$\frac{\partial B_y}{\partial x} = \frac{\partial B_x}{\partial y} = G = \frac{\gamma_0 m_0 c}{Q_0} k_1 \tag{7.83}$$

$$\frac{\partial B_x}{\partial x} = -\frac{\partial B_y}{\partial y} = \bar{G} = \frac{\gamma_0 m_0 c}{Q_0} \bar{K}_1 \tag{7.84}$$

Here, k_1 is the normalised normal quadrupole strength and $\bar{K}_1$ is the normalised skew quadrupole strength, both in units of $1/m^2$. In the following we neglect the skew quadrupole component and we assume that for the closed orbit we can assume $\gamma \simeq \gamma_0$, obtaining:

$$\frac{dP_s}{dE} = 2P_s \left[\frac{1}{E} + \frac{1}{E_0} \frac{\gamma m_0 c}{Q_0} \frac{k_1}{B^2} \left(B_y D_x + B_x D_y \right) \right] \tag{7.85}$$

The curvatures in Eqs. (7.49), (7.50) and (7.52) can be substituted, which gives:

$$\frac{dP_s}{dE} = 2\frac{P_s}{E} \left[\frac{1}{E} + \frac{1}{E_0} \frac{k_1}{h^2} \left(h_x D_x - h_y D_y \right) \right] \tag{7.86}$$

Substituting Eq. (7.69) gives:

$$\frac{dP_s}{dE} = \frac{4}{3} cr_0 E \gamma^3 \left[\frac{|h|^2}{E} + \frac{1}{E_0} k_1 \left(h_x D_x - h_y D_y \right) \right] \tag{7.87}$$

Substituting this expression back in Eq. (7.74) gives:

$$\frac{dU_s}{dE} = \frac{2}{3} \frac{cr_0 E \gamma^3}{c} \oint \left[2\frac{|h|^2}{E} (1 + h_{0x} x + h_{0y} y) + 2\frac{k_1}{E_0} \left(h_x D_x - h_y D_y \right) (1 + h_{0x} x + h_{0y} y) \right.$$
$$\left. + \frac{|h|^2}{E_0} (h_{0x} D_x + h_{0y} D_y) \right] ds \tag{7.88}$$

The first term can be identified as I_2, again we assume that $h_{0x}x + h_{0y}y \ll 1$ and, as stated above on the closed orbit we assume $E/E_0 \approx 1$. Hence, we can write:

$$\frac{\mathrm{d}U_s}{\mathrm{d}E} = \frac{2}{3}r_0\gamma^3 \left[2I_2 + \oint \left[2k_1 \left(h_x D_x - h_y D_y \right) + |h|^2 (h_{0x}D_x + h_{0y}D_y) \right] \mathrm{d}s \right] \qquad (7.89)$$

The last integral is identified as the fourth radiation integral, I_4, given by:

$$I_4 = \oint \left[2k_1 \left(h_x D_x - h_y D_y \right) + |h|^2 (h_{0x}D_x + h_{0y}D_y) \right] \mathrm{d}s \qquad (7.90)$$

Hence we can write:

$$\frac{\mathrm{d}U_s}{\mathrm{d}E} = \frac{2}{3}r_0\gamma^3 (2I_2 + I_4) \qquad (7.91)$$

The longitudinal damping rate is obtained by substituting this expression in Eq. (7.73):

$$\alpha_\epsilon = \frac{1}{3} \frac{r_0\gamma^3}{T_{\mathrm{rev}}} (2I_2 + I_4) \qquad (7.92)$$

7.3.1.3   Energy Spread and Third Radiation Integral

From Hofmann, the variance in the amplitude of a damped oscillator that is excited by a short pulse $a\delta(t)$ is given by [28]:

$$\left\langle x^2 \right\rangle = \frac{\dot{n} \left\langle a^2 \right\rangle}{4\alpha} \qquad (7.93)$$

Here, x is the deflection of the oscillator, $\dot{n}$ is the average rate at which excitation occurs, a is the amplitude of the excitation and α is the damping rate of the oscillator. For quantum excitation of the longitudinal emittance, we identify x as the RMS energy $\mathrm{d}E$, $\dot{n}$ as the average rate of photon emission, a as the photon energy and α as α_ϵ, the longitudinal damping rate. The normalised variance is then:

$$\frac{\left\langle \mathrm{d}E^2 \right\rangle}{E_0^2} = \frac{\dot{n} \left\langle E_\gamma^2 \right\rangle}{4\alpha_\epsilon E_0^2} \qquad (7.94)$$

The rate of photon emission is given by:

$$\dot{n} = \frac{60\sqrt{3}}{72} \frac{r_0 c Q B}{\hbar} \qquad (7.95)$$

The variance in the photon energy is given by:

$$\left\langle E_\gamma^2 \right\rangle = \frac{11}{12} \frac{Q^2 \hbar^2 \gamma^4 B^2}{m_0^2} \qquad (7.96)$$

and the longitudinal damping rate is given by Eq. (7.92): Combining all these terms leads to

$$\frac{\left\langle \mathrm{d}E^2 \right\rangle}{E_0^2} = \frac{60\sqrt{3}}{72} \frac{11}{12} \frac{3}{4} \frac{r_0 c Q B}{\hbar} \frac{Q^2 \hbar^2 \gamma^4 B^2}{m_0^2 E_0^2} \frac{C_0}{c r_0 \gamma^3} \frac{1}{2I_2 + I_4} \qquad (7.97)$$

This simplifies to

$$\frac{\langle dE^2 \rangle}{E_0^2} = \frac{55\sqrt{3}}{96} \frac{Q^3 \hbar \gamma B^3 C_0}{m_0^2 E_0^2} \frac{1}{2I_2 + I_4} \tag{7.98}$$

The curvature h can be substituted for B, which gives

$$\frac{\langle dE^2 \rangle}{E_0^2} = \frac{55\sqrt{3}}{96} \frac{\hbar m_0 \gamma^4 c^3 C_0}{E_0^2} \frac{h^3}{2I_2 + I_4} \tag{7.99}$$

Now averaging over the entire circumference of the ring gives

$$\left\langle \frac{\langle dE^2 \rangle}{E_0^2} \right\rangle_{\text{ring}} = \frac{55\sqrt{3}}{96} \frac{\hbar \gamma^2 C_0}{m_0 c} \frac{\frac{1}{C_0} \oint h^3 \, ds'}{2I_2 + I_4} = \frac{55\sqrt{3}}{96} \frac{\hbar \gamma^2}{m_0 c} \frac{\oint h^3 \, ds'}{2I_2 + I_4} \tag{7.100}$$

The integral in the numerator can be defined as

$$I_3 = \oint |h|^3 \, ds' = \oint |h|^3 (1 + h_{0x} x + h_{0y} y) \, ds \tag{7.101}$$

This is the third radiation integral. This way, the energy spread becomes

$$\left\langle \frac{\langle dE^2 \rangle}{E_0^2} \right\rangle_{\text{ring}} = \frac{55\sqrt{3}}{96} \frac{\hbar \gamma^2}{m_0 c} \frac{I_3}{2I_2 + I_4} \tag{7.102}$$

7.3.1.4   Transverse Damping Rates

The derivation in this section is valid for either x or y. To this end, u will be used as a substitute for either x or y. The goal is to find the rate at which the transverse emittance, ϵ_u, decreases. The emittance is given by

$$\epsilon_u = \gamma_u u_\beta^2 + 2\alpha_u u_\beta u_\beta' + \beta_u u_\beta'^2 \tag{7.103}$$

Here, subscript β indicates that the betatron component of the coordinate value. The total coordinates, u and u' are a combination of the to betatron and an energy deviation δ parts, that is

$$u = u_\beta + u_\delta \tag{7.104}$$
$$u' = u_\beta' + u_\delta' \tag{7.105}$$

When a photon is emitted, the coordinate does not change. This means that

$$du = du_\beta + du_\delta = 0 \tag{7.106}$$

The change in position due to an energy deviation is related to the dispersion through

$$du_\delta = D_u d\delta = D_u \frac{dE}{E_0} = -D_u \frac{dE_\gamma}{E_0} \tag{7.107}$$

Therefore

$$\mathrm{d}u_\beta = -\mathrm{d}u_\delta = D_u \frac{\mathrm{d}E_\gamma}{E_0} \qquad (7.108)$$

where $\mathrm{d}E_\gamma$ is the energy of the emitted photon. The angle is allowed to change due to the photon emission, that is

$$\mathrm{d}u' = \mathrm{d}u'_\beta + \mathrm{d}u'_\delta \qquad (7.109)$$

We want to express $\mathrm{d}u'$ in terms of the photon energy. To this end, assume that the particle before photon emission is on-momentum, such that

$$u'_1 = u'_\beta \qquad (7.110)$$

Following Hoffman we can write [28]:

$$u'_{2\beta} - u'_{1\beta} = \mathrm{d}u_\beta = -\left(u'_{1\beta} - D'\right)\frac{\mathrm{d}E_\gamma}{E_0} \qquad (7.111)$$

Note that the emittance only depends on u_β and u'_β. The change in emittance is:

$$\mathrm{d}\epsilon_u = 2\left(\gamma_u u_\beta \,\mathrm{d}u_\beta + \alpha_u(u_\beta \,\mathrm{d}u'_\beta + u'_\beta \,\mathrm{d}u_\beta) + \gamma_u u'_\beta \,\mathrm{d}u'_\beta\right) \qquad (7.112)$$

Substituting Equations (7.108) and (7.111) gives

$$\mathrm{d}\epsilon_u = 2\left[\gamma_u u_\beta D_u \frac{\mathrm{d}E_\gamma}{E_0} + \alpha_u\left(-u_\beta\left(u'_\beta - D'\right)\frac{\mathrm{d}E_\gamma}{E_0} + u'_\beta D_u \frac{\mathrm{d}E_\gamma}{E_0}\right) - \beta_u u'_\beta\left(u'_\beta - D'\right)\frac{\mathrm{d}E_\gamma}{E_0}\right]$$

$$(7.113)$$

$$= -2\frac{\mathrm{d}E_\gamma}{E_0}\left[\left(\alpha_u u_\beta u'_\beta + \beta_u u'^2_\beta\right) - \left(\gamma_u D_u u_\beta + \alpha_x(D_u u'_\beta + D'_u u_\beta) + \beta_u D'_u u'_\beta\right)\right]$$

$$(7.114)$$

The instantaneous power radiated by a particle undergoing betatron oscillations can be expressed as:

$$P_{s'} = P_s + \frac{\mathrm{d}P_s}{\mathrm{d}u}u_\beta \qquad (7.115)$$

Using the chain rule for the derivative gives:

$$\frac{\mathrm{d}P_s}{\mathrm{d}u} = \frac{\mathrm{d}P_s}{\mathrm{d}B}\frac{\mathrm{d}B}{\mathrm{d}u} = 2\frac{P_s}{B}\left(\frac{\mathrm{d}B}{\mathrm{d}B_w}\frac{\partial B_w}{\partial u} + \frac{\mathrm{d}B}{\mathrm{d}B_u}\frac{\partial B_u}{\partial u}\right) = 2\frac{P_s}{B^2}\left(B_w\frac{\partial B_w}{\partial u} + B_u\frac{\partial B_u}{\partial u}\right) \quad (7.116)$$

Here, w denotes the other component from u. That is, if u is chosen to be x, then $w = y$ and vice versa. As has been done in Section 7.3.1.2, $\frac{\partial B_u}{\partial u}$ represents the skew quadrupole gradients, whereas $\frac{\partial B_w}{\partial u}$ represents the normal quadrupole gradients. The following step is similar as deriving Eq. 7.86, which results in

$$\frac{\mathrm{d}P_s}{\mathrm{d}u} = 2\frac{P_s}{B^2}B_w\frac{\partial B_w}{\partial u} = 2P_s\frac{h_u}{h^2}k_1 \qquad (7.117)$$

The radiated power then becomes

$$P_{s'} = P_s \left[1 + 2\frac{h_u}{h^2}k_1 u_\beta \right]$$

(7.118)

The energy radiated in a time interval ds'/c is then given by

$$
\begin{aligned}
dE_\gamma = P_{s'}\frac{ds'}{c} &= \frac{P_s}{c}\left[1 + 2\frac{h_u}{h^2}k_1 u_\beta \right]\, ds' \\
&= \frac{P_s}{c}\left[1 + 2\frac{h_u}{h^2}k_1 u_\beta \right](1 + h_{0u}u_\beta)\, ds \\
&= \frac{P_s}{c}\left[1 + \left(h_{0u} + 2\frac{h_u}{h^2}k_1 \right) u_\beta \right]\, ds
\end{aligned}
$$

(7.119)

Here, only the u-component of h_0 was used, because we study betatron oscillations only in the selected place. Furthermore, terms of second order in u_β were neglected. This result can be substituted back in Eq. 7.114, which gives

$$
\begin{aligned}
d\epsilon_u = -2\frac{P_s}{cE_0} &\left[1 + \left(h_{0u} + 2\frac{h_u}{h^2}k_1 \right) u_\beta \right] \\
&\times \left[\left(\alpha_u u_\beta u'_\beta + \beta_u u'^2_\beta \right) - \left(\gamma_u D_u u_\beta + \alpha_x(D_u u'_\beta + D'_u u_\beta) + \beta_u D'_u u'_\beta \right) \right]\, ds
\end{aligned}
$$

(7.120)

Using the same reasoning as before, the odd terms average to zero. This means only the even terms need to be kept. This results in

$$
\begin{aligned}
d\epsilon_u = -2\frac{P_s}{cE_0} &\left[\left(\alpha_u u_\beta u'_\beta + \beta_u u'^2_\beta \right) \right. \\
&\left. - \left(h_{0u} + 2\frac{h_u}{h^2}k_1 \right)\left(\gamma_u D_u u^2_\beta + \alpha_x(D_u u_\beta u'_\beta + D'_u u^2_\beta) + \beta_u D'_u u_\beta u'_\beta \right) \right]\, ds
\end{aligned}
$$

(7.121)

The averages of the squared terms are

$$\left\langle u^2_\beta \right\rangle = \frac{1}{2}\epsilon_u \beta_u$$

(7.122)

$$\left\langle u_\beta u'_\beta \right\rangle = -\frac{1}{2}\epsilon_u \alpha_u$$

(7.123)

$$\left\langle u'^2_\beta \right\rangle = \frac{1}{2}\epsilon_u \gamma_u$$

(7.124)

Substituting these averages gives

$$
\begin{aligned}
d\epsilon_u = -2\frac{P_s}{cE_0} &\left[\left(-\frac{1}{2}\alpha^2_u \epsilon_u + \frac{1}{2}\beta_u \gamma_u \epsilon_u \right) \right. \\
&\left. - \left(h_{0u} + 2\frac{h_u}{h^2}k_1 \right)\left(\frac{1}{2}\gamma_u \beta_u \epsilon_u D_u + \alpha_x\left(-\frac{1}{2}\alpha_u \epsilon_u D_u + \frac{1}{2}\beta_u \epsilon_u D'_u \right) - \frac{1}{2}\alpha_u \beta_u \epsilon_u D'_u \right) \right]\, ds
\end{aligned}
$$

(7.125)

Note that $\beta_u \gamma_u - \alpha_u^2 = 1$ and that the cross terms between $\alpha_u \beta_u$ cancel. This way, the expression simplifies to

$$\mathrm{d}\epsilon_u = -\epsilon_u \frac{P_s}{E_0} \left[1 - \left(h_{0u} + 2\frac{h_u}{h^2} k_1 \right) D_u \right] \mathrm{d}s \tag{7.126}$$

To arrive at the change in emittance per unit time, we divide by T_{rev}

$$\frac{\mathrm{d}\epsilon_u}{\mathrm{d}t} = -\epsilon_u \oint \frac{P_s}{C_0 E_0} \left[1 - \left(h_{0u} + 2\frac{h_u}{h^2} k_1 \right) D_u \right] \mathrm{d}s \tag{7.127}$$

Finally, Eq. 7.69 may be substituted, which results in

$$\frac{\mathrm{d}\epsilon_u}{\mathrm{d}t} = -\epsilon_u \frac{2}{3} \frac{cr_0 \gamma^3}{C_0} \oint \left[h^2 - \left(h^2 h_{0u} + 2h_u k_1 \right) D_u \right] \mathrm{d}s \tag{7.128}$$

Here, the second radiation integral is identified. Furthermore, the u-component of the fourth radiation integral is found to be

$$I_{4u} = \oint \left(h^2 h_{0u} + 2h_u k_1 \right) D_u \, \mathrm{d}s \tag{7.129}$$

Thus,

$$\frac{\mathrm{d}\epsilon_u}{\mathrm{d}t} = -\epsilon_u \frac{2}{3} \frac{cr_0 \gamma^3}{C_0} (I_2 - I_{4u}) \tag{7.130}$$

This is a first-order ODE, with a damping rate given by

$$\frac{2}{3} \frac{cr_0 \gamma^3}{C_0} (I_2 - I_{4u}) \tag{7.131}$$

Since the betatron amplitude is proportional to $\sqrt{\epsilon_u}$, the 2 in the numerator disappears. This leads to the damping constant

$$\alpha_u = \frac{cr_0 \gamma^3}{3C_0} (I_2 - I_{4u}) \tag{7.132}$$

7.3.1.5 Transverse Equilibrium Emittances and the Fifth Radiation Integral

The derivation in this section is valid for either x or y. To this end, u will be used as a substitute for either x or y. The change in betatron position and angle when a photon is emitted, denoted by u_β and u'_β respectively, are given by

$$\delta u_\beta = D_u \frac{\delta E \gamma}{E_0} \tag{7.133}$$

$$\delta u'_\beta = D'_u \frac{\delta E \gamma}{E_0} \tag{7.134}$$

Here, δE is the energy carried away by the photon. The emittance before the emission of the photon, ϵ_{u1}, is given by

$$\epsilon_{u1} = \gamma_u u_\beta^2 + 2\alpha_u u_\beta u'_\beta + \beta_u u'^2_\beta \tag{7.135}$$

After the emission of the photon, the emittance has increased. The resulting emittance, ϵ_{u2} is

$$
\begin{aligned}
\epsilon_{u2} &= \gamma_u(u_\beta + \delta u_\beta)^2 + 2\alpha_u(u_\beta + \delta u_\beta)(u'_\beta + \delta u'_\beta) + \beta_u(u'_\beta + \delta u'_\beta)^2 \\
&= \epsilon_{u1} + 2\left(\gamma_u u_\beta \delta u_\beta + \alpha_u(u_\beta \delta u'_\beta + u'_\beta \delta u_\beta) + \beta_u u'_\beta \delta u'_\beta\right) \\
&\quad + \gamma_u \delta u_\beta^2 + 2\alpha_u \delta u_\beta \delta u'_\beta + \beta_u \delta u_\beta^2
\end{aligned}
\tag{7.136}
$$

The change in the emittance is then

$$
\begin{aligned}
\mathrm{d}\epsilon_u = \epsilon_{u2} - \epsilon_{u1} &= 2\left(\gamma_u u_\beta \mathrm{d}u_\beta + \alpha_u(u_\beta \mathrm{d}u'_\beta + u'_\beta \mathrm{d}u_\beta) + \beta_u u'_\beta \mathrm{d}u'_\beta\right) \\
&\quad + \gamma_u \mathrm{d}u_\beta^2 + 2\alpha_u \mathrm{d}u_\beta \mathrm{d}u'_\beta + \beta_u \mathrm{d}u'^2_\beta
\end{aligned}
\tag{7.137}
$$

Equations (7.133) and (7.134) can now be substituted, which results in

$$
\begin{aligned}
\mathrm{d}\epsilon_u &= \left(\gamma_u D_u^2 + 2\alpha_u D_u D'_u + \beta_u D'^2_u\right)\left(\frac{\mathrm{d}E_\gamma}{E_0}\right)^2 \\
&\quad + 2\left(\gamma_u u_\beta D_x + \alpha_u\left(u_\beta D'_x + u'_\beta D_x\right) + \beta_u u'_\beta D'_x\right)\frac{\mathrm{d}E_\gamma}{E_0}
\end{aligned}
\tag{7.138}
$$

The terms that are linear in u_β and u'_β will average to zero over many photon emissions. Hence:

$$
\langle \mathrm{d}\epsilon_u \rangle = \left(\gamma_u D_u^2 + 2\alpha_u D_u D'_u + \beta_u D'^2_u\right)\frac{\left\langle \mathrm{d}E_\gamma^2 \right\rangle}{E_0^2}
\tag{7.139}
$$

To this end, we define $\mathcal{H}_u$ as

$$
\mathcal{H}_u = \gamma_u D_u^2 + 2\alpha_u D_u D'_u + \beta_u D'^2_u
\tag{7.140}
$$

Thus, the expectation on the change in emittance is

$$
\langle \mathrm{d}\epsilon_u \rangle = \mathcal{H}_u \frac{\left\langle \mathrm{d}E_\gamma^2 \right\rangle}{E_0^2}
\tag{7.141}
$$

Now, Eq. 7.94 can be used, on the transverse coordinate [28]:

$$
\langle \mathrm{d}\epsilon_u \rangle = \mathcal{H}_u \frac{\left\langle \mathrm{d}E^2 \right\rangle}{E_0^2} = \mathcal{H}_u \frac{\dot{n}\left\langle E_\gamma^2 \right\rangle}{4\alpha_u E_0^2}
\tag{7.142}
$$

This gives a result very similar to Eq. 7.99

$$
\langle \mathrm{d}\epsilon_u \rangle = \frac{55\sqrt{3}}{96}\frac{\hbar \gamma^2}{m_0 c}\frac{h^3 \mathcal{H}_u}{I_2 - I_{4u}}
\tag{7.143}
$$

Integrating over the entire ring gives

$$
\begin{aligned}
\langle \epsilon_u \rangle &= \frac{55\sqrt{3}}{96}\frac{\hbar \gamma^2}{m_0 c}\frac{1}{I_2 - I_{4u}}\oint h^3 \mathcal{H}_u \,\mathrm{d}s' \\
&= \frac{55\sqrt{3}}{96}\frac{\hbar \gamma^2}{m_0 c}\frac{1}{I_2 - I_{4u}}\oint h^3 \mathcal{H}_u \,(1 + h_{0u}u)\,\mathrm{d}s
\end{aligned}
\tag{7.144}
$$

Again we assume $h_{0u}u \ll 1$. We can then define the fifth radiation integral, I_{5u}, as follows:

$$I_{5u} = \oint h^3 \mathcal{H}_u \, \mathrm{d}s \tag{7.145}$$

The expectation value of the emittance can be written as:

$$\langle \epsilon_u \rangle = \frac{55\sqrt{3}}{96} \frac{\hbar \gamma^2}{m_0 c} \frac{I_{5u}}{I_2 - I_{4u}} \tag{7.146}$$

Chapter 8

Spin tracking and polarization

8.1   Spin tracking

This section is based on [31, 32].

The spin precession for a particle traveling in a magnetic field $\boldsymbol{B}$ can be written in terms of the precession angular velocity:

$$\boldsymbol{\Omega}_{\text{BMT}} = -\frac{1}{B\rho_{\text{part}}} \left[(1 + a\gamma)\boldsymbol{B}_{\perp} + (1 + a)\boldsymbol{B}_{\parallel} \right] \tag{8.1}$$

where a is the anomalous magnetic moment and $\boldsymbol{B}_{\parallel}$ and $\boldsymbol{B}_{\perp}$ are referred to the velocity of the particle.

The precession angle for a particle traveling a path length ℓ is given by:

$$\phi = |\boldsymbol{\Omega}|\ell \tag{8.2}$$

We call:

$$\boldsymbol{\omega} = \frac{\boldsymbol{\Omega}}{|\boldsymbol{\Omega}|} \tag{8.3}$$

and we define:

$$t_0 = \cos\left(\frac{\phi}{2}\right) \tag{8.4}$$

$$t_x = \omega_x \sin\left(\frac{\phi}{2}\right) \tag{8.5}$$

$$t_y = \omega_y \sin\left(\frac{\phi}{2}\right) \tag{8.6}$$

$$t_s = \omega_z \sin\left(\frac{\phi}{2}\right) \tag{8.7}$$

The spin vector of the particle is transformed by the following rotation matrix:

$$M = \begin{bmatrix} (t_0^2 + t_x^2) - (t_s^2 + t_y^2) & 2(t_x t_y - t_0 t_s) & 2(t_x t_s + t_0 t_y) \\ 2(t_x t_y + t_0 t_s) & (t_0^2 + t_y^2) - (t_x^2 + t_s^2) & 2(t_s t_y - t_0 t_x) \\ 2(t_x t_s - t_0 t_y) & 2(t_s t_y + t_0 t_x) & (t_0^2 + t_s^2) - (t_x^2 + t_y^2) \end{bmatrix} \tag{8.8}$$

8.2   Linear transport matrix including spin

The coordinate vector including the spin is defined as:

$$
z = \begin{pmatrix} x \\ p_x \\ y \\ p_y \\ \zeta \\ \delta \\ s_x \\ s_y \\ s_z \end{pmatrix}
\quad \text{We call } z_{\text{orb}} = \begin{pmatrix} x \\ p_x \\ y \\ p_y \\ \zeta \\ \delta \end{pmatrix}, \quad z_{\text{spin}} = \begin{pmatrix} s_x \\ s_y \\ s_z \end{pmatrix}
\tag{8.9}
$$

The corresponding 9D transport matrix can be written as

$$
\mathbf{R} = \begin{pmatrix} \mathbf{R}_{\text{orb}} & 0 \\ \mathbf{D} & \mathbf{A} \end{pmatrix}
\tag{8.10}
$$

We call $e_1, \ldots, e_9$ the eigenvectors and $\lambda_1, \ldots, \lambda_9$ the eigenvalues so that

$$
\mathbf{R} e_i = \lambda_i e_i
\tag{8.11}
$$

From the definition of eigenvectors (doing the matrix product in blocks), we can write:

$$
\mathbf{R}_{\text{orb}} \, e_{i,\text{orb}} = \lambda_i e_{i,\text{orb}}
\tag{8.12}
$$

$$
\mathbf{D} \, e_{i,\text{orb}} + \mathbf{A} \, e_{i,\text{spin}} = \lambda_i e_{i,\text{spin}}
\tag{8.13}
$$

From this:

$$
\mathbf{D} \, e_{i,\text{orb}} = (\lambda_i \mathbf{I} - \mathbf{A}) \, e_{i,\text{spin}}
\tag{8.14}
$$

$$
e_{i,\text{spin}} = (\lambda_i \mathbf{I} - \mathbf{A})^{-1} \mathbf{D} \, e_{i,\text{orb}}
\tag{8.15}
$$

8.3   Invariant Spin Field - first order computation

This section is based on [33].
We expand the Invariant Spin Field [31] function to first order

$$
n(z_{\text{orb}}) = n_0 + \mathbf{N} \left(z_{\text{orb}} - z_{\text{orb}}^{\text{CO}} \right)
\tag{8.16}
$$

In the following we drop all the constant terms so we simply write $n(z_{\text{orb}}) = \mathbf{N} z_{\text{orb}}$.
We now call z_1^{spin} the ISF at z_1^{orb}, i.e.

$$
z_1^{\text{spin}} = \mathbf{N} z_1^{\text{orb}}
\tag{8.17}
$$

We call z_2 the coordinate after one revolution. By definition of the ISF, the spin part of z_2 is the ISF at z_2^{orb}, i.e.

$$z_2^{\text{spin}} = \mathbf{N} z_2^{\text{orb}} \tag{8.18}$$

We know from the structure of the one-turn matrix:

$$z_2^{\text{orb}} = \mathbf{R}_{\text{orb}} z_1^{\text{orb}} \tag{8.19}$$

$$z_2^{\text{spin}} = \mathbf{D} z_1^{\text{orb}} + \mathbf{A} z_1^{\text{spin}} \tag{8.20}$$

Combining, Eqs. 8.18, 8.19 and 8.20, we obtain:

$$\mathbf{N} \mathbf{R}_{\text{orb}} z_1^{\text{orb}} = \mathbf{D} z_1^{\text{orb}} + \mathbf{A} \mathbf{N} z_1^{\text{orb}} \tag{8.21}$$

We specialize it for the case $z_1^{\text{orb}} = e_1^{\text{orb}}$ obtaining:

$$\lambda_1 \mathbf{N} e_1^{\text{orb}} = \mathbf{D} e_1^{\text{orb}} + \mathbf{A} \mathbf{N} e_1^{\text{orb}} \tag{8.22}$$

From Eq. 8.12, we obtain:

$$\mathbf{D} e_1^{\text{orb}} = \lambda_1 e_1^{\text{spin}} - \mathbf{A} e_1^{\text{spin}} \tag{8.23}$$

Replacing into Eq. 8.12, we obtain:

$$(\lambda_1 \mathbf{I} - \mathbf{A}) \mathbf{N} e_1^{\text{orb}} = (\lambda_1 \mathbf{I} - \mathbf{A}) e_1^{\text{spin}} \tag{8.24}$$

If $(\lambda_1 \mathbf{I} - \mathbf{A})$ is not singular:

$$\mathbf{N} e_1^{\text{orb}} = e_1^{\text{spin}} \tag{8.25}$$

Combining this result for the six orbital eigenvectors:

$$\left(\mathbf{N} e_1^{\text{orb}} \quad \cdots \quad \mathbf{N} e_6^{\text{orb}} \right) = \left(e_1^{\text{spin}} \quad \cdots \quad e_6^{\text{spin}} \right) \tag{8.26}$$

In matrix form:

$$\mathbf{N} \mathbf{E}^{\text{orb}} = \mathbf{E}^{\text{spin}} \quad \Rightarrow \quad \mathbf{N} = \mathbf{E}^{\text{spin}} \left(\mathbf{E}^{\text{orb}} \right)^{-1} \tag{8.27}$$

We note that the last column of the matrix $\mathbf{N}$ provides the derivative $\frac{d\mathbf{n}}{d\delta}$ which is relevant for the computation of equilibrium polarization.

8.4 Equilibrium polarization and polarization time

This section is based on [33, 34, 35, 32, 36, 37].
In the presence of photon emission, the polarization of the beam evolves following the equation:

$$P(t) = P(0) e^{-\frac{t}{\tau_{\text{tot}}}} + P_{\text{eq}} \left(1 - e^{-\frac{t}{\tau_{\text{tot}}}} \right) \tag{8.28}$$

The equilibrium polarization and the buildup time can be computed as:

$$P_{\text{eq}} = \frac{8}{5\sqrt{3}} \frac{\alpha_-}{\alpha_+} \tag{8.29}$$

$$\tau_{\text{tot}}^{-1} = \frac{5\sqrt{3}}{8} \frac{r_e \hbar \gamma^5}{m_e} \cdot \alpha_+ \tag{8.30}$$

where, truncating to the first order the dependence of the ISF on the phase space coordinates, we have:

$$\alpha_+ \simeq \frac{1}{C} \oint \frac{ds}{|\rho(s)|^3} \left[1 - \frac{2}{9}(\boldsymbol{n_0} \cdot \hat{\boldsymbol{i}}_v)^2 + \frac{11}{18} \left| \frac{\partial \boldsymbol{n}}{\partial \delta} \right|^2 \right]_s \tag{8.31}$$

$$\alpha_- \simeq \frac{1}{C} \oint \frac{ds}{|\rho(s)|^3} \left[\hat{\boldsymbol{i}}_B \cdot (\boldsymbol{n_0} - \frac{\partial \boldsymbol{n}}{\partial \gamma}) \right]_s \tag{8.32}$$

The buildup time can be decomposed in two terms:

$$\tau_{\text{tot}}^{-1} = \tau_{\text{pol}}^{-1} + \tau_{\text{depol}}^{-1} \tag{8.33}$$

where:

$$\tau_{\text{pol}}^{-1} = \frac{5\sqrt{3}}{8} \frac{r_e \hbar \gamma^5}{m_e} \frac{1}{C} \oint \frac{ds}{|\rho(s)|^3} \left[1 - \frac{2}{9}(\boldsymbol{n_0} \cdot \hat{\boldsymbol{i}}_v)^2 \right]_s \tag{8.34}$$

$$\tau_{\text{depol}}^{-1} = \frac{5\sqrt{3}}{8} \frac{r_e \hbar \gamma^5}{m_e} \frac{1}{C} \oint \frac{ds}{|\rho(s)|^3} \left[\frac{11}{18} \left| \frac{\partial \boldsymbol{n}}{\partial \delta} \right|^2 \right]_s \tag{8.35}$$

8.5   Monte Carlo method for equilibrium polarization

This section is based on [35, 38].
We can define:

$$P_\infty = \frac{8}{5\sqrt{3}} \frac{\oint \frac{ds}{|\rho(s)|^3} \left[\hat{\boldsymbol{i}}_B \cdot (\boldsymbol{n}_0) \right]_s}{\oint \frac{ds}{|\rho(s)|^3} \left[1 - \frac{2}{9}(\boldsymbol{n_0} \cdot \hat{\boldsymbol{i}}_v)^2 \right]_s} \tag{8.36}$$

The equilibrium polarization and the buildup rate can be written as follows:

$$P_{\text{eq}} = P_\infty \frac{1}{1 + \frac{\tau_{\text{pol}}}{\tau_{\text{depol}}}} \tag{8.37}$$

$$\tau_{\text{tot}}^{-1} = \tau_{\text{pol}}^{-1} + \tau_{\text{depol}}^{-1} \tag{8.38}$$

The term τ_{depol} can be evaluated using particle tracking, accounting for quantum excitation from synchrotron radiation. Unlike the approach used in the previous section, this method accounts for the nonlinear dependence of the ISF on the phase space coordinates. Using τ_{depol} we can get from Eqs. 8.37 and 8.38 estimates for P_{eq} and τ_{tot} that include nonlinear effects.

Chapter 9

Coasting beams

In coasting beams, different particles have different revolution frequencies depending on their momentum, so they perform a different number of turns over a given time. If in the line we have collective elements which need to measure the beam distribution at a certain location s and at a given time t, we need to ensure that all particles present at s at the instant t are present at the element.

We define for each particle and for any couple of positions $s_1 < s_2$:

$$\hat{\beta}(s_1, s_2) = \frac{1}{c} \frac{s_2 - s_1}{t(s_2) - t(s_1)} \tag{9.1}$$

We choose an auxiliary value β_{sim} such that at all times:

$$\hat{\beta}(s_1, s_2) < \beta_{\text{sim}} \quad \text{for all particles and any } s_1, s_2 \tag{9.2}$$

$$\hat{\beta}(s_1, s_2) > \frac{\beta_{\text{sim}}}{2} \quad \text{for all particles and any } s_1, s_2 \tag{9.3}$$

From β_{sim} we define an auxiliary time interval ΔT as:

$$\Delta T = \frac{L}{\beta_{\text{sim}} c} \tag{9.4}$$

At each "turn" n we want to simulate at any collective element the time frame $F_n(s)$ given by:

$$F_n(s) = \left[T_n(s) - \frac{\Delta T}{2}, T_n(s) + \frac{\Delta T}{2} \right] \tag{9.5}$$

where:

$$T_n(s) = n\Delta T + \frac{s}{\beta_{\text{sim}} c} \tag{9.6}$$

We can see that intervals are contiguous; hence at any location over N turns we are simulating a time interval of length $N\Delta T$.

From Eq. 9.6 we can simply derive the following relations, which will be useful in the following:

$$T_{n+1}(s) - T_n(s) = \Delta T \tag{9.7}$$

$$T_n(s_2) - T_n(s_1) = \frac{s_2 - s_1}{\beta_{\text{sim}} c} \tag{9.8}$$

We also note that the condition $t(s) \in F_n(s)$ can be rewritten as:

$$-\frac{\Delta T}{2} < t - n\Delta T - \frac{s}{\beta_{\text{sim}} c} < \frac{\Delta T}{2} \tag{9.9}$$

We can prove the following propositions (see Sec. 9.3):

Proposition 1: If the time $t_k(s_1)$ defining the k-th arrival of a particle at location s_1 falls in the frame $F_n(s_1)$, then the particle arrives at location $s_2 > s_1$ either in the frame $F_n(s_2)$ or in the following frame $F_{n+1}(s_2)$. In symbols:

$$t_k(s_1) \in F_n(s_1) \Rightarrow t_k(s_2) \in F_n(s_2) \cup F_{n+1}(s_2) \quad \text{for any } s_1 < s_2 \tag{9.10}$$

Proposition 2: If the time $t_k(s_2)$ defining the k-th arrival of a particle at location s_2 falls in the frame $F_n(s_2)$, then the time of $(k+1)$-th arrival at any location $s_1 < s_2$ falls in the frame $F_{n+1}(s_1)$ or in the following frame $F_{n+1}(s_1)$. In symbols:

$$t_k(s_2) \in F_n(s_2) \Rightarrow t_{k+1}(s_1) \in F_{n+1}(s_1) \cup F_{n+2}(s_1) \quad \text{for any } s_1 < s_2 \tag{9.11}$$

Proposition 3: If the time $t_k(L)$ defining the k-th arrival of a particle at the end of the line falls in the frame $F_n(L)$, than the time $t_{k+1}(0) = t_k(L)$ of the $(k+1)$-th arrival of the particle at $s = 0$ falls in the interval $F_{n+1}(0)$. In symbols:

$$t_k(L) \in F_n(L) \Rightarrow t_{k+1}(0) \in F_{n+1}(0) \tag{9.12}$$

9.1 ζ definition and update

For the tracking of coasting beams we define the longitudinal coordinate ζ as:

$$\zeta = s - \beta_0 c(t - n\Delta T) \tag{9.13}$$

where s is the distance from the start of the line for the present turn, t is the absolute time since the start of the simulation, n is the index of the present simulated time frame.
We can write t in terms of ζ as:

$$t = \frac{s}{\beta_0 c} - \frac{\zeta}{\beta_0 c} + n\Delta T \tag{9.14}$$

With this definition the ζ coordinate needs to be updated each time the particle passes at the start of the line since across the $s = 0$ we can write:

$$\zeta^- = L - \beta_0 c(t - n\Delta T) \tag{9.15}$$
$$\zeta^+ = 0 - \beta_0 c(t - (n+1)\Delta T) \tag{9.16}$$

where t is the time at which the particle passes zero (which is the same in both equations).

Combining the two equations we can write:

$$\zeta^+ = \zeta^- - (L - \beta_0 c \Delta T) \tag{9.17}$$

In standard simulations for bunched beams the simulated frame is $\Delta T = L/(\beta_0 c)$, hence the ζ coordinate is continuous.

For coasting beams ΔT is given by Eq. 9.4, hence the ζ needs to be updated at each turn using:

$$\boxed{\zeta^+ = \zeta^- - L\left(1 - \frac{\beta_0}{\beta_{\mathrm{sim}}}\right)} \tag{9.18}$$

We want to translate the condition Eq. 9.9 into a condition on ζ. Replacing Eq. 9.14 into Eq. 9.9 we obtain:

$$-\frac{\Delta T}{2} < \left(\frac{s}{\beta_0 c} - \frac{\zeta}{\beta_0 c} + n\Delta T\right) - n\Delta T - \frac{s}{\beta_{\mathrm{sim}} c} < \frac{\Delta T}{2} \tag{9.19}$$

We change signs:

$$\frac{\Delta T}{2} > -\frac{s}{\beta_0 c} + \frac{\zeta}{\beta_0 c} + \frac{s}{\beta_{\mathrm{sim}} c} > -\frac{\Delta T}{2} \tag{9.20}$$

We rearrange:

$$-\frac{\Delta T}{2} < -\frac{s}{\beta_0 c} + \frac{\zeta}{\beta_0 c} + \frac{s}{\beta_{\mathrm{sim}} c} < \frac{\Delta T}{2} \tag{9.21}$$

$$-\beta_0 c \frac{\Delta T}{2} < \zeta - s\left(1 - \frac{\beta_0}{\beta_{\mathrm{sim}}}\right) < \beta_0 c \frac{\Delta T}{2} \tag{9.22}$$

from which we can write:

$$\boxed{t \in F_n(s) \quad \Leftrightarrow \quad -\frac{\Delta\zeta}{2} < \zeta - s\left(1 - \frac{\beta_0}{\beta_{\mathrm{sim}}}\right) < \frac{\Delta\zeta}{2}} \tag{9.23}$$

where we have defined:

$$\boxed{\Delta\zeta = \beta_0 c \Delta T = \frac{\beta_0}{\beta_{\mathrm{sim}}} L} \tag{9.24}$$

9.2 Handling particles jumping to the following frame

From Proposition 1 we know that during tracking particles will either stay in the present frame or "jump" to the following one.

From Eqs. 9.5 and 9.23, we know that the jump occurs when:

$$t > T_n(s) + \frac{\Delta T}{2} \quad \Leftrightarrow \quad \zeta < -\frac{\Delta\zeta}{2} + s\left(1 - \frac{\beta_0}{\beta_{\mathrm{sim}}}\right) \tag{9.25}$$

When this condition is met, the particle tracking needs to be paused for the remainder of the frame n (based on Proposition 1 it cannot go back to frame n) and, based on Proposition 2, its tracking needs to be resumed from the same location where the

tracking was paused when tracking the following frame. As the frame index is increased, ζ needs to be updated to preserve the time of arrival:

$$\zeta_{\text{before jump}} = s - \beta_0 c \, (t - n\Delta T) \tag{9.26}$$

$$\zeta_{\text{after jump}} = s - \beta_0 c \, (t - (n+1)\Delta T) \tag{9.27}$$

from which we obtain:

$$\boxed{\zeta_{\text{after jump}} = \zeta_{\text{before jump}} + \beta_0 c \Delta T = \zeta_{\text{before jump}} + \Delta\zeta} \tag{9.28}$$

9.3   Proofs

We notice that from Eqs. 9.2 and 9.3 we can write

$$\hat{\beta} < \beta_{\text{sim}} \quad \Rightarrow \quad \frac{1}{\hat{\beta}} > \frac{1}{\beta_{\text{sim}}} \quad \Rightarrow \quad \left(\frac{1}{\hat{\beta}} - \frac{1}{\beta_{\text{sim}}} \right) > 0 \tag{9.29}$$

$$\hat{\beta} > \frac{\beta_{\text{sim}}}{2} \quad \Rightarrow \quad \frac{1}{\hat{\beta}} < \frac{2}{\beta_{\text{sim}}} \quad \Rightarrow \quad \left(\frac{1}{\hat{\beta}} - \frac{1}{\beta_{\text{sim}}} \right) < \frac{1}{\beta_{\text{sim}}} \tag{9.30}$$

Combining the two we obtain

$$0 < \left(\frac{1}{\hat{\beta}} - \frac{1}{\beta_{\text{sim}}} \right) < \frac{1}{\beta_{\text{sim}}} \tag{9.31}$$

Proof of proposition 1

By definition of $\hat{\beta}$ we can write:

$$t_k(s_2) = t_k(s_1) + \frac{s_2 - s_1}{\hat{\beta}c} \tag{9.32}$$

By the hypothesis:

$$t_k(s_1) > T_n(s_1) - \frac{\Delta T}{2} \tag{9.33}$$

hence:

$$t_k(s_2) > T_n(s_1) - \frac{\Delta T}{2} + \frac{s_2 - s_1}{\hat{\beta}c} \tag{9.34}$$

Using Eq. 9.8 we can write:

$$t_k(s_2) > T_n(s_2) - \frac{s_2 - s_1}{\beta_{\text{sim}}c} - \frac{\Delta T}{2} + \frac{s_2 - s_1}{\hat{\beta}c} \tag{9.35}$$

Rearranging:

$$t_k(s_2) > T_n(s_2) - \frac{\Delta T}{2} + \frac{s_2 - s_1}{c} \left(\frac{1}{\hat{\beta}(s)} - \frac{1}{\beta_{\text{sim}}} \right) \tag{9.36}$$

Using Eq. 9.31 and the fact that by hypotheses that $s_2 > s_1$, we know that the last term is positive. Therefore we can write:

$$t_k(s_2) > T_n(s_2) - \frac{\Delta T}{2} \tag{9.37}$$

Similarly from the hypothesis we know:

$$t_k(s_1) < T_n(s_1) + \frac{\Delta T}{2} \tag{9.38}$$

From Eq. 9.32 we can write:

$$t_k(s_2) < T_n(s_1) + \frac{\Delta T}{2} + \frac{s_2 - s_1}{\hat{\beta}c} \tag{9.39}$$

Again, using Eq. 9.8 we obtain:

$$t_k(s_2) < T_n(s_2) - \frac{s_2 - s_1}{\beta_{\text{sim}}c} - \frac{\Delta T}{2} + \frac{s_2 - s_1}{\hat{\beta}c} \tag{9.40}$$

Rearranging:

$$t_k(s_2) < T_n(s_2) + \frac{\Delta T}{2} + \frac{s_2 - s_1}{c}\left(\frac{1}{\hat{\beta}(s)} - \frac{1}{\beta_{\text{sim}}}\right) \tag{9.41}$$

Using Eq. 9.31 we obtain:

$$t_k(s_2) < T_n(s_2) + \frac{\Delta T}{2} + \frac{s_2 - s_1}{\beta_{\text{sim}}c} \tag{9.42}$$

Using the fact that $s_2 - s_1 < L$ and Eq. 9.4 we can write:

$$\frac{s_2 - s_1}{\beta_{\text{sim}}c} < \frac{L}{\beta_{\text{sim}}c} = \Delta T \tag{9.43}$$

Replacing in Eq. 9.42 we obtain:

$$t_k(s_2) < T_n(s_2) + \frac{\Delta T}{2} + \Delta T \tag{9.44}$$

Using Eq. 9.7 we obtain:

$$t_k(s_2) < T_{n+1}(s_2) + \frac{\Delta T}{2} \tag{9.45}$$

Combining Eq. 9.37 and 9.37 we obtain:

$$T_n(s_2) - \frac{\Delta T}{2} < t_k(s_2) < T_{n+1}(s_2) + \frac{\Delta T}{2} \tag{9.46}$$

which is what we wanted to prove.

Proof of proposition 2

From the hypothesis:

$$t_k(s_2) > T_n(s_2) - \frac{\Delta T}{2} \tag{9.47}$$

As $L > s_2$, using Proposition 1 we can write:

$$t_k(L) > T_n(L) - \frac{\Delta T}{2} \tag{9.48}$$

Using Proposition 3 we can write:

$$t_{k+1}(0) > T_{n+1}(0) - \frac{\Delta T}{2} \tag{9.49}$$

Using the fact that $s1 > 0$, we can apply again Proposition 1, obtaining:

$$t_{k+1}(s1) > T_{n+1}(1) - \frac{\Delta T}{2} \tag{9.50}$$

which is what we wanted to prove.

Proof of proposition 3

By definition:

$$t_{k+1}(0) = t_k(L) \tag{9.51}$$

We know that $t_k(L) \in F_n(L)$ hence, from Eq. 9.5 we can write:

$$t_{k+1}(0) > T_n(L) - \frac{\Delta T}{2} \tag{9.52}$$

From Eq. 9.6 we obtain:

$$t_{k+1}(0) > n\Delta T - \frac{\Delta T}{2} + \frac{L}{\beta_{\text{sim}}c} \tag{9.53}$$

from Eq. 9.4 we get:

$$t_{k+1}(0) > (n+1)\Delta T - \frac{\Delta T}{2} \tag{9.54}$$

and from Eq. 9.6 (with $s = 0$) we obtain:

$$t_{k+1}(0) > T_{n+1}(0) - \frac{\Delta T}{2} \tag{9.55}$$

which is what we wanted to prove.

Chapter 10

Space charge and beam-beam forces

10.1 Fields generated by a bunch of particles

We assume that the bunch travels rigidly along s with velocity $\beta_0 c$:

$$\rho\left(x, y, s, t\right) = \rho_0\left(x, y, s - \beta_0 ct\right) \tag{10.1}$$

$$\mathbf{J}\left(x, y, s, t\right) = \beta_0 c\, \rho_0\left(x, y, s - \beta_0 ct\right) \hat{\mathbf{i}}_s \tag{10.2}$$

We define an auxiliary variable ζ as the position along the bunch:

$$\zeta = s - \beta_0 ct. \tag{10.3}$$

We call K the lab reference frame in which we have defined all equations above, and we introduce a boosted frame K' moving rigidly with the reference particle. The coordinates in the two systems are related by a Lorentz transformation [39]:

$$ct' = \gamma_0\left(ct - \beta_0 s\right) \tag{10.4}$$

$$x' = x \tag{10.5}$$

$$y' = y \tag{10.6}$$

$$s' = \gamma_0\left(s - \beta_0 ct\right) = \gamma_0 \zeta \tag{10.7}$$

The corresponding inverse transformation is:

$$ct = \gamma_0\left(ct' + \beta_0 s'\right) \tag{10.8}$$

$$x = x' \tag{10.9}$$

$$y = y' \tag{10.10}$$

$$s = \gamma_0\left(s' + \beta_0 ct'\right) \tag{10.11}$$

The quantities $\left(c\rho, J_x, J_y, J_s\right)$ form a Lorentz 4-vector and therefore they are transformed between K and K' by relationships similar to the Eqs. 10.4-10.6 [39]:

$$c\rho'\left(\mathbf{r}', t'\right) = \gamma_0\left[c\rho\left(\mathbf{r}\left(\mathbf{r}', t'\right), t\left(\mathbf{r}', t'\right)\right) - \beta_0 J_s\left(\mathbf{r}\left(\mathbf{r}', t'\right), t\left(\mathbf{r}', t'\right)\right)\right] \tag{10.12}$$

$$J_s'\left(\mathbf{r}', t'\right) = \gamma_0\left[J_s\left(\mathbf{r}\left(\mathbf{r}', t'\right), t\left(\mathbf{r}', t'\right)\right) - \beta_0 c\rho\left(\mathbf{r}\left(\mathbf{r}', t'\right), t\left(\mathbf{r}', t'\right)\right)\right] \tag{10.13}$$

where the transformations $\mathbf{r}\,(\mathbf{r}', t')$ and $t\,(\mathbf{r}', t')$ are defined by Eqs. 10.8 and 10.11 respectively. The transverse components J_x and J_y of the current vector are invariant for our transformation, and are anyhow zero in our case.
Using Eq. 10.2 these become:

$$\rho'\,(\mathbf{r}', t') = \frac{1}{\gamma_0}\rho\,(\mathbf{r}\,(\mathbf{r}', t')\,, t\,(\mathbf{r}', t')) \tag{10.14}$$

$$J_s'\,(\mathbf{r}', t') = 0 \tag{10.15}$$

Using Eqs. 10.1 and 10.8-10.10, we obtain:

$$\rho\,(x', y', s(s', t'), t(s', t')) = \rho_0\,(x', y', s(s', t') - \beta_0 c\, t(s', t')) \tag{10.16}$$

From Eq. 10.7 we get:

$$s(s', t') - \beta_0 c\, t(s', t') = \frac{s'}{\gamma_0} \tag{10.17}$$

where the coordinate t' has disappeared.
We can therefore write:

$$\rho'\,(x', y', s', t') = \frac{1}{\gamma_0}\rho_0\left(x', y', \frac{s'}{\gamma_0}\right) \tag{10.18}$$

The electric potential in the bunch frame is the solution of Poisson's equation:

$$\frac{\partial^2 \phi'}{\partial x'^2} + \frac{\partial^2 \phi'}{\partial y'^2} + \frac{\partial^2 \phi'}{\partial s'^2} = -\frac{\rho'(x', y', s')}{\varepsilon_0} \tag{10.19}$$

From Eq. 10.18 we can write:

$$\frac{\partial^2 \phi'}{\partial x'^2} + \frac{\partial^2 \phi'}{\partial y'^2} + \frac{\partial^2 \phi'}{\partial s'^2} = -\frac{1}{\gamma_0 \varepsilon_0}\rho_0\left(x', y', \frac{s'}{\gamma_0}\right) \tag{10.20}$$

We now make the substitution:

$$\zeta = \frac{s'}{\gamma_0} \tag{10.21}$$

obtained from Eq. 10.7, which allows to rewrite Eq. 10.20 as:

$$\frac{\partial^2 \phi'}{\partial x^2} + \frac{\partial^2 \phi'}{\partial y^2} + \frac{1}{\gamma_0^2}\frac{\partial^2 \phi'}{\partial \zeta^2} = -\frac{1}{\gamma_0 \varepsilon_0}\rho_0\,(x, y, \zeta) \tag{10.22}$$

Here we have dropped the "$'$" sign from x and y as these coordinates are unaffected by the Lorentz boost.
The quantities $\left(\frac{\phi}{c}, A_x, A_y, A_s\right)$ form a Lorentz 4-vector, so we can write:

$$\phi = \gamma_0\,(\phi' + \beta_0 c\, A_s') \tag{10.23}$$

$$A_s = A_s' + \beta_0\frac{\phi'}{c} \tag{10.24}$$

In the bunch frame the charges are at rest therefore $A'_x = A'_y = A'_s = 0$ therefore:

$$\phi = \gamma_0 \phi' \tag{10.25}$$

$$A_s = \beta_0 \frac{\phi'}{c} = \frac{\beta_0}{\gamma_0 c} \phi \tag{10.26}$$

Combining Eq. 10.25 with Eq. 10.22 we obtain the equation in ϕ:

$$\boxed{\frac{\partial^2 \phi}{\partial x^2} + \frac{\partial^2 \phi}{\partial y^2} + \frac{1}{\gamma_0^2} \frac{\partial^2 \phi}{\partial \zeta^2} = -\frac{1}{\varepsilon_0} \rho_0(x, y, \zeta)} \tag{10.27}$$

10.1.1 2.5D approximation

For large enough values of γ_0, Eq. 10.22 can be approximated by:

$$\boxed{\frac{\partial^2 \phi}{\partial x^2} + \frac{\partial^2 \phi}{\partial y^2} = -\frac{1}{\varepsilon_0} \rho_0(x, y, \zeta)} \tag{10.28}$$

which means that we can solve a simple 2D problem for each beam slice (identified by its coordinate ζ).

10.1.2 Modulated 2D

Often the beam distribution can be factorized as:

$$\rho_0(x, y, \zeta) = q_0 \lambda_0(\zeta) \rho_\perp(x, y) \tag{10.29}$$

where:

$$\int \rho_\perp(x, y) \, dx \, dy = 1 \tag{10.30}$$

and $\lambda_0(z)$ is therefore the bunch line density.
For a bunched beam:

$$\int \lambda_0(z) \, dz = N \tag{10.31}$$

where N is the bunch population.
In this case the potential can be factorized as:

$$\phi(x, y, \zeta) = q_0 \lambda(\zeta) \phi_\perp(x, y) \tag{10.32}$$

where $\phi_\perp(x, y)$ is the solution of the following 2D Poisson equation:

$$\frac{\partial^2 \phi_\perp}{\partial x^2} + \frac{\partial^2 \phi_\perp}{\partial y^2} = -\frac{1}{\varepsilon_0} \rho_\perp(x, y) \tag{10.33}$$

10.2 Lorentz force

We now compute the Lorentz force on the particles moving in the longitudinal directions, including particles of the bunch itself (space charge forces) and particles of a colliding bunch moving in the opposite directions (beam-beam forces). The angles of such test particles are neglected as done in the usual thin-lens approximation. Therefore the velocity of a test particle can be written as:

$$\mathbf{v} = \beta c\, \hat{\mathbf{i}}_s \tag{10.34}$$

The Lorentz force can be written as:

$$
\begin{aligned}
\mathbf{F} &= q\left(-\nabla\phi - \frac{\partial \mathbf{A}}{\partial t} + \beta c\, \hat{\mathbf{i}}_s \times (\nabla \times \mathbf{A})\right) \\
&= q\left(-\nabla\phi - \frac{\beta_0}{\gamma_0 c}\frac{\partial \phi}{\partial t}\hat{\mathbf{i}}_s + \beta c\, \hat{\mathbf{i}}_s \times (\nabla \times \mathbf{A})\right)
\end{aligned}
\tag{10.35}
$$

We compute the vector product:

$$
\begin{aligned}
\hat{\mathbf{i}}_s \times (\nabla \times \mathbf{A}) &= \left(\frac{\partial A_s}{\partial x} - \frac{\partial A_x}{\partial s}\right)\hat{\mathbf{i}}_x + \left(\frac{\partial A_s}{\partial y} - \frac{\partial A_y}{\partial s}\right)\hat{\mathbf{i}}_y \\
&= \left(\frac{\partial A_s}{\partial x} - \frac{\partial A_x}{\partial s}\right)\hat{\mathbf{i}}_x + \left(\frac{\partial A_s}{\partial y} - \frac{\partial A_y}{\partial s}\right)\hat{\mathbf{i}}_y + \underbrace{\left(\frac{\partial A_s}{\partial s} - \frac{\partial A_s}{\partial s}\right)}_{=0}\hat{\mathbf{i}}_s \\
&= \nabla A_s - \frac{\partial \mathbf{A}}{\partial s}
\end{aligned}
\tag{10.36}
$$

We replace:

$$\mathbf{F} = q\left(-\nabla\phi - \frac{\beta_0}{\gamma_0 c}\frac{\partial \phi}{\partial t}\hat{\mathbf{i}}_s + \beta\beta_0\nabla\phi - \frac{\beta\beta_0}{\gamma_0}\frac{\partial \phi}{\partial s}\hat{\mathbf{i}}_s\right) \tag{10.37}$$

The potentials will have the same form as the sources (this can be shown explicitly using the Lorentz transformations):

$$\phi(x,y,s,t) = \phi\left(x,y,t - \frac{s}{\beta_0 c}\right) \tag{10.38}$$

For a function in this form we can write:

$$\frac{\partial \phi}{\partial s} = \frac{\partial}{\partial \zeta} = -\frac{1}{\beta_0 c}\frac{\partial \phi}{\partial t} \tag{10.39}$$

obtaining:

$$\mathbf{F} = q\left(-\nabla\phi + \frac{\beta_0^2}{\gamma_0}\frac{\partial \phi}{\partial \zeta}\hat{\mathbf{i}}_s + \beta\beta_0\nabla\phi - \frac{\beta\beta_0}{\gamma_0}\frac{\partial \phi}{\partial \zeta}\hat{\mathbf{i}}_s\right) \tag{10.40}$$

Reorganizing:

$$\mathbf{F} = -q(1 - \beta\beta_0)\nabla\phi - \frac{\beta_0(\beta - \beta_0)}{\gamma_0}\frac{\partial \phi}{\partial \zeta}\hat{\mathbf{i}}_s \tag{10.41}$$

Writing the dependencies explicitly:

$$F_x(x, y, \zeta(t)) = -q(1 - \beta\beta_0)\frac{\partial \phi}{\partial x}(x, y, \zeta(t)) \tag{10.42}$$

$$F_y(x, y, \zeta(t)) = -q(1 - \beta\beta_0)\frac{\partial \phi}{\partial y}(x, y, \zeta(t)) \tag{10.43}$$

$$F_z(x, y, \zeta(t)) = -q\left(1 - \beta\beta_0 - \frac{\beta_0(\beta - \beta_0)}{\gamma_0}\right)\frac{\partial \phi}{\partial \zeta}(x, y, \zeta(t)) \tag{10.44}$$

where $\zeta(t)$ is the position of the particle within the bunch.

10.3 Space charge

Over the single interaction we neglect the particle slippage[1]:

$$\beta = \beta_0 \tag{10.45}$$
$$\zeta(t) = \zeta \tag{10.46}$$

This gives the following simplification of Eqs. (10.42) - (10.44):

$$F_x(x, y, \zeta) = -q(1 - \beta_0^2)\frac{\partial \phi}{\partial x}(x, y, \zeta) \tag{10.47}$$

$$F_y(x, y, \zeta) = -q(1 - \beta_0^2)\frac{\partial \phi}{\partial y}(x, y, \zeta) \tag{10.48}$$

$$F_z(x, y, \zeta) = -q(1 - \beta_0^2)\frac{\partial \phi}{\partial \zeta}(x, y, \zeta) \tag{10.49}$$

In this way the force over the single interaction becomes independent of time and therefore we can compute the kicks simply as:

$$\Delta \mathbf{P} = \frac{L}{\beta_0 c}\mathbf{F} \tag{10.50}$$

where L is the portion of the machine on which we want to compute the e-cloud interaction.

The kicks on the normalized momenta can be expressed as (recalling that $P_0 = m_0\beta_0\gamma_0 c$):

$$\Delta p_x = \frac{m_0}{m}\frac{\Delta P_x}{P_0} = -\frac{qL(1 - \beta_0^2)}{m\gamma_0\beta_0^2 c^2}\frac{\partial \phi}{\partial x}(x, y, \zeta) \tag{10.51}$$

$$\Delta p_y = \frac{m_0}{m}\frac{\Delta P_y}{P_0} = -\frac{qL(1 - \beta_0^2)}{m\gamma_0\beta_0^2 c^2}\frac{\partial \phi}{\partial y}(x, y, \zeta) \tag{10.52}$$

$$\Delta \delta \simeq \Delta p_z = \frac{m_0}{m}\frac{\Delta P_z}{P_0} = -\frac{qL(1 - \beta_0^2)}{m\gamma_0\beta_0^2 c^2}\frac{\partial \phi}{\partial \zeta}(x, y, \zeta) \tag{10.53}$$

---

[1]In any case one would need to take into account also the dispersion in order to have the right slippage.

If the beam includes particles of different species (tracking of fragments), note that here q and m refer to the individual particle while m_0 is the mass of the reference particle.

In the modulated 2D case (see Sec. 10.1.2 and in particular Eq. 10.32), the kick can be expressed as:

$$\Delta p_x = \frac{m_0}{m} \frac{\Delta P_x}{P_0} = -\frac{q q_0 L (1 - \beta_0^2)}{m \gamma_0 \beta_0^2 c^2} \lambda_0(\zeta) \frac{\partial \phi_\perp}{\partial x}(x, y) \qquad (10.54)$$

$$\Delta p_y = \frac{m_0}{m} \frac{\Delta P_y}{P_0} = -\frac{q q_0 L (1 - \beta_0^2)}{m \gamma_0 \beta_0^2 c^2} \lambda_0(\zeta) \frac{\partial \phi_\perp}{\partial y}(x, y) \qquad (10.55)$$

$$\Delta \delta \simeq \Delta p_z = \frac{m_0}{m} \frac{\Delta P_z}{P_0} = -\frac{q q_0 L (1 - \beta_0^2)}{m \gamma_0 \beta_0^2 c^2} \frac{d\lambda_0}{d\zeta}(\zeta) \phi_\perp(x, y) \qquad (10.56)$$

In some cases, for example in the case of transversely Gaussian beams, an analytic closed form exists for the quantities $\frac{\partial \phi_\perp}{\partial x}$ and $\frac{\partial \phi_\perp}{\partial y}$ but not for the potential $\phi_\perp$ itself. In those cases, in order to compute the longitudinal kick, it is possible to obtain a function $\phi_\perp(x, y)$ generating the same transverse kicks by computing numerically the integral:

$$\phi_\perp(x, y) = \int_{(0,0)}^{(x,y)} \left(\frac{\partial \phi_\perp}{\partial x} \hat{\mathbf{i}}_x + \frac{\partial \phi_\perp}{\partial y} \hat{\mathbf{i}}_y \right) \cdot d\mathbf{r}' \qquad (10.57)$$

10.4   Beam-beam interaction (4D model)

We consider a test particle moving in the opposite direction with velocity:

$$\mathbf{v}_W = -\beta_{0W} c \, \hat{\mathbf{i}}_s \qquad (10.58)$$
$$s_W(t) = -\beta_{0W} c t \qquad (10.59)$$

Equations (10.42) - (10.44) become:

$$F_x(x, y, \zeta_W(t)) = -q(1 + \beta_{0W}\beta_{0S}) \frac{\partial \phi}{\partial x}(x, y, \zeta_W(t)) \qquad (10.60)$$

$$F_y(x, y, \zeta_W(t)) = -q(1 + \beta_{0W}\beta_{0S}) \frac{\partial \phi}{\partial y}(x, y, \zeta_W(t)) \qquad (10.61)$$

$$F_z(x, y, \zeta_W(t)) = -q \left(1 + \beta_{0W}\beta_{0S} - \frac{\beta_{0S}(\beta_{0W} + \beta_{0S})}{\gamma_0} \right) \frac{\partial \phi}{\partial \zeta}(x, y, \zeta_W(t)) \qquad (10.62)$$

where we have used the subscript S (strong) for the bunch generating the fields, and the subscript W (weak) for the test particle.

$\zeta_W(t)$ is the position of the test particle within the bunch generating the fields:

$$\zeta_W(t) = s_W(t) - \beta_{0S} c t = -(\beta_{0W} + \beta_{0S}) c t \qquad (10.63)$$

In modulated-2D case (Eq. 10.32), Eqs. (10.60) - (10.61) become:

$$F_x(x,y,\zeta_W(t)) = -qq_{0S}(1+\beta_{0W}\beta_{0S})\lambda_{0S}(\zeta_W(t))\frac{\partial\phi_\perp}{\partial x}(x,y) \tag{10.64}$$

$$F_y(x,y,\zeta_W(t)) = -qq_{0S}(1+\beta_{0W}\beta_{0S})\lambda_{0S}(\zeta_W(t))\frac{\partial\phi_\perp}{\partial y}(x,y) \tag{10.65}$$

$$F_z(x,y,\zeta_W(t)) = -qq_{0S}\left(1+\beta_{0W}\beta_{0S}-\frac{\beta_{0S}(\beta_{0W}+\beta_{0S})}{\gamma_0}\right)\frac{d\lambda_{0S}}{d\zeta}(\zeta_W(t))\phi_\perp(x,y) \tag{10.66}$$

The change in momentum for the test particle is given by:

$$\Delta\mathbf{P} = \int_{-\infty}^{+\infty}\mathbf{F}(t)\,dt \tag{10.67}$$

Therefore:

$$\Delta P_x(x,y,\zeta_W(t)) = -qq_{0S}N_S(1+\beta_{0W}\beta_{0S})\frac{\partial\phi_\perp}{\partial x}(x,y)\int_{-\infty}^{+\infty}\lambda_{0S}(\zeta_W(t))\,dt \tag{10.68}$$

$$\Delta P_y(x,y,\zeta_W(t)) = -qq_{0S}N_S(1+\beta_{0W}\beta_{0S})\frac{\partial\phi_\perp}{\partial y}(x,y)\int_{-\infty}^{+\infty}\lambda_{0S}(\zeta_W(t))\,dt \tag{10.69}$$

$$\Delta P_z(x,y,\zeta_W(t)) = -qq_{0S}\left(1+\beta_{0W}\beta_{0S}-\frac{\beta_{0S}(\beta_{0W}+\beta_{0S})}{\gamma_0}\right)\phi_\perp(x,y)\int_{-\infty}^{+\infty}\frac{d\lambda_{0S}}{d\zeta}(\zeta_W(t))\,dt \tag{10.70}$$

Using Eq. (10.63) and Eq. (10.31) we can write:

$$\int_{-\infty}^{+\infty}\lambda_{0S}(\zeta_W(t))\,dt = \frac{1}{(\beta_{0W}+\beta_{0S})c}\int_{-\infty}^{+\infty}\lambda_{0S}(\zeta)\,d\zeta = \frac{N_S}{(\beta_{0W}+\beta_{0S})c} \tag{10.71}$$

Similarly, for a bunched beam:

$$\int_{-\infty}^{+\infty}\frac{d\lambda_{0S}}{d\zeta}(\zeta_W(t))\,dt = \frac{1}{(\beta_{0W}+\beta_{0S})c}\int_{-\infty}^{+\infty}\frac{d\lambda_{0S}}{d\zeta}\,d\zeta = \frac{\lambda_{0S}(+\infty)-\lambda_{0S}(-\infty)}{(\beta_{0W}+\beta_{0S})c} = 0 \tag{10.72}$$

From which we can write:

$$\boxed{\Delta p_x = \frac{m_0}{m}\frac{\Delta P_x}{P_0} = -\frac{qq_{0S}N_S}{m\beta_{0W}\gamma_{0W}c^2}\frac{(1+\beta_{0W}\beta_{0S})}{(\beta_{0W}+\beta_{0S})}\frac{\partial\phi_\perp}{\partial x}(x,y)} \tag{10.73}$$

$$\boxed{\Delta p_y = \frac{m_0}{m}\frac{\Delta P_y}{P_0} = -\frac{qq_{0S}N_S}{m\beta_{0W}\gamma_{0W}c^2}\frac{(1+\beta_{0W}\beta_{0S})}{(\beta_{0W}+\beta_{0S})}\frac{\partial\phi_\perp}{\partial y}(x,y)} \tag{10.74}$$

$$\boxed{\Delta p_z = \frac{m_0}{m}\frac{\Delta P_z}{P_0} = 0} \tag{10.75}$$

10.5 Longitudinal profiles

10.5.1 Gaussian profile

The profile is in the form:

$$\lambda_0(z) = \frac{N}{\sqrt{2\pi}\sigma}e^{-\frac{(z-z_0)^2}{2\sigma^2}} \tag{10.76}$$

10.5.2 q-Gaussian

The profile is in the form:

$$\lambda_0(z) = \frac{N\sqrt{\beta}}{C_q} e_q \left(-\beta(z - z_0)^2 \right) \tag{10.77}$$

where e_q is the q-exponential function:

$$e_q(x) = [1 + (1 - q)x]_+^{\frac{1}{1-q}} \tag{10.78}$$

C_q is a normalization factor dependent on q alone:

$$C_q = \frac{\sqrt{\pi}\Gamma\left(\frac{3-q}{2(q-1)}\right)}{\sqrt{q-1}\Gamma\left(\frac{1}{q-1}\right)} \tag{10.79}$$

The parameter beta defines the standard deviation of the distribution:

$$\sigma = \sqrt{\frac{1}{\beta(5 - 3q)}} \iff \beta = \frac{1}{\sigma^2(5 - 3q)} \tag{10.80}$$

These expressions are valid for values of the parameter q in the range of interest:

$$1 < q < \frac{5}{3} \tag{10.81}$$

In general the q-Gaussian is defined outside this range, but for smaller values it has limited support (not of interest) and for larger values it has an undefined standard deviation.

10.6 Beam-beam interaction (6D model, Hirata method)

This chapter describes in detail the numerical method used for the simulation of beam-beam interactions in the weak-strong framework using the "Synchro Beam Mapping" approach [40, 41]. This allows correctly modeling the coupling introduced by beam-beam between the longitudinal and transverse planes. The goal of this document is in particular to provide in a compact, complete and self-consistent manner, the set of equations that are needed for the implementation in a numerical code. Complementary information can be found in [42], including graphical representations of the procedure presented in this note and several validation tests.

The effect of a "crossing angle" in an arbitrary "crossing plane" with respect to the assigned reference frame is taken into account with a suitable coordinate transformation following the approach described in [40, 9]. The employed description of the strong beam allows the correct inclusion of the hour-glass effect as well as the linear coupling at the interaction point, following the treatment presented in [9].

If not differently stated in an explicit way in the following, all coordinates are given in the reference system defined by the closed orbit of the weak beam, which is traveling

with positive speed along the s direction. The Interaction Point (IP) is located at $s=0$ and the crossing plane is defined by as the angle that the strong beam forms with the s-axis. In the presence of an offset between the beams (separation), the orientation of the reference system is defined by the closed orbit of the weak beam and the system is centered at the IP location as defined for the strong beam. Therefore the strong beam passes always through the origin of the reference frame.

10.6.1 Direct Lorentz boost (for the weak beam)

We want to transform the coordinates by moving to a Lorentz boosted frame in which the collision is head-on (i.e. $p_x = p_y = 0$ for the strong beam and for the reference particle of the weak beam). We call ϕ the half crossing angle and α the angle that the crossing plane makes with respect to the $x - z$ plane. For this purpose, we perform a transformation which actually includes four operations (more details can be found in Appendix 10.6.6.1 and in [42, 9]):

- Transform the accelerator positions and momenta into Cartesian coordinates (which can then be Lorentz boosted);

- Rotate particle coordinates to the "barycentric" reference frame;

- Perform the Lorentz boost;

- Drift all the particles back to $s = 0$ (as not all particles with $s = 0$ are fixed points of the transformation, and we are tracking with respect to s and not with respect to time).

We name the original accelerator coordinates (as defined in the SixTrack Physics Manual [43]):

$$\left(x, p_x, y, p_y, \sigma, \delta \right) \tag{10.82}$$

and the transformed coordinates:

$$\left(x^*, p_x^*, y^*, p_y^*, \sigma^*, \delta^* \right) \tag{10.83}$$

We start by computing the drift Hamiltonian in the original coordinates (we are doing a Lorentz transformation, therefore constants matter as we are assuming that h is the total energy of the particle):

$$h = \delta + 1 - \sqrt{\left(1 + \delta \right)^2 - p_x^2 - p_y^2} \tag{10.84}$$

We transform the momenta:

$$p_x^* = \frac{p_x}{\cos \phi} - h \cos \alpha \frac{\tan \phi}{\cos \phi} \tag{10.85}$$

$$p_y^* = \frac{p_y}{\cos \phi} - h \sin \alpha \frac{\tan \phi}{\cos \phi} \tag{10.86}$$

$$\delta^* = \delta - p_x \cos \alpha \tan \phi - p_y \sin \alpha \tan \phi + h \tan^2 \phi \tag{10.87}$$

In order to calculate the angles in the transformed frame, we evaluate:

$$p_z^* = \sqrt{(1+\delta^*)^2 - p_x^{*2} - p_y^{*2}} \tag{10.88}$$

We can now evaluate the following derivatives of the transformed Hamiltonian (from Hamilton's equations it can be easily seen that these are the angles in the boosted frame):

$$h_x^* = \frac{\partial h^*}{\partial p_x^*} = \frac{p_x^*}{p_z^*} \tag{10.89}$$

$$h_y^* = \frac{\partial h^*}{\partial p_y^*} = \frac{p_y^*}{p_z^*} \tag{10.90}$$

$$h_\sigma^* = \frac{\partial h^*}{\partial \delta} = 1 - \frac{\delta^* + 1}{p_z^*} \tag{10.91}$$

These can be used to build the following matrix:

$$L = \begin{pmatrix} (1 + h_x^* \cos\alpha \sin\phi) & h_x^* \sin\alpha \sin\phi & \cos\alpha \tan\phi \\ h_y^* \cos\alpha \sin\phi & \left(1 + h_y^* \sin\alpha \sin\phi\right) & \sin\alpha \tan\phi \\ h_\sigma^* \cos\alpha \sin\phi & h_\sigma^* \sin\alpha \sin\phi & \frac{1}{\cos\phi} \end{pmatrix} \tag{10.92}$$

which can then be used to transform the test-particle positions:

$$\begin{pmatrix} x^* \\ y^* \\ \sigma^* \end{pmatrix} = L \begin{pmatrix} x \\ y \\ \sigma \end{pmatrix} \tag{10.93}$$

10.6.2   Synchro-beam mapping

Following the approach introduced in [40], the strong beam is sliced along z. A common approach is to use constant-charge slices (see Appendix 10.6.6.2). For each particle in the weak beam and for each slice in the strong beam we perform the following.

We identify the position of the Collision Point (CP):

$$S = \frac{\sigma^* - \sigma_{sl}^*}{2} \tag{10.94}$$

Here σ^* is defined in the reference system of the weak beam ($\sigma^* > 0$ for particles at the head of the weak bunch) while σ_{sl}^* is defined in the reference system of the strong beam ($\sigma_{sl}^* > 0$ for particles at the head of the strong bunch). S is the coordinate of the collision point in the reference system of the weak beam (from Eq. 10.94, we can see that particles at the head of the weak bunch, collide with particles at the tail of the strong bunch at $S > 0$).

N.B. Here we are making an approximation since we are assuming that particles are moving at the speed of light along z independently on their angles. This means that the presented approach works only for small particle angles. It is for this reason that we need to Lorentz boost to get rid of the crossing angle and we cannot just move to the reference of the strong beam using a rotation (in this case the weak beam would have large angles).

We now evaluate the transverse position of the particle at the CP, with respect to the centroid of the slice, taking into account the particle angles :

$$\overline{x}^* = x^* + p_x^* S - (x_{\text{sl}}^* - p_{x,\text{sl}}^* S) \tag{10.95}$$

$$\overline{y}^* = y^* + p_y^* S - (y_{\text{sl}}^* - p_{y,\text{sl}}^* S) \tag{10.96}$$

Here x_{sl}^*, y_{sl}^*, $p_{x,\text{sl}}^*$ and $p_{y,\text{sl}}^*$ are defined in the coordinate system of the weak beam. The momenta of the strong slice appear with a negative sign since in the weak frame the strong slice is travelling "backwards".

10.6.3 Propagation of the strong beam to the collision point

The distribution of the strong beam in the transverse phase-space can be written using the Σ-matrix [12]:

$$f(\eta) = f_0 e^{-\eta^{\text{T}} \Sigma^{-1} \eta} \tag{10.97}$$

where:

$$\eta = \begin{pmatrix} x \\ p_x \\ y \\ p_y \end{pmatrix} \tag{10.98}$$

Points having same phase space density lie on hyper-elliptic manifolds defined by the equation:

$$\eta^{\text{T}} \Sigma^{-1} \eta = \text{const.} \tag{10.99}$$

Further considerations on the Σ-matrix can be found in Appendix 10.6.6.3.

We transform the Σ-matrix at the Interaction Point to take into account the Lorentz

Boost:

$$\Sigma_{11}^{*0} = \Sigma_{11}^{0} \tag{10.100}$$
$$\Sigma_{12}^{*0} = \Sigma_{12}^{0} / \cos\phi \tag{10.101}$$
$$\Sigma_{13}^{*0} = \Sigma_{13}^{0} \tag{10.102}$$
$$\Sigma_{14}^{*0} = \Sigma_{14}^{0} / \cos\phi \tag{10.103}$$
$$\Sigma_{22}^{*0} = \Sigma_{22}^{0} / \cos^2\phi \tag{10.104}$$
$$\Sigma_{23}^{*0} = \Sigma_{23}^{0} / \cos\phi \tag{10.105}$$
$$\Sigma_{24}^{*0} = \Sigma_{24}^{0} / \cos^2\phi \tag{10.106}$$
$$\Sigma_{33}^{*0} = \Sigma_{33}^{0} \tag{10.107}$$
$$\Sigma_{34}^{*0} = \Sigma_{34}^{0} / \cos\phi \tag{10.108}$$
$$\Sigma_{44}^{*0} = \Sigma_{44}^{0} / \cos^2\phi \tag{10.109}$$
$$\tag{10.110}$$

We transport the position part of the boosted Σ-matrix to the CP (here we are taking into account hourglass effect, assuming that we are in a drift space):

$$\Sigma_{11}^{*} = \Sigma_{11}^{*0} + 2\Sigma_{12}^{*0}S + \Sigma_{22}^{*0}S^2 \tag{10.111}$$
$$\Sigma_{33}^{*} = \Sigma_{33}^{*0} + 2\Sigma_{34}^{*0}S + \Sigma_{44}^{*0}S^2 \tag{10.112}$$
$$\Sigma_{13}^{*} = \Sigma_{13}^{*0} + \left(\Sigma_{14}^{*0} + \Sigma_{23}^{*0}\right) S + \Sigma_{24}^{*0}S^2 \tag{10.113}$$

The Σ-matrix is given in the reference system of the weak beam.
For singular cases we will also need to transport the other terms:

$$\Sigma_{12}^{*} = \Sigma_{12}^{*0} + \Sigma_{22}^{*0}S \tag{10.114}$$
$$\Sigma_{14}^{*} = \Sigma_{14}^{*0} + \Sigma_{24}^{*0}S \tag{10.115}$$
$$\Sigma_{22}^{*} = \Sigma_{22}^{*0} \tag{10.116}$$
$$\Sigma_{23}^{*} = \Sigma_{23}^{*0} + \Sigma_{24}^{*0}S \tag{10.117}$$
$$\Sigma_{24}^{*} = \Sigma_{24}^{*0} \tag{10.118}$$
$$\Sigma_{34}^{*} = \Sigma_{34}^{*0} + \Sigma_{44}^{*0}S \tag{10.119}$$
$$\Sigma_{44}^{*} = \Sigma_{44}^{*0} \tag{10.120}$$

We introduce the following three auxiliary quantities:

$$R\left(S\right) = \Sigma_{11}^{*} - \Sigma_{33}^{*} \tag{10.121}$$
$$W\left(S\right) = \Sigma_{11}^{*} + \Sigma_{33}^{*} \tag{10.122}$$
$$T\left(S\right) = R^2 + 4{\Sigma_{13}^{*}}^2 \tag{10.123}$$

The following derivatives will be needed in the following:

$$\frac{\partial R}{\partial S} = 2\left(\Sigma_{12}^0 - \Sigma_{34}^0\right) + 2S\left(\Sigma_{22}^0 - \Sigma_{44}^0\right) \tag{10.124}$$

$$\frac{\partial W}{\partial S} = 2\left(\Sigma_{12}^0 + \Sigma_{34}^0\right) + 2S\left(\Sigma_{22}^0 + \Sigma_{44}^0\right) \tag{10.125}$$

$$\frac{\partial \Sigma_{13}^*}{\partial S} = \Sigma_{14}^0 + \Sigma_{23}^0 + 2\Sigma_{24}^0 S \tag{10.126}$$

$$\frac{\partial T}{\partial S} = 2R\frac{\partial R}{\partial S} + 8\Sigma_{13}^*\frac{\partial \Sigma_{13}^*}{\partial S} \tag{10.127}$$

We will now compute, at the location of the CP, the coupling angle θ, defining a reference frame in which the beam is decoupled. We will call $\hat{x}$ and $\hat{y}$ the coordinates in the decoupled frame and $\hat{\Sigma}_{11}^*$, $\hat{\Sigma}_{33}^*$ the corresponding squared beam sizes. The angle θ is defined as the angle between the $\hat{x}$-axis and the x-axis.

These quantities can be found by diagonalizing the $x - y$ block of the Σ-matrix. We will make determination choices (Eqs. 10.130, 10.133 and 10.137) so that the set $(\theta, \hat{\Sigma}_{11}^*, \hat{\Sigma}_{33}^*)$ is uniquely defined and the coupling angle θ lies in the interval:

$$-\frac{\pi}{4} < \theta < \frac{\pi}{4} \tag{10.128}$$

Different cases need to be treated separately:

Case T>0, $\left|\Sigma_{13}^*\right|$>0

We evaluate the coupling angle at the position of the CP in the boosted frame:

$$\cos 2\theta = \mathrm{sgn}\left(\Sigma_{11}^* - \Sigma_{33}^*\right)\frac{\Sigma_{11}^* - \Sigma_{33}^*}{\sqrt{\left(\Sigma_{11}^* - \Sigma_{33}^*\right)^2 + 4\Sigma_{13}^{*2}}} \tag{10.129}$$

Or more synthetically:

$$\cos 2\theta = \mathrm{sgn}(R)\frac{R}{\sqrt{T}} \tag{10.130}$$

In the following we will need also the derivative of this quantity:

$$\frac{\partial}{\partial S}\left[\cos 2\theta\right] = \mathrm{sgn}(R)\left(\frac{\partial R}{\partial S}\frac{1}{\sqrt{T}} - \frac{R}{2\left(\sqrt{T}\right)^3}\frac{\partial T}{\partial S}\right) \tag{10.131}$$

It can be proved that [9]:

$$\cos\theta = \sqrt{\frac{1}{2}\left(1 + \cos 2\theta\right)} \tag{10.132}$$

$$\sin\theta = \mathrm{sgn}(R)\mathrm{sgn}(\Sigma_{13}^*)\sqrt{\frac{1}{2}\left(1 - \cos 2\theta\right)} \tag{10.133}$$

The corresponding derivatives are given by:

$$\frac{\partial}{\partial S}\cos\theta = \frac{1}{4\cos\theta}\frac{\partial}{\partial S}\cos 2\theta \tag{10.134}$$

$$\frac{\partial}{\partial S}\sin\theta = -\frac{1}{4\sin\theta}\frac{\partial}{\partial S}\cos 2\theta \tag{10.135}$$

The squared beam sizes in the rotated (un-coupled) boosted frame are given by:

$$\hat{\Sigma}_{11}^* = \frac{1}{2}\left[(\Sigma_{11}^* + \Sigma_{33}^*) + \text{sgn}\,(\Sigma_{11}^* - \Sigma_{33}^*)\sqrt{(\Sigma_{11}^* - \Sigma_{33}^*)^2 + 4\Sigma_{13}^{*\,2}}\right] \tag{10.136}$$

$$\hat{\Sigma}_{33}^* = \frac{1}{2}\left[(\Sigma_{11}^* + \Sigma_{33}^*) - \text{sgn}\,(\Sigma_{11}^* - \Sigma_{33}^*)\sqrt{(\Sigma_{11}^* - \Sigma_{33}^*)^2 + 4\Sigma_{13}^{*\,2}}\right] \tag{10.137}$$

Equation 10.137 can be written in a compact form as:

$$\hat{\Sigma}_{11}^* = \frac{1}{2}\left(W + \text{sgn}(R)\sqrt{T}\right) \tag{10.138}$$

$$\hat{\Sigma}_{33}^* = \frac{1}{2}\left(W - \text{sgn}(R)\sqrt{T}\right) \tag{10.139}$$

The corresponding derivatives, which will be needed in the following, are given by:

$$\frac{\partial}{\partial S}\left[\hat{\Sigma}_{11}^*\right] = \frac{1}{2}\left(\frac{\partial W}{\partial S} + \text{sgn}(R)\frac{1}{2\sqrt{T}}\frac{\partial T}{\partial S}\right) \tag{10.140}$$

$$\frac{\partial}{\partial S}\left[\hat{\Sigma}_{33}^*\right] = \frac{1}{2}\left(\frac{\partial W}{\partial S} - \text{sgn}(R)\frac{1}{2\sqrt{T}}\frac{\partial T}{\partial S}\right) \tag{10.141}$$

Case T>0, $\left|\Sigma_{13}^*\right|$=0:

The treatment of the previous case is still applicable with the exception of Eq. 10.135 in which the denominator becomes zero. This happens when Σ_{13}^*=0, which implies $\sqrt{T} = |R|$ and therefore $\cos 2\theta = 1$. The case $T = 0$ will be treated separately later, therefore here we can assume $|R| > 0$. We can expand with respect to Σ_{13}^*/R obtaining:

$$\cos 2\theta = \frac{|R|}{\sqrt{R^2 + 4\Sigma_{13}^{*\,2}}} = \frac{1}{\sqrt{1 + 4\frac{\Sigma_{13}^{*\,2}}{R^2}}} \simeq \frac{1}{1 + 2\frac{\Sigma_{13}^{*\,2}}{R^2}} \simeq 1 - 2\frac{\Sigma_{13}^{*\,2}}{R^2} \tag{10.142}$$

Replacing these result in Eq. 10.133 we obtain:

$$\sin\theta = \text{sgn}(R)\text{sgn}(\Sigma_{13}^*)\frac{\left|\Sigma_{13}^*\right|}{|R|} = \frac{\Sigma_{13}^*}{R} \tag{10.143}$$

We call S_0 the location at which $\Sigma_{13}^* = 0$. At this location we define the auxiliary quantities:

$$c = \Sigma_{14}^* + \Sigma_{23}^* \tag{10.144}$$

$$d = \Sigma_{24}^* \tag{10.145}$$

We introduce $\Delta S = S - S_0$ and we can write using Eqs. 10.111–10.113:

$$\Sigma_{13}^* = c\Delta S + d\Delta S^2 \tag{10.146}$$

By taking the derivative of Eq. 10.143 and using Eq. 10.146 we obtain:

$$\frac{\partial}{\partial S} \sin \theta = \frac{1}{R^2} \left[(c + 2d\Delta S)\, R - \frac{\partial R}{\partial S} \left(c\Delta S + d\Delta S^2 \right) \right] \tag{10.147}$$

In the implementation we need only the value for ΔS=0, which is simply given by:

$$\frac{\partial}{\partial S} \sin \theta = \frac{c}{R} \tag{10.148}$$

Case T=0, $|c|$>0

Special care has to be taken at sections S_0 at which $\Sigma_{11}^* = \Sigma_{33}^*$ and $\Sigma_{13}^* = 0$ as Eqs. 10.130 and 10.141 cannot be evaluated directly. Also in this case we define:

$$\Delta S = S - S_0 \tag{10.149}$$

At the location of the apparent singularity (ΔS=0) we define the auxiliary quantities:

$$a = \Sigma_{12}^* - \Sigma_{34}^* \tag{10.150}$$
$$b = \Sigma_{22}^* - \Sigma_{44}^* \tag{10.151}$$
$$c = \Sigma_{14}^* + \Sigma_{23}^* \tag{10.152}$$
$$d = \Sigma_{24}^* \tag{10.153}$$

and therefore, using Eqs. 10.111–10.113, we can write:

$$R = 2a\Delta S + b\Delta S^2 \tag{10.154}$$
$$\Sigma_{13}^* = c\Delta S + d\Delta S^2 \tag{10.155}$$

With these definitions the function T (defined by Eq. 10.123) can be expanded around $\Delta S = 0$ (using the Eqs. 10.111, 10.112, 10.113):

$$T = \Delta S^2 \left[(2a + b\Delta S)^2 + 4\,(c + d\Delta S)^2 \right] \tag{10.156}$$

Replacing Eq. 10.156 in Eq. 10.130 allows removing the apparent singularity:

$$\cos 2\theta = \frac{|2a + b\Delta S|}{\sqrt{(2a + b\Delta S)^2 + 4\,(c + d\Delta S)^2}} \tag{10.157}$$

This can be derived obtaining:

$$\frac{\partial}{\partial S} \left[\cos 2\theta \right] = \mathrm{sgn}(2a + b\Delta S) \left[\frac{b}{\sqrt{(2a + b\Delta S)^2 + 4\,(c + d\Delta S)^2}} \right.$$

$$\left. - \frac{(2a + b\Delta S)(2ab + b^2\Delta s + 4cd + 4d^2\Delta S)}{\left(\sqrt{(2a + b\Delta S)^2 + 4\,(c + d\Delta S)^2} \right)^3} \right] \tag{10.158}$$

Similarly, replacing Eq. 10.156 in Eq. 10.139 we obtain:

$$\hat{\Sigma}_{11}^* = \frac{W}{2} + \frac{1}{2}\text{sgn}\left(2a\Delta S + b\Delta S^2\right)|\Delta S|\sqrt{(2a + b\Delta S)^2 + 4(c + d\Delta S)^2} \qquad (10.159)$$

$$\hat{\Sigma}_{33}^* = \frac{W}{2} - \frac{1}{2}\text{sgn}\left(2a\Delta S + b\Delta S^2\right)|\Delta S|\sqrt{(2a + b\Delta S)^2 + 4(c + d\Delta S)^2} \qquad (10.160)$$

This can be derived obtaining:

$$\frac{\partial}{\partial S}\left[\hat{\Sigma}_{11}^*\right] = \frac{1}{2}\frac{\partial W}{\partial S} + \frac{1}{2}\text{sgn}\left(2a\Delta S + b\Delta S^2\right)\text{sgn}(\Delta S)\left[\sqrt{(2a + b\Delta S)^2 + 4(c + d\Delta S)^2}\right.$$
$$\left. + \frac{\Delta S\left(2ab + b^2\Delta s + 4cd + 4d^2\Delta S\right)}{\sqrt{(2a + b\Delta S)^2 + 4(c + d\Delta S)^2}}\right] \qquad (10.161)$$

$$\frac{\partial}{\partial S}\left[\hat{\Sigma}_{33}^*\right] = \frac{1}{2}\frac{\partial W}{\partial S} - \frac{1}{2}\text{sgn}\left(2a\Delta S + b\Delta S^2\right)\text{sgn}(\Delta S)\left[\sqrt{(2a + b\Delta S)^2 + 4(c + d\Delta S)^2}\right.$$
$$\left. + \frac{\Delta S\left(2ab + b^2\Delta s + 4cd + 4d^2\Delta S\right)}{\sqrt{(2a + b\Delta S)^2 + 4(c + d\Delta S)^2}}\right] \qquad (10.162)$$

In the implementation only the values at $\Delta S = 0$ are needed. For this case the obtained results above can be simplified as:

$$\cos 2\theta = \frac{|2a|}{2\sqrt{a^2 + c^2}} \qquad (10.163)$$

$$\frac{\partial}{\partial S}\left[\cos 2\theta\right] = \text{sgn}(2a)\left[\frac{b}{2\sqrt{a^2 + c^2}} - \frac{a(ab + 2cd)}{2\left(\sqrt{a^2 + c^2}\right)^3}\right] \qquad (10.164)$$

$$\hat{\Sigma}_{11}^* = \frac{W}{2} \qquad (10.165)$$

$$\hat{\Sigma}_{33}^* = \frac{W}{2} \qquad (10.166)$$

$$\frac{\partial}{\partial S}\left[\hat{\Sigma}_{11}^*\right] = \frac{1}{2}\frac{\partial W}{\partial S} + \text{sgn}(2a)\sqrt{a^2 + c^2} \qquad (10.167)$$

$$\frac{\partial}{\partial S}\left[\hat{\Sigma}_{33}^*\right] = \frac{1}{2}\frac{\partial W}{\partial S} - \text{sgn}(2a)\sqrt{a^2 + c^2} \qquad (10.168)$$

Eqs. 10.133 and 10.135 can still be used to evaluate $\sin\theta$ and $\cos\theta$ and the corresponding derivatives, once we assume that $\text{sgn}(0) = 1$ and noticing from Eqs. 10.154 and 10.155 that for small ΔS:

$$\text{sgn}(R)\text{sgn}(\Sigma_{13}^*) = \text{sgn}(a)\text{sgn}(c) \qquad (10.169)$$

Case T=0, c=0, $|a|>0$

The treatment of the previous case is still applicable with the exception of Eq. 10.135 in which the denominator becomes zero.
For this case we can write (from Eq. 10.157) around the point where this condition is verified:

$$\cos 2\theta = \frac{1}{\sqrt{1 + \frac{4d^2\Delta S^2}{(2a+b\Delta S)^2}}} \simeq 1 - \frac{2d^2\Delta S^2}{(2a + b\Delta S)^2} \tag{10.170}$$

We notice from Eqs. 10.154 and 10.155 that for small ΔS:

$$\text{sgn}(R)\text{sgn}(\Sigma^*_{13}) = \text{sgn}(a)\text{sgn}(d)\text{sgn}(\Delta S) \tag{10.171}$$

Replacing Eq. 10.170 and 10.171 into in Eq. 10.133 we obtain:

$$\sin \theta = \frac{d\Delta S}{2a} \left| 1 - \frac{b\Delta S}{2a} \right| \tag{10.172}$$

which can be derived in $\Delta S = 0$ obtaining:

$$\frac{\partial}{\partial S} \sin \theta = \frac{d}{2a} \tag{10.173}$$

The case in which also $d = 0$ is (or is equivalent to) the uncoupled case as Σ^*_{13} is zero for all S.

Case T=0, c=0, a=0

Around the apparently singular point we can write:

$$R = b\Delta S^2 \tag{10.174}$$
$$\Sigma^*_{13} = d\Delta S^2 \tag{10.175}$$

Therefore:

$$T = S^4 \left(b^2 + 4d^2 \right) \tag{10.176}$$

and:

$$\cos 2\theta = \frac{|b|}{\sqrt{b^2 + 4d^2}} \tag{10.177}$$

which is a constant. Eqs. 10.133 and 10.135 can still be used to evaluate $\sin \theta$ and $\cos \theta$ while the corresponding derivatives vanish:
This can be derived obtaining:

$$\frac{\partial}{\partial S} \cos \theta = 0 \tag{10.178}$$

$$\frac{\partial}{\partial S} \sin \theta = 0 \tag{10.179}$$

Replacing $a = c = 0$ into Eq 10.160 we obtain:

$$\hat{\Sigma}_{11}^* = \frac{W}{2} + \frac{1}{2}\text{sgn}(b)\Delta S^2 \sqrt{b^2 + 4d^2} \tag{10.180}$$

$$\hat{\Sigma}_{33}^* = \frac{W}{2} - \frac{1}{2}\text{sgn}(b)\Delta S^2 \sqrt{b^2 + 4d^2} \tag{10.181}$$

and:

$$\frac{\partial}{\partial S}\left[\hat{\Sigma}_{11}^*\right] = \frac{1}{2}\frac{\partial W}{\partial S} \tag{10.182}$$

$$\frac{\partial}{\partial S}\left[\hat{\Sigma}_{33}^*\right] = \frac{1}{2}\frac{\partial W}{\partial S} \tag{10.183}$$

The case in which also $d = 0$ is (or is equivalent to the uncoupled case) as Σ_{13}^* is zero for all S.

10.6.4 Forces and kicks on weak beam particles

The positions of the weak beam particle in the un-coupled boosted frame are given by:

$$\hat{\bar{x}}^* = \bar{x}^* \cos\theta + \bar{y}^* \sin\theta \tag{10.184}$$

$$\hat{\bar{y}}^* = -\bar{x}^* \sin\theta + \bar{y}^* \cos\theta \tag{10.185}$$

In the following we will also need to evaluate:

$$\frac{\partial}{\partial S}\left[\hat{\bar{x}}^*\left(\theta(S)\right)\right] = \frac{\partial \bar{x}^*}{\partial S}\cos\theta + \bar{x}^*\frac{\partial}{\partial S}\left[\cos\theta\right] + \frac{\partial \bar{y}^*}{\partial S}\sin\theta + \bar{y}^*\frac{\partial}{\partial S}\left[\sin\theta\right] \tag{10.186}$$

$$\frac{\partial}{\partial S}\left[\hat{\bar{y}}^*\left(\theta(S)\right)\right] = -\frac{\partial \bar{x}^*}{\partial S}\sin\theta - \bar{x}^*\frac{\partial}{\partial S}\left[\sin\theta\right] + \frac{\partial \bar{y}^*}{\partial S}\cos\theta + \bar{y}^*\frac{\partial}{\partial S}\left[\cos\theta\right] \tag{10.187}$$

In this boosted, rotated and re-centered frame, closed formulas exist to evaluate the following quantities:

$$\hat{F}_x^* = -K_{sl}\frac{\partial \hat{U}^*}{\partial \hat{\bar{x}}^*}\left(\hat{\bar{x}}^*, \hat{\bar{y}}^*, \hat{\Sigma}_{11}^*, \hat{\Sigma}_{33}^*\right) \tag{10.188}$$

$$\hat{F}_y^* = -K_{sl}\frac{\partial \hat{U}^*}{\partial \hat{\bar{y}}^*}\left(\hat{\bar{x}}^*, \hat{\bar{y}}^*, \hat{\Sigma}_{11}^*, \hat{\Sigma}_{33}^*\right) \tag{10.189}$$

$$\hat{G}_x^* = -K_{sl}\frac{\partial \hat{U}^*}{\partial \hat{\Sigma}_{11}^*}\left(\hat{\bar{x}}^*, \hat{\bar{y}}^*, \hat{\Sigma}_{11}^*, \hat{\Sigma}_{33}^*\right) \tag{10.190}$$

$$\hat{G}_y^* = -K_{sl}\frac{\partial \hat{U}^*}{\partial \hat{\Sigma}_{33}^*}\left(\hat{\bar{x}}^*, \hat{\bar{y}}^*, \hat{\Sigma}_{33}^*, \hat{\Sigma}_{33}^*\right) \tag{10.191}$$

where $\hat{U}^*$ is the electric potential associated to the normalized transverse distribution and:

$$K_{sl} = \frac{N_{sl}q_{sl}q_0}{P_0 c} \tag{10.192}$$

where N_{sl} is the number of particles in the strong-beam slice, q_{sl} and q_0 are the particle charges for the strong and weak beam respectively, P_0 is the reference momentum of the weak beam.

The minus sign in the Eqs. 10.188-10.191 comes from the definition of electric potential, i.e. $E = -\nabla U$.

For a bi-Gaussian beam (elliptic) [40]:

$$
\hat{f}_x^* = -\frac{\partial \hat{U}^*}{\partial \hat{\bar{x}}^*} = \frac{1}{2\epsilon_0 \sqrt{2\pi \left(\hat{\Sigma}_{11}^* - \hat{\Sigma}_{33}^*\right)}} \mathrm{Im}\left[w\left(\frac{\hat{\bar{x}}^* + i\hat{\bar{y}}^*}{\sqrt{2\left(\hat{\Sigma}_{11}^* - \hat{\Sigma}_{33}^*\right)}} \right) \right.
$$

$$
\left. - \exp\left(-\frac{(\hat{\bar{x}}^*)^2}{2\hat{\Sigma}_{11}^*} - \frac{(\hat{\bar{y}}^*)^2}{2\hat{\Sigma}_{33}^*} \right) w\left(\frac{\hat{\bar{x}}^* \sqrt{\frac{\hat{\Sigma}_{33}^*}{\hat{\Sigma}_{11}^*}} + i\hat{\bar{y}}^* \sqrt{\frac{\hat{\Sigma}_{11}^*}{\hat{\Sigma}_{33}^*}}}{\sqrt{2\left(\hat{\Sigma}_{11}^* - \hat{\Sigma}_{33}^*\right)}} \right) \right]
$$

$$(10.193)$$

$$
\hat{f}_y^* = -\frac{\partial \hat{U}^*}{\partial \hat{\bar{x}}^*} = \frac{1}{2\epsilon_0 \sqrt{2\pi \left(\hat{\Sigma}_{11}^* - \hat{\Sigma}_{33}^*\right)}} \mathrm{Re}\left[w\left(\frac{\hat{\bar{x}}^* + i\hat{\bar{y}}^*}{\sqrt{2\left(\hat{\Sigma}_{11}^* - \hat{\Sigma}_{33}^*\right)}} \right) \right.
$$

$$
\left. - \exp\left(-\frac{(\hat{\bar{x}}^*)^2}{2\hat{\Sigma}_{11}^*} - \frac{(\hat{\bar{y}}^*)^2}{2\hat{\Sigma}_{33}^*} \right) w\left(\frac{\hat{\bar{x}}^* \sqrt{\frac{\hat{\Sigma}_{33}^*}{\hat{\Sigma}_{11}^*}} + i\hat{\bar{y}}^* \sqrt{\frac{\hat{\Sigma}_{11}^*}{\hat{\Sigma}_{33}^*}}}{\sqrt{2\left(\hat{\Sigma}_{11}^* - \hat{\Sigma}_{33}^*\right)}} \right) \right]
$$

$$(10.194)$$

$$
\hat{g}_x^* = -\frac{\partial \hat{U}^*}{\partial \hat{\Sigma}_{11}^*} = -\frac{1}{2\left(\hat{\Sigma}_{11}^* - \hat{\Sigma}_{33}^*\right)} \left\{ \hat{\bar{x}}^* \hat{E}_x^* + \hat{\bar{y}}^* \hat{E}_y^* + \frac{1}{2\pi\epsilon_0}\left[\sqrt{\frac{\hat{\Sigma}_{33}^*}{\hat{\Sigma}_{11}^*}} \exp\left(-\frac{(\hat{\bar{x}}^*)^2}{2\hat{\Sigma}_{11}^*} - \frac{(\hat{\bar{y}}^*)^2}{2\hat{\Sigma}_{33}^*} \right) - 1 \right] \right\}
$$

$$(10.195)$$

$$
\hat{g}_y^* = -\frac{\partial \hat{U}^*}{\partial \hat{\Sigma}_{33}^*} = \frac{1}{2\left(\hat{\Sigma}_{11}^* - \hat{\Sigma}_{33}^*\right)} \left\{ \hat{\bar{x}}^* \hat{E}_x^* + \hat{\bar{y}}^* \hat{E}_y^* + \frac{1}{2\pi\epsilon_0}\left[\sqrt{\frac{\hat{\Sigma}_{11}^*}{\hat{\Sigma}_{33}^*}} \exp\left(-\frac{(\hat{\bar{x}}^*)^2}{2\hat{\Sigma}_{11}^*} - \frac{(\hat{\bar{y}}^*)^2}{2\hat{\Sigma}_{33}^*} \right) - 1 \right] \right\}
$$

$$(10.196)$$

where w is the Faddeeva function.

For a round beam, i.e. $\hat{\Sigma}^*_{11} = \hat{\Sigma}^*_{33} = \hat{\Sigma}^*$:

$$\hat{f}^*_x = -\frac{\partial \hat{U}^*}{\partial \hat{\hat{x}}^*} = \frac{1}{2\pi\epsilon_0} \left[1 - \exp\left(-\frac{(\hat{\hat{x}}^*)^2 + (\hat{\hat{y}}^*)^2}{2\hat{\Sigma}^*} \right) \right] \frac{x}{(\hat{\hat{x}}^*)^2 + (\hat{\hat{y}}^*)^2} \tag{10.197}$$

$$\hat{f}^*_y = -\frac{\partial \hat{U}^*}{\partial \hat{\hat{x}}^*} = \frac{1}{2\pi\epsilon_0} \left[1 - \exp\left(-\frac{(\hat{\hat{x}}^*)^2 + (\hat{\hat{y}}^*)^2}{2\hat{\Sigma}^*} \right) \right] \frac{y}{(\hat{\hat{x}}^*)^2 + (\hat{\hat{y}}^*)^2} \tag{10.198}$$

$$\hat{g}^*_x = -\frac{\partial \hat{U}^*}{\partial \hat{\Sigma}^*_{11}} = \frac{1}{2\left[(\hat{\hat{x}}^*)^2 + (\hat{\hat{y}}^*)^2\right]} \left[\hat{\hat{y}}^* \hat{E}^*_y - \hat{\hat{x}}^* \hat{E}^*_x + \frac{1}{2\pi\epsilon_0} \frac{\left(\hat{\hat{x}}^*\right)^2}{\hat{\Sigma}^*} \exp\left(-\frac{(\hat{\hat{x}}^*)^2 + (\hat{\hat{y}}^*)^2}{2\hat{\Sigma}^*} \right) \right] \tag{10.199}$$

$$\hat{g}^*_y = -\frac{\partial \hat{U}^*}{\partial \hat{\Sigma}^*_{33}} = \frac{1}{2\left[(\hat{\hat{x}}^*)^2 + (\hat{\hat{y}}^*)^2\right]} \left[\hat{\hat{x}}^* \hat{E}^*_x - \hat{\hat{y}}^* \hat{E}^*_y + \frac{1}{2\pi\epsilon_0} \frac{\left(\hat{\hat{y}}^*\right)^2}{\hat{\Sigma}^*} \exp\left(-\frac{(\hat{\hat{x}}^*)^2 + (\hat{\hat{y}}^*)^2}{2\hat{\Sigma}^*} \right) \right] \tag{10.200}$$

We have used lower-case symbols to indicate that the factor given by Eq. 10.192 is not yet applied.

The transverse kicks in the coupled (but still boosted) reference frame are given by:

$$F^*_x = \hat{F}^*_x \cos\theta - \hat{F}^*_y \sin\theta \tag{10.201}$$

$$F^*_y = \hat{F}^*_x \sin\theta + \hat{F}^*_y \cos\theta \tag{10.202}$$

To compute the longitudinal kick we notice from Eq. 10.94 that:

$$\frac{\partial}{\partial z} = \frac{1}{2}\frac{\partial}{\partial S} \tag{10.203}$$

Therefore:

$$F^*_z = \frac{1}{2}\frac{\partial}{\partial S} \left[\hat{U}^* \left(\hat{\hat{x}}^* (\theta(S)), \hat{\hat{y}}^* (\theta(S)), \hat{\Sigma}^*_{11}(S), \hat{\Sigma}^*_{33}(S) \right) \right] \tag{10.204}$$

This can be rewritten as:

$$F^*_z = \frac{1}{2}\left(\hat{F}^*_x \frac{\partial}{\partial S}\left[\hat{\hat{x}}^*(\theta(S)) \right] + \hat{F}^*_y \frac{\partial}{\partial S}\left[\hat{\hat{y}}^*(\theta(S)) \right] + \hat{G}^*_x \frac{\partial}{\partial S}\left[\hat{\Sigma}^*_{11}(S) \right] + \hat{G}^*_y \frac{\partial}{\partial S}\left[\hat{\Sigma}^*_{33}(S) \right] \right) \tag{10.205}$$

where all the terms have been evaluated before.
The quantities evaluated so far can be used to compute the effect of the beam-beam interaction on the particles coordinates and momenta [40]:

$$x^*_{new} = x^* - SF^*_x \tag{10.206}$$

$$p^*_{x,new} = p^*_x + F^*_x \tag{10.207}$$

$$y^*_{new} = y^* - SF^*_y \tag{10.208}$$

$$p^*_{y,new} = p^*_y + F^*_y \tag{10.209}$$

$$z^*_{new} = z^* \tag{10.210}$$

$$\delta^*_{new} = \delta^* + F^*_z + \frac{1}{2}\left[F^*_x \left(p^*_x + \frac{1}{2}F^*_x + p^*_{x,\text{sl}} \right) + F^*_y \left(p^*_y + \frac{1}{2}F^*_y + p^*_{y,\text{sl}} \right) \right] \tag{10.211}$$

The physical meaning of the different terms in these equations is illustrated in [42].

10.6.5 Inverse Lorentz boost (for the weak beam)

Now we need to go back to the accelerator coordinates by undoing the transformation described in Sec. 10.6.1.
As before we evaluate:

$$p_z^* = \sqrt{(1+\delta^*)^2 - p_x^{*2} - p_y^{*2}} \tag{10.212}$$

and then:

$$h_x^* = \frac{p_x^*}{p_z^*} \tag{10.213}$$

$$h_y^* = \frac{p_y^*}{p_z^*} \tag{10.214}$$

$$h_\sigma^* = 1 - \frac{\delta^* + 1}{p_z^*} \tag{10.215}$$

We invert the matrix (10.92) using Cramer's rule:

$$\mathrm{Det}\,(L) = \frac{1}{\cos\phi} + \left(h_x^* \cos\alpha + h_y^* \sin\alpha - h_\sigma^* \sin\phi \right) \tan\phi \tag{10.216}$$

$$
L^{\mathrm{inv}} = \frac{1}{\mathrm{Det}\,(L)} \times
$$
$$
\begin{pmatrix}
\left(\frac{1}{\cos\phi} + \sin\alpha\tan\phi\left(h_y^* - h_\sigma^*\sin\alpha\sin\phi\right) \right) & \sin\alpha\tan\phi\left(h_\sigma^*\cos\alpha\sin\phi - h_x^*\right) & -\tan\phi\left(\cos\alpha - h_x^*\sin^2\alpha\sin\phi + h_y^*\cos\alpha\sin\alpha\sin\phi\right) \\
\cos\alpha\tan\phi\left(-h_y^* + h_\sigma^*\sin\alpha\sin\phi\right) & \left(\frac{1}{\cos\phi} + \cos\alpha\tan\phi\left(h_x^* - h_\sigma^*\cos\alpha\sin\phi\right) \right) & -\tan\phi\left(\sin\alpha - h_y^*\cos^2\alpha\sin\phi + h_x^*\cos\alpha\sin\alpha\sin\phi\right) \\
-h_\sigma^*\cos\alpha\sin\phi & -h_\sigma^*\sin\alpha\sin\phi & \left(1 + h_x^*\cos\alpha\sin\phi + h_y^*\sin\alpha\sin\phi\right)
\end{pmatrix}
\tag{10.217}
$$

This can be used to transform the positions:

$$
\begin{pmatrix} x \\ y \\ \sigma \end{pmatrix} = L^{\mathrm{inv}} \begin{pmatrix} x^* \\ y^* \\ \sigma^* \end{pmatrix} \tag{10.218}
$$

The Hamiltonian can be transformed with a re-scaling:

$$h = h^* \cos^2\phi = \left(\delta^* + 1 - \sqrt{(1+\delta^*)^2 - p_x^{*2} - p_y^{*2}} \right) \cos^2\phi \tag{10.219}$$

This can be used to transform the transverse momenta (inverting Eqs. 10.85 and following):

$$p_x = p_x^* \cos\phi + h\cos\alpha\tan\phi \tag{10.220}$$
$$p_y = p_y^* \cos\phi + h\sin\alpha\tan\phi \tag{10.221}$$

The longitudinal momentum can be calculated using directly Eq. 10.87:

$$\delta = \delta^* + p_x\cos\alpha\tan\phi + p_y\sin\alpha\tan\phi - h\tan^2\phi \tag{10.222}$$

10.6.6   Additional material

10.6.6.1   Detailed explanation of "the boost" transformation

The reference frame transformation used in Sec. 10.6.1 can be written as [40, 9]:

$$
\begin{pmatrix} \sigma^* \\ x^* \\ s^* \\ y^* \end{pmatrix} = A^{-1} R_{\mathrm{CP}}^{-1} L_{\mathrm{boost}} R_{\mathrm{CA}} R_{\mathrm{CP}} A \begin{pmatrix} \sigma \\ x \\ s \\ y \end{pmatrix}
\tag{10.223}
$$

Here A is the matrix transforming the accelerator coordinates (Courant-Snyder) to Cartesian coordinates:

$$
\begin{pmatrix} ct \\ X \\ Z \\ Y \end{pmatrix} = A \begin{pmatrix} \sigma \\ x \\ s \\ y \end{pmatrix} = \begin{pmatrix} -1 & 0 & 1 & 0 \\ 0 & 1 & 0 & 0 \\ 0 & 0 & 1 & 0 \\ 0 & 0 & 0 & 1 \end{pmatrix} \begin{pmatrix} \sigma \\ x \\ s \\ y \end{pmatrix}
\tag{10.224}
$$

R_{CP} is a rotation matrix bringing the crossing plane to the $X - Z$ plane:

$$
R_{\mathrm{CP}} = \begin{pmatrix} 1 & 0 & 1 & 0 \\ 0 & \cos\alpha & 0 & \sin\alpha \\ 0 & 0 & 1 & 0 \\ 0 & -\sin\alpha & 0 & \cos\alpha \end{pmatrix}
\tag{10.225}
$$

R_{CA} is a rotation matrix moving to the barycentric reference frame (in which the two beams are symmetric with respect to the s-axis):

$$
R_{\mathrm{CA}} = \begin{pmatrix} 1 & 0 & 0 & 0 \\ 0 & \cos\phi & \sin\phi & 0 \\ 0 & -\sin\phi & \cos\phi & 0 \\ 0 & 0 & 0 & 1 \end{pmatrix}
\tag{10.226}
$$

L_{boost} is the matrix defining a Lorentz boost in the direction of the rotated X-axis:

$$
L_{\mathrm{boost}} = \begin{pmatrix} 1/\cos\phi & -\tan\phi & 0 & 0 \\ -\tan\phi & 1/\cos\phi & 0 & 0 \\ 0 & 0 & 1 & 0 \\ 0 & 0 & 0 & 1 \end{pmatrix}
\tag{10.227}
$$

The momenta are transformed similarly [9]:

$$
\begin{pmatrix} \delta^* \\ p_x^* \\ h^* \\ p_y^* \end{pmatrix} = B^{-1} R_{CP}{}^{-1} L_{\text{boost}} R_{CA} R_{CP} B \begin{pmatrix} \delta \\ p_x \\ h \\ p_y \end{pmatrix}
\tag{10.228}
$$

where the transformation from accelerator to Cartesian coordinates given by:

$$
\begin{pmatrix} E/c - p_0 \\ P_x \\ P_z - p_0 \\ P_y \end{pmatrix} = p_0 \begin{pmatrix} 1 & 0 & 0 & 0 \\ 0 & 1 & 0 & 0 \\ 0 & 0 & -1 & 0 \\ 0 & 0 & 0 & 1 \end{pmatrix} \begin{pmatrix} \delta \\ p_x \\ h \\ p_y \end{pmatrix}
\tag{10.229}
$$

As explaned in Sec.10.6.1 not all particles with $s = 0$ are fixed points of the transformation, therefore a drift back to s=0 needs to be performed as we are tracking w.r.t. s and not w.r.t. time. The net effect of the transformation is to move from the reference frame of the weak beam to the boosted barycentric frame.

10.6.6.2 Constant charge slicing

We consider a Gaussian longitudinal bunch distribution:

$$
\lambda(z) = \frac{1}{\sigma_z \sqrt{2\pi}} e^{-\frac{z^2}{2\sigma_z^2}}
\tag{10.230}
$$

We introduce the cumulative distribution function:

$$
Q(z) = \int_{-\infty}^{z} \lambda(z') dz' = \frac{1}{2} + \frac{1}{2} \text{erf}\left(\frac{z}{\sqrt{2}\sigma_z} \right)
\tag{10.231}
$$

We define longitudinal cuts z_n^{cut} such that the bunch is sliced in N sections having the same charge:

$$
Q(z_n^{\text{cut}}) = \frac{n}{N}
\tag{10.232}
$$

Replacing 10.232 in 10.231 we obtain:

$$
z_n^{\text{cut}} = \sqrt{2}\sigma_z \text{erf}^{-1}\left(\frac{2n}{N} - 1 \right)
\tag{10.233}
$$

For each slice we need to find the longitudinal centroid position. For generic slice having edges z_1 and z_2 the centroid position can be written as:

$$
z^{centroid} = \frac{1}{Q(z_2) - Q(z_1)} \int_{z_1}^{z_2} z\lambda(z) dz = \frac{\sigma_z}{\sqrt{2\pi}\left(Q(z_2) - Q(z_1)\right)} \left(e^{-\frac{z_1^2}{2\sigma_z^2}} - e^{-\frac{z_2^2}{2\sigma_z^2}} \right)
\tag{10.234}
$$

10.6.6.3   Considerations on the Σ-matrix description

Given the reduced Σ-matrix of the beam (including only position terms, no momenta):

$$\Sigma = \begin{pmatrix} \Sigma_{11} & \Sigma_{13} \\ \Sigma_{13} & \Sigma_{33} \end{pmatrix} \tag{10.235}$$

the distribution for a Gaussian beam can be written as:

$$\rho(\mathbf{x}) = \rho_0 e^{-\mathbf{x}^T \Sigma^{-1} \mathbf{x}} \tag{10.236}$$

Points having same density lie con ellipses defined by the equation:

$$\mathbf{x}^T \Sigma^{-1} \mathbf{x} = \text{const.} \tag{10.237}$$

As Σ is symmetric, it can be diagonalized:

$$\Sigma = \mathbf{V}\mathbf{W}\mathbf{V}^T \tag{10.238}$$

where the matrix $\mathbf{V}$ has in its columns the eigenvectors of Σ and $\mathbf{W}$ is a diagonal matrix with the corresponding eigenvalues:

$$W = \begin{pmatrix} \hat{\Sigma}_{11} & 0 \\ 0 & \hat{\Sigma}_{33} \end{pmatrix} \tag{10.239}$$

$\mathbf{V}$ is a unitary matrix (eigenvectors are ortho-normal):

$$\mathbf{V}\mathbf{V}^T = \mathbf{I} \Rightarrow \mathbf{V}^{-1} = \mathbf{V}^T \tag{10.240}$$

$\mathbf{V}$ can be used to transform coordinates from the initial frame to the de-coupled frame: where $\hat{\mathbf{x}}$ are the coordinates in the decoupled frame, i.e. the projections of of $\mathbf{x}$ on the eigenvectors:

$$\hat{\mathbf{x}} = \mathbf{V}^T \mathbf{x} \tag{10.241}$$

Combining Eqs. 10.238 and 10.240 we can write:

$$\Sigma^{-1} = \mathbf{V}\mathbf{W}^{-1}\mathbf{V}^T \tag{10.242}$$

This can be replaced in Eq. 10.237, re-writing the equation of the ellipse as:

$$\mathbf{x}^T \mathbf{V}\mathbf{W}^{-1}\mathbf{V}^T \mathbf{x} = \text{const.} \tag{10.243}$$

Using Eq. 10.241 we obtain the equation of the ellipse in the reference system of the eigenvectors:

$$\hat{\mathbf{x}}^T \mathbf{W}^{-1} \hat{\mathbf{x}} = \text{const.} \tag{10.244}$$

which can be rewritten in the familiar form:

$$\frac{\hat{x}^2}{\hat{\Sigma}_{11}} + \frac{\hat{y}^2}{\hat{\Sigma}_{33}} = \text{const.} \tag{10.245}$$

Once the Σ-matrix is assigned, the one-sigma ellipse can be drawn by the following procedure:

- We diagonalize Σ and we generate an auxiliary matrix defined as:

$$\mathbf{A} = \mathbf{V}\sqrt{\mathbf{W}}\mathbf{V}^T \tag{10.246}$$

- We generate a set of points in the unitary circle

$$\mathbf{z} = \begin{bmatrix} \cos t \\ \sin t \end{bmatrix} \tag{10.247}$$

- We apply $\mathbf{A}$ to t to generate points on the one-sigma ellipse:

$$\mathbf{x}_{1\sigma} = \mathbf{Az} \tag{10.248}$$

This can be verified as follows:

$$
\begin{aligned}
\mathbf{x}_{1\sigma}{}^{\mathrm{T}}\Sigma^{-1}\mathbf{x}_{1\sigma} &= \mathbf{z}^{\mathrm{T}}\mathbf{A}^{\mathrm{T}}\Sigma^{-1}\mathbf{Az} = \mathbf{z}^{\mathrm{T}}(\mathbf{V}\sqrt{\mathbf{W}}\mathbf{V})(\mathbf{V}^T\mathbf{W}^{-1}\mathbf{V}^T)(\mathbf{V}\sqrt{\mathbf{W}}\mathbf{V}^T)\mathbf{z} \\
&= \mathbf{z}^{\mathrm{T}}\mathbf{V}\sqrt{\mathbf{W}}\mathbf{W}^{-1}\sqrt{\mathbf{W}}\mathbf{V}^T\mathbf{z} = \mathbf{z}^{\mathrm{T}}\mathbf{V}\mathbf{V}^T\mathbf{z} = \mathbf{z}^{\mathrm{T}}\mathbf{z} = 1
\end{aligned}
\tag{10.249}
$$

10.7 Beam-beam interaction (6d model, Particle In Cell)

To simulate self-consistently the interaction between two bunches of particles, it is possible to use the Particle In Cell method. The computation is done in a boosted reference frame in which the bunches move mainly along s as illustrated in the previous section.

For this purpose, as for space charge simulations, we define a uniform 3D grid with grid sizes Δx, Δy, $\Delta \zeta$. We note that each value of ζ corresponds to a different time of arrival at the Interaction Point (IP):

$$\zeta = s_{\mathrm{IP}} - \beta_0 c t \ \Leftrightarrow \ t = \frac{s_{\mathrm{IP}} - \zeta}{\beta_0 c} \tag{10.250}$$

We simulate the interaction in discrete time intervals corresponding to the passage of the different slices. The duration of each interval is

$$\Delta t = \frac{\Delta \zeta}{\beta_0 c} \tag{10.251}$$

We call t_i the time at which the i-th slice is passing at the IP. The is is related to the ζ_i coordinate of the slice by the relation

$$t_i = \frac{s_{\mathrm{IP}} - \zeta_i}{\beta_0 c} \tag{10.252}$$

10.7.1   Propagation of particles during the interaction

From the conventional tracking using s as independent variable we get for all particles the coordinates at the IP, which we call x_{IP}, $p_{x\,IP}$, y_{IP}, $p_{y\,IP}$, $zeta_{IP} = s_{y\,IP} - \beta_0 ct_{IP}$, where t_{IP} is the time of arrival of the particle at the IP. Assuming the motion is in a drift space, for each time step, we propagate the particles from the IP to their positions at the time t_i:

$$x\left(t_i\right) = x_{IP} + \beta_x c\left(t_i - t_{IP}\right) = x_{IP} + \beta_x c\left(\frac{s_{IP} - \zeta_i}{\beta_0 c} - \frac{s_{IP} - \zeta_{IP}}{\beta_0 c}\right) \tag{10.253}$$

Using the fact that:

$$p_x = \frac{P_x}{P_0} = \frac{m_0 \gamma \beta_x c}{m_0 \gamma_0 \beta_0 c} = \frac{\gamma \beta_x}{\gamma_0 \beta_0} \tag{10.254}$$

we can write:

$$x\left(t_i\right) = x_{IP} + p_x \frac{\gamma_0}{\gamma}\left(\zeta_{IP} - \zeta_i\right) \tag{10.255}$$

With the coordinates of the propagated particles we can solve a Poisson problem having as source the 3D particle distribution at time t_i. Using the fact that the bunches are elongated and relativistic, we can solve the 2D Poisson equation instead of the full 3D problem. This procedure needs to be performed for the two colliding bunches.

10.7.2   Time relation between the two beams

For a particle of beam 1 having longitudinal coordinate ζ_{IP}^{B1} we want to know the longitudinal coordinate ζ_{IP}^{B2} corresponding to the section of beam 2 crossing the particle at time t_i.

We assume that the reference systems of the two beams are antiparallel and coincident in transverse:

$$s^{B2} - s_{IP}^{B2} = -\left(s^{B1} - s_{IP}^{B1}\right) \tag{10.256}$$

$$x^{B2} = -x^{B1} \tag{10.257}$$

$$y^{B2} = +x^{B1} \tag{10.258}$$

Similarly as done in Sec. 10.7.1, we can write the s position at the time t_i for the particles of beam 1 and beam 2:

$$s^{B1}\left(t_i\right) = s_{IP}^{B1} + \frac{\beta_s^{B1}}{\beta_0^{B1}}\left(\zeta_{IP}^{B1} - \zeta_i^{B1}\right) \tag{10.259}$$

$$s^{B2}\left(t_i\right) = s_{IP}^{B2} + \frac{\beta_s^{B2}}{\beta_0^{B2}}\left(\zeta_{IP}^{B2} - \zeta_i^{B2}\right) \tag{10.260}$$

To find particles that are at the same s at time t_i we replace Eqs. 10.259-10.260 in 10.256 we obtain:

$$\zeta_{IP}^{B2} = \zeta_i^{B2} - \frac{\beta_s^{B1} \beta_0^{B2}}{\beta_0^{B1} \beta_s^{B2}}\left(\zeta_{IP}^{B1} - \zeta_i^{B1}\right) \tag{10.261}$$

This relation can be used to probe the field map generated by the other bunch at the position of each particle.

10.7.3 Computation of the kick

The transverse kick at each time step can be written as:

$$\Delta p_x^{\mathrm{B1}} = \frac{\Delta P_x^{\mathrm{B1}}}{P_0^{\mathrm{B1}}} = \frac{F_x \Delta t}{P_0^{\mathrm{B1}}} \tag{10.262}$$

Using Eqs. 10.42 and 10.251, taking onto account that the beams move in opposite directions, we obtain:

$$\Delta p_x^{\mathrm{B1}} = -\frac{q \Delta \zeta^{\mathrm{B1}}}{m_0^{\mathrm{B1}} \gamma_0^{\mathrm{B1}} (\beta_0^{\mathrm{B1}})^2 c^2} \left(1 + \beta^{\mathrm{B1}} \beta^{\mathrm{B2}} \right) \frac{\partial \phi^{\mathrm{B2}}}{\partial x} (x, y, \zeta^{\mathrm{B2}}) \tag{10.263}$$

10.8 Configuration of beam-beam lenses for tracking simulations (weak-strong)

The effects of the non-linear forces introduced by beam-beam interactions in the Large Hadron Collider (LHC) are studied with tracking simulations using, for example, the SixTrack and sixtracklib codes [43, 44]. In these simulations the beam-beam interactions are modeled by a set of "thin" non-linear lenses around the collision points. "6D beam-beam lenses" based on Hirata's synchro-beam method [40, 45, 42] are used to model the Head-On (HO) interactions at the for interaction points (IPs) while simpler "4D lenses" are used to model parasitic Long-Range encounters [46].

This document describes a method to configure the beam-beam lenses in tracking simulations based on the model of the accelerator, which has been recently developed as an evolution of existing tools in MAD-X scripting language [47][2]

In particular, in Sec. 10.8.1, we discuss how to reconstruct the absolute position of the two beams with respect to the lab frame using the twiss and survey tables; in Sec. 10.8.2 we discuss how to compute the separation between the two beams; in Sec. 10.8.3 we describe how to identify the crossing plane and crossing angle; in Sec. 10.8.6 we describe how to configure the anticlockwise beam (conventionally called beam 4) from the MAD-X model based on two clockwise-oriented sequences; in Sec. 10.8.7 we introduce the effect of crab cavities on the beam-beam configuration.

10.8.1 Identification of the beam position and direction

The position and orientation of the beams at a certain machine element can be obtained from MAD-X combining the information from the survey and twiss tables. We assume that:

- The sequences start from an element at which the reference trajectories of the two beams are known to be parallel;

- Both beams (B1 and B2) have the same orientation (clockwise);

- Markers or beam-beam lenses are installed at the s-locations of the beam-beam interactions.

The survey provides the coordinates in the lab frame of the two beams:

$$\mathbf{P}^{\mathrm{su}} = \begin{pmatrix} x^{\mathrm{su}} \\ y^{\mathrm{su}} \\ s^{\mathrm{su}} \end{pmatrix} \tag{10.264}$$

and the corresponding set of angles $(\theta^{\mathrm{su}}, \phi^{\mathrm{su}}, \psi^{\mathrm{su}})$ defining the orientation of the local reference system used by the twiss [1]. The origin and the orientation of the lab frame are defined by the first element in the sequence.

The components of the unit vectors defining the local reference frame with respect to the lab frame can be obtained from the following relationship:

$$\left(\hat{\mathbf{e}}_x, \hat{\mathbf{e}}_y, \hat{\mathbf{e}}_s \right) =$$

$$\begin{pmatrix} \cos\theta^{\mathrm{su}} & 0 & \sin\theta^{\mathrm{su}} \\ 0 & 1 & 0 \\ -\sin\theta^{\mathrm{su}} & 0 & \cos\theta^{\mathrm{su}} \end{pmatrix} \times \begin{pmatrix} 1 & 0 & 0 \\ 0 & \cos\phi^{\mathrm{su}} & \sin\phi^{\mathrm{su}} \\ 0 & -\sin\phi^{\mathrm{su}} & \cos\phi^{\mathrm{su}} \end{pmatrix} \times \begin{pmatrix} \cos\psi^{\mathrm{su}} & -\sin\psi^{\mathrm{su}} & 0 \\ \sin\psi^{\mathrm{su}} & \cos\psi^{\mathrm{su}} & 0 \\ 0 & 0 & 1 \end{pmatrix}.$$

$$\tag{10.265}$$

The MAD-X twiss provides the transverse position of the beam in the local reference frame $(x^{\mathrm{tw}}, y^{\mathrm{tw}})$, so that the absolute position of the beam in the lab frame can written as

$$\mathbf{P} = \mathbf{P}^{\mathrm{su}} + x^{\mathrm{tw}}\hat{\mathbf{e}}_x + y^{\mathrm{tw}}\hat{\mathbf{e}}_y. \tag{10.266}$$

At the beam-beam locations the local reference frames for the two beams are assumed to be aligned. This is not strictly the case in the regions between the separation-recombination magnets (D1 and D2), but also in that case that case the existing small divergence can be considered negligible. The beam-beam module of pymask checks the conditions:

$$||\hat{\mathbf{e}}_x^{\mathrm{b1}} - \hat{\mathbf{e}}_x^{\mathrm{b2}}|| \ll 1, \tag{10.267}$$

$$||\hat{\mathbf{e}}_y^{\mathrm{b1}} - \hat{\mathbf{e}}_y^{\mathrm{b2}}|| \ll 1. \tag{10.268}$$

Therefore we will simply define:

$$\hat{\mathbf{e}}_x = \hat{\mathbf{e}}_x^{\mathrm{b1}} = \hat{\mathbf{e}}_x^{\mathrm{b2}}, \tag{10.269}$$

$$\hat{\mathbf{e}}_y = \hat{\mathbf{e}}_y^{\mathrm{b1}} = \hat{\mathbf{e}}_y^{\mathrm{b2}}. \tag{10.270}$$
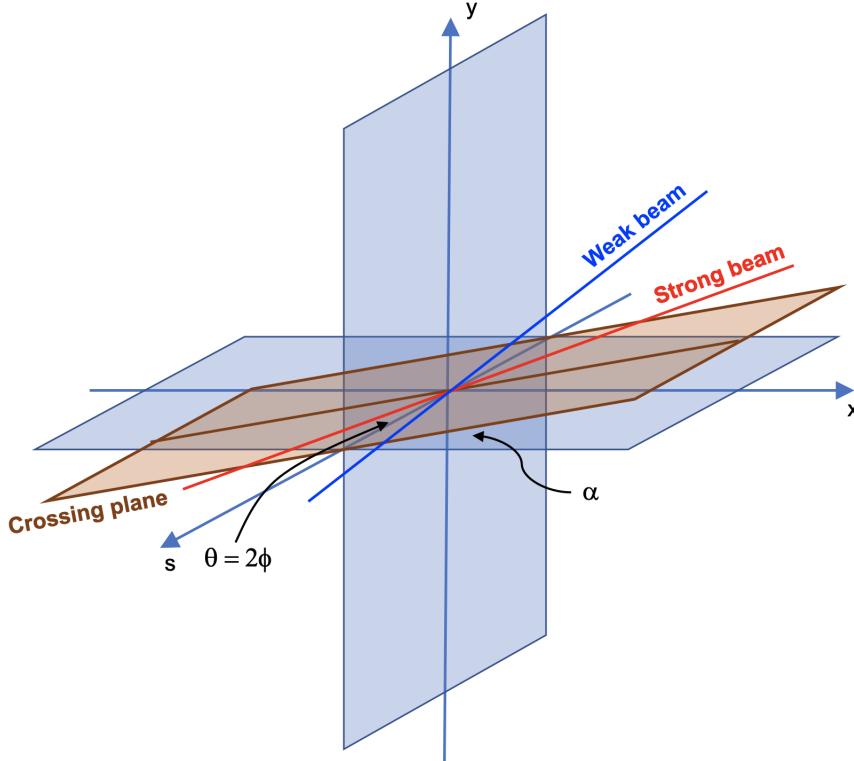
Figure 10.1: Schematic illustration of the crossing plane.

10.8.2   Computation of beam-beam separations

The beam-beam separations are defined as the transverse coordinates of the strong beam with respect to the weak beam. They can be computed as:

$$\Delta x = \hat{\mathbf{e}}_x \cdot \left(\mathbf{P}^S - \mathbf{P}^W \right) , \tag{10.271}$$

$$\Delta y = \hat{\mathbf{e}}_y \cdot \left(\mathbf{P}^S - \mathbf{P}^W \right) , \tag{10.272}$$

where the superscripts identify the weak (W) and the strong (S) beam.

Typically the accuracy of the survey table is insufficient to computed the separations correctly, especially for elements that are too far from the first element in the sequence, due to accumulation of errors along the sequence. A correction can be computed looking as the apparent displacement of the closest Interaction Point (IP) between the two surveys, as the IPs are supposed to coincide.

10.8.3   Crossing plane and crossing angle

At the beam-beam encounters the local reference frames for the two beams share the same orientation. Therefore the elevation angle α of the crossing plane and the crossing angle θ can be computed in the local reference frame, as will be illustrated in the following.

10.8.4 The crossing plane

The directions defined by the local trajectories of the two beams are identified by the unit vectors

$$\hat{\mathbf{p}}^W = \left(p_x^W, p_y^W, p_s^W \right), \tag{10.273}$$

$$\hat{\mathbf{p}}^S = \left(p_x^S, p_y^S, p_s^S \right), \tag{10.274}$$

containing the angles of the closed orbit obtained from the twiss of the two beams. The plane defined by these two directions is called Crossing Plane (XP), as illustrated in Fig. 10.1, and its equation is given by:

$$\mathbf{v}_{XP}(w_1, w_2) = w_1 \hat{\mathbf{p}}^W + w_2 \hat{\mathbf{p}}^S. \tag{10.275}$$

The line defined by the intersection of the crossing plane and the transverse plane identified by the unit vectors $\hat{\mathbf{e}}_x$ and $\hat{\mathbf{e}}_y$ is given by the condition:

$$\mathbf{v}_{XP}(w_1, w_2) \cdot \hat{\mathbf{e}}_s = 0. \tag{10.276}$$

Replacing Eq. (10.275) into Eq. (10.276) we obtain:

$$w_1 p_s^W + w_2 p_s^S = 0, \tag{10.277}$$

and replacing this condition in Eq. (10.275) we obtain the equation of the intersection line

$$\mathbf{v}_T(w_1) = w_1 \left(\hat{\mathbf{p}}^W - \frac{p_s^W}{p_s^S} \hat{\mathbf{p}}^S \right). \tag{10.278}$$

The elevation angle α of the intersection line with respect to the local x-direction ($\hat{\mathbf{e}}_x$) can be written as:

$$\alpha = \arctan \frac{\mathbf{v}_T \cdot \hat{\mathbf{e}}_y}{\mathbf{v}_T \cdot \hat{\mathbf{e}}_x}. \tag{10.279}$$

Using Eq. (10.278) we obtain:

$$\alpha = \arctan \frac{\left(p_y^W - \frac{p_s^W}{p_s^S} p_y^S \right)}{\left(p_x^W - \frac{p_s^W}{p_s^S} p_x^S \right)}. \tag{10.280}$$

In the paraxial approximation ($p_s^S \simeq p_s^W \simeq 1$) this simply becomes:

$$\alpha = \arctan \frac{\Delta p_y}{\Delta p_x}, \tag{10.281}$$

where we have defined:

$$\Delta p_x = p_x^W - p_x^S, \tag{10.282}$$

$$\Delta p_y = p_y^W - p_y^S. \tag{10.283}$$

In the legacy beam-beam macros as well as in the configuration pymask tool, the following logic is implemented

$$
\alpha = \begin{cases} \arctan\left(\dfrac{\Delta p_y}{\Delta p_x}\right) & \text{if } |\Delta p_x| \geq |\Delta p_y| \\ \dfrac{\pi}{2} - \arctan\left(\dfrac{\Delta p_x}{\Delta p_y}\right) & \text{if } |\Delta p_x| < |\Delta p_y| \end{cases} ,
\tag{10.284}
$$

for which α is limited to the range:

$$
-\frac{\pi}{4} \leq \alpha \leq \frac{3}{4}\pi .
\tag{10.285}
$$

In particular, for a purely horizontal crossing we have $\alpha = 0$ and for a purely vertical crossing we have $\alpha = \frac{\pi}{2}$.

10.8.5 The crossing angle

The crossing angle θ between the two beams can be found from the relation:

$$
\cos\theta = \hat{\mathbf{p}}^W \cdot \hat{\mathbf{p}}^S .
\tag{10.286}
$$

The half crossing angle

$$
\phi = \frac{\theta}{2}
\tag{10.287}
$$

is often used instead of θ.
In the paraxial approximation

$$
p_x \ll 1 ,
\tag{10.288}
$$
$$
p_y \ll 1 ,
\tag{10.289}
$$
$$
\tag{10.290}
$$

the scalar product in Eq. (10.286) can be rewritten as

$$
\begin{aligned}
\hat{\mathbf{p}}^W \cdot \hat{\mathbf{p}}^S &= p_x^W p_x^S + p_y^W p_y^S + p_s^W p_s^S \\
&= p_x^W p_x^S + p_y^W p_y^S + \sqrt{1 - (p_x^W)^2 - \left(p_y^W\right)^2}\sqrt{1 - (p_x^S)^2 - (p_y^S)^2} \\
&\simeq p_x^W p_x^S + p_y^W p_y^S + \left(1 - \frac{(p_x^W)^2}{2} - \frac{\left(p_y^W\right)^2}{2}\right)\left(1 - \frac{(p_x^S)^2}{2} - \frac{\left(p_y^S\right)^2}{2}\right) \\
&\simeq p_x^W p_x^S + p_y^W p_y^S + 1 - \frac{(p_x^W)^2}{2} - \frac{\left(p_y^W\right)^2}{2} - \frac{(p_x^S)^2}{2} - \frac{\left(p_y^S\right)^2}{2} ,
\end{aligned}
\tag{10.291}
$$

which can be written in compact form as:

$$
\hat{\mathbf{p}}^W \cdot \hat{\mathbf{p}}^S \simeq 1 - \frac{(p_x^W - p_x^S)^2 + \left(p_y^W - p_y^S\right)^2}{2} .
\tag{10.292}
$$

For small crossing angle we can write:

$$\cos\theta \simeq 1 - \frac{\theta^2}{2}. \tag{10.293}$$

Replacing Eqs. (10.292) and (10.293) into Eq. (10.286) we obtain

$$|\theta| = \sqrt{\Delta p_x^2 + \Delta p_y^2}. \tag{10.294}$$

The sign of θ is defined positive when the weak beam needs to rotate in the clockwise sense in the crossing plane in order to be brought on the strong beam. This corresponds to the following sign choices:

	$|\Delta p_x| > |\Delta p_y|$	$|\Delta p_x| < |\Delta p_y|$
$\Delta p_x \geq 0,\ \Delta p_y \geq 0$	$\theta > 0$	$\theta > 0$
$\Delta p_x < 0,\ \Delta p_y \geq 0$	$\theta < 0$	$\theta > 0$
$\Delta p_x < 0,\ \Delta p_y < 0$	$\theta < 0$	$\theta < 0$
$\Delta p_x \geq 0,\ \Delta p_y < 0$	$\theta > 0$	$\theta < 0$

which are consistent with the sign convention used in LHC operation.

10.8.6 Transformations for the counterclockwise beam (B4)

The typically used MAD-X model of the LHC consists of two sequences both having clockwise (CW) orientation, conventionally called Beam 1 and Beam 2. To perform tracking simulations of the anticlockwise (ACW) beam, an anticlockwise sequence needs to be generated, which is conventionally called Beam 4. The beam-beam lenses in the Beam 4 sequence can be configured based on the beam-beam lenses defined in Beam 2, taking into account that the two are related by the following change of coordinates:

$$x^{\text{ACW}} = -x^{\text{CW}}, \tag{10.295}$$
$$y^{\text{ACW}} = +y^{\text{CW}}, \tag{10.296}$$
$$s^{\text{ACW}} = -s^{\text{CW}}. \tag{10.297}$$

The corresponding transformation for the transverse momenta is:

$$p_x^{\text{ACW}} = +p_x^{\text{CW}}, \tag{10.298}$$
$$p_y^{\text{ACW}} = -p_y^{\text{CW}}. \tag{10.299}$$

This can be easily seen from the fact that:

$$p_x \simeq \frac{dx}{ds}, \tag{10.300}$$

$$p_y \simeq \frac{dy}{ds}. \tag{10.301}$$

Additionally, from Eqs. (10.295) - (10.299) it is possible to derive the following relations to transform the Σ-matrix [45] of the strong beam:

$$\Sigma_{11}^{ACW} = +\Sigma_{11}^{CW}, \tag{10.302}$$
$$\Sigma_{12}^{ACW} = -\Sigma_{12}^{CW}, \tag{10.303}$$
$$\Sigma_{13}^{ACW} = -\Sigma_{13}^{CW}, \tag{10.304}$$
$$\Sigma_{14}^{ACW} = +\Sigma_{14}^{CW}, \tag{10.305}$$
$$\Sigma_{22}^{ACW} = +\Sigma_{22}^{CW}, \tag{10.306}$$
$$\Sigma_{23}^{ACW} = +\Sigma_{23}^{CW}, \tag{10.307}$$
$$\Sigma_{24}^{ACW} = -\Sigma_{24}^{CW}, \tag{10.308}$$
$$\Sigma_{33}^{ACW} = +\Sigma_{33}^{CW}, \tag{10.309}$$
$$\Sigma_{34}^{ACW} = -\Sigma_{34}^{CW}, \tag{10.310}$$
$$\Sigma_{44}^{ACW} = +\Sigma_{44}^{CW}. \tag{10.311}$$
$$\tag{10.312}$$

10.8.7 Crab crossing

To discuss the effect of crab cavities, we define along the bunches of Beam 1 and Beam 2 (sharing the same s coordinate as in the MAD-X model), the longitudinal coordinates z_1 and z_2, oriented like s.

Assuming that the slices with $z_1 = z_2 = 0$ collide at s=0, the collision point (CP) for two generic slices z_1 and z_2 is at the location:

$$s_{CP} = \frac{z_1 + z_2}{2}. \tag{10.313}$$

In the absence of crab crossing, the transverse position of the two beams is independent from z:

$$x_1 = +\phi s, \tag{10.314}$$
$$x_2 = -\phi s. \tag{10.315}$$

Ideal crab cavities, in the linear approximation, introduce a z-dependent orbit correction such that:

$$x_1(s) = +\phi s + \phi_c z_1, \tag{10.316}$$
$$x_2(s) = -\phi s - \phi_c z_2, \tag{10.317}$$

where ϕ_c is the crabbing angle and we assume, without loss of generality, horizontal crabbing plane.

The separation of the two slices at their collision point is obtained replacing (10.313) into (10.316) and (10.317):

$$\Delta x(s_{CP}) = x_2(s_{CP}) - x_1(s_{CP}) = -(\phi + \phi_c)(z_1 + z_2). \tag{10.318}$$

If $\phi_c = -\phi$, the separation is zero independently of z_1 and z_2 (perfect crabbing).

The crab crossing in the IPs of the HL-LHC for the clockwise and anticlockwise beams is illustrated with the relevant sign conventions in Figs. 10.2 - 10.5.
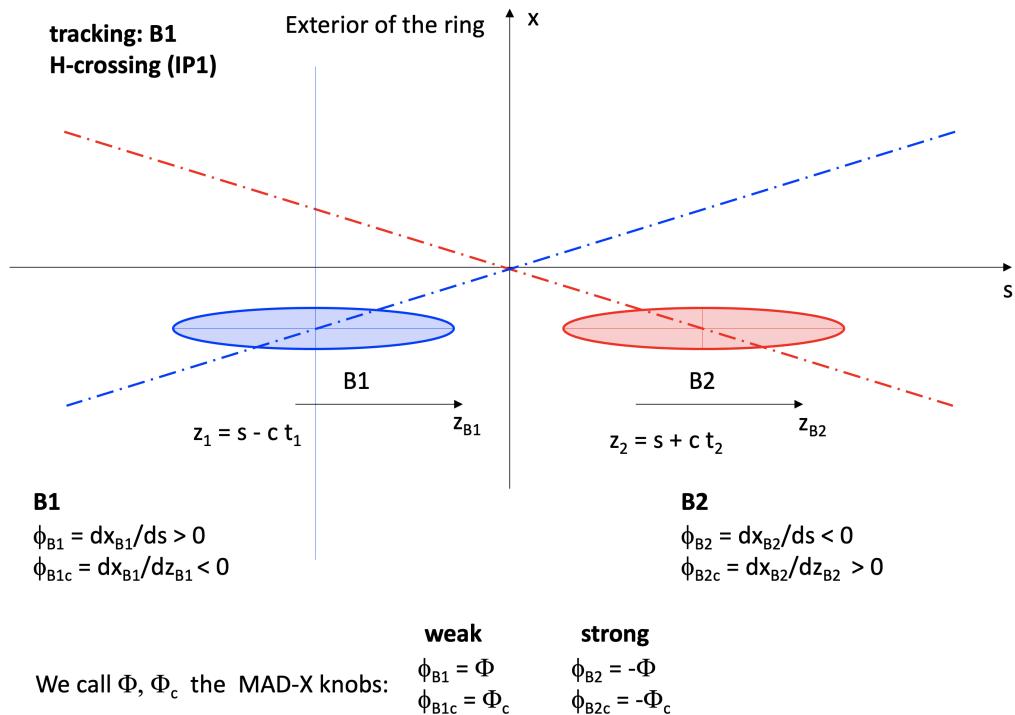
Figure 10.2: Crab crossing in the IP1 of the HL-LHC modeled for the tracking of the clockwise beam (beam 1).
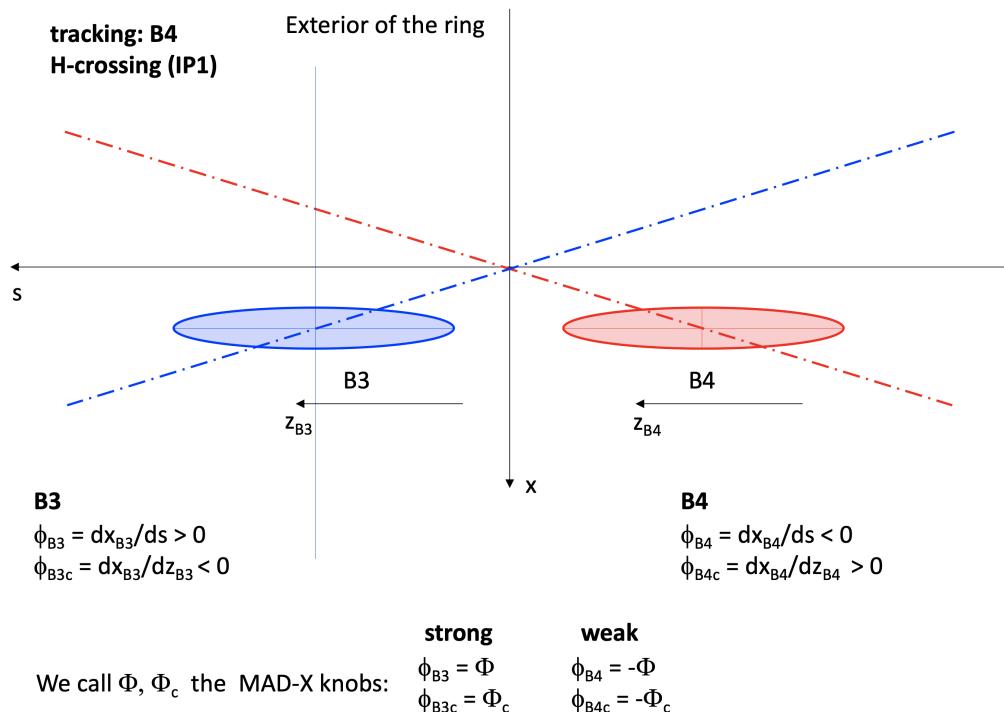
Figure 10.3: Crab crossing in the IP1 of the HL-LHC modeled for the tracking of the anti-clockwise beam (beam 4).

tracking: B1
V-crossing (IP5)

Sky   y

S

B1

B2

z_{B1}

z_{B2}

B1
$\phi_{B1} = dy_{B1}/ds > 0$
$\phi_{B1c} = dy_{B1}/dz_{B1} < 0$

B2
$\phi_{B2} = dy_{B2}/ds < 0$
$\phi_{B2c} = dy_{B2}/dz_{B2} > 0$

	weak	**strong**
We call Φ, Φ_c the MAD-X knobs:	$\phi_{B1} = \Phi$ $\phi_{B1c} = \Phi_c$	$\phi_{B2} = -\Phi$ $\phi_{B2c} = -\Phi_c$
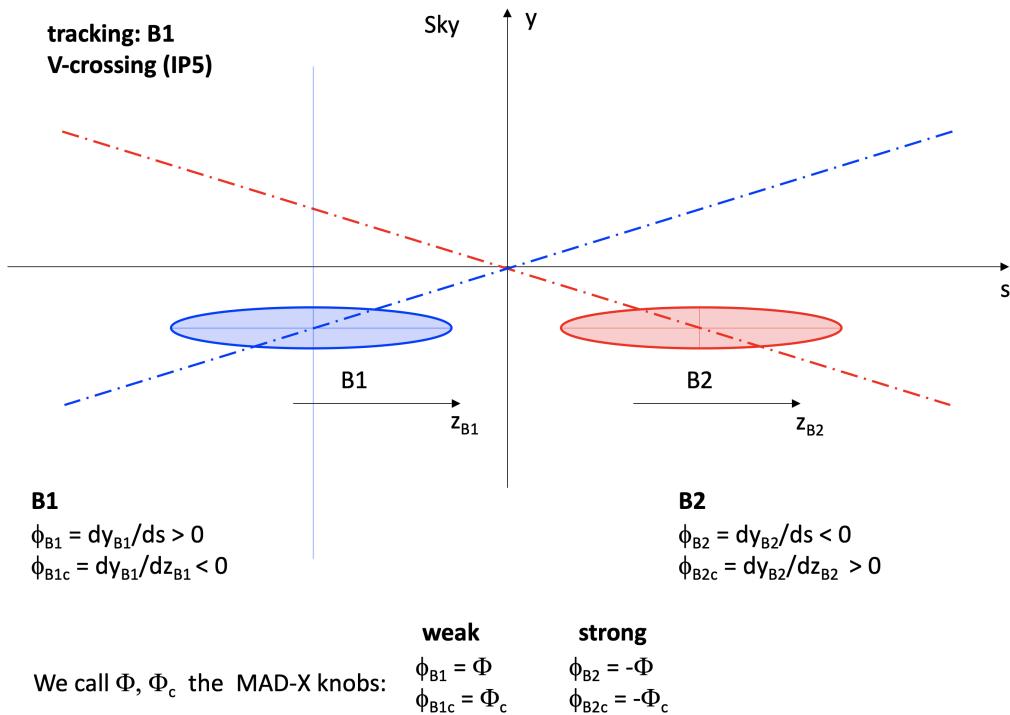
Figure 10.4: Crab crossing in the IP5 of the HL-LHC modeled for the tracking of the clockwise beam (beam 1).

tracking: B4
V-crossing (IP5)

Sky   y

S

B3

B4

z_{B3}

z_{B4}

B3
$\phi_{B3} = dy_{B3}/ds < 0$
$\phi_{B3c} = dy_{B3}/dz_{B3} > 0$

B4
$\phi_{B4} = dy_{B4}/ds > 0$
$\phi_{B4c} = dy_{B4}/dz_{B4} < 0$

|	**strong**	**weak**
We call Φ, Φ_c the MAD-X knobs:	$\phi_{B3} = -\Phi$ $\phi_{B3c} = -\Phi_c$	$\phi_{B4} = +\Phi$ $\phi_{B4c} = +\Phi_c$
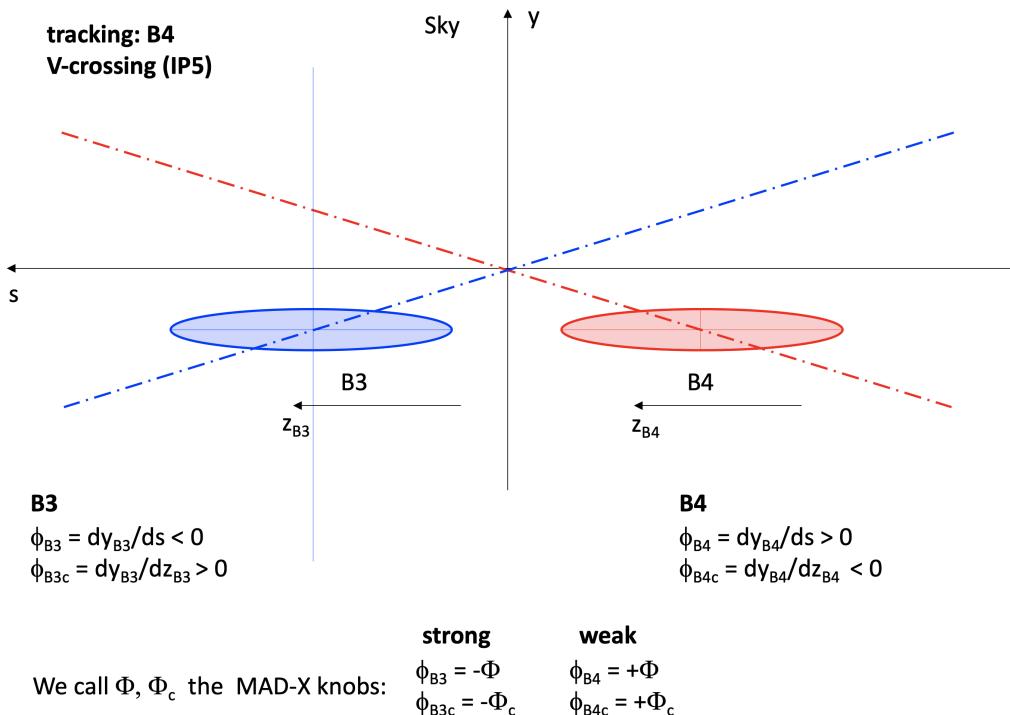
Figure 10.5: Crab crossing in the IP5 of the HL-LHC modeled for the tracking of the anti-clockwise beam (beam 4).

### 10.8.7.1   Configuration of beam-beam lenses for beam 1

In order to model the HO interaction for a crab crossing, the "strong bunch" is sliced longitudinally using the constant charge method, and one beam-beam lens for each slice is installed in the sequence.

In particular, in the sequence of beam 1, the lens corresponding to a slice of the strong beam (beam 2) having longitudinal coordinate $z_2 = Z_2$ is installed at the location where the slice encounters the synchronous particle of the weak beam (see Eq. (10.313) with $z_1 = 0$):

$$s_{\text{lens}} = +\frac{Z_2}{2} \, . \tag{10.319}$$

The position of the strong beam at the lens can be found replacing Eq. (10.319) into Eq. (10.317):

$$X_2 = -s_{\text{lens}}(\phi + 2\phi_c) \, . \tag{10.320}$$

The effect of the crab bump alone is given by:

$$X_2^{\text{crab}} = -2\phi_c s_{\text{lens}} = -\phi_c Z_2 \, . \tag{10.321}$$

Taking into account the RF curvature coming from the crab cavity frequency, the position of the slice at the beam-beam lens can be written as:

$$X_2^{\text{crab}} = -\phi_c \frac{L_{\text{ring}}}{2\pi h_{\text{CC}}} \sin\left(\frac{2\pi h_{\text{CC}}}{L_{\text{ring}}} Z_2\right) = -\phi_c \frac{L_{\text{ring}}}{2\pi h_{\text{CC}}} \sin\left(\frac{2\pi h_{\text{CC}}}{L_{\text{ring}}} 2s_{\text{lens}}\right) , \tag{10.322}$$

where h_{CC} is the harmonic number of the crab cavity and L_{ring} is the circumference of the ring.

10.8.8   Configuration of beam-beam lenses for beam 2

In the sequence of beam 2, we install the beam-beam lens for a slice of the strong beam (beam 1) having longitudinal coordinate $z_1 = Z_1$ at the location where the slice encounters the synchronous particle of the weak beam, (see Eq. (10.313) with $z_2 = 0$):

$$s_{\text{lens}} = \frac{Z_1}{2} \, . \tag{10.323}$$

The position of the strong beam at the lens can be found replacing Eq. (10.323) into Eq. (10.316):

$$X_1 = s_{\text{lens}}(\phi + 2\phi_c) \, . \tag{10.324}$$

The effect of the crab bump alone is given by:

$$X_1^{\text{crab}} = 2\phi_c s_{\text{lens}} = \phi_c Z_1 \, . \tag{10.325}$$

Taking into account the RF curvature coming from the crab cavity frequency, the position of the slice at the beam-beam lens can be written as:

$$X_1^{\text{crab}} = \phi_c \frac{L_{\text{ring}}}{2\pi h_{\text{CC}}} \sin\left(\frac{2\pi h_{\text{CC}}}{L_{\text{ring}}} Z_1\right) = \phi_c \frac{L_{\text{ring}}}{2\pi h_{\text{CC}}} \sin\left(\frac{2\pi h_{\text{CC}}}{L_{\text{ring}}} 2s_{\text{lens}}\right) . \tag{10.326}$$

From Eqs. (10.322) and (10.326), we find that for lenses at the same longitudinal position s_{lens} the corresponding slices of the two beams $Z_1 = Z_2 = 2s_{\text{lens}}$ have opposite transverse coordinates:

$$X_1^{\text{crab}} = -X_2^{\text{crab}} \, . \tag{10.327}$$

10.8.8.1 Crab bump from twiss table

For a non-ideal crabbing, for example in the presence of a non-closure of the crab-bump, the realistic z-dependent orbit distortion introduced by the crab cavities can be characterized using the twiss, by installing orbit correctors at the position of the crab cavities that introduce the crab cavity deflection as seen at a certain reference position along the bunch z_{ref}. To obtain the effect on particles at different positions along bunch it is possible to apply the following scaling:

$$x\left(z\right) = x\left(z_{\text{ref}}\right) \frac{\sin\left(\frac{2\pi h_{\text{CC}}}{L_{\text{ring}}} z\right)}{\sin\left(\frac{2\pi h_{\text{CC}}}{L_{\text{ring}}} z_{\text{ref}}\right)}. \tag{10.328}$$

10.8.9 Step-by-step configuration procedure

Based on the method introduced in the previous sections, the following procedure has been implemented in pymask to configure the beam-beam lenses in the sixtrack and sixtracklib tracking model:

1. Inactive beam-beam lenses (not configured) are installed in both clockwise sequences (Beam 1 and Beam 2) at the locations of the HO and LR beam-beam encounters. As discussed in Sec. 10.8.7, at each IP a set of lenses is installed to model the HO, one corresponding to each bunch slice.

2. The MAD-X twiss and survey tables are computed for both clockwise sequences.

3. The transverse beam shapes (Σ-matrix) are extracted from the twiss table for all beam-beam lenses.

4. The positions of the beams at the beam-beam lenses in the lab frame are computed combining the information from the survey and twiss tables, as discussed in Sec. 10.8.1.

5. The beam-beam separations are computed, as discussed in Sec. 10.8.2.

6. For all HO interactions, the crossing plane and the crossing angle are identified, as discussed in Sec. 10.8.3.

7. The relevant quantities for the beam-beam lenses in the anticlockwise sequences (Beam 3 and Beam 4) are obtained from the data computed for the lenses in the clockwise sequences (Beam 1 and Beam 2), using the transformations described in Sec. 10.8.6.

8. The effect of the crab cavities is introduced by using the shape of the crab bumps obtained from twiss tables computed with orbit correctors at the locations of the cavities, as discussed in Sec. 10.8.7.

9. The information computed before is used to configure the beam-beam lenses in the MAD-X model of the sequence for which the tracking simulation will be performed, typically either Beam 1 or Beam 4.

10. The SixTrack input and the pysixtrack/sixtracklib input files are generated using the MAD-X model and the additional information computed as described above.

11. The closed orbit as computed from the MAD-X sequences is saved on file, for the generation of matched beam distributions and for the computation of the beam-beam dipolar kicks on the closed orbit, which are usually subtracted in weak-strong tracking simulations.

Chapter 11

Bhabha scattering and beamstrahlung

11.1 Bhabha scattering

In quantum electrodynamics (QED), the Coulomb attraction of two opposite charges (e.g. an electron and a positron) is called Bhabha scattering [48]. The mathematical treatment of Bhabha scattering can be done using the method of equivalent photons (Weizsäcker-Williams approach) [49, 50]. The essence of this method lies in the fact that the electromagnetic field of a relativistic charged particle, say the positron, is almost transversal and can therefore accurately be substituted by an appropriately chosen equivalent radiation field of photons. Thus, the cross section for the scattering of an electron with this positron (Bhabha scattering) can be approximated by that of the electron and an "equivalent" photon (Compton scattering). In this case, the equivalent photon corresponds to the exchanged virtual photon between the scattering primaries. The whole process, including the subsequent emission of bremsstrahlung photons can be treated in a numerical simulation as an inverse Compton scattering process [51]. In this, the virtual photons emitted by the positron will collide with the electron. Due to the relativistic dynamics of the participating leptons, the virtual photons have an energy which is often negligible compared to that of the leptons, thus we can treat them as real. The process is called inverse since here the electron will lose energy while the photons will gain energy, contrary to standard Compton scattering. The scattered photons are real and typically end up with an energy E'_γ comparable to the initial lepton energy E_e [52].

The generation of photons from radiative Bhabha scattering in Xsuite can be divided into 3 steps. First, the charge density of the opposite bunch slice at the location of the macroparticle in the soft-Gaussian approximation is computed [53]. From this one computes the integrated luminosity of the collision of the macroparticle with the virtual photons represented by the slice, integrated over the time of passing through the slice. Second, a set of virtual photons is generated corresponding to the total energy of the opposite slice. Third, the code iterates over these virtual photons and simulates the bremsstrahlung process as a series of inverse Compton scattering events between the macroparticle and each virtual photon.
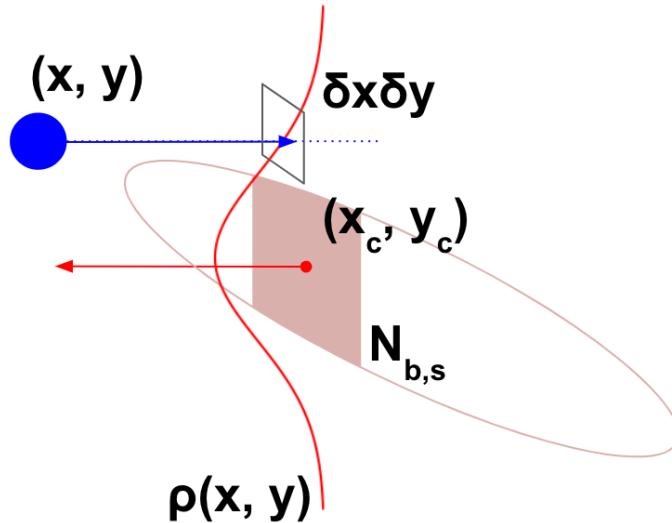
Figure 11.1: Schematic illustration of a single macroparticle from bunch 1 (blue) colliding with a single longitudinal slice of the opposing bunch 2 (red).

11.1.1   Luminosity Computation

Figure 11.1 illustratres how `Xfields` computes the integrated luminosity in a collision of a single macroparticle from one beam with a single slice of the opposing beam[1]. On the figure x, y denote the transverse coordinates of a macroparticle in the boosted and uncoupled frame, at the collision point with a slice of the opposing bunch, corresponding to the notation $\hat{\bar{x}}^*, \hat{\bar{y}}^*$ in the previous sections. The centroid (mean) coordinate of the opposing slice, with a bunch intensity of $N_{b,s}$, is denoted by x_c, y_c, in the boosted, uncoupled, transported reference frame of its own bunch. `Xfields` models the charge density of a longitudinal slice as a 2D Gaussian distribution $\rho(x, y)$. Considering an infinitesimal area $\delta x \delta y$ around the transverse position x, y of a given macroparticle at the collision point with the slice, one can write the number of charges with which this macroparticle will interact:

$$N_e(x, y) = N_{b,s}\rho(x, y)\delta x \delta y, \qquad (11.1)$$

and the integrated luminosity of the macroparticle-slice collision:

$$L = \frac{N_{b,m} \cdot N_e(x, y)}{\delta x \delta y} = N_{b,m}N_{b,s}\rho(x, y), \qquad (11.2)$$

where $N_{b,m}$ denotes the number of elementary charges per macroparticle.

---

[1]Note that this luminosity can be recorded in a table with the **flag_luminosity** flag of the `BeamBeamGaussian3D` element and **lumitable** keyword in the `Xline` internal log. The recorded entries must be summed up to get the total integrated luminosity of the collision. This method has an uncertainty of $\pm 10\%$ compared to the analytical formula.

11.1.2 Virtual Photon Generation

Equation (11.2) describes the integrated luminosity of primary-primary collisions. In order to simulate the collision of the primaries with virtual photons instead, `Xfields` uses the assumption that the virtual photon distribution $N_\gamma(x, y)$ is proportional to that of the primary charges:

$$N_\gamma(x, y) = n N_e(x, y), \tag{11.3}$$

where n is a proportionality factor denoting the number of virtual photons corresponding to one elementary charge. The number density spectrum of virtual photons is given by:

$$\frac{dn}{dx dQ^2} = \frac{\alpha}{2\pi} \frac{1 + (1 - x)^2}{x} \frac{1}{Q^2}, \tag{11.4}$$

where $x = \frac{\hbar\omega}{E_e} = \frac{E_\gamma}{E_e}$ is the total energy of the virtual photon normalized to the primary energy and Q^2 is the squared virtuality of the virtual photon [54].

The virtual photon energies and virtualities can be drawn using the method of inverse CDF (Cumulative Distribution Function) sampling. The sampling algorithm in `Xsuite` has been adapted from `GUINEA-PIG` [55], a Particle In Cell (PIC) based single beam-beam collision simulation software. For each macroparticle in the beam, we first compute the total amount of equivalent photons using the energy of the opposite bunch slice. Subsequently, the energy and virtuality of each photon will be sampled. In the current implementation all virtual photons inherit the dynamical variables of the strong bunch slice centroid. Note that the virtual photons sampled this way will also be "macroparticles" in the sense that they represent the dynamics of all virtual photons generated by all charges in a primary macroparticle.

11.1.3 Inverse Compton Scattering of Virtual Photons

We account for the proportionality of the primary charge and virtual photon distributions described by Eq. (11.3) by resampling the virtual photons for each macroparticle. With each photon, we simulate the bremsstrahlung process in the form of a set of inverse Compton scattering events. The number of Compton events can be described as:

$$R = \sigma_{C,tot}(s) L = \sigma_{C,tot}(s) N_{b,m} N_{b,s} \rho(x, y), \tag{11.5}$$

where $s \approx \frac{4 E_\gamma E_e}{m_e^2 c^4}$ is the center of mass energy squared of the photon-primary Compton interaction, normalized to the rest mass of the primary [56], and $\sigma_{C,tot}(s)$ denotes the total Compton scattering cross section, given by:

$$\sigma_{C,tot}(s) = \frac{2\pi r_e^2}{s} \left[\ln(s + 1) \left(1 - \frac{4}{s} - \frac{8}{s^2} \right) \cdot + \frac{1}{2} + \frac{8}{s} - \frac{1}{2(s+1)^2} \right], \tag{11.6}$$

with r_e being the classical electron radius. For each event, we sample the scattered photon energy from the differential cross section:

$$\frac{d\sigma_C}{dy} = \frac{2\pi r_e^2}{s} \left[\frac{1}{1-y} + 1 - y - \frac{4y}{s(1-y)} + \frac{4y^2}{s^2(1-y)^2} \right], \tag{11.7}$$

which describes the scattering of a beam of unpolarized photons on the primary charge [51]. Here $y = \dfrac{\hbar\omega'}{E_e} = \dfrac{E'_\gamma}{E_e}$ is the energy of the scattered photon in units of the total energy of the colliding primary. Given the energy E'_γ, we can compute the scattering angle of the primary and the photon as well as their momenta, using the constraints given by energy and momentum conservation. While the emitted photon spectrum corresponds to the sum of all charges represented by a macroparticle, a given macroparticle should represent the dynamics of a single primary charge. Thus, the dynamical variables of the macroparticles are updated according to energy and momentum conservation accounting for the emission of only a fraction of the photons. The latter are picked randomly based on a probability corresponding to the inverse of the number of charges per macroparticle.

11.2   Beamstrahlung

The implementation of beamstrahlung in `Xfields` is based on `GUINEA-PIG` [55]. In this section a high level summary of the modeling is presented. Further details can be found in [57].

`Xfields` samples the quantum theoretical synchrotron radiation spectrum $G(v, \xi)$:

$$G(v, \xi) = \frac{v^2}{(1-(1-\xi)v^3)^2} \left(G_1(y) + \frac{\xi^2 y^2}{1+\xi y} G_2(y) \right), \tag{11.8}$$

which is normalized such that $G(v = 0, \xi) = 1$ and $G(v, \xi) \leq 1$ for all v and ξ. The variable ξ is defined as:

$$\xi = \frac{E_{crit}}{E} \tag{11.9}$$

and denotes the magnitude of the quantum correction, i.e. the critical energy normalized to the energy E of the primary particle in GeV undergoing the beamstrahlung process. The critical beamstrahlung energy is defined in the classical way as:

$$E_{crit} = \frac{3\hbar c \gamma^3}{2\rho} \tag{11.10}$$

The unitless variable y is related to the energy of the emitted beamstrahlung photon E_γ:

$$y = \frac{E_\gamma}{E_{crit}} \frac{1}{1 - \frac{E_\gamma}{E}}. \tag{11.11}$$

Equation 11.11 can be expressed with the help of a uniform random variable v as follows:

$$y = \frac{v^3}{1 - v^3}; \ v \in U[0, 1]. \tag{11.12}$$

With these the number of beamstrahlung photons emitted in the interval $[v, v + \Delta v]$ during a time interval δ_t can be given as:

$$\Delta N_\gamma = p_0 G(v, \xi) \Delta v, \tag{11.13}$$

where

$$p_0 = \frac{2^{\frac{2}{3}}}{\Gamma(\frac{4}{3})} \frac{\alpha \gamma \delta_t}{\rho} \approx 25.4 \cdot \frac{E \delta_t}{\rho} \tag{11.14}$$

is a scaling factor dependent on the relativistic γ of the primary, the instantaneous bending radius ρ and the fine structure constant α. The bending radius of each macroparticle in the electromagnetic field of a given longitudinal slice of the opposite bunch is obtained from the radial kick:

$$F_r^* = r_{pp} \sqrt{F_x^{*2} + F_y^{*2}}, \tag{11.15}$$

$$\rho = \frac{1}{F_r^*}, \tag{11.16}$$

with $r_{pp} = \frac{1}{1+\delta} = \frac{p}{p_0}$. In the `Xfields` `BeamBeamGaussian3D` element the time interval δ_t is expressed as a longitudinal distance Δz, which is the distance the macroparticle travels between two consecutive longitudinal slices and it corresponds to the bin width of the longitudinal slicing.

Figure 11.2 shows the beamstrahlung photon number density $p_0 G(v, \xi)$ for a fixed value of p_0 and ξ. The area in the region C is the mean number of beamstrahlung photons emitted during an interval δ_t, i.e. a passage through one longitudinal slice of width Δz.

The functions $G_1(y)$ and $G_2(y)$ are defined as follows:

$$\begin{aligned} G_1(y) &= \frac{\sqrt{3}\Gamma(\frac{1}{3})}{2^{\frac{5}{3}}\pi} \int_y^\infty K_{\frac{5}{3}}(x) dx, \\ G_2(y) &= \frac{\sqrt{3}\Gamma(\frac{1}{3})}{2^{\frac{5}{3}}\pi} K_{\frac{2}{3}}(y). \end{aligned} \tag{11.17}$$

Equations 11.17 are evaluated numerically with the below approximate formulas:

$0 \leq y \leq 1.54$

$$\begin{aligned} G_1(y) &= y^{-\frac{2}{3}}(1 - 0.8432885317 \cdot y^{\frac{2}{3}} + 0.1835132767 \cdot y^2 \\ &\quad - 0.0527949659 \cdot y^{\frac{10}{3}} + 0.0156489316 \cdot y^4) \\ G_2(y) &= y^{-\frac{2}{3}}(0.4999456517 - 0.5853467515 \cdot y^{\frac{4}{3}} \\ &\quad + 0.3657833336 \cdot y^2 - 0.0695055284 \cdot y^{\frac{10}{3}} + 0.0191803860 \cdot y^4) \end{aligned} \tag{11.18}$$
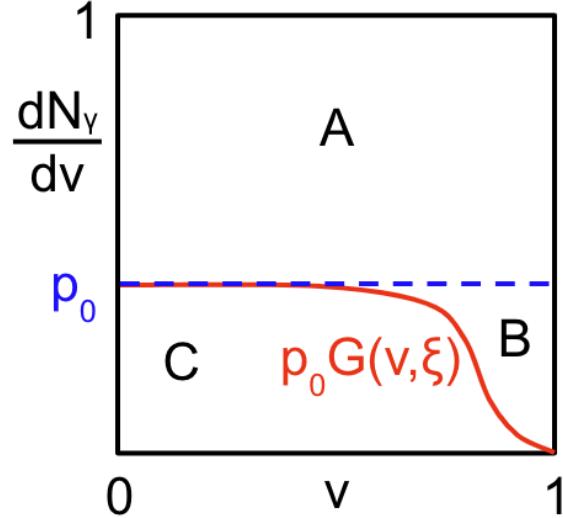
Figure 11.2: Schematic illustration of the number density function of beamstrahlung photons $p_0 G(v, \xi)$ (red curve) for a given p_0 (blue dashed line) and ξ, as a function of v.

$1.54 < y \leq 4.48$

$$G_1(y) = \frac{2.066603927 - 0.5718025331 \cdot y + 0.04243170587 \cdot y^2}{-0.9691386396 + 5.651947051 \cdot y - 0.6903991322 \cdot y^2 + y^3}$$

$$G_2(y) = \frac{1.8852203645 - 0.5176616313 \cdot y + 0.03812218492 \cdot y^2}{-0.4915880600 + 6.1800441958 \cdot y - 0.6524469236 \cdot y^2 + y^3}$$

(11.19)

$4.48 < y \leq 165.0$

$$G_1(y) = \frac{e^{-y}}{\sqrt{y}} \cdot \frac{1.0174394594 + 0.5831679349 \cdot y}{0.9949036186 + y}$$

(11.20)

$$G_2(y) = \frac{e^{-y}}{\sqrt{y}} \cdot \frac{0.2847316689 + 0.5830684600 \cdot y}{0.3915531539 + y}.$$

For $y > 165$ the model assumes no radiation. With these one can simulate beamstrahlung emission by first drawing a random uniform number p. The condition $p > p_0$ corresponds to region A on Fig. 11.2, therefore no photons are emitted. In the other case a second random uniform number v is drawn, and Eq. 11.8 is computed. If $p < p_0 G(v, \xi)$ is satisfied (region C) a photon is emitted with an energy

$$\frac{E_\gamma}{E} = \frac{\xi v^3}{1 - (1 - \xi)v^3},$$

(11.21)

otherwise no photon is emitted (region B). The generated beamstrahlung photons are themselves macroparticles in the sense that they represent the dynamics of all photons generated by all charges in a primary macroparticle.

Chapter 12

Wakefields and impedances

12.1   Transverse wakefields

Transverse wakefields are defined such that the corresponding transverse kicks can be written as:

$$\Delta p_x = \frac{q^2 e^2}{m_0 \gamma \beta_0^2 c^2} \sum_{i,j,k,l \geq 0} x^k y^l \int_{-\infty}^{\infty} \bar{x}^i(z') \bar{y}^j(z') \lambda(z') W_x^{i,j,k,l}(z - z') \, dz' \tag{12.1}$$

$$\Delta p_y = \frac{q^2 e^2}{m_0 \gamma \beta_0^2 c^2} \sum_{i,j,k,l \geq 0} x^k y^l \int_{-\infty}^{\infty} \bar{x}^i(z') \bar{y}^j(z') \lambda(z') W_y^{i,j,k,l}(z - z') \, dz' \tag{12.2}$$

where $\bar{x}(z)$ and $\bar{y}(z)$ are the transverse centroid positions along the beam.
The convolution can be obtained numerically using the method of Section 14.2.
The lower order terms of the summation are often called as:

- $W_x^{0,0,0,0}$ constant x

- $W_y^{0,0,0,0}$ constant y

- $W_x^{1,0,0,0}$ dipolar x, or driving x

- $W_y^{0,1,0,0}$ dipolar y, or driving y

- $W_x^{0,1,0,0}$ dipolar xy, or driving xy

- $W_y^{1,0,0,0}$ dipolar yx, or driving yx

- $W_x^{0,0,1,0}$ quadrupolar x, or detuning x

- $W_y^{0,0,0,1}$ quadrupolar y, or detuning y

- $W_x^{0,0,0,1}$ quadrupolar xy, or detuning xy

- $W_y^{0,0,1,0}$ quadrupolar yx, or detuning yx

The z variable can be written as a function of time in the lab frame as:

$$z = -\beta_0 ct, \tag{12.3}$$

We call $\widehat{W}_{x,y}$ the wakefield defined as a function of time t:

$$\widehat{W}_{x,y}(t) = W_{x,y}(-\beta_0 ct) \tag{12.4}$$

$$W_{x,y}(z) = \widehat{W}_{x,y}\left(-\frac{z}{\beta_0 c}\right) \tag{12.5}$$

For ultrarelativistic beams we have:

$$\widehat{W}_{x,y}(t) = 0 \qquad\qquad\qquad \text{for } t < 0 \tag{12.6}$$

$$W_{x,y}(z) = 0 \qquad\qquad\qquad \text{for } z > 0 \tag{12.7}$$

The coefficient $1/\gamma\beta_0^2$ in Eqs. 12.1 and 12.2 comes from the fact that, if we have a force F_x acting on a length Δs, we can derive the corresponding kick as follows:

$$\Delta P_x = F_x \Delta t, \tag{12.8}$$

and substituting the P_x with the normalized one $p_x = \frac{P_x}{P_0}$ we find

$$\Delta p_x = \frac{F_x}{P_0}\Delta t = \frac{F_x}{P_0}\frac{\Delta s}{\beta_0 c}, \tag{12.9}$$

hence substituting $P_0 = m_0\gamma\beta_0 c$ we find

$$\Delta p_x = \frac{F_x}{m_0\gamma\beta_0^2 c^2}\Delta s. \tag{12.10}$$

12.2   Transverse impedances

The transverse beam coupling impedances $Z_{x,y}(\omega)$ are related to the wakefields through a Fourier transform (see [58, Eq. 1.216]):

$$\widehat{W}_{x,y}(t) = -\frac{j}{2\pi}\int_{-\infty}^{+\infty} d\omega\, e^{j\omega t}Z_{x,y}(\omega)\,, \tag{12.11}$$

$$Z_{x,y}(\omega) = j\int_{-\infty}^{+\infty} dt\, e^{-j\omega t}\widehat{W}_{x,y}(t)\,. \tag{12.12}$$

The equivalence between the two equations can be seen multiplying both sides of Eq. 12.11 by $e^{-j\omega' t}$ and integrating over t

$$\int_{-\infty}^{\infty} dt\, e^{-j\omega' t}\widehat{W}_{x,y}(t) = -\frac{j}{2\pi}\int_{-\infty}^{\infty} dt\int_{-\infty}^{+\infty} d\omega Z_{x,y}(\omega)e^{j(\omega-\omega')t} \tag{12.13}$$

$$= -\frac{j}{2\pi}\int_{-\infty}^{+\infty} d\omega\, Z_{x,y}(\omega)\int_{-\infty}^{\infty} dt\, e^{j(\omega-\omega')t}. \tag{12.14}$$

We now apply the following property of the Dirac δ function

$$\delta(\omega - \omega') = \frac{j}{2\pi} \int_{-\infty}^{\infty} dt\, e^{j(\omega-\omega')t}, \qquad (12.15)$$

and we find

$$\int_{-\infty}^{\infty} dt\, e^{-j\omega't}\widehat{W}_{x,y}(t) = -j \int_{-\infty}^{+\infty} d\omega\, Z_{x,y}(\omega)\delta(\omega - \omega') = -jZ_{x,y}(\omega'). \qquad (12.16)$$

We can write the impedances also in terms of the wakefield expressed as a function of $z = -\beta_0 ct$ (using Eqs. 12.4 and 12.5):

$$W_{x,y}(z) = -\frac{j}{2\pi} \int_{-\infty}^{+\infty} d\omega\, e^{-j\omega \frac{z}{\beta_0 c}} Z_{x,y}(\omega), \qquad (12.17)$$

$$Z_{x,y}(\omega) = \frac{j}{\beta_0 c} \int_{-\infty}^{+\infty} dz e^{j\omega \frac{z}{\beta_0 c}} W_{x,y}(z). \qquad (12.18)$$

As the transverse wakes are real functions, the impedances satisfy the following symmetry properties:

$$\text{Re}\left\{Z_{x,y}(-\omega)\right\} = -\text{Re}\left\{Z_{x,y}(\omega)\right\} \qquad (12.19)$$

$$\text{Im}\left\{Z_{x,y}(-\omega)\right\} = \text{Im}\left\{Z_{x,y}(\omega)\right\} \qquad (12.20)$$

12.3 Longitudinal wakefield

Longitudinal wakefields are defined such that the corresponding kicks can be written as:

$$\Delta\delta = -\frac{q^2 e^2}{m_0 \gamma \beta_0^2 c^2} \int_{-\infty}^{+\infty} dz'\, \lambda(z')W_s(z - z'). \qquad (12.21)$$

The minus sign is introduced such that a positive wake causes the particles to lose energy. The convolution can be obtained numerically using the method of Section 14.2.
Also in this case, we call $\widehat{W}_s$ the wakefield defined as a function of time t:

$$\widehat{W}_s(t) = W_s\left(\beta_0 ct\right) \qquad (12.22)$$

$$W_s(z) = \widehat{W}_s\left(-\frac{z}{\beta_0 c}\right) \qquad (12.23)$$

12.4 Longitudinal impedance

The longitudinal beam coupling impedances $Z_s(\omega)$ are related to the wakefields through a Fourier transform (see [58, Eq. 1.216]):

$$\widehat{W}_s(t) = \frac{1}{2\pi} \int_{-\infty}^{+\infty} d\omega\, e^{j\omega t} Z_s(\omega), \qquad (12.24)$$

$$Z_s(\omega) = \int_{-\infty}^{+\infty} dt\, e^{-j\omega t}\widehat{W}_s(t). \qquad (12.25)$$

We can write the impedances also in terms of the wakefield expressed as a function of $z = -\beta_0 ct$ (using Eqs. 12.22 and 12.23):

$$W_s(z) = \frac{1}{2\pi} \int_{-\infty}^{+\infty} d\omega\, e^{-j\omega \frac{z}{\beta_0 c}} Z_s(\omega)\,, \tag{12.26}$$

$$Z_s(\omega) = \frac{1}{\beta_0 c} \int_{-\infty}^{+\infty} dz e^{j\omega \frac{z}{\beta_0 c}} W_s(z)\,. \tag{12.27}$$

As the longitudinal wake is a real function, the conrresponding impedance satisfies the following symmetry properties:

$$\mathrm{Re}\,\{Z_s(-\omega)\} = \mathrm{Re}\,\{Z_s(\omega)\} \tag{12.28}$$

$$\mathrm{Im}\,\{Z_s(-\omega)\} = -\,\mathrm{Im}\,\{Z_s(\omega)\} \tag{12.29}$$

12.5 Analytical wakes

Resonator

Ultra-relativistic resonator with shunt impedance R, quality factor $Q > 1$ and resonant frequency f_r

- Longitudinal:

$$W_s(t) = \frac{\omega_r R}{Q} e^{-\alpha t} \left(\cos(\widehat{\omega}_r t) - \frac{\alpha}{\widehat{\omega}_r} \sin(\widehat{\omega}_r t) \right)\,, \tag{12.30}$$

$$Z_s(\omega) = \frac{R}{1 - jQ \left(\frac{\omega_r}{\omega} - \frac{\omega}{\omega_r} \right)}\,. \tag{12.31}$$

- Transverse:

$$W_{x,y}(t) = \frac{\omega_r^2 R}{Q \widehat{\omega}_r} e^{-\alpha t} \sin(\widehat{\omega}_r t)\,, \tag{12.32}$$

$$Z_{x,y}(\omega) = \frac{\omega_r}{\omega} \frac{R}{1 - jQ \left(\frac{\omega_r}{\omega} - \frac{\omega}{\omega_r} \right)}\,. \tag{12.33}$$

where $\omega_r = 2\pi f_r$, $\widehat{\omega}_r = \omega_r \sqrt{1 - \frac{1}{4Q^2}}$, $\alpha = \frac{\omega_r}{2Q}$. Ref: [58, Section 2.2]

Cylindrical thick wall

Cylindrical resistive wall wake, based on the "classic thick wall formula" (see e.g. [59, Chapter 2]) with resistivity ρ, permeability μ, radius r and length L:

- Longitudinal:

$$W_s(t) = -L \frac{1}{4\pi r} \sqrt{\frac{Z_0 \rho}{\pi c}} t^{-\frac{3}{2}}\,, \tag{12.34}$$

$$Z_s(\omega) = L \left(1 + j\,\mathrm{sign}(\omega)\right) \frac{\rho}{2\pi r} \frac{1}{\delta_s(\omega)}\,, \tag{12.35}$$

where $\delta_s(\omega) = \sqrt{\frac{2\rho}{|\omega|}}$ is the frequency-dependent skin depth.

Note: the longitudinal resistive wall wake is negative for any value of t, while, with the adopted sign convention, longitudinal wakes should be positive for $t \to 0+$. This happens because the thick wall approximation is not valid for small t. Computing the wake numerically with IW2D shows that the resistive wall wake is actually positive close to zero and performs a few oscillations after which it agrees very well with the formula above. For applications where short range effects are relevant this model should not be used.

- Transverse:

$$W_{x,y}(t) = L\frac{1}{\pi r^3}\sqrt{\frac{cZ_0\rho}{\pi}}t^{-\frac{1}{2}}\,, \tag{12.36}$$

$$Z_{x,y}(\omega) = L(1+j\,\mathrm{sign}(\omega))\frac{\rho}{\pi r^3}\frac{1}{\omega\sqrt{\varepsilon_0\mu_0}}\frac{1}{\delta_s(\omega)}\,. \tag{12.37}$$

Chapter 13

Intra-Beam Scattering

Intra-beam scattering (IBS) is the process of small angle, multiple Coulomb scattering of charged particles within the beam. It leads to a redistribution of the particle momenta in six-dimentional phase space.

13.1 Analytical Growth Rates

Theoretical models commonly characterize the effect of intra-beam scattering through growth rates, or growth times. The former is expressed in $[s^{-1}]$) and the latter in $[s]$. These govern the evolution of the rms beam sizes or rms emittances of the beam, depending on the convention used.

Growth rates (and growth times) can be expressed in either amplitude or emittance convention. The former governs the evolution of rms beam sizes while the latter governs that of rms emittances. The two conventions are equivalent by a factor 2 and conversion can be done as:

$$
\begin{array}{ccc}
\text{Emit. Times} & \xrightleftharpoons[\times 2]{\div 2} & \text{Amp. Times} \\[2em]
\Big\updownarrow \text{\itshape inverse} & & \Big\updownarrow \text{\itshape inverse} \\[2em]
\text{Emit. Rates} & \xrightleftharpoons[\div 2]{\times 2} & \text{Amp. Rates}
\end{array}
$$
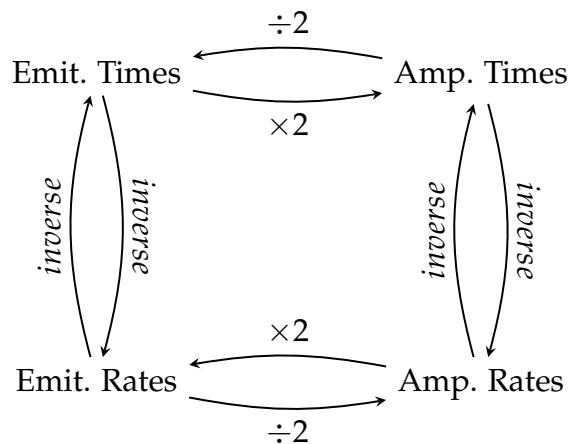
Figure 13.1: Illustration of the conversions between IBS growth rates and times, across emittance and amplitude conventions.

The growth rates themselves are expressed from the lattice optics as well as the beam properties.

In Xsuite, for consistency with synchrotron radiation damping times (see section 7.1), **the amplitude growth rates are computed**. The horizontal (K_x), vertical (K_y) and longitudinal (K_z) amplitude growth rates are defined as:

$$
\begin{aligned}
K_x &= \frac{1}{\tau_x} = \frac{1}{\varepsilon_x^{1/2}} \frac{d\varepsilon_x^{1/2}}{dt}, \\[2mm]
K_y &= \frac{1}{\tau_y} = \frac{1}{\varepsilon_y^{1/2}} \frac{d\varepsilon_y^{1/2}}{dt}, \\[2mm]
K_z &= \frac{1}{\tau_z} = \frac{1}{\varepsilon_z^{1/2}} \frac{d\varepsilon_z^{1/2}}{dt},
\end{aligned}
\tag{13.1}
$$

where (τ_x), (τ_y) and (τ_z) are the amplitude growth times.

Currently two different formalism are available to compute these growth rates. Both assume transverse and longitudinal Gaussian bunch profiles. Both rely on the computation of the Coulomb logarithm L_C, which in *xfields* is computed according to the expression in the Physics Vade Mecum [60]:

$$
L_C = \ln\left(\frac{r_{max}}{r_{min}}\right).
\tag{13.2}
$$

In Eq (13.2) r_{max} is taken as the smaller of σ_x and the Debye length, while r_{min} is taken as the larger of the classical distance of closest approach and the quantum diffraction limit from the nuclear radius.

13.1.1 Nagaitsev Formalism

One available formalism follows the approach introduced by S. Nagaitsev in [61]. It provides a fast computation method through symmetric elliptic integrals of the second kind, $R_D(x, y, z)$, defined as:

$$
R_D(x, y, z) = \frac{3}{2} \int_0^\infty \frac{dt}{\sqrt{(t+x)(t+y)(t+z)^3}}.
\tag{13.3}
$$

Interestingly, this elliptic integral has the following special properties:

$$
R_D(x, x, x) = x^{-3/2},
\tag{13.4}
$$

$$
R_D(x, y, z) + R_D(y, z, x) + R_D(z, x, y) = \frac{3}{\sqrt{xyz}}.
\tag{13.5}
$$

Thanks to Eq (13.5) only two evaluations of this integral are needed to obtain various simple terms from which one can compute the growth rates. Importantly, the computation time of this integral in Nagaitsev's approach does not scale with the size of the lattice.

First the a_x, a_y, a_s, a_1 and a_2 terms are computed:

$$a_x = \frac{\beta_x}{\varepsilon_x}, a_y = \frac{\beta_y}{\varepsilon_y}, a_s = a_x \left(\frac{D_x^2}{\beta_x^2} + \Phi_x^2 \right) + \frac{1}{\sigma_p^2},$$

$$a_1 = \frac{1}{2}(a_x + \gamma^2 a_s), a_2 = \frac{1}{2}(a_x - \gamma^2 a_s),$$

(13.6)

where the $\Phi_{x,y}$ term is defined as:

$$\Phi_{x,y} = D'_{x,y} - \frac{\beta'_{x,y} D_{x,y}}{2\beta_{x,y}}.$$

(13.7)

Then the λ_1, λ_2 and λ_3 terms are computed:

$$\lambda_1 = a_y, \lambda_2 = a_1 + \sqrt{a_2^2 + \gamma^2 a_x^2 \Phi_x^2}, \lambda_3 = a_1 - \sqrt{a_2^2 + \gamma^2 a_x^2 \Phi_x^2}.$$

(13.8)

and used to compute three integrals R_1, R_2 and R_3 (though with Eq (13.5) only two need to be computed):

$$R1 = \frac{1}{\lambda_1} R_D(\frac{1}{\lambda_2}, \frac{1}{\lambda_3}, \frac{1}{\lambda_1}),$$

$$R2 = \frac{1}{\lambda_2} R_D(\frac{1}{\lambda_3}, \frac{1}{\lambda_1}, \frac{1}{\lambda_2}),$$

(13.9)

$$R3 = \frac{1}{\lambda_3} R_D(\frac{1}{\lambda_1}, \frac{1}{\lambda_2}, \frac{1}{\lambda_3}).$$

Using all the above the S_p, S_x and S_{xp} terms are computed according to Eq (13.10):

$$S_p = \frac{\gamma^2}{2} \left[2R_1 - R_2 \left(1 - \frac{3a_2}{\sqrt{a_2^2 + \gamma^2 a_x^2 \Phi_x^2}} \right) - R_3 \left(1 + \frac{3a_2}{\sqrt{a_2^2 + \gamma^2 a_x^2 \Phi_x^2}} \right) \right],$$

$$S_x = \frac{1}{2} \left[2R_1 - R_2 \left(1 + \frac{3a_2}{\sqrt{a_2^2 + \gamma^2 a_x^2 \Phi_x^2}} \right) - R_3 \left(1 - \frac{3a_2}{\sqrt{a_2^2 + \gamma^2 a_x^2 \Phi_x^2}} \right) \right], \quad (13.10)$$

$$S_{xp} = \frac{3\gamma^2 \Phi_x^2 a_x}{\sqrt{a_2^2 + \gamma^2 a_x^2 \Phi_x^2}} (R_3 - R_2).$$

From these, one computes the integrals - called the *Nagaitsev integrals* in the *xfields* code base - I_x, I_y and I_z:

$$I_x = \int_0^C \frac{\beta_x ds}{L\sigma_x\sigma_y} \left[S_x + \left(\frac{D_x^2}{\beta_x^2} + \Phi_x^2 \right) S_p + S_{xp} \right],$$

$$I_y = \int_0^C \frac{\beta_y ds}{L\sigma_x\sigma_y} (R_2 + R_3 - 2R_1),$$

(13.11)

$$I_z = \int_0^C \frac{ds}{L\sigma_x\sigma_y} S_p.$$

with C the circumference (or length) of the machine. Finally, the *emittance growth rates* in the horizontal, vertical and longitudinal planes are computed as:

$$\boxed{\frac{1}{\varepsilon_x}\frac{d\varepsilon_x}{dt} = \frac{1}{\varepsilon_x}\frac{Nr_0^2 c L_C}{12\pi\beta^3\gamma^5\sigma_z}I_x}$$ (13.12)

$$\boxed{\frac{1}{\varepsilon_y}\frac{d\varepsilon_y}{dt} = \frac{1}{\varepsilon_y}\frac{Nr_0^2 c L_C}{12\pi\beta^3\gamma^5\sigma_z}I_y}$$ (13.13)

$$\boxed{\frac{1}{\varepsilon_z}\frac{d\varepsilon_z}{dt} = \frac{1}{\sigma_p^2}\frac{Nr_0^2 c L_C}{12\pi\beta^3\gamma^5\sigma_z}I_z}$$ (13.14)

In the above N is the total beam intensity, r_0 the classical particle radius, c the speed of light in vacuum, L_C the Coulomb logarithm from Eq (13.2), β and γ the relativistic parameters of the beam and σ_z the bunch length.

Please note: Nagaitsev's computations yield emittance growth rates. In Xsuite these are computed as exposed above, and converted to amplitude growth rates before being returned to the user, as shown in Fig. 13.1.

Importantly, this formalism does not take into account vertical dispersion, and in the presence of D_y will yield an erroneous vertical growth rate. For machines with vertical dispersion, the Bjorken-Mtingwa formalism presented below is recommended.

13.1.2   Bjorken-Mtingwa Formalism

The IBS growth rates can also be computed according to the theory by Bjorken and Mtingwa [62]. The specific implementation follows that of the MAD-X code, for which modifications to the terms of B&M's theory have been made by Antoniou and Zimmermann to account for vertical dispersion non-ultrarelativistic beams [63].

In this formalism, growth rates are computed at every element in the lattice and averaged over the machine. For a given plane u (horizontal, vertical or longitudinal), the *emittance growth rate* is computed as:

$$T_u = \frac{Nr_0^2 c m^3 L_C \pi^2}{\gamma\Gamma}\left\langle \int_0^\infty \frac{d\lambda\,\lambda^{1/2}}{[\det(L+\lambda I)]^{1/2}}\left\{ \mathrm{Tr}\,L^{(u)}\,\mathrm{Tr}\left(\frac{1}{L+\lambda I}\right) - 3\,\mathrm{Tr}\,L^{(u)}\left(\frac{1}{L+\lambda I}\right)\right\}\right\rangle$$ (13.15)

in which N is the total beam intensity, r_0 the classical particle radius, c the speed of light in vacuum, m the mass of the considered particle, L_C the Coulomb logarithm from Eq (13.2), γ the relativistic parameter of the beam, and Γ the six-dimensional phase space volume of the beam, defined as:

$$\Gamma = (2\pi)^3\,(\beta\gamma)^3\,m^3\varepsilon_x\varepsilon_y\sigma_\delta\sigma_z$$ (13.16)

with σ_δ the relative momentum spread and σ_z the bunch length. One should note the expression for Γ is corrected by a factor $\sqrt{2}$ for coasting beams.

In Eq (13.15) λ is simply the integration variable, I is the 3x3 identity matrix, and L is the 3x3 matrix and the matrix L is defined as:

$$L = L^{(x)} + L^{(y)} + L^{(z)} , \qquad (13.17)$$

where the plane-dependent matrices $L^{(x)}, L^{(y)}$ and $L^{(z)}$ are defined as:

$$L^{(x)} = \frac{\beta_x}{\epsilon_x} \begin{pmatrix} 1 & -\gamma\phi_x & 0 \\ -\gamma\phi_x & \gamma^2 H_x/\beta_x & 0 \\ 0 & 0 & 0 \end{pmatrix} , \qquad (13.18)$$

$$L^{(y)} = \frac{\beta_y}{\epsilon_y} \begin{pmatrix} 0 & 0 & 0 \\ 0 & \gamma^2 H_y/\beta_y & -\gamma\phi_y \\ 0 & -\gamma\phi_y & 1 \end{pmatrix} , \qquad (13.19)$$

$$L^{(z)} = \frac{\gamma^2}{\sigma_\delta^2} \begin{pmatrix} 0 & 0 & 0 \\ 0 & 1 & 0 \\ 0 & 0 & 0 \end{pmatrix} . \qquad (13.20)$$

The $\Phi_{x,y}$ and $H_{x,y}$ terms are defined as:

$$\phi_{x,y} = D'_{x,y} - \frac{\beta'_{x,y} D_{x,y}}{2\beta_{x,y}} , \qquad (13.21)$$

and

$$H_{x,y} = \frac{D_{x,y}^2 + \beta_{x,y}^2 \phi_{x,y}^2}{\beta_{x,y}} . \qquad (13.22)$$

In [63] a new expression was derived for each growth rates, which is the implemented approach. In *xfields*, the computation of the growth rates takes the following steps. First the $a, b, c, a_x, b_x, a_y, b_y, a_z$ and b_z terms are computed as defined below:

$$a = \gamma^2 \left(\frac{H_x}{\epsilon_x} + \frac{H_y}{\epsilon_y} \right) + \frac{\gamma^2}{\sigma_\delta^2} + \left(\frac{\beta_x}{\epsilon_x} + \frac{\beta_y}{\epsilon_y} \right) , \qquad (13.23)$$

$$b = \left(\frac{\beta_x}{\epsilon_x} + \frac{\beta_y}{\epsilon_y} \right) \left(\frac{\gamma^2 D_x^2}{\epsilon_x \beta_x} + \frac{\gamma^2 D_y^2}{\epsilon_y \beta_y} + \frac{\gamma^2}{\sigma_\delta^2} \right) + \frac{\beta_x \beta_y}{\epsilon_x \epsilon_y} \gamma^2 \left(\Phi_x^2 + \Phi_y^2 \right) + \frac{\beta_x \beta_y}{\epsilon_x \epsilon_y} , \qquad (13.24)$$

$$c = \frac{\beta_x \beta_y}{\epsilon_x \epsilon_y} \left(\frac{\gamma^2 D_x^2}{\epsilon_x \beta_x} + \frac{\gamma^2 D_y^2}{\epsilon_y \beta_y} + \frac{\gamma^2}{\sigma_\delta^2} \right) , \qquad (13.25)$$

$$a_x = 2\gamma^2 \left(\frac{H_x}{\varepsilon_x} + \frac{H_y}{\varepsilon_y} + \frac{1}{\sigma_\delta^2} \right) - \frac{\beta_x H_y}{H_x \varepsilon_y} + \frac{\beta_x}{H_x \gamma^2} \left(\frac{2\beta_x}{\varepsilon_y} - \frac{\beta_y}{\varepsilon_y} - \frac{\gamma^2}{\sigma_\delta^2} \right)$$
$$- 2\frac{\beta_x}{\varepsilon_x}\frac{\beta_y}{\varepsilon_y} + \frac{\beta_x}{\gamma^2 H_x} \left(\frac{6\beta_x}{\varepsilon_x} \gamma^2 \Phi_x^2 \right) \ , \tag{13.26}$$

$$b_x = \left(\frac{\beta_x}{\varepsilon_x} + \frac{\beta_y}{\varepsilon_y} \right) \left(\frac{\gamma^2 H_x}{\varepsilon_x} + \frac{\gamma^2 H_y}{\varepsilon_y} + \frac{\gamma^2}{\sigma_\delta^2} \right) - \gamma^2 \left(\frac{\beta_x^2}{\varepsilon_x^2} \Phi_x^2 + \frac{\beta_y^2}{\varepsilon_y^2} \Phi_y^2 \right) + \left(\frac{\beta_x}{\varepsilon_x} - \frac{4\beta_y}{\varepsilon_y} \right) \frac{\beta_x}{\varepsilon_x}$$
$$+ \frac{\beta_x}{\gamma^2 H_x} \left(\frac{\gamma^2}{\sigma_\delta^2} \left(\frac{\beta_x}{\varepsilon_x} - \frac{2\beta_y}{\varepsilon_y} \right) + \frac{\beta_x \beta_y}{\varepsilon_x \varepsilon_y} + \frac{6\beta_x \beta_y}{\varepsilon_x \varepsilon_y} \gamma^2 \Phi_x^2 + \gamma^2 \left(\frac{2\beta_y^2 \Phi_y^2}{\varepsilon_y^2} - \frac{\beta_x^2 \Phi_x^2}{\varepsilon_x^2} \right) \right)$$
$$+ \frac{\beta_x H_y}{\varepsilon_y H_x} \left(\frac{\beta_x}{\varepsilon_x} - \frac{2\beta_y}{\varepsilon_y} \right)$$

$$\tag{13.27}$$

$$a_y = -\gamma^2 \left(\frac{H_x}{\varepsilon_x} + \frac{2H_y}{\varepsilon_y} + \frac{\beta_x}{\beta_y}\frac{H_y}{\varepsilon_x} + \frac{1}{\sigma_\delta^2} \right) + 2\gamma^4 \frac{H_y}{\beta_y} \left(\frac{H_y}{\varepsilon_y} + \frac{H_x}{\varepsilon_x} \right)$$
$$+ \frac{2\gamma^4 H_y}{\beta_y \sigma_\delta^2} - \left(\frac{\beta_x}{\varepsilon_x} - \frac{2\beta_y}{\varepsilon_y} \right) + \left(\frac{6\beta_y}{\varepsilon_y} \gamma^2 \Phi_y^2 \right) \tag{13.28}$$

$$b_y = \gamma^2 \left(\frac{\beta_y}{\varepsilon_y} - \frac{2\beta_x}{\varepsilon_x} \right) \left(\frac{H_x}{\varepsilon_x} + \frac{1}{\sigma_\delta^2} \right) + \left(\frac{\beta_y}{\varepsilon_y} - \frac{4\beta_x}{\varepsilon_x} \right) \frac{\gamma^2 H_y}{\varepsilon_y} + \frac{\beta_x \beta_y}{\varepsilon_x \varepsilon_y}$$
$$+ \gamma^2 \left(\frac{2\beta_x^2 \Phi_x^2}{\varepsilon_x^2} - \frac{\beta_y^2 \Phi_y^2}{\varepsilon_y^2} \right) + \frac{\gamma^4 H_y}{\beta_y} \left(\frac{\beta_x}{\varepsilon_x} + \frac{\beta_y}{\varepsilon_y} \right) \left(\frac{H_y}{\varepsilon_y} + \frac{1}{\sigma_\delta^2} \right) \tag{13.29}$$
$$+ \left(\frac{\beta_x}{\varepsilon_x} + \frac{\beta_y}{\varepsilon_y} \right) \gamma^4 \frac{H_x H_y}{\beta_y \varepsilon_x} - \gamma^4 \frac{H_y}{\beta_y} \left(\frac{\beta_x^2}{\varepsilon_x^2} \Phi_x^2 + \frac{\beta_y^2}{\varepsilon_y^2} \Phi_y^2 \right) + \frac{6\beta_x \beta_y}{\varepsilon_x \varepsilon_y} \gamma^2 \Phi_y^2$$

$$a_z = 2\gamma^2 \left(\frac{H_x}{\varepsilon_x} + \frac{H_y}{\varepsilon_y} + \frac{1}{\sigma_\delta^2} \right) - \frac{\beta_x}{\varepsilon_x} - \frac{\beta_y}{\varepsilon_y} \tag{13.30}$$

$$b_z = \left(\frac{\beta_x}{\varepsilon_x} + \frac{\beta_y}{\varepsilon_y} \right) \gamma^2 \left(\frac{H_x}{\varepsilon_x} + \frac{H_y}{\varepsilon_y} + \frac{1}{\sigma_\delta^2} \right) - 2\frac{\beta_x \beta_y}{\varepsilon_x \varepsilon_y} - \gamma^2 \left(\frac{\beta_x^2 \Phi_x^2}{\varepsilon_x^2} + \frac{\beta_y^2 \Phi_y^2}{\varepsilon_y^2} \right) \tag{13.31}$$

Finally, the *emittance growth rates* in the horizontal, vertical and longitudinal planes are computed as:

$$\boxed{\frac{1}{\varepsilon_x}\frac{d\varepsilon_x}{dt} = \frac{Nr_0^2 cm^3 L_C \pi^2}{\gamma \Gamma} \left\langle \left[\frac{\gamma^2 H_x}{\varepsilon_x} \right] \int_0^\infty \frac{\lambda^{1/2} \left[a_x \lambda + b_x \right]}{(\lambda^3 + a\lambda^2 + b\lambda + c)} d\lambda \right\rangle} \tag{13.32}$$

$$\boxed{\frac{1}{\varepsilon_y}\frac{d\varepsilon_y}{dt} = \frac{Nr_0^2 cm^3 L_C \pi^2}{\gamma \Gamma} \left\langle \left[\frac{\beta_y}{\varepsilon_y} \right] \int_0^\infty \frac{\lambda^{1/2} \left[a_y \lambda + b_y \right]}{(\lambda^3 + a\lambda^2 + b\lambda + c)} d\lambda \right\rangle} \tag{13.33}$$

$$\boxed{\frac{1}{\varepsilon_z}\frac{d\varepsilon_z}{dt} = \frac{Nr_0^2 cm^3 L_C \pi^2}{\gamma\Gamma}\left\langle\left[\frac{\gamma^2}{\sigma_\delta^2}\right]\int_0^\infty \frac{\lambda^{1/2}\left[a_z\lambda + b_z\right]}{(\lambda^3 + a\lambda^2 + b\lambda + c)}d\lambda\right\rangle} \tag{13.34}$$

where the constants in the common fraction term are the same as for Eq (13.15), λ is an integration variable and the angled bracket signify the averaging over the lattice, given the terms contained inside are arrays with one value per element.

Please note: Bjorken and Mtingwa's computations yield emittance growth rates. In Xsuite these are computed as exposed above, and converted to amplitude growth rates before being returned to the user, as shown in Fig. 13.1. where the constants in the common fraction term are the same as for Eq (13.15), λ is an integration variable and the angled bracket signifies the averaging over the lattice, given the terms contained inside are arrays with one value per element.

13.2   Steady-state emittances

The steady-state emittances in the presence of Synchrotron Radiation (SR), Quantum Excitation (QE), and Intra-Beam Scattering (IBS) emerge from a dynamic equilibrium, where the combined effect of these three phenomena balances each other out. More specifically, the QE and SR are accounted for through the natural emittances and SR damping constants, the IBS is described by its growth rates. Each of these effects depends on the optical functions along the storage ring. All the following equations remain valid independently of which formalism (Nagaitsev or Bjorken-Mtingwa) is used when computing the IBS growth rates. In addition, the SR damping constants and IBS growth rates follow the amplitude convention as defined in Eq. (7.15).

13.2.1   Steady-state emittances with QE, SR, and IBS

The steady-state emittances are solutions to a system of three ordinary differential equations describing the dynamic interplay of the QE, SR, and IBS. The system of differential equations can be solved numerically by computing the emittance evolution for a succession of infinitesimal time steps. The equations are as follows:

$$\frac{d\varepsilon_u}{dt} = -2\alpha_u^{SR}\left(\varepsilon_u - \varepsilon_{u,0}\right) + 2\alpha_u^{IBS}\varepsilon_u, \quad u = x, y, z \tag{13.35}$$

$\varepsilon_{u,0}$ is the natural emittance, ε_u the emittance, α_u^{SR} the SR damping constant and α_u^{IBS} the IBS growth rate. It can be noted that the IBS growth rates are a function of all three emittances ($\alpha_u^{IBS}(\varepsilon_x, \varepsilon_y, \varepsilon_z)$).
The steady-state emittance is reached when the emittance evolution reaches zero and leads to:

$$\varepsilon_u = \frac{\varepsilon_{u,0}}{1 - \alpha_u^{IBS}/\alpha_u^{SR}}, \quad u = x, y, z \tag{13.36}$$

Although mathematically correct, the equation assumes a finite vertical emittance. In the case of lepton storage rings, the vertical emittance is often negligible in the absence

of vertical dispersion or betatron coupling. As a result, the IBS growth rates would reach extremely large values when a near zero vertical emittance is considered. A finite vertical emittance is introduced through betatron coupling or an external excitation to overcome this limitation.

13.2.2   Steady-state emittances due to betatron coupling

In the presence of betatron coupling, emittance sharing occurs between the two transverse planes. The treatment of betatron coupling can be simplified by expressing it through the emittance coupling factor $\kappa = \tilde{\varepsilon}_y / \tilde{\varepsilon}_x$, the ratio of the perturbed vertical emittance to the horizontal one.

Based on the natural emittance, defined in Eq. (7.39) but written in a form [64] so that the horizontal damping partition number j_x appears:

$$\varepsilon_0 = C_q \frac{\gamma^2}{j_x} \frac{I_5}{I_2},$$

where $C_q = \frac{55}{32\sqrt{3}} \frac{\hbar}{m_e c} \approx 3.84 \times 10^{-13}$ m for electrons, γ the relativistic gamma and I_2, I_5 respectively the second and fifth radiation integrals.

$$\tilde{\varepsilon}_0 = C_q \frac{\gamma^2}{\tilde{j}_x} \frac{\langle K^3 \mathcal{H} \rangle}{K^2}, \qquad \text{where} \quad \tilde{j}_x = \frac{j_x}{1+\kappa} + \frac{\kappa j_y}{1+\kappa} \tag{13.37}$$

Here, j_y represents the vertical damping partition number. After some simplifications and remembering $\tilde{\varepsilon}_0 = \tilde{\varepsilon}_x + \tilde{\varepsilon}_y$ we finally obtain:

$$\tilde{\varepsilon}_{x,0} = \frac{\tilde{\varepsilon}_0}{1+\kappa} = \frac{\tilde{\varepsilon}_0}{1+\kappa\frac{j_y}{j_x}}, \qquad \tilde{\varepsilon}_{y,0} = \frac{\kappa\tilde{\varepsilon}_0}{1+\kappa} = \frac{\kappa\tilde{\varepsilon}_0}{1+\kappa\frac{j_y}{j_x}} \tag{13.38}$$

Furthermore, the perturbed horizontal and vertical emittances can be expressed as a function of the ones without betatron coupling:

$$\tilde{\varepsilon}_x = \frac{\varepsilon}{1+\kappa\frac{j_y}{j_x}}, \quad \tilde{\varepsilon}_y = \frac{\kappa\varepsilon}{1+\kappa\frac{j_y}{j_x}}$$

It can be noted that total transverse emittance conservation occurs solely if $j_x = j_y$. As a result, the transverse emittance evolution can be rewritten as:

$$\frac{d\tilde{\varepsilon}_u}{dt} = -2\alpha_u^{SR}\left(\tilde{\varepsilon}_u - \tilde{\varepsilon}_{u,0}\right) + 2\alpha_u^{IBS}\tilde{\varepsilon}_u, \quad u = x,y \tag{13.39}$$

And the steady-state transverse emittances become:

$$\tilde{\varepsilon}_u = \frac{\tilde{\varepsilon}_{u,0}}{1 - \frac{\alpha_u^{IBS}}{\alpha_u^{SR}\left(1+\kappa j_y/j_x\right)}}, \quad u = x,y \tag{13.40}$$

13.2.3 Steady-state emittances due to an external excitation

Alternatively, a finite vertical emittance can also be obtained by exciting the beam using the Pulse-Picking by Resonant Excitation (PPRE) method [65] in the vertical plane. In this situation, the horizontal and vertical planes are left uncoupled while the vertical emittance can be controlled. Nonetheless, the emittance coupling factor can still be employed. In this scenario, the emittance evolution follows Eq. (13.39) and the final emittance Eq. (13.36). Compared to the previous case, the total transverse emittance is not conserved even if $j_x = j_y$.

13.3 IBS Kicks

The approach of using analytical growth rates does not provide a way to study the interplay of IBS with arbitrary effects, such as space charge, electron clouds, beam-beam, etc. To do so, it is necessary to include IBS effects in tracking simulations together with other desired effects. In *xfields* two elements are available to model IBS effects in tracking simulations, both providing momenta kicks to tracked particles according to a specific formalism.

13.3.1 Analytical Kicks

A first element is available to provide momenta kicks based on analytical growth rates, according to the approach introduced by R. Bruce [66]. In *xfields* the computation of the kick is done as follows.

First, the beam intensity N, bunch length σ_z, momentum deviation σ_δ, and geometric emittances $\varepsilon_{x,y}$ are inferred from the tracked particles object. These are used to compute the analytical IBS growth rates. From these, each particle is given a momentum kick in each dimension according to:

$$\boxed{\Delta p_u = R\sigma_{p_u}\sqrt{2T_{IBS,u}T_{rev}\sigma_z\sqrt{\pi}\rho(z)} \; ; u = x, y, z} \qquad (13.41)$$

Here R is a random number from the standard normal distribution; σ_{p_u} is the standard deviation of the momentum in plane u; $T_{IBS,u}$ is the *emittance growth rate* for plane u; T_{rev} is the revolution frequency and $\rho(z)$ is the longitudinal line density.

Note from the form of Eq (13.41) that only zero or strictly positive growth rates are valid, and as such this formalism is traditionally available above transition energy.

The longitudinal line density $\rho(z)$ is used as a weighting factor to provide a stronger kick to particles in the denser regions of the bunch. It is obtained by binning the longitudinal plane of the particle distribution and normalizing the values.

13.3.2   Kinetic Kicks

A second element is available to provide momenta kicks based on diffusion and friction terms from the kinetic theory of gases, as introduced by P. Zenkevich [67]. The momentum kick has a form similar to the Langevin equation:

$$\Delta p_u = -K_u p_u \sigma_z \sqrt{\pi} \rho(z) \Delta t + R \sigma_{p_u} \sqrt{2 C_u \sigma_z \sqrt{\pi} \rho(z) \Delta t} \; ; u = x, y, z \qquad (13.42)$$

where K_u and C_u are functions of the friction and diffusion terms, respectively.

In *xfields* the exact implementation makes use of terms from the Nagaitsev formalism (see 13.1.1) as derived by M. Zampetakis [68]. First the a_x, a_y, a_s, a_1 and a_2 terms are computed according to Eq (13.6). Then the λ_1, λ_2 and λ_3 terms are computed according to Eq (13.8), to obtain the R_1, R_2 and R_3 elliptic integrals according to Eq (13.9).

New forms equivalent to the original diffusion and friction terms of the Approximate Model can be expressed from these. By first defining

$$q = \sqrt{a_2^2 + \gamma^2 a_x^2 \Phi_x^2} \, , \qquad (13.43)$$

one can first compute:

$$D_{x,x} = \frac{1}{2} \left[2R_1 + R2 \left(1 - \frac{a_2}{q} \right) + R_3 \left(1 + \frac{a_2}{q} \right) \right] ,$$

$$D_{x,z} = \frac{3\gamma^2 \Phi_x^2 a_x}{q} \left(R_3 - R_2 \right) ,$$

$$D_{y,y} = R_2 + R_3, \qquad (13.44)$$

$$D_{z,z} = \frac{\gamma^2}{2} \left[2R_1 + R_2 \left(1 + \frac{a_2}{q} \right) + R_3 \left(1 - \frac{a_2}{q} \right) \right] ,$$

and then:

$$K_x = R_2 \left(1 + \frac{a_2}{q} \right) + R_3 \left(1 - \frac{a_2}{q} \right) ,$$

$$K_y = 2R_1, \qquad (13.45)$$

$$K_z = \gamma^2 \left[R_2 \left(1 - \frac{a_2}{q} \right) + R_3 \left(1 + \frac{a_2}{q} \right) \right] .$$

The following integrals are computed from the above:

$$D_{xi} = \int_0^C \frac{\beta_x ds}{C \sigma_x \sigma_y} \left[D_{x,x} + \left(\frac{D_x^2}{\beta_x^2} + \Phi_x^2 \right) D_{z,z} + D_{x,z} \right] ,$$

$$D_{yi} = \int_0^C \frac{\beta_y ds}{C \sigma_x \sigma_y} D_{y,y}, \qquad (13.46)$$

$$D_{zi} = \int_0^C \frac{ds}{C \sigma_x \sigma_y} D_{z,z} .$$

$$F_{xi} = \int_0^C \frac{\beta_x ds}{C\sigma_x\sigma_y} \left[K_x + \left(\frac{D_x^2}{\beta_x^2} + \Phi_x^2 \right) K_z \right],$$

$$F_{yi} = \int_0^C \frac{\beta_y ds}{C\sigma_x\sigma_y} K_x, \tag{13.47}$$

$$F_{zi} = \int_0^C \frac{ds}{C\sigma_x\sigma_y} K_z .$$

with C the circumference of the machine. Finally, the new diffusion coefficients are computed according to:

$$G_x = \frac{1}{\varepsilon_x} \frac{Nr_0^2 c L_C}{12\pi\beta^3\gamma^5\sigma_z} D_{xi} \tag{13.48}$$

$$G_y = \frac{1}{\varepsilon_y} \frac{Nr_0^2 c L_C}{12\pi\beta^3\gamma^5\sigma_z} D_{yi} \tag{13.49}$$

$$G_z = \frac{1}{\sigma_\delta^2} \frac{Nr_0^2 c L_C}{12\pi\beta^3\gamma^5\sigma_z} D_{zi} \tag{13.50}$$

and the friction coefficients according to:

$$F_x = \frac{1}{\varepsilon_x} \frac{Nr_0^2 c L_C}{12\pi\beta^3\gamma^5\sigma_z} F_{xi} \tag{13.51}$$

$$F_y = \frac{1}{\varepsilon_y} \frac{Nr_0^2 c L_C}{12\pi\beta^3\gamma^5\sigma_z} F_{yi} \tag{13.52}$$

$$F_z = \frac{1}{\sigma_\delta^2} \frac{Nr_0^2 c L_C}{12\pi\beta^3\gamma^5\sigma_z} F_{zi} \tag{13.53}$$

In the above N is the total beam intensity, r_0 the classical particle radius, c the speed of light in vacuum, L_C the Coulomb logarithm from Eq (13.2). β and γ are the relativistic parameters of the beam and σ_z the bunch length.

From these coefficients, each particle is given a momentum kick in each dimension according to:

$$\Delta p_u = -F_u p_u T_{rev} 2\sqrt{\pi}\sigma_z\rho(z) + R\sigma_{p_u} \sqrt{T_{rev} G_u 2\sqrt{\pi}\sigma_z\rho(z)} \; ; u = x, y, z \tag{13.54}$$

Here R is a random number from the standard normal distribution; p_u and σ_{p_u} are the momentum and its standard deviation in plane u; T_{rev} is the revolution frequency and $\rho(z)$ is the longitudinal line density as defined previously (see 13.3.1).

Chapter 14

FFT solvers and convolutions

14.1 Notation for Discrete Fourier Transform

We will use the following notation for the Discrete Fourier Transform of a sequence of length M:

$$\hat{a}_k = \mathrm{DFT}_M(a_m) = \sum_{m=0}^{M-1} a_m\, e^{-j2\pi\frac{km}{M}} \quad \text{for } k \in 0, ..., M \tag{14.1}$$

The corresponding inverse transform is defined as:

$$a_m = \mathrm{DFT}_M^{-1}(\hat{a}_k) = \frac{1}{M} \sum_{k=0}^{M-1} \hat{a}_k\, e^{j2\pi\frac{km}{M}} \quad \text{for } m \in 0, ..., M \tag{14.2}$$

Multidimensional Discrete Fourier Transforms are obtained by applying sequentially 1D DFTs.. For example, in two dimensions:

$$
\begin{aligned}
\hat{a}_{k_x k_y} &= \mathrm{DFT}_{M_x M_y} \left\{ a_{m_x m_y} \right\} = \mathrm{DFT}_{M_y} \left\{ \mathrm{DFT}_{M_x} \left\{ a_{m_x m_y} \right\} \right\} \\
&= \sum_{m_x=0}^{M_x-1} e^{-j2\pi\frac{k_x m_x}{M_x}} \sum_{m_y=0}^{M_y-1} e^{-j2\pi\frac{k_y m_y}{M_y}} a_{m_x m_y}
\end{aligned}
\tag{14.3}
$$

$$
\begin{aligned}
a_{m_x m_y} &= \mathrm{DFT}_{M_x M_y}^{-1} \left\{ a_{k_x k_y} \right\} = \mathrm{DFT}_{M_y}^{-1} \left\{ \mathrm{DFT}_{M_x}^{-1} \left\{ \hat{a}_{k_x k_y} \right\} \right\} \\
&= \frac{1}{M_x M_y} \sum_{k_x=0}^{M_x-1} e^{j2\pi\frac{k_x m_x}{M_x}} \sum_{k_y=0}^{M_y-1} e^{j2\pi\frac{k_y m_y}{M_y}} \hat{a}_{k_x k_y}
\end{aligned}
\tag{14.4}
$$

14.2 FFT convolution - 1D case

The potential can be written as the convolution of a Green function with the charge distribution:

$$\phi(x) = \int_{-\infty}^{+\infty} \rho(x')\, G(x - x') dx' \tag{14.5}$$

We assume that the source is limited to the region $[0, L]$:

$$\rho(x) = \rho(x) \, \Pi_{[0,L]}(x) \tag{14.6}$$

where $\Pi_{[a,b]}(x)$ is a rectangular window function defined as:

$$\Pi_{[a,b]}(x) = \begin{cases} 1 & \text{for } x \in [a, b] \\ 0 & \text{elsewhere} \end{cases} \tag{14.7}$$

We are interested in the electric potential only the region occupied by the sources, so we can compute:

$$\phi_L(x) = \phi(x)\Pi_{[0,L]}(x) \tag{14.8}$$

We replace Eq. (14.6) and Eq. (14.8) into Eq.(14.5), obtaining:

$$\phi_L(x) = \Pi_{[0,L]}(x) \int_{-\infty}^{+\infty} \Pi_{[0,L]}(x') \, \rho(x') \, G(x - x') dx' \tag{14.9}$$

We apply the change of variable $x'' = x - x'$:

$$\phi_L(x) = \int_{-\infty}^{+\infty} \Pi_{[0,L]}(x) \, \Pi_{[0,L]}(x - x'') \, \rho(x - x'') \, G(x'') \, dx'' \tag{14.10}$$

The integrand vanishes outside the set of the (x, x'') defined by:

$$\begin{cases} 0 < x < L \\ 0 < (x - x'') < L \end{cases} \tag{14.11}$$

We flip the signs in the second equation, obtaining:

$$\begin{cases} 0 < x < L \\ -L < (x'' - x) < 0 \end{cases} \tag{14.12}$$

Combining the two equations we obtain:

$$-L < -L + x < x'' < x < L \tag{14.13}$$

i.e. the integrand is zero for $-L < x'' < L$. Therefore in Eq. (14.10) we can replace $G(x'')$ with its truncated version:

$$G_{2L}(x'') = G(x'') \, \Pi_{[-L,L]}(x'') \tag{14.14}$$

obtaining:

$$\phi_L(x) = \int_{-\infty}^{+\infty} \Pi_{[0,L]}(x) \, \Pi_{[0,L]}(x - x'') \, \rho(x - x'') \, G_{2L}(x'')dx'' \tag{14.15}$$

Since the two window functions force the integrand to zero outside the region $|x''| < L$ we can replace $G_{2L}(x'')$ with its replicated version:

$$G_{2LR}(x'') = \sum_{n=-\infty}^{+\infty} G_{2L}(x'' - 2nL) = \sum_{n=-\infty}^{+\infty} G(x'' - 2nL) \, \Pi_{[-L,L]}(x'' - 2nL) \tag{14.16}$$

obtaining:

$$\phi_L(x) = \int_{-\infty}^{+\infty} \Pi_{[0,L]}(x)\,\Pi_{[0,L]}(x - x'')\,\rho(x - x'')\,G_{2LR}(x'')dx'' \tag{14.17}$$

We can go back to the initial coordinate by substituting $x'' = x - x'$:

$$\phi_L(x) = \Pi_{[0,L]}(x) \int_{-\infty}^{+\infty} \rho(x')\,G_{2LR}(x - x')dx' \tag{14.18}$$

This is a cyclic convolution, so we can proceed as follows. We split the integral:

$$\phi_L(x) = \Pi_{[0,L]}(x) \sum_{n=-\infty}^{+\infty} \int_{2nL}^{2(n+1)L} \rho(x')\,G_{2LR}(x - x')\,dx' \tag{14.19}$$

In each term we replace $x''' = x' + 2nL$:

$$\phi_L(x) = \Pi_{[0,L]}(x) \sum_{n=-\infty}^{+\infty} \int_{0}^{2L} \rho(x''' - 2nL)\,G_{2LR}(x - x''' - 2nL)\,dx''' \tag{14.20}$$

We use the fact that $G_{2LR}(x)$ is periodic:

$$\phi_L(x) = \Pi_{[0,L]}(x) \sum_{n=-\infty}^{+\infty} \int_{0}^{2L} \rho(x''' - 2nL)\,G_{2LR}(x - x''')dx'''$$

$$\tag{14.21}$$

$$= \Pi_{[0,L]}(x) \int_{0}^{2L} \sum_{n=-\infty}^{+\infty} \rho(x''' - 2nL)\,G_{2LR}(x - x''')dx'''$$

We can define a replicated version of $\rho(x)$:

$$\rho_{2LR}(x) = \sum_{n=-\infty}^{+\infty} \rho(x - 2nL) \tag{14.22}$$

noting that this implies:

$$\rho_{2LR}(x) = 0 \quad \text{for } x \in [L, 2L] \tag{14.23}$$

We obtain:

$$\phi_L(x) = \Pi_{[0,L]}(x) \int_{0}^{2L} \rho_{2LR}(x')\,G_{2LR}(x - x')dx' \tag{14.24}$$

The function:

$$\phi_{2LR}(x) = \int_{0}^{2L} \rho_{2LR}(x')\,G_{2LR}(x - x')dx' \tag{14.25}$$

is periodic of period $2L$. From it the potential of interest can be simply calculated by selecting the first half period $[0, L]$:

$$\phi_L(x) = \Pi_{[0,L]}(x)\,\phi_{2LR}(x) \tag{14.26}$$

To compute the convolution in Eq. 14.25 we expand $\phi_{2LR}(x)$ in Fourier series:

$$\phi_{2LR}(x) = \sum_{k=-\infty}^{+\infty} \tilde{\phi}_k \, e^{j2\pi k \frac{x}{2L}} \tag{14.27}$$

where the Fourier coefficients are given by:

$$\tilde{\phi}_k = \frac{1}{2L} \int_0^{2L} \phi_{2LR}(x) \, e^{-j2\pi k \frac{x}{2L}} \, dx \tag{14.28}$$

We replace Eq. (14.25) into Eq. (14.28) obtaining:

$$\hat{\phi}_k = \frac{1}{2L} \int_0^{2L} \int_0^{2L} \rho_{2LR}(x') \, G_{2LR}(x - x') \, e^{-j2\pi k \frac{x}{2L}} \, dx' \, dx \tag{14.29}$$

With the change of variable $x'' = x - x'$ we obtain:

$$\tilde{\phi}_k = \frac{1}{2L} \int_0^{2L} \rho_{2LR}(x') e^{-j2\pi k \frac{x'}{2L}} dx' \int_0^{2L} G_{2LR}(x'') e^{-j2\pi k \frac{x''}{2L}} \, dx'' \tag{14.30}$$

where we recognize the Fourier coefficients of $\rho_{2LR}(x)$ and $G_{2LR}(x)$:

$$\tilde{\rho}_k = \frac{1}{2L} \int_0^{2L} \rho_{2LR}(x) \, e^{-j2\pi k \frac{x}{2L}} \, dx \tag{14.31}$$

$$\tilde{G}_k = \frac{1}{2L} \int_0^{2L} G_{2LR}(x) \, e^{-j2\pi k \frac{x}{2L}} \, dx \tag{14.32}$$

obtaining simply:

$$\hat{\phi}_k = 2L \, \hat{G}_k \, \hat{\rho}_k \tag{14.33}$$

I assume to have the functions $\rho_{2LR}(x)$ and $G_{2LR}(x)$ sampled (or averaged) with step:

$$h_x = \frac{2L}{M} = \frac{L}{N} \tag{14.34}$$

I can approximate the integrals in Eqs. (14.31) and (14.32) as:

$$\tilde{\rho}_k = \frac{1}{M} \sum_{n=0}^{M-1} \rho_{2LR}(x_n) \, e^{-j2\pi \frac{kn}{M}} = \frac{1}{M} \hat{\rho}_k \tag{14.35}$$

$$\tilde{G}_k = \frac{1}{M} \sum_{n=0}^{M-1} G_{2LR}(x_n) \, e^{-j2\pi \frac{kn}{M}} = \frac{1}{M} \hat{G}_k \tag{14.36}$$

where we recognize the Discrete Fourier Transforms:

$$\hat{\rho}_k = \text{DFT}_M \{\rho_{2LR}(x_n)\} \tag{14.37}$$

$$\hat{G}_k = \text{DFT}_M \{G_{2LR}(x_n)\} \tag{14.38}$$

Using Eq. (14.27) we can obtain a sampled version of $\phi(x)$:

$$\phi_{2LR}(x_n) = \sum_{n=0}^{M-1} \tilde{\phi}_k \, e^{j2\pi \frac{kn}{M}} \tag{14.39}$$

where we have assumed that $\phi(x)$ is sufficiently smooth to allow truncating the sum. Using Eqs. (14.33), (14.35) and (14.36) we obtain:

$$\phi_{2LR}(x_n) = 2L \sum_{n=0}^{M-1} \tilde{G}_k \, \tilde{\rho}_k \, e^{j2\pi \frac{kn}{M}} = \frac{2L}{M^2} \sum_{n=0}^{M-1} \hat{G}_k \, \hat{\rho}_k \, e^{j2\pi \frac{kn}{M}} \tag{14.40}$$

This can be rewritten as:

$$\phi_{2LR}(x_n) = \frac{1}{M} \sum_{n=0}^{M-1} (h_x \hat{G}_k) \, \hat{\rho}_k \, e^{j2\pi \frac{kn}{M}} = \text{DFT}_M^{-1} \{\phi_k\} \tag{14.41}$$

where

$$\hat{\phi}_k = h_x \hat{G}_k \, \hat{\rho}_k \tag{14.42}$$

We call "Integrated Green Function" the quantity:

$$G_{2LR}(x_n) = h_x G_{2LR}(x_n) \tag{14.43}$$

we introduce the corresponding Fourier transform:

$$\hat{G}_k^{\text{int}} = \text{DFT}_M \left\{ G_{2LR}^{\text{int}}(x_n) \right\} \tag{14.44}$$

Eq. (14.42) can be rewritten as:

$$\boxed{\hat{\phi}_k = \hat{G}_k^{\text{int}} \, \hat{\rho}_k} \tag{14.45}$$

In summary the potential at the grid nodes can be computed as follows:

1. We compute the Integrated Green function at the grid points in the range $[0, L]$:

$$G_{2LR}^{\text{int}}(x_n) = \int_{x_n - \frac{h_x}{2}}^{x_n + \frac{h_x}{2}} G(x) dx \tag{14.46}$$

2. We extend to the interval $[L, 2L]$ using the fact that in this interval:

$$G_{2LR}^{\text{int}}(x_n) = G_{2LR}^{\text{int}}(x_n - 2L) = G_{2LR}^{\text{int}}(2L - x_n) \tag{14.47}$$

    where the first equality comes from the periodicity of $G_{2LR}^{\text{int}}(x)$ and the second from the fact that $G(x)$ is an even function (i.e. $G(x) = G(-x)$). Note that for $x_n \in [L, 2L]$ we have that $2L - x_n \in [0, L]$ so we can reuse the values computed at the previous step.

3. We transform it:
$$\hat{G}_k^{\text{int}} = \text{DFT}_{2N} \{G_{2LR}(x_n)\} \tag{14.48}$$

4. We assume that we are given $\rho(x_n)$ in the interval $[0, L]$. From this we can obtain $\rho_{2LR}(x_n)$ over the interval $[0, 2L]$ simply extending the sequence with zeros (see Eq. (14.23)).

5. We transform it:
$$\hat{\rho}_k = \text{DFT}_{2N} \{\rho_{2LR}(x_n)\} \tag{14.49}$$

6. We compute the potential in the transformed domain:

$$\hat{\phi}_k = \hat{G}_k^{\text{int}}\hat{\rho}_k \quad \text{for } k \in [0, 2N] \tag{14.50}$$

7. We inverse-transform:

$$\phi_{2LR}(x_n) = \text{DFT}_{2N}^{-1}\{\hat{\phi}_k\} \tag{14.51}$$

which provides the physical potential in the range $[0, L]$:

$$\phi(x_n) = \phi_{2LR}(x_n) \quad \text{for } x_n \in [0, L] \tag{14.52}$$

14.3   Extension to multiple dimensions

The procedure described above can be extended to multiple dimensions by applying the same reasoning for all coordinates. This gives the following procedure:

1. We compute the Integrated Green function at the grid points in the volume $[0, L_x] \times [0, L_y] \times [0, L_z]$:

$$G_{2LR}^{\text{int}}(x_{n_x}, y_{n_y}, z_{n_z}) = \int_{x_{n_x} - \frac{h_x}{2}}^{x_{n_x} + \frac{h_x}{2}} dx \int_{y_{n_y} - \frac{h_y}{2}}^{y_{n_y} + \frac{h_y}{2}} dy \int_{z_{n_z} - \frac{h_z}{2}}^{z_{n_z} + \frac{h_z}{2}} dz\, G(x, y, z) \tag{14.53}$$

2. We extend to the region $[0, 2L_x] \times [0, 2L_y] \times [0, 2L_z]$ using the fact that:

$$G_{2LR}^{\text{int}}(x_n, y_n, z_n) = G_{2LR}^{\text{int}}(x_n - 2L_x, y_n, z_n) = G_{2LR}^{\text{int}}(2L_x - x_n, y_n, z_n)$$
$$\text{for } x_n \in [L_x, 2L_x], y_n \in [0, 2L_y], z_n \in [0, 2L_z] \tag{14.54}$$

$$G_{2LR}^{\text{int}}(x_n, y_n, z_n) = G_{2LR}^{\text{int}}(x_n, y_n - 2L_y, z_n) = G_{2LR}^{\text{int}}(x_n, 2L_y - y_n, z_n)$$
$$\text{for } y_n \in [L_y, 2L_y], x_n \in [0, 2L_x], z_n \in [0, 2L_z] \tag{14.55}$$

$$G_{2LR}^{\text{int}}(x_n, y_n, z_n) = G_{2LR}^{\text{int}}(x_n, y_n, z_n - 2L_z) = G_{2LR}^{\text{int}}(x_n, y_n, 2L_z - z_n)$$
$$\text{for } z_n \in [L_z, 2L_z], x_n \in [0, 2L_x], y_n \in [0, 2L_y] \tag{14.56}$$

This allows reusing the values computed at the previous step.

3. We transform it:

$$\hat{G}_{k_x k_y k_z}^{\text{int}} = \text{DFT}_{2N_x 2N_y 2N_z}\{G_{2LR}(x_n, y_n, z_n)\} \tag{14.57}$$

4. We assume that we are given $\rho(x_n, y_n, z_n)$ in the region $[0, L_x] \times [0, L_y] \times [0, L_z]$. From this we can obtain $\rho_{2LR}(x_n)$ over the region $[0, 2L_x] \times [0, 2L_y] \times [0, 2L_z]$ simply extending the matrix with zeros (see Eq. (14.23)).

5. We transform it:

$$\hat{\rho}_{k_x k_y k_z}^{\text{int}} = \text{DFT}_{2N_x 2N_y 2N_z}\{\rho_{2LR}(x_n, y_n, z_n)\} \tag{14.58}$$

6. We compute the potential in the transformed domain:

$$\hat{\phi}_{k_x k_y k_z} = \hat{G}^{\text{int}}_{k_x k_y k_z} \, \hat{\rho}_{k_x k_y k_z} \quad \text{for } k_{x/y/z} \in [0, 2N_{x/y/z}] \tag{14.59}$$

7. We inverse-transform:

$$\phi_{2LR}(x_n, y_n, z_n) = \text{DFT}^{-1}_{2N_x 2N_y 2N_z} \left\{ \hat{\phi}_{k_x k_y k_z} \right\} \tag{14.60}$$

which provides the physical potential in the region $[0, L_x] \times [0, L_y] \times [0, L_z]$:

$$\phi(x_n, y_n, z_n) = \phi_{2LR}(x_n, y_n, z_n) \text{ for } (x_n, y_n, z_n) \in [0, L_x] \times [0, L_y] \times [0, L_z] \tag{14.61}$$

14.4 Green functions for 2D and 3D Poisson problems

3D Poisson problem, free space boundary conditions

For the equation:

$$\nabla^2 \phi(x, y, z) = -\frac{1}{\varepsilon_0} \rho(x, y, z) \tag{14.62}$$

where:

$$\nabla = \left(\frac{\partial}{\partial x}, \frac{\partial}{\partial y}, \frac{\partial}{\partial z} \right) \tag{14.63}$$

the solution can be written as

$$\phi(x, y, z) = \iiint_{-\infty}^{+\infty} \rho(x', y', z') \, G(x - x', y - y', z - z') \, dx' \, dy' \, dz' \tag{14.64}$$

where:

$$G(x, y, z) = \frac{1}{4\pi\varepsilon_0} \frac{1}{\sqrt{x^2 + y^2 + z^2}} \tag{14.65}$$

The corresponding integrated Green function [69]. can be written as:

$$G_{2LR}^{int}(x_{n_x}, y_{n_y}, z_{n_z}) = \int_{x_{n_x}-\frac{h_x}{2}}^{x_{n_x}+\frac{h_x}{2}} dx \int_{y_{n_y}-\frac{h_y}{2}}^{y_{n_y}+\frac{h_y}{2}} dy \int_{z_{n_z}-\frac{h_z}{2}}^{x_{n_z}+\frac{h_z}{2}} dz \, G(x,y,z) \tag{14.66}$$

$$= + F\left(x_{n_x} + \frac{h_x}{2}, y_{n_x} + \frac{h_y}{2}, z_{n_x} + \frac{h_z}{2}\right) \tag{14.67}$$

$$- F\left(x_{n_x} + \frac{h_x}{2}, y_{n_x} + \frac{h_y}{2}, z_{n_x} - \frac{h_z}{2}\right) \tag{14.68}$$

$$- F\left(x_{n_x} + \frac{h_x}{2}, y_{n_x} - \frac{h_y}{2}, z_{n_x} + \frac{h_z}{2}\right) \tag{14.69}$$

$$+ F\left(x_{n_x} + \frac{h_x}{2}, y_{n_x} - \frac{h_y}{2}, z_{n_x} - \frac{h_z}{2}\right) \tag{14.70}$$

$$- F\left(x_{n_x} - \frac{h_x}{2}, y_{n_x} + \frac{h_y}{2}, z_{n_x} + \frac{h_z}{2}\right) \tag{14.71}$$

$$+ F\left(x_{n_x} - \frac{h_x}{2}, y_{n_x} + \frac{h_y}{2}, z_{n_x} - \frac{h_z}{2}\right) \tag{14.72}$$

$$+ F\left(x_{n_x} - \frac{h_x}{2}, y_{n_x} - \frac{h_y}{2}, z_{n_x} + \frac{h_z}{2}\right) \tag{14.73}$$

$$- F\left(x_{n_x} - \frac{h_x}{2}, y_{n_x} - \frac{h_y}{2}, z_{n_x} - \frac{h_z}{2}\right) \tag{14.74}$$

where $F(x,y,z)$ is a primitive of $G(x,y,z)$, which can be obtained as:

$$F(x,y,z) = \int_{x_0}^{x} dx \int_{y_0}^{y} dy \int_{z_0}^{x} dz \, G(x,y,z) \tag{14.75}$$

with (x_0, y_0, z_0) being an arbitrary starting point.
An expression for $F(x,y,z)$ is the following

$$F(x,y,z) = \frac{1}{4\pi\varepsilon_0} \iiint \frac{1}{\sqrt{x^2 + y^2 + z^2}} dx dy dz \tag{14.76}$$

$$= \frac{1}{4\pi\varepsilon_0}\left[-\frac{z^2}{2}\arctan\left(\frac{xy}{z\sqrt{x^2+y^2+z^2}}\right) - \frac{y^2}{2}\arctan\left(\frac{xz}{y\sqrt{x^2+y^2+z^2}}\right)\right. \tag{14.77}$$

$$- \frac{x^2}{2}\arctan\left(\frac{yz}{x\sqrt{x^2+y^2+z^2}}\right) + yz\ln\left(x + \sqrt{x^2+y^2+z^2}\right) \tag{14.78}$$

$$\left. + xz\ln\left(y + \sqrt{x^2+y^2+z^2}\right) + xy\ln\left(z + \sqrt{x^2+y^2+z^2}\right)\right] \tag{14.79}$$

Note that we need to choose the first cell center to be in (0,0,0) for evaluation of the integrated Green function. Therefore the cell edges have non zero coordinates and the denominators in the formula will always be non-vanishing.

2D Poisson problem, free space boundary conditions

For the equation:

$$\nabla_\perp^2 \phi(x, y) = -\frac{1}{\varepsilon_0}\rho(x, y) \tag{14.80}$$

where:

$$\nabla = \left(\frac{\partial}{\partial x}, \frac{\partial}{\partial y} \right) \tag{14.81}$$

the solution can be written as

$$\phi(x, y) = \iiint_{-\infty}^{+\infty} \rho(x', y')\, G(x - x', y - y')\, dx'\, dy' \tag{14.82}$$

where:

$$G(x, y) = -\frac{1}{4\pi\varepsilon_0} \log\left(\frac{x^2 + y^2}{r_0^2} \right) \tag{14.83}$$

where r_0 is arbitrary constant which has no effect on the evaluated fields (changes the potential by an additive constant).

The corresponding integrated Green function can be written as:

$$G_{2LR}^{\text{int}}(x_{n_x}, y_{n_y}) = \int_{x_{n_x} - \frac{h_x}{2}}^{x_{n_x} + \frac{h_x}{2}} dx \int_{y_{n_y} - \frac{h_y}{2}}^{y_{n_y} + \frac{h_y}{2}} dy\, G(x, y, z) \tag{14.84}$$

$$= + F\left(x_{n_x} + \frac{h_x}{2}, y_{n_x} + \frac{h_y}{2} \right) \tag{14.85}$$

$$- F\left(x_{n_x} + \frac{h_x}{2}, y_{n_x} - \frac{h_y}{2} \right) \tag{14.86}$$

$$- F\left(x_{n_x} - \frac{h_x}{2}, y_{n_x} + \frac{h_y}{2} \right) \tag{14.87}$$

$$+ F\left(x_{n_x} - \frac{h_x}{2}, y_{n_x} - \frac{h_y}{2} \right) \tag{14.88}$$

where $F(x, y)$ is a primitive of $G(x, y)$, which can be obtained as:

$$F(x, y) = \int_{x_0}^{x} dx \int_{y_0}^{y} dy\, G(x, y) \tag{14.89}$$

where (x_0, y_0) is an arbitrary starting point.

An expression for $F(x, y)$ is the following (where we have chosen $r_0 = 1$):

$$F(x, y) = -\frac{1}{4\pi\varepsilon_0} \iint \ln\left(x^2 + y^2 \right) dx/, dy \tag{14.90}$$

$$= \frac{1}{4\pi\varepsilon_0} \left[3xy - x^2 \arctan(y/x) - y^2 \arctan(x/y) - xy \ln\left(x^2 + y^2 \right) \right] \tag{14.91}$$

Note that we need to choose the first cell center to be in (0,0) for evaluation of the integrated Green function. Therefore the cell edges have non zero coordinates and the denominators in the formula will always be non-vanishing.

14.5   Generalization to observation interval different from source interval

The potential generated by a source $\rho(x)$ can be written as the convolution of a Green function with the charge distribution:

$$\phi(x) = \int_{-\infty}^{+\infty} \rho(x')\, G(x - x')dx' \tag{14.92}$$

We assume that the source is limited to the region $[a, b]$:

$$\rho(x) = \rho(x)\, \Pi_{[a,b]}(x) \tag{14.93}$$

where $\Pi_{[a,b]}(x)$ is a rectangular window function defined as:

$$\Pi_{[a,b]}(x) = \begin{cases} 1 & \text{for } x \in [a, b] \\ 0 & \text{elsewhere} \end{cases} \tag{14.94}$$

We are interested in the electric potential in a given region $[c, d]$, so we can compute:

$$\phi_{cd}(x) = \phi(x)\Pi_{[c,d]}(x) \tag{14.95}$$

We combine Eqs. (14.93), (14.95) and (14.92), obtaining:

$$\phi_{cd}(x) = \Pi_{[c,d]}(x) \int_{-\infty}^{+\infty} \Pi_{[a,b]}(x')\, \rho(x')\, G(x - x')dx' \tag{14.96}$$

We apply the change of variable $x'' = x - x'$:

$$\phi_{cd}(x) = \int_{-\infty}^{+\infty} \Pi_{[c,d]}(x)\, \Pi_{[a,b]}(x - x'')\, \rho(x - x'')\, G(x'')\, dx'' \tag{14.97}$$

The integrand vanishes outside the set of the (x, x'') defined by the two window functions:

$$\begin{cases} c < x < d \\ a < (x - x'') < b \end{cases} \tag{14.98}$$

We flip the signs in the second equation, obtaining:

$$\begin{cases} c < x < d \\ -b < (x'' - x) < -a \end{cases} \tag{14.99}$$

Combining the two equations we obtain:

$$c - b < -b + x < x'' < -a + x < d - a \tag{14.100}$$

i.e. the integrand is not zero for $c - b < x'' < d - a$. Therefore in Eq. (14.97) we can replace $G(x'')$ with its truncated version:

$$G_{\text{tr}}(x'') = G(x'')\, \Pi_{[c-b,\, d-a]}(x'') \tag{14.101}$$

obtaining:

$$\phi_{cd}(x) = \int_{-\infty}^{+\infty} \Pi_{[c,d]}(x) \, \Pi_{[a,b]}\left(x - x''\right) \rho(x - x'') \, G_{\text{tr}}(x'')dx'' \tag{14.102}$$

We can go back to the initial coordinate by substituting $x'' = x - x'$:

$$\phi_{cd}(x) = \Pi_{[c,d]}(x) \int_{-\infty}^{+\infty} \rho(x') \, G_{\text{tr}}(x - x')dx' \tag{14.103}$$

We call:

$$L_1 = b - a \tag{14.104}$$
$$L_2 = d - c \tag{14.105}$$

The measure of the set on which $G_{\text{tr}}(x'')$ is non zero is

$$(d - a) - (c - b) = L_1 + L_2 \tag{14.106}$$

We define L such that:

$$L_1 + L_2 = 2L \tag{14.107}$$

Since the two window functions in Eq. 14.102 force the integrand to zero outside the region $c - b < x'' < d - a$ of measure $2L$, we can replace $G_{\text{tr}}(x'')$ with its replicated version:

$$G_R(x'') = \sum_{n=-\infty}^{+\infty} G_{\text{tr}}(x'' - 2nL) = \sum_{n=-\infty}^{+\infty} G(x'' - 2nL) \, \Pi_{[c-b,\, d-a]}\left(x'' - 2nL\right) \tag{14.108}$$

obtaining:

$$\phi_{cd}(x) = \int_{-\infty}^{+\infty} \Pi_{[c,d]}(x) \, \Pi_{[a,b]}\left(x - x''\right) \rho(x - x'') \, G_R(x'')dx'' \tag{14.109}$$

We can go back to the initial coordinate by substituting $x'' = x - x'$:

$$\phi_{cd}(x) = \Pi_{[c,d]}(x) \int_{-\infty}^{+\infty} \rho(x') \, G_R(x - x')dx' \tag{14.110}$$

This is a cyclic convolution, so we can proceed as follows. We split the integral:

$$\phi_{cd}(x) = \Pi_{[c,d]}(x) \sum_{n=-\infty}^{+\infty} \int_{2nL}^{2(n+1)L} \rho(x') \, G_R(x - x') \, dx' \tag{14.111}$$

In each term we replace $x''' = x' + 2nL$:

$$\phi_{cd}(x) = \Pi_{[c,d]}(x) \sum_{n=-\infty}^{+\infty} \int_{0}^{2L} \rho(x''' - 2nL) \, G_R(x - x''' - 2nL) \, dx''' \tag{14.112}$$

We use the fact that $G_R(x)$ is periodic:

$$\phi_{cd}(x) = \Pi_{[c,d]}(x) \sum_{n=-\infty}^{+\infty} \int_0^{2L} \rho(x''' - 2nL)\, G_R(x - x''')dx'''$$

(14.113)

$$= \Pi_{[c,d]}(x) \int_0^{2L} G_R(x - x''') \sum_{n=-\infty}^{+\infty} \rho(x''' - 2nL)\, dx'''$$

We can define a replicated version of $\rho(x)$:

$$\rho_R(x) = \sum_{n=-\infty}^{+\infty} \rho(x - 2nL) \tag{14.114}$$

We obtain:

$$\phi_{cd}(x) = \Pi_{[c,d]}(x) \int_0^{2L} \rho_R(x')\, G_R(x - x')dx' \tag{14.115}$$

The function:

$$\phi_R(x) = \int_0^{2L} \rho_R(x')\, G_R(x - x')dx' \tag{14.116}$$

is periodic of period $2L$. Replacing in Eq. 14.115 we see that the potential of interest can be simply calculated by selecting the right interval $[c, d]$:

$$\phi_{cd}(x) = \Pi_{[c,d]}(x)\, \phi_R(x) \tag{14.117}$$

To compute the convolution in Eq. 14.116 we expand $\phi_R(x)$ in a Fourier series starting from $x = c$:

$$\phi_R(x) = \sum_{k=-\infty}^{+\infty} \tilde{\phi}_k\, e^{j2\pi k \frac{x}{2L}} \tag{14.118}$$

where the Fourier coefficients are given by:

$$\tilde{\phi}_k = \frac{1}{2L} \int_0^{2L} \phi_R(x)\, e^{-j2\pi k \frac{x}{2L}}\, dx \tag{14.119}$$

We replace Eq. (14.116) into Eq. (14.119) obtaining:

$$\tilde{\phi}_k = \frac{1}{2L} \int_0^{2L} \int_0^{2L} \rho_R(x')\, G_R(x - x')\, e^{-j2\pi k \frac{x}{2L}}\, dx'\, dx \tag{14.120}$$

With the change of variable $x'' = x - x'$ we obtain:

$$\tilde{\phi}_k = \frac{1}{2L} \int_0^{2L} \rho_R(x')e^{-j2\pi k \frac{x'}{2L}}dx' \int_0^{2L} G_R(x'')e^{-j2\pi k \frac{x''}{2L}}\, dx'' \tag{14.121}$$

where we recognize the Fourier coefficients of $\rho_R(x)$ and $G_R(x)$:

$$\tilde{\rho}_k = \frac{1}{2L} \int_0^{2L} \rho_R(x)\, e^{-j2\pi k \frac{x}{2L}}\, dx \tag{14.122}$$

$$\tilde{G}_k = \frac{1}{2L} \int_0^{2L} G_R(x)\, e^{-j2\pi k \frac{x}{2L}}\, dx \tag{14.123}$$

obtaining simply:

$$\tilde{\phi}_k = 2L\,\tilde{G}_k\,\tilde{\rho}_k \tag{14.124}$$

We assume to have the functions $\rho_R(x)$ and $G_R(x)$ sampled (or averaged) with step:

$$h_x = \frac{2L}{M} \tag{14.125}$$

We assume that all intervals have size multiple of h_x. So we can define:

$$N_1 = L_1/h_x \tag{14.126}$$
$$N_2 = L_2/h_x \tag{14.127}$$

We call:

$$\rho_{Rn} = \rho_R\left(a + nh_x\right) \tag{14.128}$$
$$\phi_{Rn} = \phi_R\left(c + nh_x\right) \tag{14.129}$$
$$G_{Rn} = G_R\left(c - b + nh_x\right) \tag{14.130}$$

By construction in the range $0 \le n < M$:

$$\rho_{Rn} \equiv \rho_n = \begin{cases} \rho\left(a + nh_x\right) & \text{for } 0 \le n < N_1 \\ 0 & \text{for } N_1 \le n < M \end{cases} \tag{14.131}$$

$$G_{Rn} \equiv G_n = G\left(c - b + nh_x\right) \quad \text{for } 0 \le n < M \tag{14.132}$$

We can approximate the integral as follows:

$$\tilde{\rho}_k = \frac{1}{2L}\int_0^{2L} \rho_R(x)\,e^{-j2\pi k\frac{x}{2L}}\,dx = \frac{1}{2L}\int_a^{a+2L} \rho_R(x)\,e^{-j2\pi k\frac{x}{2L}}\,dx \tag{14.133}$$

$$\simeq \frac{h_x}{2L}\sum_{n=0}^{M-1} \rho_R(a + nh_x)\,e^{-j2\pi k\frac{a+nh_x}{2L}} = e^{-j2\pi k\frac{a}{2L}}\frac{1}{M}\sum_{n=0}^{M-1} \rho_{Rn}e^{-j2\pi\frac{kn}{M}} \tag{14.134}$$

We recognize the Discrete Fourier Transform:

$$\tilde{\rho}_k = e^{-j2\pi k\frac{a}{2L}}\frac{1}{M}\text{DFT}_M\left\{\rho_{Rn}\right\} = e^{-j2\pi k\frac{a}{2L}}\frac{1}{M}\hat{\rho}_k \tag{14.135}$$

and similarly we can obtain

$$\tilde{\phi}_k = e^{-j2\pi k\frac{c}{2L}}\frac{1}{M}\text{DFT}_M\left\{\phi_{Rn}\right\} = e^{-j2\pi k\frac{c}{2L}}\frac{1}{M}\hat{\phi}_k \tag{14.136}$$

$$\tilde{G}_k = e^{-j2\pi k\frac{c-b}{2L}}\frac{1}{M}\text{DFT}_M\left\{G_{Rn}\right\} = e^{-j2\pi k\frac{c-b}{2L}}\frac{1}{M}\hat{G}_k \tag{14.137}$$

Replacing in Eq. 14.124 we obtain

$$\hat{\phi}_k = h_x e^{j2\pi k\frac{b-a}{2L}}\hat{\rho}_k\hat{G}_k = h_x e^{j2\pi k\frac{N_1}{M}}\hat{\rho}_k\hat{G}_k \tag{14.138}$$

14.6   Compressed FFT convolution

We assume that the source has the form

$$\rho(x) = \sum_{j=A}^{B-1} \rho_j^{\text{loc}}(x - jP) \tag{14.139}$$

where $\rho_j^{\text{loc}}(x)$ is limited to the interval $[a, b]$.
We are interested in the potential in a set of intervals given by:

$$[c + iP, \, d + iP] \quad \text{for } i = C, ..., D - 1 \tag{14.140}$$

The contribution of the j-th term of ρ to ϕ int the i-th interval:

$$\phi_{ij}(x) = \int_{-\infty}^{+\infty} \rho_j^{\text{loc}}(x' - jP) \, G_{i-j}^{\text{tr}}(x - x')dx' \tag{14.141}$$

where:

$$G_l^{\text{tr}}(x'') = G(x'') \, \Pi_{[c-b+lP, \, d-a+lP]}(x'') \tag{14.142}$$

We define a local version of G^{tr} as

$$G_l^{\text{tr, loc}}(x) = G_l^{\text{tr}}(x + lP) = G(x + lP) \, \Pi_{[c-b, \, d-a]}(x) \tag{14.143}$$

obtaining:

$$\phi_{ij}(x) = \int_{-\infty}^{+\infty} \rho_j^{\text{loc}}(x' - jP) \, G_{i-j}^{\text{tr, loc}}(x - x' - (i - j)P)dx' \tag{14.144}$$

We replace $x' = x' - jP$:

$$\phi_{ij}(x) = \int_{-\infty}^{+\infty} \rho_j^{\text{loc}}(x') \, G_{i-j}^{\text{tr, loc}}(x - x' - iP)dx' \tag{14.145}$$

We define a local version of ϕ:

$$\phi_{ij}^{\text{loc}}(x) = \phi_{ij}(x + iP) \tag{14.146}$$

obtaining:

$$\phi_{ij}^{\text{loc}}(x) = \int_{-\infty}^{+\infty} \rho_j^{\text{loc}}(x') \, G_{i-j}^{\text{tr, loc}}(x - x')dx' \tag{14.147}$$

I explicit all the pies:

$$\phi_{ij}^{\text{loc}}(x) = \int_{-\infty}^{+\infty} \Pi_{[a,b]}(x')\Pi_{[c-b, \, d-a]}(x - x')\rho_j^{\text{loc}}(x') \, G_{i-j}^{\text{tr, loc}}(x - x')dx' \tag{14.148}$$

Again, we want to find the region in x where this is non-zero:

$$a < x' < b \tag{14.149}$$

$$c - b < x - x' < d - a \tag{14.150}$$

from which:

$$c - b + x' < x < d - a + x' \tag{14.151}$$
$$c - b + a < x < d - a + b \tag{14.152}$$

So we find that $\phi_{ij}^{\text{loc}}(x)$ is non-zero in the region:

$$c - L_1 < x < d + L_1 \tag{14.153}$$

The total potential in the i-th interval of interest:

$$\phi_i^{\text{loc}}(x) = \sum_{j=A}^{B-1} \phi_{ij}^{\text{loc}}(x) = \sum_{j=A}^{B-1} \int_{-\infty}^{+\infty} \rho_j^{\text{loc}}(x') \, G_{i-j}^{\text{tr, loc}}(x - x') dx' \tag{14.154}$$

Since all terms in the sum are zero outside the region defined by Eq. 14.153 also $\phi_i^{\text{loc}}(x)$ is zero outside the same interval, which is larger by $2L_1$ compared to the set of interest $[c, d]$.
We build:

$$G^{\text{aux}}(x) = \sum_{l=C-B+1}^{D-A-1} G_l^{\text{tr, loc}}(x - lL_{\text{aux}}) \tag{14.155}$$

where:

$$L_{\text{aux}} = L_1 + L_2 \tag{14.156}$$

and

$$\rho^{\text{aux}}(x) = \sum_{j=A}^{B-1} \rho_j^{\text{loc}}(x - jL_{\text{aux}}) \tag{14.157}$$

and we define

$$\phi^{\text{aux}}(x) = \int_{-\infty}^{+\infty} \rho^{\text{aux}}(x') \, G^{\text{aux}}(x - x') dx' \tag{14.158}$$

We extract a segment of it:

$$\phi_i^{\text{aux, loc}}(x) = \phi^{\text{aux}}(x + iL_{\text{aux}}) \Pi_{[c,d]}(x) \tag{14.159}$$

We replace Eq. 14.155:

$$\phi_i^{\text{aux, loc}}(x) = \Pi_{[c,d]}(x) \int_{-\infty}^{+\infty} \rho^{\text{aux}}(x') \, G^{\text{aux}}(x - x' + iL_{\text{aux}}) dx' \tag{14.160}$$

We replace Eq. 14.157 and Eq. 14.155:

$$\phi_i^{\text{aux, loc}}(x) = \Pi_{[c,d]}(x) \int_{-\infty}^{+\infty} \sum_{j=A}^{B-1} \rho_j^{\text{loc}}(x' - jL_{\text{aux}}) \sum_{l=C-B+1}^{D-A-1} G_l^{\text{tr, loc}}(x - x' + (i - l)L_{\text{aux}}) dx' \tag{14.161}$$

$$= \Pi_{[c,d]}(x) \sum_{l=C-B+1}^{D-A-1} \sum_{j=A}^{B-1} \int_{-\infty}^{+\infty} \rho_j^{\text{loc}}(x' - jL_{\text{aux}}) \, G_l^{\text{tr, loc}}(x - x' + (i - l)L_{\text{aux}}) dx' \tag{14.162}$$

We change variable $x'' = x' - (i - l)L_{\text{aux}}$

$$\phi_i^{\text{aux, loc}}(x) = \sum_{l=C-B+1}^{D-A-1} \sum_{j=A}^{B-1} \int_{-\infty}^{+\infty} \Pi_{[c,d]}(x)\rho_j^{\text{loc}}(x'' + (i-l-j)L_{\text{aux}}) \, G_l^{\text{tr, loc}}(x - x'')dx''$$

(14.163)

The integrand is nonzero for:

$$c < x < d \tag{14.164}$$
$$a < x'' + (i-l-j)L_{\text{aux}}) < b \tag{14.165}$$
$$c - b < x - x'' < d - a \tag{14.166}$$

I subtract the first and the last:

$$a < x'' + (i-l-j)L_{\text{aux}}) < b \tag{14.167}$$
$$-b < -x'' < -a \tag{14.168}$$

I flip the last

$$a < x'' + (i-l-j)L_{\text{aux}}) < b \tag{14.169}$$
$$a < x'' < b \tag{14.170}$$

The two are compatible only if

$$l = i - j \tag{14.171}$$

This means that in the double sum only the terms satisfying Eq. 14.171 are nonzero, hence:

$$\phi_i^{\text{aux, loc}}(x) = \Pi_{[c,d]}(x) \sum_{j=A}^{B-1} \int_{-\infty}^{+\infty} \rho_j^{\text{loc}}(x''+) \, G_{i-j}^{\text{tr, loc}}(x - x'')dx'' \tag{14.172}$$

Comparing against Eq. 14.154 we find:

$$\Pi_{[c,d]}(x)\phi_i^{\text{aux, loc}}(x) = \Pi_{[c,d]}(x)\phi_i^{\text{loc}}(x) \tag{14.173}$$

Using Eq. 14.159 we obtain:

$$\Pi_{[c,d]}(x)\phi_i^{\text{loc}}(x) = \Pi_{[c,d]}(x)\phi^{\text{aux}}(x + iL_{\text{aux}}) \tag{14.174}$$

To compute the convolution in Eq. 14.158 we can use the results from the previous section.
We call:

$$N_S = B - A \tag{14.175}$$
$$N_T = D - C \tag{14.176}$$
$$\tag{14.177}$$

The support of $\rho^{\text{aux}}(x)$ is:

$$[a + AL_{\text{aux}}, a + BL_{\text{aux}}] \text{ having size } N_S L_{\text{aux}} \tag{14.178}$$

The support of $G^{\text{aux}}(x)$ is:

$$[c - b + (C - B + 1)L_{\text{aux}}, c - b + (D - A)L_{\text{aux}}] \text{ having size } (N_S + N_T - 1)L_{\text{aux}} \tag{14.179}$$

Using a sampling step h_x, we can define:

$$N_1 = L_1/h_x \tag{14.180}$$
$$N_2 = L_2/h_x \tag{14.181}$$
$$N_{\text{aux}} = L_{\text{aux}}/h_x = N_1 + N_2 \tag{14.182}$$

The number of samples in the support of $G^{\text{aux}}(x)$ is

$$M_{\text{aux}} = (N_S + N_T - 1)N_{\text{aux}} \tag{14.183}$$

We define

$$G_m^{\text{aux}} = G^{\text{aux}}\left(c - b + (C - B + 1)L_{\text{aux}} + mh_x\right) \text{ for } 0 \le m < M_{\text{aux}} \tag{14.184}$$

Replacing Eq. 14.155:

$$G_m^{\text{aux}} = \sum_{l=C-B+1}^{D-A-1} G_l^{\text{tr, loc}}\left(c - b + (C - B + 1)L_{\text{aux}} + mh_x - lL_{\text{aux}}\right) \tag{14.185}$$

$$= \sum_{l=C-B+1}^{D-A-1} G\left(c - b + (C - B + 1)L_{\text{aux}} + lP + h_x(m - lN_{\text{aux}})\right) \times \tag{14.186}$$

$$\Pi_{[c-b,\, d-a]}\left(c - b + (C - B + 1)L_{\text{aux}} + h_x(m - lN_{\text{aux}})\right) \tag{14.187}$$

We define:

$$G_{l,n}^{\text{segm}} = G\left(c - b + (C - B + 1)L_{\text{aux}} + lP + nh_x\right)\Pi_{[c-b,\, d-a]}\left(c - b + (C - B + 1)L_{\text{aux}} + nh_x\right)$$
$$\text{for } 0 \le n < N_{\text{aux}} \text{ and } (C - B + 1) \le l < (D - A) \tag{14.188}$$

So we can write:

$$G_m^{\text{aux}} = \sum_{l=C-B+1}^{D-A-1} G_{l,m-lN_{\text{aux}}}^{\text{segm}} \tag{14.189}$$

We define:

$$\rho_m^{\text{aux}} = \begin{cases} \rho^{\text{aux}}\left(a + AL_{\text{aux}} + mh_x\right) & \text{for } 0 \le m < N_S N_{\text{aux}} \\ 0 & \text{for } N_S N_{\text{aux}} \le m < M_{\text{aux}} \end{cases} \tag{14.190}$$

We can use the result from before linking the DFTs of these sequences:

$$\hat{\phi}_k^{\text{aux}} = h_x e^{j2\pi k \frac{(B-A-1)L_{\text{aux}}+(b-a)}{(N_S+N_T-1)L_{\text{aux}}}} = h_x e^{j2\pi k \frac{(N_S-1)N_{\text{aux}}+N_1}{(N_S+N_T-1)N_{\text{aux}}}} \hat{\rho}_k^{\text{aux}} \hat{G}_k^{\text{aux}} \tag{14.191}$$

The inverse DFT of $\hat{\phi}_k^{\text{aux}}$ provides:

$$\phi_m^{\text{aux}} = \phi^{\text{aux}}\left(c + CL_{\text{aux}} + mh_x\right) \quad \text{for } 0 \le m < N_T N_{\text{aux}} \tag{14.192}$$

Bibliography

[1] MAD-X Project website. `http://cern.ch/madx`.

[2] F. C. Iselin. The mad program (methodical accelerator design) - physics methods manual. Technical Report CERN/SL/92-?? (AP), CERN, 1992.

[3] F. Schmidt. SIXTRACK: Single particle tracking code treating transverse motion with synchrotron oscillations in a symplectic manner. Technical Report 94-56, CERN, 1994.

[4] G. Ripken. Non-linear canonical equations of coupled synchro-betatron motion and their solutions within the framework of a non-linear six-dimensional (symplectic) tracking program for ultrarelativistic protons. Technical Report 85-084, DESY, 1985.

[5] D.P. Barber, G. Ripken, and F. Schmidt. A non-linear canonical formalism for the coupled synchro-betatron motion of protons with arbitrary energy. Technical Report 87-36, DESY, 1987.

[6] G. Ripken and F. Schmidt. A symplectic six-dimensional thin-lens formalism for tracking. Technical Report DESY 95-63 and CERN/SL/95-12(AP), DESY, CERN, 1995.

[7] K. Heinemann, G. Ripken, and F. Schmidt. Construction of nonlinear symplectic six-dimensional thin-lens maps by exponentiation. Technical Report 95-189, DESY, 1995.

[8] D.P. Barber, K. Heinemann, G. Ripken, and F. Schmidt. Symplectic thin-lens transfer maps for SIXTRACK: Treatment of bending magnets in terms of the exact hamiltonian. Technical Report 96-156, DESY, 1996.

[9] L.H.A. Leunissen, F. Schmidt, and G. Ripken. 6D beam-beam kick including coupled motion. Technical report, 2001.

[10] A. Latina and R. De Maria. RF multipole implementation. Technical report, CERN-ATS. 2012-088.

[11] E. Forest. *Beam Dynamics: A New Attitude and Framework.* Harcourt Academic Publisher, 1999.

[12] Andrzej Wolski. *Beam dynamics in high energy particle accelerators.* World Scientific, 2014.

[13] R Talman. Representation of thick quadrupoles by thin lenses. Technical report, Lawrence Berkeley Nat. Lab., Berkeley, CA, 1985.

[14] Helmut Burkhardt, Riccardo De Maria, Massimo Giovannozzi, and Thys Risse-lada. Improved TEAPOT Method and Tracking with Thick Quadrupoles for the LHC and its Upgrade. page MOPWO027, 2013.

[15] Haruo Yoshida. Construction of higher order symplectic integrators. *Physics Letters A*, 150(5):262–268, 1990.

[16] Étienne Forest, Simon C. Leemann, and Frank Schmidt. Fringe Effects in MAD PART I, Second Order Fringe in MAD-X for the Module PTC. *KEK-PREPRINT-2005-109, https://cds.cern.ch/record/2857004.*

[17] Silke Van Der Schueren. Impact of fringe fields on beam dynamics. *ABP-CAP Section Meeting, CERN, 4 Jul 2025, https://indico.cern.ch/event/1533185/*, 2025.

[18] Silke Van Der Schueren. Dipole fringing fields. *Meeting on fringe fields, CERN, 30 Sept 2024, https://indico.cern.ch/event/1462429*, 2025.

[19] Helmut Poth. Electron cooling: theory, experiment, application. *Physics reports*, 196(3-4):135–297, 1990.

[20] F. Willeke and G. Ripken. Methods of beam optics. Technical Report 88-114, DESY, 1988.

[21] Y. Luo, P. Cameron, S. Peggs, and D. Trbojevic. Possible phase loop for the global betatron decoupling. Technical Report CAD/AP/174, Brookhaven National Laboratory, Upton, NY 11973, USA, October 4 2004.

[22] Rhodri Jones. Measuring Tune, Chromaticity and Coupling. 5 2020.

[23] Eirik Jaccheri Hoydalsvik, Tobias Hakan Bjorn Persson, and Rogelio Tomas Garcia. Evaluation of the closest tune approach and its MAD-X implementation. 2021.

[24] Laurent Deniau. Linear coupling treatment in MAD-X. *Presentation at ABP-HSS meeting, CERN, 25 Oct 2017, https://indico.cern.ch/event/672801/.*

[25] Laurent Deniau. Linear coupling treatment in MAD-X: part 2. *Presentation at ABP-HSS meeting, CERN, 22 Nov 2017, https://indico.cern.ch/event/679893/.*

[26] A. Franchi, L. Farvacque, F. Ewald, G. Le Bec, and K. B. Scheidt. First simultaneous measurement of sextupolar and octupolar resonance driving terms in a circular accelerator from turn-by-turn beam position monitor data. *Phys. Rev. ST Accel. Beams*, 17:074001, Jul 2014.

[27] Andrea Franchi, Simone Maria Liuzzo, and Zeus Marti. Analytic formulas for the rapid evaluation of the orbit response matrix and chromatic functions from lattice parameters in circular accelerators, 2023.

[28] Albert Hofmann. *The Physics of Synchrotron Radiation*. Cambridge Monographs on Particle Physics, Nuclear Physics and Cosmology. Cambridge University Press, 2004.

[29] H Burkhardt. Monte Carlo generator for synchrotron radiation. Technical report, CERN, Geneva, 1990.

[30] Alexander W. Chao. Evaluation of beam distribution parameters in an electron storage ring. *Journal of Applied Physics*, 50(2):595–598, 07 2008.

[31] Georg H. Hoffstaetter. *High-Energy Polarized Proton Beams: A Modern View*, volume 218 of *Springer Tracts in Modern Physics*. Springer, Berlin, Heidelberg, 2006.

[32] David C. Sagan. *Bmad Reference Manual*. Cornell Laboratory for Accelerator-Based Sciences and Education, 2025. Available at `https://www.classe.cornell.edu/bmad/`.

[33] A. W. Chao. Evaluation of Radiative Spin Polarization in an Electron Storage Ring. *Nucl. Instrum. Meth.*, 180:29, 1981.

[34] Ya. S. Derbenev and A. M. Kondratenko. Polarization kinematics of particles in storage rings. *Sov. Phys. JETP*, 37:968–973, 1973.

[35] Michael Boge. Analysis of spin depolarizing effects in electron storage rings. Other thesis, 5 1994.

[36] S. R. Mane. Electron Spin Polarization in High-Energy Storage Rings. 1. Derivation of the Equilibrium Polarization. *Phys. Rev. A*, 36:105–119, 1987.

[37] D. P. Barber and G. Ripken. Radiative polarization, computer algorithms and spin matching in electron storage rings. 7 1999.

[38] Zhe Duan, Mei Bai, Desmond P. Barber, and Qing Qin. A monte-carlo simulation of the equilibrium beam polarization in ultra-high energy electron (positron) storage rings. *Nuclear Instruments and Methods in Physics Research Section A: Accelerators, Spectrometers, Detectors and Associated Equipment*, 793:81–91, 2015.

[39] John David Jackson. *Classical Electrodynamics*. Wiley, New York, 3 edition, 1998.

[40] K Hirata, H Moshammer, and F Ruggiero. A Symplectic Beam-Beam Interaction with Energy Change. *SLAC-PUB-10055*, Dec 2017.

[41] Kohji Hirata. Don't be afraid of beam-beam interactions with a large crossing angle. Technical Report SLAC-PUB-6375, 1994.

[42] G Iadarola, R De Maria, and Y Papaphilippou. Modelling and implementation of the "6D" beam-beam interaction. *CERN-ACC- SLIDES-2018-001*, Dec 2017.

[43] SixTrack Project website. `http://cern.ch/sixtrack`.

[44] SixTrackLib source code repository. `http://github.com/SixTrack/SixTrackLib`.

[45] G Iadarola, R De Maria, and Y Papaphilippou. 6D beam-beam interaction step-by-step. *CERN-ACC-NOTE-2018-0023*, Dec 2017.

[46] W Herr and T Pieloni. Beam-Beam Effects. *in Proceedings of CAS - CERN Accelerator School: Advanced Accelerator Physics Course, 18 - 29 Aug 2013, Trondheim, Norway, CERN-2014-009*, 2014.

[47] Mad-X beam-beam macros, source code repository. `https://github.com/lhcopt/beambeam_macros`.

[48] D. Griffiths. *Introduction to elementary particles*. 2nd rev. version, Wiley, 2008.

[49] C. Weizsäcker. Ausstrahlung bei Stössen sehr schneller Elektronen. *in Zeitschrift Für Physik, vol. 88, Sep. 1934, pp. 612-625.* `https://doi.org/10.1007/BF01333110`.

[50] E. Williams. Correlation of certain collision problems with radiation theory. *in Kong. Dan. Vid. Sel. Mat. Fys. Med., vol. 13N4, 1935, pp. 1-50.* `https://inspirehep.net/literature/1377275`.

[51] D. Schulte. Study of electromagnetic and hadronic background in the interaction region of the TESLA collider. Apr. 1997. `https://cds.cern.ch/record/331845`.

[52] F. Arutyunian and V. Tumanian. The Compton effect on relativistic electrons and the possibility of obtaining high energy beams. *in Physics Letters, vol. 4, 1963, pp. 176-178.* `https://doi.org/10.1016/0031-9163(63)90351-2`.

[53] M. Bassetti and G. Erskine. Closed expression for the electrical field of a two-dimensional Gaussian charge. 1980. `https://cds.cern.ch/record/122227`.

[54] F. Halzen and A. Martin. *Quarks and Leptons: An Introductory Course in Modern Particle Physics.* 1984. `http://www.gammaexplorer.com/wp-content/uploads/2014/03/Quarks-and-Leptons-An-Introductory-Course-in-Modern-Particle-Physics.pdf`.

[55] `GUINEA-PIG` repository. `https://gitlab.cern.ch/clic-software/guinea-pig-legacy`.

[56] I. Ginzburg, G. Kotkin, V. Serbo, and V. Telnov. Colliding ge and gg beams based on the single-pass e±e- colliders (VLEPP type). *in Nuclear Instruments And Methods In Physics Research, vol. 205, pp. 47-68.*, 1983. `https://www.sciencedirect.com/science/article/pii/0167508783901734`.

[57] Kaoru Yokoya. A Computer Simulation Code for the Beam-beam Interaction in Linear Colliders. 10 1985. `https://inspirehep.net/literature/218375`.

[58] Nicolas Mounet. The LHC Transverse Coupled-Bunch Instability, 2012. Presented 2012.

[59] A. W. Chao. *Physics of collective beam instabilities in high-energy accelerators.* 1993.

[60] H. L, Anderson. *AIP 50th Anniversary: Physics Vade Mecum.* American Institute of Physics, 1981.

[61] Sergei Nagaitsev. Intrabeam Scattering Formulas for Fast Numerical Evaluation. *Phys. Rev. ST Accel. Beams*, 8:064403, 5 2005.

[62] James Bjorken and Sekazi Mtingwa. Intrabeam scattering. In *Particle Accelerators*, pages 115–143. Gordon and Breach Science Publishers, 1983.

[63] F. Antoniou and F. Zimmermann. Revision of Intrabeam Scattering with Non-Ultrarelativistic Corrections and Vertical Dispersion for MAD-X. Technical report, Cern, Geneva, 2012.

[64] Shyh-yuan Lee. *Accelerator Physics (Fourth Edition).* World Scientific Publishing Company, 2018.

[65] Ji-Gwang Hwang, Marten Koopmans, Markus Ries, Andreas Schälicke, and Roman Muller. Analytical and numerical analysis of longitudinally coupled transverse dynamics of pulse picking by resonant excitation in storage rings serving timing and high-flux users simultaneously. *Nuclear Instruments and Methods in Physics Research Section A: Accelerators, Spectrometers, Detectors and Associated Equipment*, 2019.

[66] Bruce R, Jowett J. M, Blaskiewicz M, and Fischer W. Time Evolution of the Luminosity of Colliding Heavy-Ion Beams in BNL Relativistic Heavy Ion Collider and CERN Large Hadron Collider. *Physical Review Special Topics - Accelerators and Beams*, 13(9), 2010.

[67] Zenkevich P, Boine-Frankenheim O, and Bolshakov A. A new Algorithm for the Kinetic Analysis of Intra-Beam Scattering in Storage Rings. *Nuclear Instruments and Methods in Physics Research Section A: Accelerators, Spectrometers, Detectors and Associated Equipment*, 561(2):284–288, 2006.

[68] M. Zampetakis, F. Antoniou, F. Asvesta, H. Bartosik, Y. Papaphilippou, and A.S. Hernández. Interplay of Space Charge and Intra-Beam Scattering in the LHC Ion Injector Chain. 2023.

[69] Ji Qiang, Miguel A. Furman, and Robert D. Ryne. A parallel particle-in-cell model for beam–beam interaction in high energy ring colliders. *Journal of Computational Physics*, 198(1):278–294, 2004.